Addressing Fundamental Questions in Chemical Biology through Biochemical Investigations of Natural Products

Inauguraldissertation

zur

Erlangung der Würde eines Doktors der Philosophie

vorgelegt der

Philosophisch-Naturwissenschaftlichen Fakultät

der Universität Basel

von

Simon Sieber

Aus Fribourg, Schweiz

Basel, 2015

Genehmigt von der Philosophisch-Naturwissenschaftlichen Fakultät
auf Antrag von:

Prof. Dr. Karl Gademann
Prof. Dr. Matthias Hamburger

Basel, den 23. Juni 2015

Prof. Dr. Jörg Schibler
Dekan

Pour Carlotta
et ma famille

Table of Content

Abstract

This thesis is separated in three main parts including a general introduction, three chapters based on research projects and the last chapters with the experimental procedures and analytical data. The focus of this work is based on the isolation of natural products and their application in chemistry and biology.

Chapter 1

The first chapter consists in a general introduction about natural products, where their importance in drug discovery and in the interaction between living organisms is highlighted. Several examples of natural products from different origins are described.

Chapter 2

The study of a system living in obligatory symbiosis is addressed in this chapter. *Psychotria kirkii* is a plant having the particularity to be in symbiosis with a bacterial strain named *Candidatus Burkholderia kirkii* and the presence of this microorganism was found to be essential for the plant's survival. Interestingly, the bacterial genomic sequencing and analysis revealed the presence of a putative C_7N aminocyclitol. This project led to the isolation, total synthesis and biological evaluation of kirkamide, a new C_7N aminocyclitol from *Candidatus Burkholderia kirkii*. In the course of the chemical composition analysis of *Psychotria kirkii*, another new natural product (streptol glucoside) was isolated and its structure was elucidated. The last part of this chapter focuses on detection and quantification methods for the analysis of these natural products.

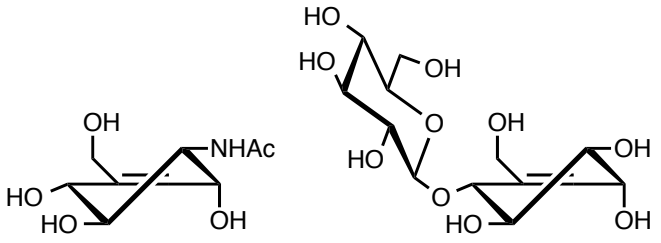

kirkamide streptol glucoside

Chapter 3

After completing a genome-driven bioassay-guided fractionation, a natural product possessing an unusual *N*-nitrosohydroxylamine functional group was isolated. The formation of the N-N bond in biological system has yet to be elucidated. Chapter 3 addresses the question regarding the biosynthetic analysis of the *N*-nitrosohydroxylamine compound. Furthermore, the mechanism of the N-N bond formation was investigated in detail using model compounds.

Chapter 4

The potential of secondary metabolites has been recognized for the discovery of biological active compounds. The strength of natural products resides in the diversity and complexity of their chemical structures. In this chapter the isolation, structure elucidation and biological evaluation of new natural products from cyanobacteria are described.

Three new cyanobactins were isolated from the cyanobacteria *Microcystis aeruginosa* EAWAG 251. The stereoassignement of these natural products, named balgacyclamides A–C, is presented with their biological activity investigations against the parasite *Plasmodium falciparum*.

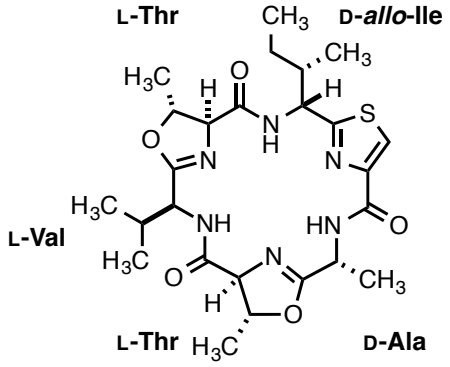

balgacyclamide A (**177**)

The last part of the chapter describes a bioassay-guided fractionation leading to the discovery of two new glycolipopeptides from cyanobacteria. The efforts achieved towards the structure elucidation using HRMS tandem mass spectrometry, NMR and amino acid analysis are presented.

Acknowledgements

I want to express my sincere gratitude to my supervisor Prof. Dr. *Karl Gademann* who gave me the opportunity to be a member of his group and carry out fascinating research projects. His guidance, support and most particularly his trust, were essential contributions and motivational factors during my Ph.D.

I would like to thank Prof. Dr. *Matthias Hamburger* for accepting to be co-examintor of my Ph.D. thesis.

I am thankful to Prof. Dr. *Dennis Gillingham* for chairing the defense of this thesis.

I am really grateful to my students *Silvan Wirthensohn* and *Darja Kolbin*, which brought substantial contributions to my projects in isolation of natural products during their master thesis. Also, I want to thank *Joël Rösslein* for his positive attitude, his help and ideas during his Wahlpraktikum.

I would like to thank Prof. Dr. *Leo Eberl*, Dr. *Aurelien Carlier* and *Christian Jenul* from the University of Zürich for having the opportunity to collaborate on captivating projects.

I want to acknowledge *Carlotta Foletti, Robin Wehlauch*, Dr. *Regina Berg*, *Elias Kaufmann*, *Christophe Daeppen* and Dr. *Nadine Bohni* for the critical proofreading of this thesis.

I truly appreciate the advices, fruitful discussions and friendship from Dr. *Suman De Sarkar*, Dr. *Hideki Miyatake-Ondozabal* and Dr. *Christof Sparr*. Also, a special thank goes to *Elias Kaufmann* and *Isabel Kerschgens* for the fantastic time spend during weddings in India and Poland and to *Christophe Daeppen* for his essential contribution on a common project and his critical advices.

I would like to thank the current and former group members of Gademann and Sparr groups for their contribution in creating a friendly and family working atmosphere and for their multiple participation on diverse committees: Dr. *Fabian Schmid*, *Hiromu Hattori*, *Ellen Piel*, Dr. *Johannes Hoecker*, Dr. *José Gomes*, Dr. *Verena Grundler*, Dr. *Malika Makhlouf*, *Mathieu Szponarski*, Dr. *Erika Crane*, *Christophe Thommen*, Dr. *Patrick Burch*, Dr. *Elamparuthi Elangovan*, *Manuel Scherer*, *Raphael Liffert*, Dr. *Samuel*

Bader, *Simone Grendelmeier*, *Jan Hanusch*, *Achim Link*, *Christian Fischer* and *Vincent Fäseke*.

I am grateful for the great work of Dr. *Markus Neuburger*, Dr. *Daniel Häussinger* and Dr. *Heinz Nadig* on analytical measurements.

I want to thank *Marina Mambelli Johnson* for her administrative help and for always being so welcoming.

I am thankful to the Werkstatt and other technical staff of the department of organic chemistry at University of Basel for always being so helpful.

I want to thank the NCCR Chemical Biology for their financial support.

A special thank goes to *Carlotta* that has helped and supported me so much during these last few years.

Je termine cette section en disant un grand merci à ma famille qui m'a toujours soutenue et je vous en serai éternellement reconnaissant. Aussi vous m'avez apporté le courage, la persévérance et la passion pour la science, merci encore à vous.

Publications List

Part of this thesis have been published in the following articles:

M. Pinto-Carbó, **S. Sieber**, S. Dessein, T. Wicker, B. Verstraete, K. Gademann, L. Eberl, A. Carlier, *manuscript submitted*.

Simon Sieber, Aurélien Carlier, Markus Neuburger, Giselher Grabenweger Leo Eberl and Karl Gademann: Isolation and Total Synthesis of Kirkamide, an Aminocyclitol from an Obligate Leaf Nodule Symbiont. *Angew. Chem. Int. Ed.* **2015**, *54*, 7968–7970.

Cyril Portmann, **Simon Sieber**, Silvan Wirthensohn, Judith F. Blom, Laeticia Da Silva, Emilie Baudat, Marcel Kaiser, Reto Brun and Karl Gademann: Balgacyclamides, Antiplasmodial Heterocyclic Peptides from *Microcystis Aeruguinosa* EAWAG 251. *J. Nat. Prod.* **2014**, *77*, 557–562.

Karl Gademann and **Simon Sieber**: Chemical interference of biological systems with natural products. *Chimia*, **2011**, *65*, 835–838.

List of Abbreviations, Acronyms and Symbols

A	adenylation
Ac	acetyl
AcOH	acetic acid
ADDA	(all-S,all-E)-3-amino-9-methoxy-2,6,8-trimethyl-10-phenyldeca-4,6-dienoic acid
AHL	*N*-acyl-L-homoserine lactone
Ala	alanine
APCI	atmospheric pressure chemical ionization
aq.	aqueous
Ara	arabinose
B.	*Burkholderia*
Bn	benzyl
Bu	butyl
°C	degrees centigrade
c	concentration
CAM	ceric ammonium molybdate
COSY	correlation spectroscopy
CSA	camphor-10-sulfonic acid
d	doublet
dd	doublet of doublet
ddd	doublet of doublet of doublet
dddd	doublet of doublet of doublet of doubet
D	deuterium
Dhb	dehydroaminobutyric acid
Dhh	dihydroxy hexadecanoic acid
diox	dioxane
DMF	dimethylformamide
DMSO	dimethyl sulfoxide
dpi	days post innoculation
dq	doublet of quartet

EAWAG	Eidgenössische Anstalt für Wasserversorgung (Swiss Federal Institute of Aquatic Science and Technology)
ED_{100}	effective dose with an inhibition effect of 100%
ED_{50}	effective dose with an inhibition effect of 50%
ESI	electrospray ionization
Et_3N	triethylamine
Et_2O	diethyl ether
EtOAc	ethyl acetate
FDAA	*N*-(2,4-dinitro-5-fluorophenyl)-L-alaninamide
g	gram(s)
GalA	galacturonic acid
Glc	glucose
GLCP	glycolipocyclopeptide
Gln	glutamine
GlnNAc	*N*-acetyl-D-glucosamine
Glu	glutamic acid
Gly	glycine
h	hour(s)
HMBC	heteronuclear multiple bond correlation
HMDS	hexamethyldisilazane
HPLC	high-performance liquid chromatography
HRMS	high-resolution mass spectrometry
$HRMS^2$	high-resolution tandem mass spectrometry
Hz	hertz (s^{-1})
Ile	isoleucine
imid	imidazole
J	coupling constant
KS	β-ketoacyl synthase
L	liter(s)
L.	*Leishmania*

LC_{50}	median lethal dose
M	molarity (mol./L^{-1})
m	multiplet
M.	*Microcystis*
M.p.	melting point
MeCN	acetonitrile
MeOH	methanol
min	minute(s)
Mm	millimeter
MS	mass spectrometry
MSTFA	*N*-methyl-*N*-(trimethylsilyl)trfifluoroacetamide
n.d.	not determined
neg.	negative
NMR	nuclear magnetic resonance spectroscopy
NOESY	nuclear Overhauser effect spectroscopy
NRPS	nonribosomal peptide synthetase
P.	*Psychotria*
P. aeruginosa	*Pseudomonas aeruginosa*
P. falciparum	*Plasmodium falciparum*
PCC	Pasteur Culture Collection of Cyanobacteria, Paris, France
Ph	phenyl
PPh	triphenylphosphine
Phe	phenylalanine
PKS	polyketide synthase
ppm	parts per million
positive	pos.
PCP	peptidyl carrier protein
*p*TSOH	*p*-toluenesulfonic acid
Red	reductase
R_f	retention time

RP	reversed phase
RT	room temperature
s	singlet
S.	*Streptomyces*
SD	standard deviation
sat.	saturated
soln.	solution
sp.	species
SPE	solid phase extraction
t	triplet
T. b.	*Trypanosoma brucei*
TBAF	tertbutylammonium fluoride
TBS	tert-butyldimethylsilyl
Tf	trifluoromethanesulfonyl
TFA	trifluoroacetic acid
TFAA	trifluoroacetic anhydride
THF	tetrahydrofuran
Thr	threonine
TLC	thin layer chromatography
Ts	tosyl
Tyr	tyrosine
U. ornatrix	*Utetheisa ornatrix*
UV	ultraviolet
ν	wavenumber
Val	valine
μM	micromolar

1. Natural Products: a Prolific Source of Knowledge

Isolation of natural products has been since many years a powerful tool for the discovery of new biologically active compounds and to gain a better understanding of biological systems. In this chapter, the importance of natural products in drug discovery will be presented followed by the role of these compounds in interactions between organisms.

1.1. Natural Products in Drug Discovery

The development of combinatorial libraries has brought a new route for the discovery of biological active compounds without the requirement for isolation nor structure elucidation. One of the main limitations of this approach is the generation of a library covering a broad diversity in chemical space.[1] For this reason, the interest was brought back to natural products, which were found to provide a wide chemical structure variation and accessiblility at moderate costs. Examples of natural products will be described in the following sections.[2]

1.1.1. Natural Products Isolated from Plants

In the 17th century, the bark of the cinchona tree was used to treat malaria. In 1820, Pelletier and Caventou isolated the natural product responsible for the antiprotozoal activity and the structure was elucidated to be quinine (**1**) in 1908.[3] The first total synthesis, reported in 1944, confirmed the structure of the natural product.[4]

The discovery of artemisinin (**2**) is another example of traditional medicine leading to the isolation of an antimalarial drug. *Artemisia annua* (sweet wormwood or qinghao in Chinese) is an herb that was recognized for a long time in China for its antimalarial property. The active compound was isolated in 1972 and the structure was characterized in 1979. The natural product was named artemisinin or qinghaosu (**2**), meaning active principle of qinghao in chinese.[5] Interestingly, artemisinin (**2**) is the only natural product possessing a 1,2,4 trioxane (figure **1**). A semisynthetic derivative of artemisinin in

1 J. Hong, *Curr. Opin. Chem. Biol.* **2011**, *15*, 350–354.
2 G. M. Cragg, D. J. Newman, *Biochim. Biophys. Acta* **2013**, *1830*, 3670–3695.
3 A. R. Butler, Y. L. Wu, *Chem. Soc. Rev.* **1992**, 85–90.
4 R. B. Woodward, W. E. Doering, *J. Am. Chem. Soc.* **1944**, *66*, 849–849.
5 D. L. Klayman, A. J. Lin, N. Acton, J. P. Scovill, J. M. Hoch, W. K. Milhous, A. D. Theoharides, A. S. Dobek, *J. Nat. Prod.* **1984**, *47*, 715–717.

combination with lumefantrine was recently approved by FDA and is now an available antimalarial drug (Coartem®).[6]

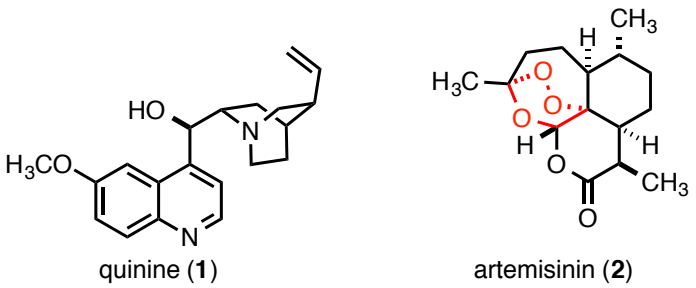

*Figure **1**: Antimalarial natural products quinine (**1**) and artemisinin (**2**).The 1,2,4 trioxane is highlighted in red.*

1.1.2. Natural Product Isolated from Marine Organisms

In an early stage, some secondary metabolites of the marine sponge *Halichondria okadai* (*H. okadai*) were found to possess potent anticancer properties.[7] To further investigate the potential of this marine organism, 600 kg of *H. okadai* were collected, the compounds were extracted and subject to a bioassay-guided fractionation to finally obtain 12.5 mg of halichondrin B (**3**). The natural product **3** was found to possess an IC_{50} value of 0.093 ng/mL against B-16 melanoma cells, which encouraged the development of an alternative route to obtain the natural product.[8] The first total synthesis was achieved by Kishi and coworkers in 47 steps for the longest linear sequence.[9] During the course of this work the activity of synthetic precursors was tested and a truncated analogue was shown to possess similar anticancer activity as halichondrin B (**3**). After structure and reactivity studies, eribulin mesylated (**4**)[7] was chosen for clinical trials and was recently approved by the FDA for the treatment of breast cancer.[10]

---

6 Z. G. Premji, *Malar. J.* **2009**, *8*, S3.
7 K. L. Jackson, J. A. Henderson, A. J. Phillips, *Chem. Rev.* **2009**, *109*, 3044–3079.
8 Y. Hirata, D. Uemura, *Pure Appl. Chem.* **1986**, *58*, 701–710.
9 T. D. Aicher, K. R. Buszek, F. G. Fang, C. J. Forsyth, S. H. Jung, Y. Kishi, M. C. Matelich, P. M. Scola, D. M. Spero, S. K. Yoon, *J. Am. Chem. Soc.* **1992**, *114*, 3162–3164.
10 U. Swami, I. Chaudhary, M. H. Ghalib, S. Goel, *Crit. Rev. Oncol. Hematol.* **2012**, *81*, 163–184.

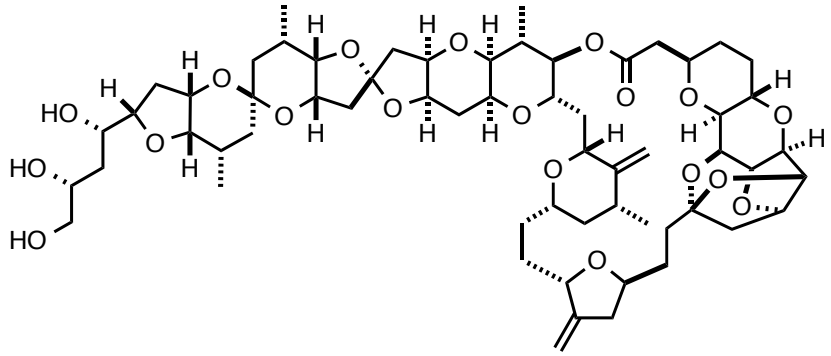

halichondrin B (**3**)

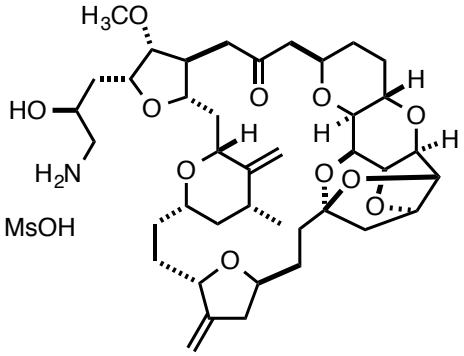

eribulin mesylate (**4**)

1.1.3. Natural Product Isolated from Microorganisms

During a search for new antifungal compounds directed by Merck, two natural products, pneumocandins A_0 and B_0 (**5**), were isolated from an extract of the fungus *Glarea lozoyensis*.[11] Pneumocandin B_0 (**5**) was selected for further investigation due to its potent antifungal activity against several *Candida* species.[12] The development of the natural product to the FDA approved drug CANCIDAS® included: 1) genetic modifications of *Glarea lozoyensis* to obtain a mutant producing larger amount of pneumocandin B_0 (**5**), 2) optimization of the isolation strategy using different extraction procedures combined with normal phase HPLC separation and finally, 3) chemical modifications to improve pharmacokinetic and pharmacodynamic properties.[11]

[11] J. M. Balkovec, D. L. Hughes, P. S. Masurekar, C. A. Sable, R. E. Schwartz, S. B. Singh, *Nat. Prod. Rep.* **2014**, *31*, 15–34.

[12] D. M. Schmatz, G. Abruzzo, M. A. Powles, D. C. Mcfadden, J. M. Balkovec, R. M. Black, K. Nollstadt, K. Bartozal, *J. Antibiot.* **1992**, *45*, 1886–1891.

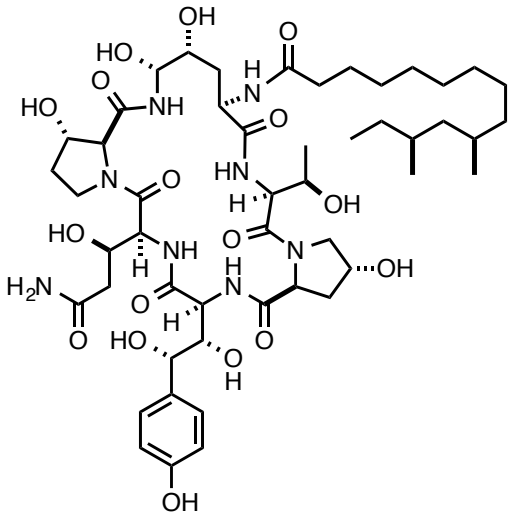

pneumocandin B_0 (**5**)

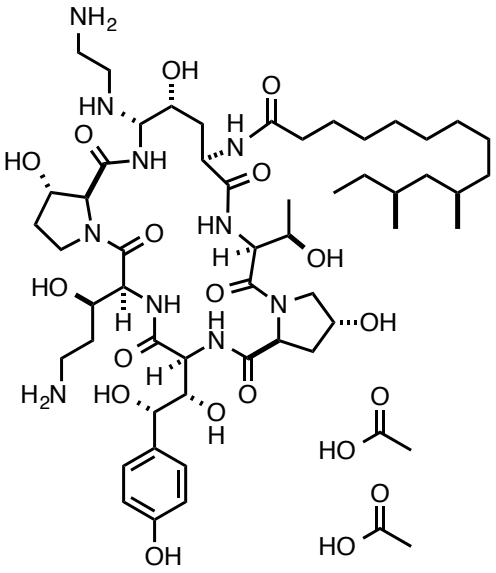

CANCIDAS®

1.2. Natural Products as Chemical Messengers

The communications between various living organisms occurs *via* an exchange of natural product(s). The isolation of these compounds and the study of their biological role provide crucial information for the understanding of the interaction between various species. Herein we will present two example of natural product acting as the chemical language between different organisms.[13]

1.2.1. Hydroxydanaidal

Meinwald and coworkers reported a particular behavior of the moth *Utetheisa ornatrix* (*U. ornatrix*). The authors observed that male moths fed with the plant *Crotalaria* sp. were more successful in courtship when compared to male moths fed with pinto bean. Hydroxydanaidal (**6**) was isolated from the successful males and was proposed to be the pheromone responsible for this behavior. Additionally, this natural product **6** was proposed to be biosynthetically prepared from the plant alkaloid monocrotaline (**7**).[14] It was later found that males fed with the plant *Crotalaria* sp. accumulate the alkaloid **7**, which is feeding deterrent, and can transfer the compound to

[13] J. Meinwald, *J. Org. Chem.* **2009**, *74*, 1813–1825.
[14] W. E. Conner, T. Eisner, R. K. Vander Meer, A. Guerrero, J. Meinwald, *Behav. Ecol. Sociobiol.* **1981**, *9*, 227–235.

the eggs and to the female.[15] It was proposed that hydroxydanaidal (**6**) was an indication for the female that the male possesses the toxic alkaloid monocrotaline (**7**).[13]

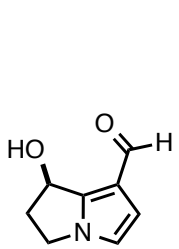

hydroxydanaidal (**6**)

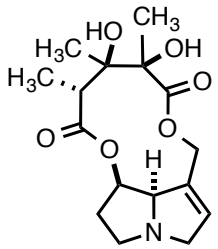

monocrotaline (**7**)

1.2.2. Bacterium Messengers *N*-Acyl-L-homoserine Lactones

Bacteria have developed a communication system based on the production of *N*-acyl-L-homoserine lactones (AHLs) acting as signaling molecules. For example, one bacterium will produce and export these natural products into the media, which will be detected *via* a specific receptor (LasR) by another congener. It was found that this communication is essential for biofilm formation and virulence of theses organisms. AHLs were found to possess a similar lactone core structure with variation in the oxidation and length of the acyl chain.[16] The natural products *N*-butyryl-L-homoserine lactone (C4-HSL, **8**)[17] and *N*-(3′-oxodecanoyl)-L-homoserine lactone (3-oxo-C_{12}-HSL, **9**)[18] were isolated from *Pseudomonas aeruginosa* (*P. aeruginosa*) culture.

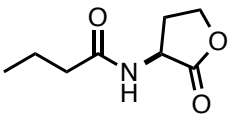

C_4-HSL (**8**)

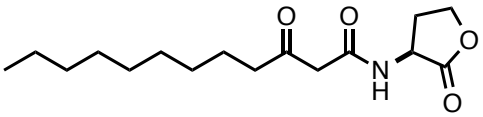

3-oxo-C_{12}-HSL (**9**)

*Figure **2**: Examples of AHLs produced by P. aeruginosa.*

[15] D. E. Dussourd, K. Ubik, C. Harvis, J. Resch, J. Meinwald, T. Eisner, *Proc. Natl. Acad. Sci. U. S. A.* **1988**, *85*, 5992–5996.
[16] J. S. Dickschat, *Nat. Prod. Rep.* **2010**, *27*, 343–369.
[17] J. P. Pearson, K. M. Gray, L. Passador, K. D. Tucker, A. Eberhard, B. H. Iglewski, E. P. Greenberg, *Proc. Natl. Acad. Sci. U. S. A.* **1994**, *91*, 197–201.
[18] J. P. Pearson, L. Passador, B. H. Iglewski, E. P. Greenberg, *Proc. Natl. Acad. Sci. U. S. A.* **1995**, *92*, 1490–1494.

2. C_7N Aminocyclitol Kirkamide and Streptol Glucoside

2.1. The C_7N Aminocylitol Natural Products Family

The natural products of the C_7N aminocyclitol family are characterized by a cylcohexane or cyclohexene core structure having attached to the ring a CH_2OH, one amine and 3 to 5 hydroxyl groups (figure **3**). Most of the members possess the amino group at C-2 and a saccharide or polysaccharide as R_1 and/or R_2.[19] Additionally, these natural products shared a common biosynthetic pathway with the use of 2-*epi*-5-*epi*-valiolone synthases.[20,21,22]

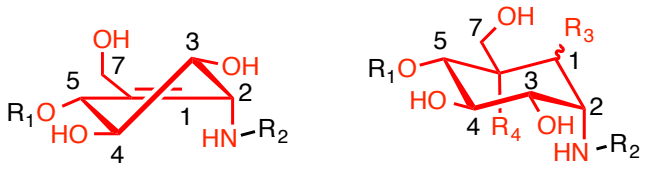

*Figure **3**: General structure of the C_7N aminocyclitols, where R_1 and R_2 can be hydrogen or carbohydrate and R_3 and R_4 can be hydrogen or hydroxyl group.*

Herein, the C_7N aminocyclitol natural products will be presented in relation to their numerous biological activities such as antifungal, α-glucosidase inhibitor, antibacterial and cytotoxicity.

[19] T. Mahmud, *Nat. Prod. Rep.* **2003**, *20*, 137–166.
[20] P. M. Flatt, T. Mahmud, *Nat Prod Rep* **2007**, *24*, 358–392.
[21] T. Mahmud, P. M. Flatt, X. Wu, *J. Nat. Prod.* **2007**, *70*, 1384–1391.
[22] T. Mahmud, *Curr. Opin. Chem. Boil.* **2009**, *13*, 161–170.

2.1.1. Antifungal and Insecticide

Validamycin A (**10**) and B (**11**) were isolated from *Streptomyces hygroscopicus* var. *limoneus* in 1970, in an effort to find new antifungal compounds to control the sheath blight causing damage to rice production.[23,24] These two natural products were the first from the C_7N aminocyclitol family to be discovered.

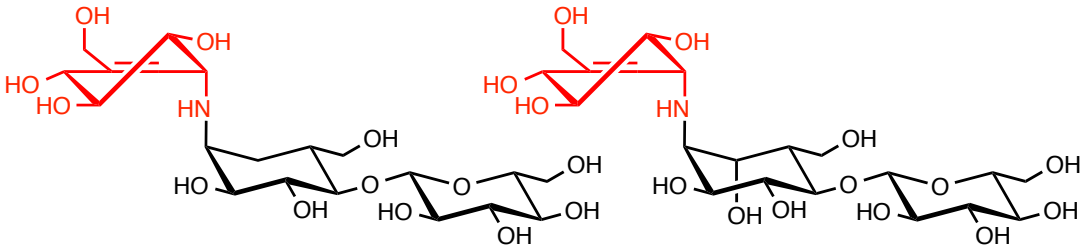

Many compounds sharing similar scaffold with variation in the number of carbohydrates were isolated from the same bacteria and named validamycins C–H (**12-17**) for those that contains 2 or more carbohydrates,[25,26,27] validoxylamine A (**18**), B (**19**) and G (**20**) with one carbohydrate[25,26] and valienamine (**21**) for the core structure (table **1**).[28]

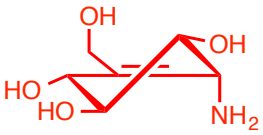

valienamine (**21**)

[23] T. Iwasa, H. Yamamoto, M. Shibata, *J. Antibiot.* **1970**, *23*, 595–602.
[24] T. Iwasa, E. Higashide, H. Yamamoto, M. Shibata, *J. Antibiot.* **1971**, *24*, 107–113.
[25] S. Horii, Y. Kameda, K. Kawahara, *J. Antibiot.* **1972**, *25*, 48–53.
[26] Y. Kameda, N. Asano, T. Yamaguchi, K. Matsui, S. Horii, H. Fukase, *J. Antibiot.* **1986**, *39*, 1491–1494.
[27] N. Asano, Y. Kameda, K. Matsui, S. Horii, H. Fukase, *J. Antibiot.* **1990**, *43*, 1039–1041.
[28] Y. Kameda, N. Asano, M. Yoshikawa, M. Takeuchi, T. Yamaguchi, K. Matsui, S. Horii, H. Fukase, *J. Antibiot.* **1984**, *37*, 1301–1307.

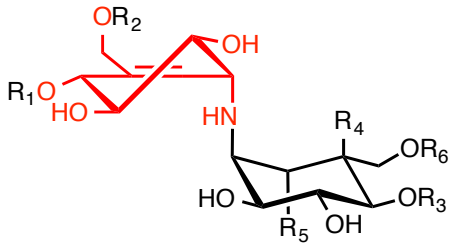

Table **1.** The natural products validamycins and validoxylamines.

	R_1	**R_2**	**R_3**	**R_4**	**R_5**	**R_6**
validamycin A (**10**)	H	H	β-D-Glc	H	H	H
validamycin B (**11**)	H	H	β-D-Glc	H	OH	H
validamycin C (**12**)	H	α-D-Glc	β-D-Glc	H	H	H
validamycin D (**13**)	H	H	H	H	H	α-D-Glc
validamycin E (**14**)	H	H	α-D-Glc-(1-4)-β-D-Glc	H	H	H
validamycin F (**15**)	α-D-Glc	H	β-D-Glc	H	H	H
validamycin G (**16**)	H	H	β-D-Glc	OH	H	H
validamycin H (**17**)	H	H	α-D-Glc-(1-4)-β-D-Glc	H	H	H
validoxylamine A (**18**)	H	H	H	H	H	H
validoxylamine B (**19**)	H	H	H	H	OH	H
validoxylamine G (**20**)	H	H	H	OH	H	H

Antifungal activities were reported for validamycin A (**10**), B (**11**), E (**14**), F (**15**), G (**16**), H (**17**) and validoxylamine A (**18**) and G (**20**). The inhibition of the enzyme trehalase was suggested as the mechanism of action, which prevents the degradation of trehalose (**22**) into glucose. The activity of the compounds was tested *in vitro* and validoxylamine A (**18**) was found to be the most potent compound from this family with an IC_{50} value of 0.14 µM. Surprisingly, **14** and **15** showed no inhibition up to a concentration of 10 mM although they exhibit an antifungal activity. Furthermore, validamycin A (**10**) exhibited a strong antifungal activity but only a weak trehalase inhibition and for validoxylamine A (**18**) exactly the reverse phenomenon was observed, strong trehalase inhibition and weak antifungal activity. **10** was suggested to be a prodrug harboring good pharmacokinetic properties and activated within the organism into **18**

after glucolysis. The same mode of action could be applied to **14** and **15** as they would be converted to validoxylamine A (**18**) after glucolysis.[27,29]

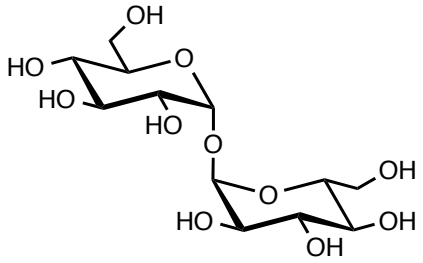

trehalose (**22**)

Validamycins A–E (**10**-**14**) and validoxylamine A (**18**), B (**19**) and G (**20**) were tested for their insecticide activity performing *in vivo* and *in vitro* assays. **10**, **12**, **13**, **14** and **18** were found to be active *in vivo* using 20 larvae. Validoxylamin A (**18**) showed the strongest activity. Furthermore, all the compounds were found to possess IC_{50} values in the micromolar and even nanomolar range for their inhibition against trehalase, from insect origin, with the most potent activity for validoxylamine A (**18**).[30]

Salbostatin (**23**) and suidatrestin were found to possess a trehalase inhibition in the nanomolar range and picomolar range respectively.[31,32] The promising activity of suidatrestin was further investigated on insect and essentially no effect was observed.[33] Additionally, the structure of this natural product remained unknown and was proposed to be similar as validoxylamin A (**18**) based on C NMR data analysis.[33]

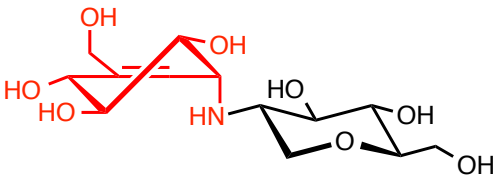

salbostatin (**23**)

[29] N. Asano, T. Yamaguchi, Y. Kameda, K. Matsui, *J. Antibiot*. **1987**, *40*, 526–532.
[30] N. Asano, M. Takeuchi, Y. Kameda, K. Matsui, Y. Kono, *J. Antibiot.* **1990**, *43*, 722–726.
[31] L. Vértesy, H. W. Fehlhaber, A. Schulz, *Angew. Chem. Int. Ed.* **1994**, *33*, 1844–1846.
[32] S. Murao, T. Shin, K. Sugawa, A. Teruo (S. Murao) US005494812A, **1996**
[33] I. Knuesel, S. Murao, T. Shin, T. Amachi, H. Kayser, *Comp. Biochem. Physiol. B, Biochem. Mol. Biol.* **1998**, *120*, 639–646.

2.1.2. α-Glucosidase Inhibitor

Acarbose (**24**), discovered in 1977, is one of the mostly used α-glucosidase inhibitor,[34] nowadays to treat patients suffering from type 2 diabetes.[35] The compound is ingested at the same time as the meal and its inhibitor effect will prevent that the concentration of glucose rises in the blood.[35] The mechanism of action was suggested to be related to the presence of valienamine (**21**), which its half chair conformation would mimic an oxocarbenium (degradation intermediate of glucose) and block the active site of the enzyme.[19] Several other naturals products containing **21** were reported to possess α-glucosidase activities as adiposin-1 (**25**),[36] adiposin-2 (**26**)[36] and the more complex trestatins A-C (**27**-**29**),[37,38] Ro 09-0766 (**30**),[39] Ro 09-0767 (**31**)[39] and Ro 09-0768 (**32**).[39] The structure of these natural products was elucidated by NMR spectroscopy data analysis and degradation studies.

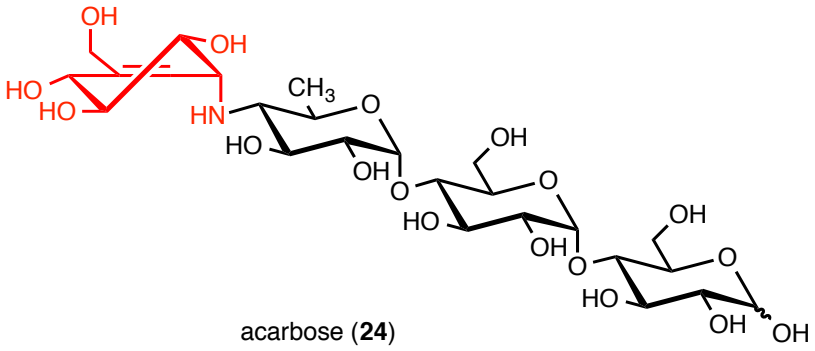

acarbose (**24**)

[34] D. D. Schmidt, W. Frommer, B. Junge, L. Müller, W. Wingender, E. Truscheit, D. Schäfer, *Naturwissenschaften* **1977**, *64*, 535–536.
[35] M. F. McCarty, J. J. DiNicolantonio, *Open Heart* **2015**, *2*, e000205.
[36] S. Namiki, K. Kangouri, T. Nagate, H. Hara, K. Sugita, S. Omura, *J. Antibiot*. **1982**, *35*, 1234–1236.
[37] K. Yokose, K. Ogawa, T. Sano, K. Watanabe, H. B. Maruyama, Y. Suhara, *J. Antibiot.* **1983**, *36*, 1157–1165.
[38] K. Yokose, K. Ogawa, Y. Suzuki, I. Umeda, Y. Suhara, *J. Antibiot.* **1983**, *36*, 1166–1175.
[39] K. Yokose, M. Ogawa, K. Ogawa, *J. Antibiot.* **1984**, *37*, 182–186.

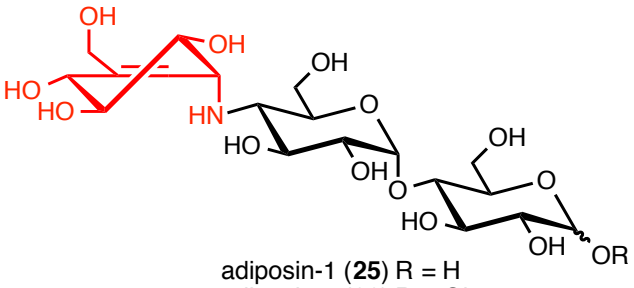

adiposin-1 (**25**) R = H
adiposin-2 (**26**) R = Glc

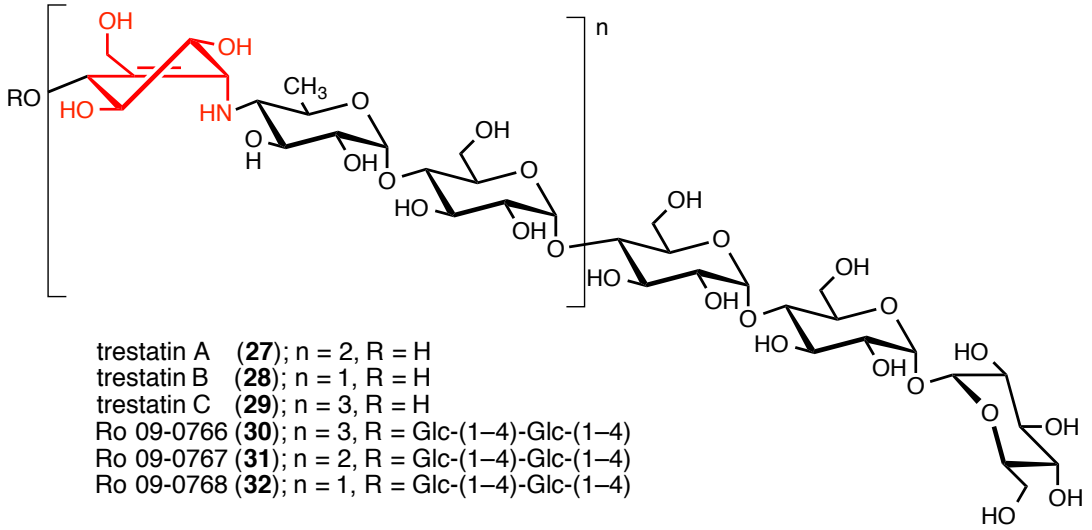

trestatin A (**27**); n = 2, R = H
trestatin B (**28**); n = 1, R = H
trestatin C (**29**); n = 3, R = H
Ro 09-0766 (**30**); n = 3, R = Glc-(1–4)-Glc-(1–4)
Ro 09-0767 (**31**); n = 2, R = Glc-(1–4)-Glc-(1–4)
Ro 09-0768 (**32**); n = 1, R = Glc-(1–4)-Glc-(1–4)

It was also found that valienamine (**21**), hydroxyvalidamine (**33**), valiolamine (**34**) and validamine (**35**) were active at a micromolar and even nanomolar range, for **35**, against some α-glucosidase.[28] This result was unexpected due the fact that these carbohydrates are not all in a half-chair conformation. Furthermore, the C_7N aminocylitol oligostatins C–E (**36**–**38**) possessing a core structure in chair conformation was found to be active against α-amylase.[40,41]

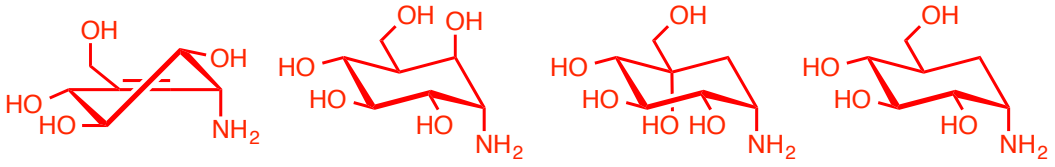

valienamine (**21**) hydroxyvalidamine (**33**) valiolamine (**34**) validamine (**35**)

[40] J. Itoh, S. Omoto, T. Shomura, H. Ogino, K. Iwamatsu, S. Inouye, H. Hidaka, *J. Antibiot.* **1981**, *34*, 1424–1428.
[41] S. Omoto, J. Itoh, H. Ogino, K. Iwamatsu, N. Nishizawa, S. Inouye, *J. Antibiot.* **1981**, *34*, 1429–1433.

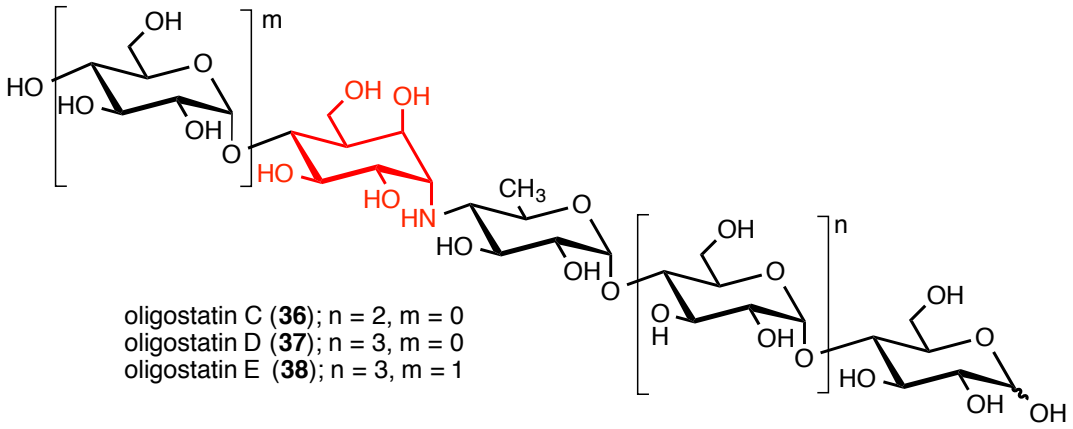

Several oxirane pseudooligosaccharides were isolated and patented for their use as α-glucosidase inhibitors. The compounds W-46 A (**39**), W-46 B (**40**), W-46 C (**41**), W-46 H (**42**), W-46 P (**43**),[42] CKD-711 (**44**)[43], CKD-711a (**45**)[43] and from the NS and CK-4416 complexes,[44,45] contained carbohydrates attached at C-2 and/or C-4 to the C_7N core structure.

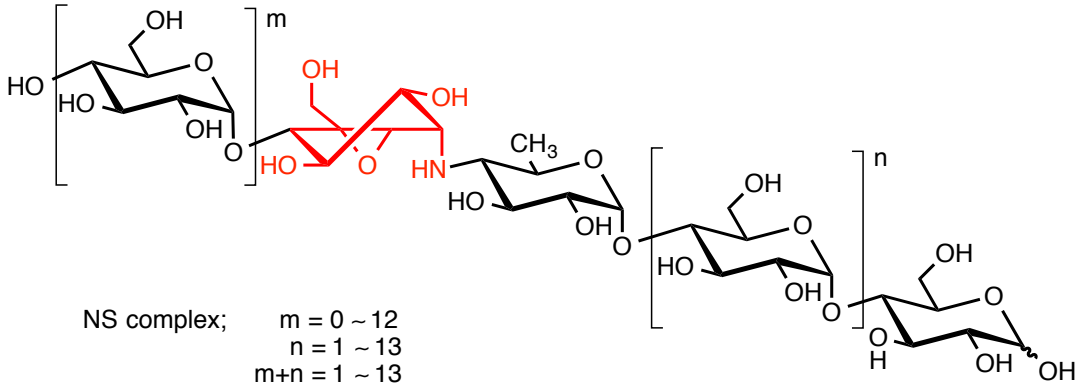

[42] L. Vertesy, J. Betz, H.-W. Felhaber, K. Geisen (Hoechst Aktiengesellschaft) US4990500, **1991**.
[43] H.-B. Chang, S.-H. Kim, Y.-I. Kwon, D.-H. Choung, W.-K. Choi, T. W. Kang, S. Lee, J.-G. Kim, H.-S. Chun, S. K. Ahn, C. I. Hong, K.-H. Han, *J. Antibiot.* **2002**, *55*, 467–471.
[44] J. W. Kim, K. M. Lee, H. S. Chun, J. G. Kim, H. B. Chang, S. H. Kim, K. B. Min, K. S. Moon (Chong Kun Dang Corporation) US5866377A, **1999**.
[45] T. Haruki, N. Yoshio, K. Akira (Tokyo Tanabe CO), JPS58172400, **1983**.

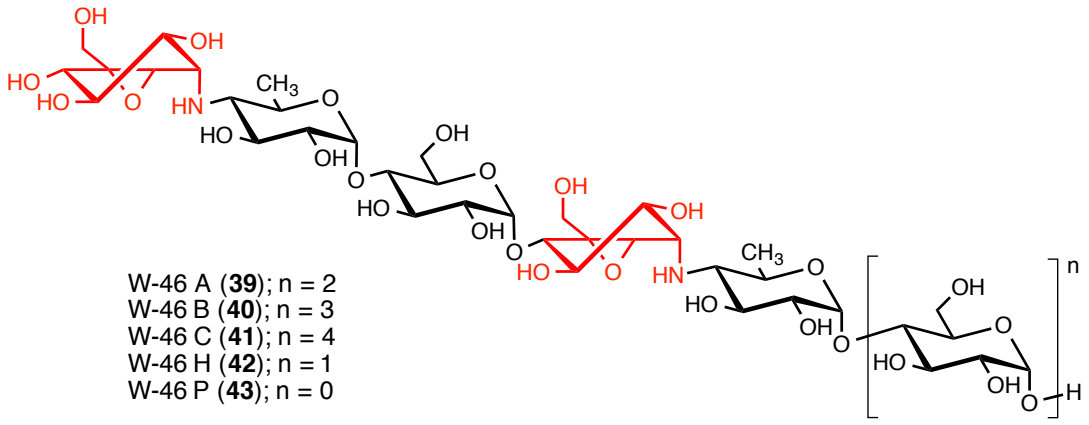

W-46 A (**39**); n = 2
W-46 B (**40**); n = 3
W-46 C (**41**); n = 4
W-46 H (**42**); n = 1
W-46 P (**43**); n = 0

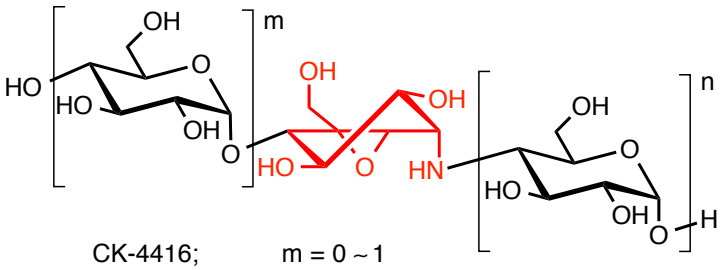

CK-4416; m = 0 ~ 1
n = 3 ~ 7
m+n = 3 ~ 6

CKD-711(**44**); m = 0, n = 3

CKD-711a (**45**); m = 0, n = 6

2.1.3. Antibacterial Activity

Pyralomicin 1a–1d (**46-49**) were isolated from a *Microtetraspora spiralis* strain and their structures were elucidated by NMR spectroscopic data analysis and by X-ray crystallography analysis on the bromo derivative of **46**.[46,47] The natural products were found to be active against various bacterial strains especially against *Micrococcus luteus*.[46] Pyralomicin 1d (**49**), which contained an additional chloride attached to the cyclopentadiene, had a significantly lower potency indicating the importance of this position for the biological activity.

[46] N. Kawamura, R. Sawa, Y. Takahashi, K. Issiki, T. Sawa, N. Kinoshita, H. Naganawa, M. Hamada, T. Takeuchi, *J. Antibiot.* **1995**, *48*, 435–437.

[47] N. Kawamura, N. Kinoshita, R. Sawa, Y. Takahashi, T. Sawa, H. Naganawa, M. Hamada, T. Takeuchi, *J. Antibiot.* **1996**, *49*, 706–709; N. Kawamura, R. Sawa, Y. Takahashi, K. Isshiki, T. Sawa, H. Naganawa, T. Takeuchi, *J. Antibiot.* **1996**, *49*, 651–656; N. Kawamura, H. Nakamura, R. Sawa, Y. Takahashi, T. Sawa, H. Naganawa, T. Takeuchi, *J. Antibiot*. **1997**, *50*, 147–149.

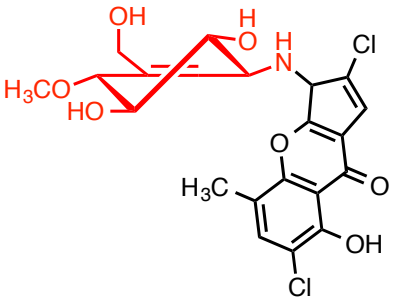

pyralomicin 1a (**46**)

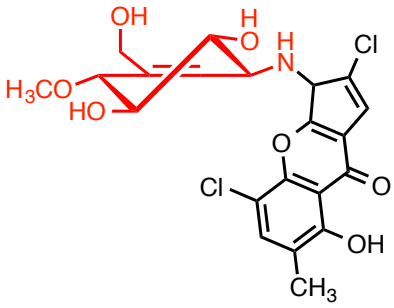

pyralomicin 1b (**47**)

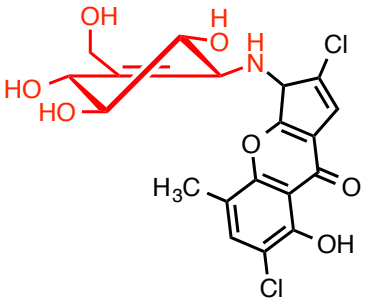

pyralomicin 1c (**48**)

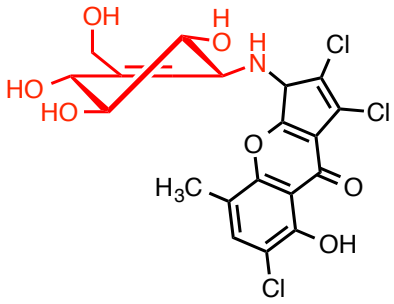

pyralomicin 1d (**49**)

The natural products epoxyquinomicins A-D (**50-53**), produced by *Amycolatopsis* sp., were discovered during a screening for new antibiotics.[48,49] Epoxyquinomicins A and B (**50-51**) inhibited the growth of several bacteria but their reduced forms **52** and **53** lost their activities.[48] Additionally, the compounds possessed an antiarthritic effect by inhibiting the articular lesions without antiinflammatory properties.[50]

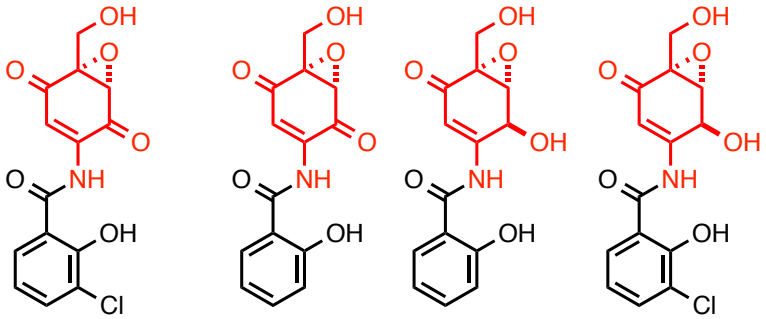

epoxyquinomicin A (**50**), B (**51**), C (**52**) and D (**53**)

[48] T. Tsuchida, M. Umekita, N. Kinoshita, H. Iinuma, H. Nakamura, K. Nakamura, H. Naganawa, T. Sawa, M. Hamada, T. Takeuchi, *J. Antibiot.* **1996**, *49*, 326–328.

[49] N. Matsumoto, T. Tsuchida, M. Umekita, N. Kinoshita, H. Iinuma, T. Sawa, M. Hamada, T. Takeuchi, *J. Antibiot.* **1997**, *50*, 900–905; N. Matsumoto, T. Tsuchida, R. Sawa, H. Iinuma, H. Nakamura, H. Naganawa, T. Sawa, T. Takeuchi, *J. Antibiot.* **1997**, *50*, 912–915.

[50] N. Matsumoto, H. Iinuma, T. Sawa, T. Takeuchi, S. Hirano, T. Yoshioka, M. Ishizuka, *J. Antibiot.* **1997**, *50*, 906–911.

Others compounds discussed previously were identified as antibacterial agents as adiposins (**25-26**), oligostatins (**36-38**), CKD-711 (**44**) and CKD-711a (**45**)

2.1.4. Antitumor Activity

Cetoniacytones A and B (**54-55**) were isolated from the insect, *Cetonia aurata,* bacterial endosymbiont. The epoxide **54** was tested against human cancer cell lines and was found to be active at a few µg/mL.[51] Interestingly the natural products epoxyquinomicins A and B (**50-51**) and not C nor D (**52-53**), which shared the same core structure as **54**, have been also reported for their cytotoxicity activity.

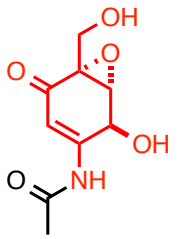

cetoniacytone A (**54**)

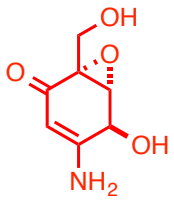

cetoniacytone B (**55**)

[51] O. Schlörke, P. Krastel, I. Müller, I. Usón, K. Dettner, A. Zeeck, *J. Antibiot.* **2002**, *55*, 635–642.

2.2. *Psychotria kirkii*, an Obligatory Symbiosis System

Psychotria kirkii (*P. kirkii*) is a flowering plant from the Rubiaceae family that lives in obligatory symbiosis with bacteria from the genus Burkholderia.[52] *Candidatus Burkholderia kirkii* (*B. kirkii*) forms nodules on the lower surface of the plant's leaves and the presence of the microorganism is essential for the development of the plant host.[53] However, it is unknown how the formation of these nodules by *B. kirkii* can account for the survival of the plant. This gap in the understanding of their symbiosis is mainly due to the impracticality of culturing the *B. kirkii* bacteria in the absence of their plant host.[54]

Analysis of the genome of uncultured *B. kirkii* revealed that there is a biochemical pathway leading to the production of a C_7N aminocyclitol compound.[55,56] This family of secondary metabolites features a wide range of biological activities. It was thus hypothesized that this unknown C_7N aminocyclitol compound might be the key molecule for the establishment of the obligate symbiosis between the bacteria and the plant. To verify this hypothesis, we decided to embark on the isolation and structure elucidation of the C_7N aminocyclitol from the symbiont of *P. kirkii*.

[52] A. Zimmermann, *Jahrb. Wiss. Bot.* **1902**, *37*, 1–11.
[53] S. Van Oevelen, R. De Wachter, P. Vandamme, E. Robbrecht, E. Prinsen, *Int. J. Syst. Evol. Microbiol.* **2004**, *54*, 2237–2239.
[54] I. M. Miller, in *Advances in Botanical Research* (Ed.: J.A. Callow), Academic Press, **1990**, pp. 163–234.
[55] A. L. Carlier, L. Eberl, *Environ. Microbiol.* **2012**, *14*, 2757–2769.
[56] A. L. Carlier, U. Omasits, C. H. Ahrens, L. Eberl, *Mol. Plant-Microbe Interact.* **2013**, *26*, 1325–1333.

2.3. Results and Discussion[57]

This project was carried out in collaboration with Dr. Aurélien Carlier from the research group of Professor Leo Eberl at the Institute of Plant Biology, University of Zürich. My contribution was the isolation and structure elucidation as well as the development methods for the detection and quantification of kirkamide (**56**) and streptol glucoside (**57**). I also devised and successfully carried out a total synthesis of kirkamide. For the preparation of synthetic kirkamide, I want to mention the help of M. Sc. Darja Kolbin, M. Sc. Ina Ontiveros Casas and B. Sc. Joel Rösslein in the course of their project during their master program. This chapter will be separated into three parts, starting with the isolation, structure elucidation, total synthesis and biological investigations of kirkamide (**56**), followed by the isolation and structure elucidation of streptol glucoside (**57**) and finally the last chapter will be dedicated to the analytical methods developed for the detection and quantification of kirkamide (**56**) and streptol glucoside (**57**).

2.3.1. Isolation of Kirkamide

It is crucial for the isolation of natural products to find a unique chemical or biological characteristic of the desired compound. Bio-guided fractionation is a method frequently used, which consists of the separation of a bioactive extract by chromatography generating fractions that are further tested in biological assays. The active fractions are further separated and the process is then repeated until a pure natural product is obtained.

The project started with the isolation of the putative C_7N aminocyclitol predicted, by genomic analysis, to be present in the *P. kirkii* leaves extract. The first isolation strategy applied was based on a bio-guided fractionation targeting the biological activities shared by most of the members of the C_7N aminocyclitol family members. Unfortunately neither a α-glucosidase inhibitor nor antibacterial or antifungal activity was observed.[19] For this reason we decided to analyze the chemical properties of the members from the C_7N aminocylitol family taking validamycin A (**10**) as an example. The ^1H NMR spectrum of this natural product displays a characteristic methylene proton around δ = 6

[57] Part of this project is currently subject of two publications and a Sinergia grant; S. Sieber, A. Carlier, M. Neuburger, G. Grabenweger, L. Eberl, K. Gademann, *Ang. Chem. Int. Ed. Engl.* **2015**, *54*, 7968–7970; M. Pinto-Carbó, S. Sieber, S. Dessein, T. Wicker, B. Verstraete, K. Gademann, L. Eberl, A. Carlier, *manuscript submitted*; Sinergia grant CRSII3_154430.

ppm (figure **4**), and this property is ideally suited to serve as a characteristic mark in ^{1}H NMR guided fractionation.[58] This isolation strategy is similar to bio-guided fractionation. The crude extract is separated in several fractions, which are analyzed by ^{1}H NMR and those possessing the specific chemical shift are further separated by chromatography methods.

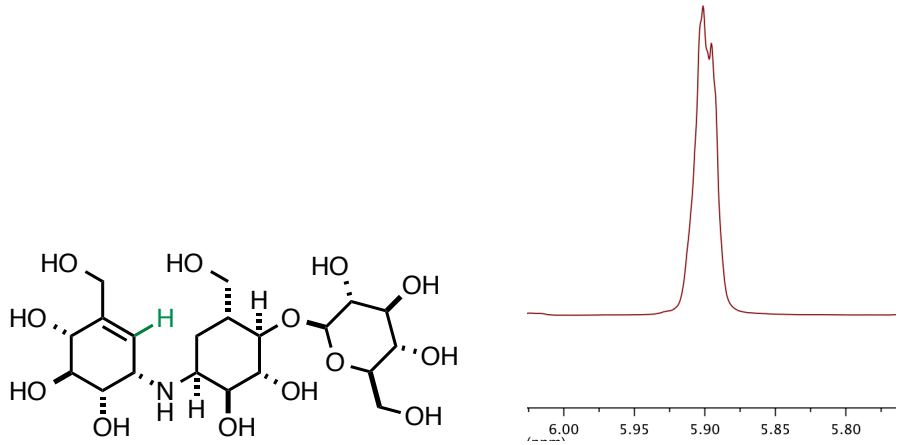

*Figure **4**: Structure of validamycin A (**10**) and characteristic ^{1}H NMR peak at 5.9.*

2.3.1.1. Methods for the Separation and Detection of Kirkamide

The high polarity and the absence of chromophore were the two main challenges that had to be addressed for the isolation of the unknown C_7N aminocylitol compound from the leaves plant extract of *P. kirkii.* To overcome these difficulties and to avoid any derivatization, reversed phase high performance liquid chromatography (RP-HPLC) was used with water and acetonitrile as eluents. A Synergi Hydro column consisting of a polar endcapped C-18 stationary phase, was chosen due to its ability to retain polar compounds while using a RP solvent system.[59] The UV detector was set at a wavelength of $\lambda = 190$ nm and mass spectrometric (MS) detection was used in negative atmospheric pressure chemical ionization (APCI) mode, as this method has been previously reported for the analysis of saccharide.[60]

[58] W. Z. Jin, K. L. Rinehart, T. Toyokuni, *J. Antibiot*. **1987**, *40*, 329–339.
[59] Z. Liu, S. Rochfort, *J. Chromatogr. B* **2013**, *912*, 8–15.
[60] G. Ricochon, C. Paris, M. Girardin, L. Muniglia, *J. Chromatogr. B* **2011**, *879*, 1529–1536.

2.3.1.2. ^{1}H NMR-Guided Fractionation of the Leaves Extract of *P. kirkii*

The crude extracts from *P. kirkii* leaves were subjected to multiple RP-HPLC separations using a semi-preparative Synergi Hydro column operating at a flow of 2 mL/min. A natural product possessing a ^{1}H NMR peak with a chemical shift at 5.86 ppm was found in a fraction. However, the separation of the desired compound was found to be difficult due to the presence of a contaminant possessing an identical rentention time. Fortunately, the contaminant was identified to be sucrose, based on the NMR comparison between the fraction and the sugar. To remove sucrose, the crude extract was treated under acidic conditions to cleave the glycosidic bond of the disaccharide. The separation of the mixture was then achieved by a combination of RP-HPLC using the Synergi Hydro column and a Cu(II)-coated preparative thin layer chromatography, which has been previously reported for the separation of saccharides.[61] With this strategy a new C_7N aminocyclitol (figure **5**), named kirkamide (**56**), was isolated from the leaves of the plant *P. kirkii*.

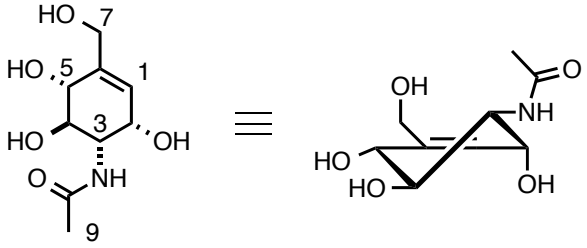

kirkamide (**56**)

*Figure **5**: Configuration and conformation of kirkamide (**56**).*

2.3.2. Structure Elucidation of Kirkamide

High resolution ESI-MS of kirkamide (**56**) displayed an exact mass of *m/z* 240.0844 Da, which supports the molecular formula $C_9H_{15}NO_5Na$ for the $[M+Na]^+$ pseudo-molecular ion. ^{1}H and ^{13}C NMR spectroscopic data (DMSO-d_6) of kirkamide (**56**) were compared with those reported for streptol (**58**),[62] which suggested a different functionality at C-2, as well as the presence of an acetyl group. This group was established as an NH-acetyl fragment based on ^{1}H ^{13}C HMBC correlations between the

[61] O. Hadžija, B. Špoljar, L. Sesartić, *Fresenius' J. Anal. Chem.* **1994**, *348*, 782–782.; R. Bhushan, S. Kaur, *Biomed. Chromatogr.* **1997**, *11*, 59–60.
[62] P. Sedmera, P. Halada, S. Pospíšil, *Magn. Reson. Chem.* **2009**, *47*, 519–522.

quaternary carbonyl C-8 with the NH and H-9 proton signals. The assignment of the carbocyclic core structure was then deduced based on ^{1}H ^{13}C HMBC correlations between H-5, H-7a and H-7b with C-6 as well as between H-5 and C-1. ^{1}H ^{1}H COSY correlations between H-1 and H-2, H-2 and H-3, H-3 and H-4, NH and H-3, H-4 and H-5 and H-5 and H-1 further supported this structural proposition. The relative configuration was assigned comparing the $^{3}J_{H\text{-}H}$ coupling constants between H-2 and H-3, H-3 and H-4, and H-4 and H-5 in DMSO-*d*6 (table **2**) with those reported for streptol (**58**) in D_2O.[62] To exclude the influence of the solvent, the recorded NMR spectroscopic data of kirkamide were compared to those of valienamine (**21**) in DMSO-d_6, which showed that theses two compounds feature the same conformation with H-2 in equatorial position and H-3, H-4 and H-5 in axial position. Finally, single crystal X-ray structure analysis (Figure **6**) unambiguously established the constitution and configuration of kirkamide (**56**).

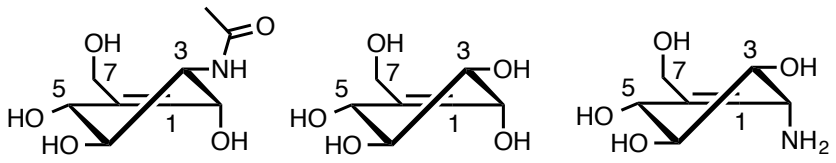

Table **2.** NMR spectroscopic data (500 MHz, DMSO-d_6) of kirkamide (**56**).

C/N no.	δ_C, type	δ_H ($^{3}J_{H\text{-}H}$ in Hz)	HMBC[a]
1	121.5, CH	5.63, dq[b] (4.8, 1.5)	3, 5, 7
2	64.3, CH	3.99, m	
3	53.1, CH	3.63, ddd (10.9, 8.1, 3.9)	
NH		7.36, d (8.1)	8
4	70.4, CH	3.56, dd (10.9, 7.1)	3, 5
5	72.9, CH	3.79, d (7.1)	1, 4, 6
6	142.5, C		
7a	60.8, CH_2	4.01, d (14.8)	1, 6
7b		3.95 d (14.8)	1, 6
8	169.2, C		
9	23.0, CH_3	1.85, s	8

[a] HMBC correlations are given from proton(s) stated to the indicated carbon atom.

[b] Apparent splitting pattern.

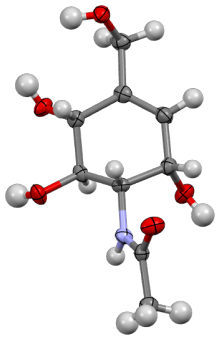

*Figure **6**: Single crystal X-ray analysis of kirkamide (**56**). Cambridge Crystallographic Data Centre accession number: CCDC 1054238.*

2.3.3. Enantioselective Total Synthesis of Kirkamide

A total synthesis was developed using a cheap and readily available starting material in order to obtain larger quantities of the compound for biological tests regarding its role in the symbiosis with *P. kirkii*.

2.3.3.1. Overview of Existing Syntheses of Valienamine

During the past decades, many studies have been directed towards the synthesis of C_7N aminocyclitol compounds particularly valienamine (**21**). Paulsen and coworkers developed the first enantioselective synthesis of this natural product in 1972 using quebrachitol (**59**) as the initial reagent (scheme **1**).[63] The synthesis started with the installation of the protective groups followed by an oxidation with ruthenium tetraoxide/sodium periodate affording the ketone intermediate **60**. Using sequentially Corey-Chaykovsky and basic conditions furnished the diol **61**, which was activated and its protection groups exchanged to obtain the mono or di mesylated **62** and **63**. With both compounds **62** and **63,** the formation of an epoxide followed by its elimination afforded the cyclohexene **64**. The insertion of the amine was achieved *via* azide formation and the final deprotections delivered valienamine (**21**). Many synthetic strategies have been focus on the variation of the starting material with different key step for the ring formation; e.g an alkene or enyne ring-closing metathesis or an aldol reaction with amino acids or carbohydrate derivatives,[64,65,66] or a Diels-Alder cycloaddition with achiral substrates.[67] Furthermore quininic acid and inositol were investigated as chiral pool.[68]

---

[63] H. Paulsen, F. R. Heiker, *Angew. Chem., Int. Ed. Engl.* **1980**, *19*, 904–905.

[64] Selected examples: R. R. Schmidt, A. Köhn, *Angew. Chem. Int. Ed.* **1987**, *26*, 482–483; P. Kapferer, F. Sarabia, A. Vasella, *Helv. Chim. Acta* **1999**, *82*, 645–656; K. Tatsuta, H. Mukai, M. Takahashi, *J. Antibiot.* **2000**, *53*, 430–435; I. Cumpstey, *Tetrahedron Lett.* **2005**, *46*, 6257–6259; Y.-K. Chang, B.-Y. Lee, D. J. Kim, G. S. Lee, H. B. Jeon, K. S. Kim, *J. Org. Chem.* **2005**, *70*, 3299–3302; I. Cumpstey, S. Gehrke, S. Erfan, R. Cribiu, *Carbohydr. Res.* **2008**, *343*, 1675–1692; T. K. M. Shing, H. M. Cheng, *J. Org. Chem.* **2010**, *75*, 3522–3525; Q. R. Li, S. I. Kim, S. J. Park, H. R. Yang, A. R. Baek, I. S. Kim, Y. H. Jung, *Tetrahedron* **2013**, *69*, 10384–10390.

[65] P. Radha Krishna, P. Srinivas Reddy, *Synlett* **2009**, 0209–0212; B. Zhou, Z. Luo, S. Lin, Y. Li, *Synlett* **2012**, *23*, 913–916.

[66] Y.-K. Chang, H. J. Lo, T. H. Yan, *Org. Lett.* **2009**, *11*, 4278–4281; H. J. Lo, C. Y. Chen, W. L. Zheng, S. M. Yeh, T. H. Yan, *Eur. J. Org. Chem.* **2012**, 2780–2785.

[67] B. M. Trost, L. S. Chupak, T. Lübbers, *J. Am. Chem. Soc.* **1998**, *120*, 1732–1740.

[68] Selected examples: Tony K M Shing, A. Tin Y Li, S. H. L. Kok, *J. Org. Chem.* **1999**, *64*, 1941–1946; S. Mondal, A. Prathap, K. M. Sureshan, *J. Org. Chem.* **2013**, *78*, 7690–7700; S. Ogawa, N. Chida, T. Suami, *J. Org. Chem.* **1983**, *48*, 1203–1207.

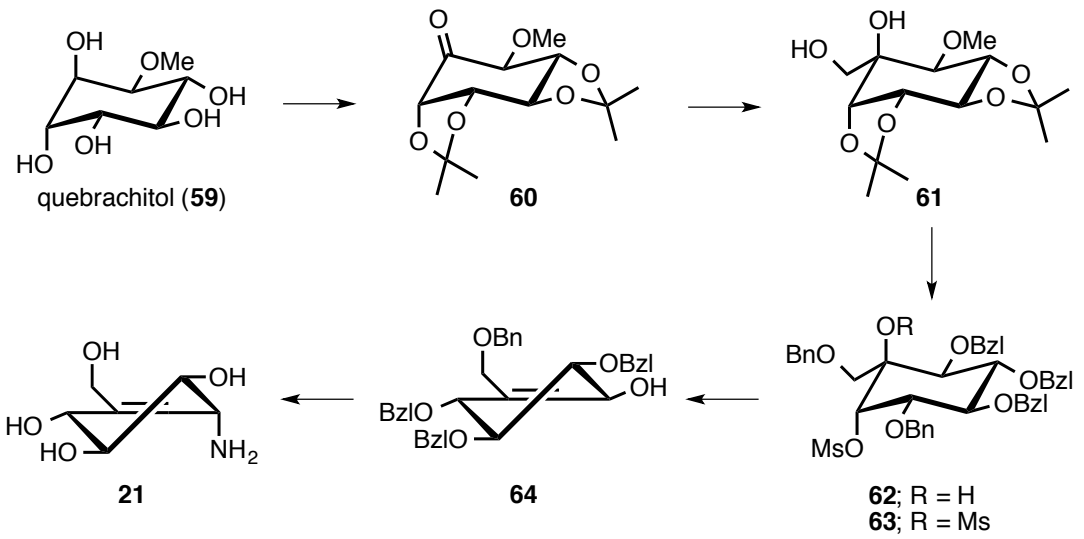

*Scheme **1**: First enantioselective synthesis of valienamine (**21**).*

2.3.3.2. Retrosynthetic Analysis of Kirkamide

Bearing the results of other aminocyclitol syntheses in mind (2.3.3.1), a D-glucose derivative appeared to be a good starting material due to its availability and low cost. For the retrosynthetic analysis of kirkamide (**56**) (scheme **3**), we were inspired by Scaffidi's work on β-*N*-acetylglucosaminidase inhibitors. Starting from *N*-acetyl-D-glucosamine (**65**), Scaffidi's synthetic route to cyclohexanone **66** features a Ferrier carbocyclization as key step (scheme **2**).[69,70]

[69] A. Scaffidi, K. A. Stubbs, R. J. Dennis, E. J. Taylor, G. J. Davies, D. J. Vocadlo, R. V. Stick, *Org. Biomol. Chem.* **2007**, *5*, 3013–3019.
[70] A. Scaffidi, K. A. Stubbs, D. J. Vocadlo, R. V. Stick, *Carbohydr. Res.* **2008**, *343*, 2744–2753.

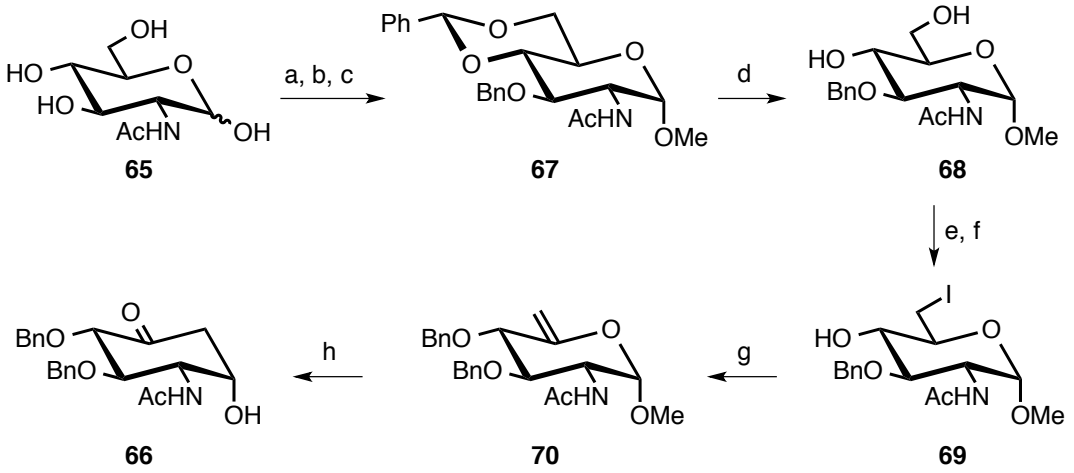

Scheme **2**: Synthetic strategy of Scaffidi and coworkers affording the cyclohexanone **66** a) HCl, MeOH; b) $PhCH(OMe)_2$, CSA, DMF; c) BnBr, NaH, THF; d) aq. AcOH soln. (80%); e) TsCl, Et_3N, CH_2Cl_2; f) NaI, DMF; g) NaH, BnBr, DMF; h) $HgSO_4$, dioxane: aq. H_2SO_4 (5 mM) 2:1.

Cyclohexanone **72** was chosen as a key intermediate for the synthesis of kirkamide (**56**). This compound could be transformed to the enol triflate **71** using Comins' reagent in the presence of a hindered base. Kirkamide (**56**) could then by prepared *via* a Stille cross-coupling followed by final deprotections. This synthetic pathway was chosen for the availability of the starting material and its flexibility.

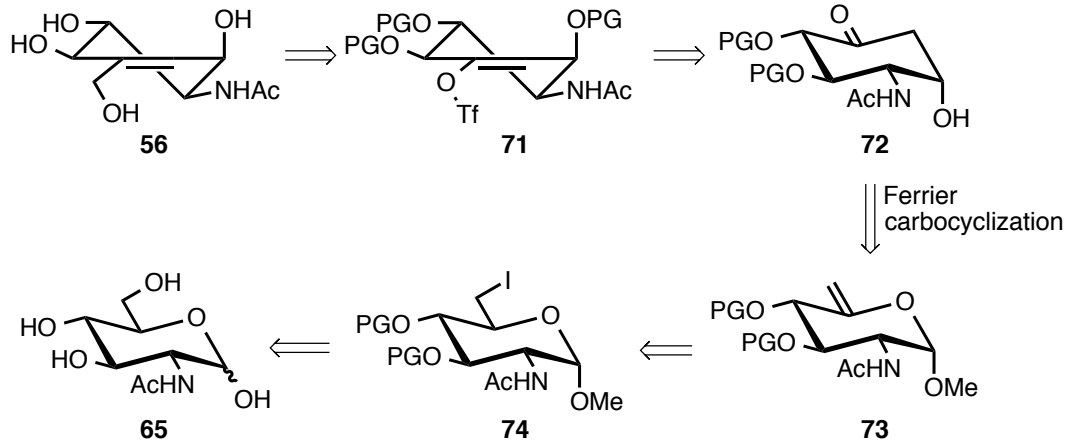

*Scheme **3**: Retrosynthetic analysis of kirkamide (**56**).*

2.3.3.3. Towards Enol Ether, Strategy I

The first strategy (scheme **4**), for our total synthesis of the natural product kirkamide (**56**), is based on the synthesis of valienamine (**21**) by Scaffidi and coworkers.[69] We started with methyl ether protection of the *N*-acetyl-D-glucosamine's (**65**) anomeric position using an acidic resin.[71] Next, the hydroxyl groups at C-4 and C-6 were jointly protected by reaction with (dimethoxymethyl)benzene to give the corresponding benzylidene.[72,73] After installation of a benzyl protecting group at the C-3 hydroxyl group, the benzylidene protecting group was selectively cleaved by treating the fully protected pyranose **67** with acetic acid. The free hydroxyl group at C-6 was activated by tosylation to form a good leaving group. Nucleophilic substitution with sodium iodide then gave compound **69** with 29% over six steps from **65** to **69**. After the first column chromatography required in this route, elimination of the iodide and protection of the free OH group at C-4 were achieved in one pot by treating **69** with benzyl bromide and sodium hydride. The desired enol ether key intermediate **70** was obtained from this step in 77% yield. This strategy proved to be robust, and all steps were suitable for multigram scale preparation.

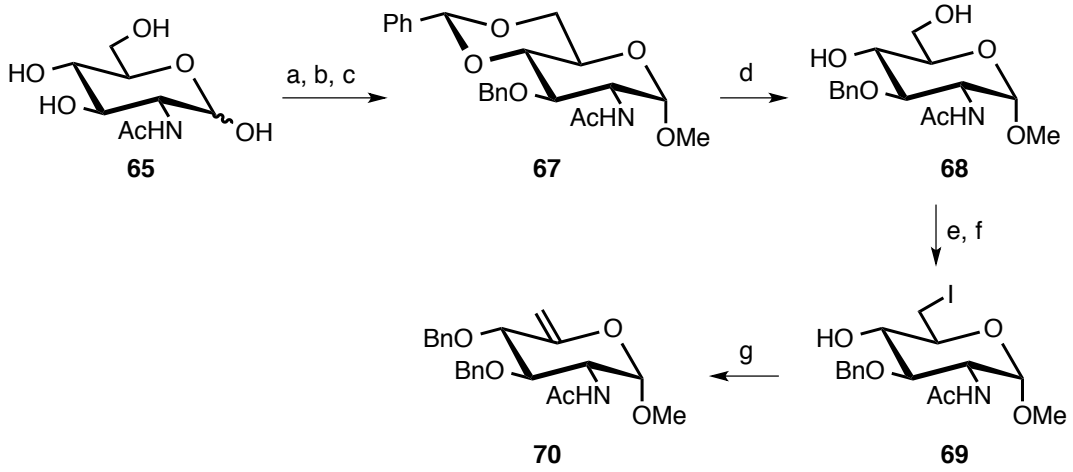

Scheme **4**: a) Amberlite® IR-120 (H^+ form), MeOH reflux, 16 h; b) $PhCH(OMe)_2$, *p*TSOH, DMF; c) BnBr, BaO, $Ba(OH)_2$, DMF, 2 h 40, RT; d) aq. AcOH soln. (aq., 80%), 70 °C, 1 h; e) TsCl, Et_3N, CH_2Cl_2, 0 °C to RT, 3 h 20; f) NaI, DMF, 100 °C, 3 h, 29% over 6 steps; g) NaH, BnBr, DMF, RT, 1 h, 77%.

[71] F. Gao, X. Yan, T. Shakya, O. M. Baettig, S. Ait-Mohand-Brunet, A. M. Berghuis, G. D. Wright, K. Auclair, *J. Med. Chem.* **2006**, *49*, 5273–5281.
[72] D. P. G. Emmerson, W. P. Hems, B. G. Davis, *Tetrahedron: Asymmetry* **2005**, *16*, 213–221.
[73] E. Petrakova, U. Spohr, R. U. Lemieux, *Can. J. Chem.* **1992**, *70*, 233–240.

2.3.3.4. Towards Enol Ether, Strategy II

In order to develop a shorter synthetic pathway another strategy was developed to obtain the key intermediate **70** in large amount (scheme **5**). The known methyl-*N*-acetyl-D-glucosamine (**75**) was subject to a Garegg-Samuelsson reaction using Ph_3P, I_2 and imidazole and we were pleased to report the formation of the iodide **76** in good yield.[74] However, due to the high polarity of the product **76** separation by column chromatography was found to be challenging on a large scale (20 g). Therefore, the crude product mixture, containing iodide **76** and imidazole, was used directly for the next synthetic step without any purification. Various methods were tested for the direct introduction of the benzyl protecting groups, but nucleophilic attack of the hydroxyl group on C-3 on C-6 forming bicycle **77** was always observed as a side reaction. Consequently, the two free hydroxyl groups in diol **76** were protected by acetylation. Then, AgF-mediated elimination was successfully executed.[75] Finally the protection groups were exchanged to obtain the desired benzyl-protected enol ether **70** in five steps, on a multigram scale and only requiring two purifications by column chromatography.[75]

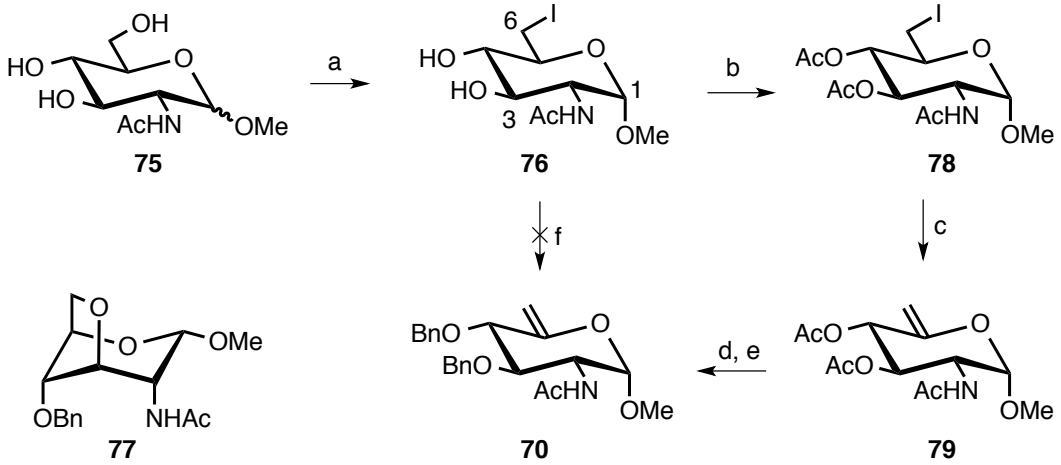

Scheme **5**: a) Ph_3P, imidazole, I_2, THF, reflux, 15 min; b) Ac_2O, pyridine, RT, 24 h; c) AgF, pyridine, RT, 48 h, exclusion of light, 50% over 3 steps; d) $NH_{3(gas)}$, MeOH, RT, 3 h; e) NaH, BnBr, DMF, 0°C, 12 h, 36% over 2 steps.

[74] P. J. Garegg, B. Samuelsson, *J. Chem. Soc., Chem. Commun.* **1979**, 978–980.
[75] F. Chretien, R. Wolf, Y. Chapleur, *Nat. Prod. Lett.* **1993**, *2*, 69–75.

2.3.3.5. Ferrier Carbocylization

The Ferrier carbocyclization was developed by Ferrier in 1979 using mercury chloride to transform an enol ether in a cyclohexanone.[76] Following this result other transition metals, for example palladium or titanium salts were found to catalyze this reaction.[77,78] As for the reaction conditions, the use of a microwave reactor was shown to improve the yield and diastereoselectivity of the reaction (figure **7**, line 2).[79] Scaffidi and coworkers reported the use of $HgSO_4$ as catalyst under acidic conditions to give the desired cyclohexanone **66** (figure **7**, line 1).[70] To optimize the reaction conditions, we tested palladium chloride as a less toxic catalyst, but unfortunately the yield dropped substantially. However, by use of microwave irradiation the reaction time was lowered and the yield of the cyclohexanone **66** improved to 74 % (figure **7**, line 3)

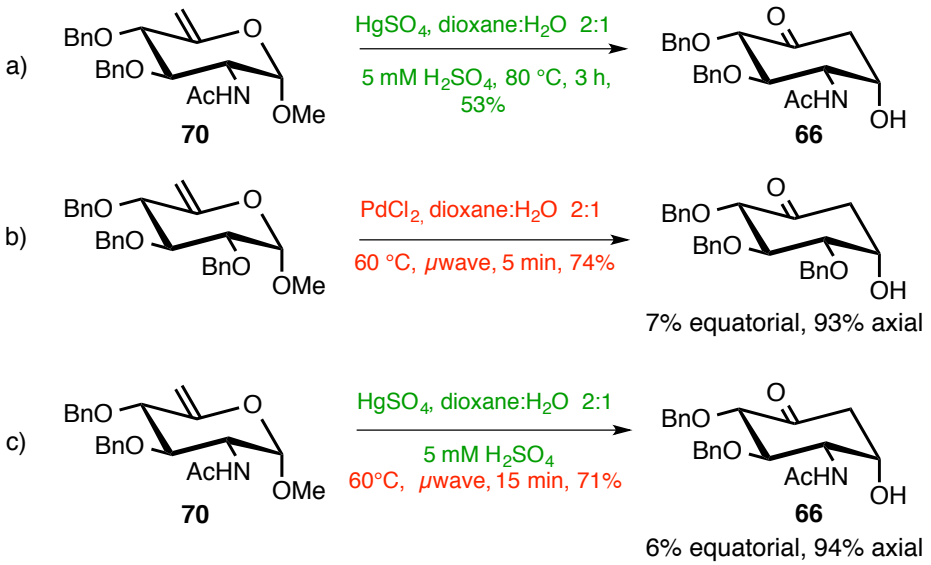

*Figure 7:Ferrier carbocylization reaction conditions: a) reported by Scaffidi and coworkers,[70] b) reported by Ko and coworkers[79] and c) used for the synthesis of kirkamide **56**.*

[76] R. J. Ferrier, *J. Chem. Soc., Perkin Trans. 1* **1979**, 1455–1458.
[77] S. Adam, *Tetrahedron Lett.* **1988**, *29*, 6589–6592.
[78] M. Sollogoub, J.-M. Mallet, P. Sinaÿ, *Tetrahedron Lett.* **1998**, *39*, 3471–3472.
[79] K.-S. Ko, C. J. Zea, N. L. Pohl, *J. Am. Chem. Soc.* **2004**, *126*, 13188–13189.

2.3.3.6. Final Steps of Kirkamide Synthesis

Cyclohexanone **66** obtained by Ferrier carbocyclization (1.1.3.5) was directly protected with TBS[80] to prevent the elimination of the free hydroxyl group. A single crystal X-ray structure of the protected cyclohexanone **80** confirmed the antiperiplanar relation between the oxygen from C-2 and the axial hydrogen of C-1 (Figure **8**).

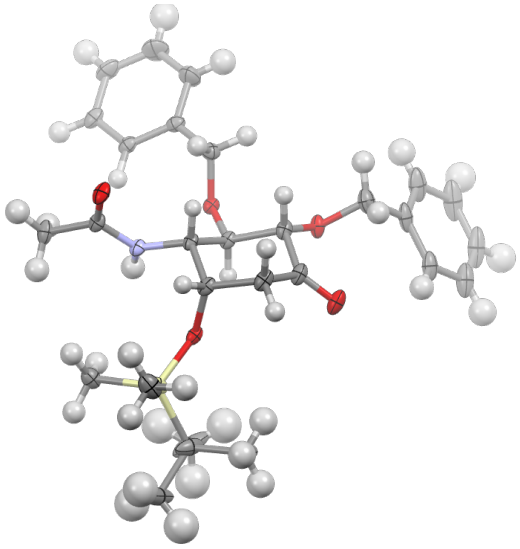

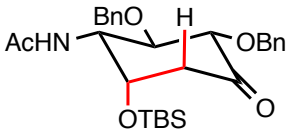

80

*Figure **8**: Single crystal X-ray structure of the protected cyclohexanone **80** and its representation with the antiperiplanar relation between the TBS protective group and the hydrogen at C-2 highlighted in red.*

The reaction conditions had to be carefully controlled for the formation of the enol triflate **81**. It was mandatory to premix the starting material cyclohexanone **80** with Comins' reagent before the base (NaHMDS) was slowly added at –78 °C.[81] When the reaction was executed on a gram scale, the temperature was controlled with a cryostat and the solution of NaHMDS was added using a syringe pump. Furthermore, triethyl amine was required as an additive to the eluent for the purification of product **81** by column chromatography in order to prevent its degradation.

A Stille cross-coupling gave primary alcohol **82**. This strategy was inspired by the work of Li and coworkers, who used similar conditions on an enol triflate substrate for

[80] M. Nevalainen, A. M. P. Koskinen, *J. Org. Chem.* **2002**, *67*, 1554–1560.
[81] P. Jakubec, A. Hawkins, W. Felzmann, D. J. Dixon, *J. Am. Chem. Soc.* **2012**, *134*, 17482–17485.

the synthesis of (±)-minfiensine.[82] Having the core structure completed, TBS was smoothly removed. For the benzyl deprotection, various reagents were tested: standard literature procedures using Pd/C with H_2 or HCOOH,[83,84] EtSH[85] or $FeCl_3$[69] only led to decomposition of the starting material. Finally, we successfully achieved the total synthesis of kirkamide (**56**) by applying Birch conditions.[86]

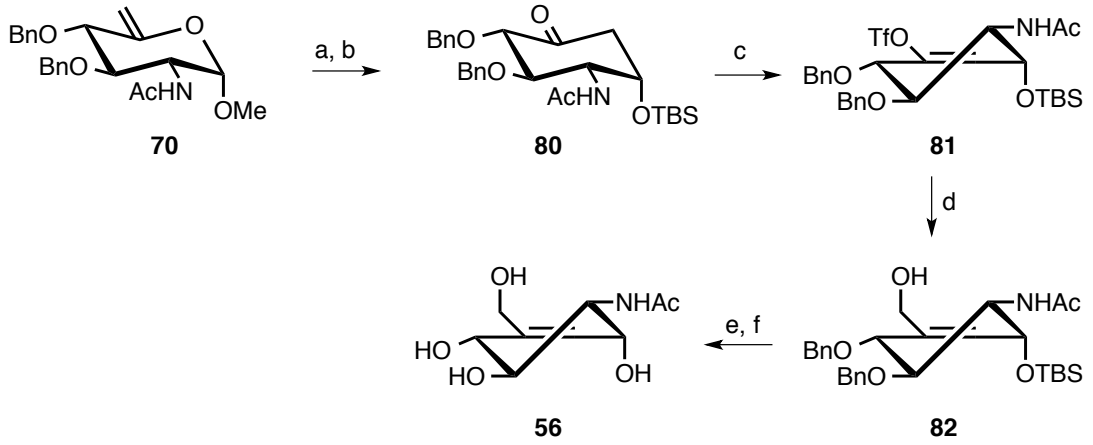

Scheme **6**: a) $HgSO_4$ dioxane: aq. H_2SO_4 (aq., 5 mM) 2:1, µw, 60 °C, 15 min; b) TBSOTf, 2,6-lutidine, THF, 0°C, 12 h, 63% over 2 steps; c) Comins' reagent, NaHMDS, THF, −78°C, 5 min, 62%; d) *n*-Bu_3SnCH_2OH, $Pd(PPh_3)_4$, LiCl, dioxane, µw, 105°C, 1 h, 85%; e) TBAF, THF, RT, 3 h, 98%; f) $Na/NH_{3(liq)}$, THF, −78 °C, 30 min, 59 %.

[82] G. Li, A. Padwa, *Org. Lett.* **2011**, *13*, 3767–3769.
[83] J. Chen, P.-Q. Huang, Y. Queneau, *J. Org. Chem.* **2009**, *74*, 7457–7463.
[84] Y. Oikawa, T. Tanaka, K. Horita, O. Yonemitsu, *Tetrahedron Lett.* **1984**, *25*, 5397–5400.
[85] Z. Liu, H.-S. Byun, R. Bittman, *J. Org. Chem.* **2011**, *76*, 8588–8598.
[86] A. J. Birch, *J. Chem. Soc.* **1944**, 430–436; X. Lu, G. Arthur, R. Bittman, *Org. Lett.* **2005**, *7*, 1645–1648.

2.3.4. Biological Activity of Kirkamide

The biological activity of kirkamide (**56**) was investigated in order to understand its role in the relation between the symbiont *B. kirkii* and the plant host *P. kirkii*. A protective role of the C_7N aminocyclitol was postulated by Aurelien Carlier *et al.* to explain the unique obligatory character of the symbiosis.[55,56] Since the natural product kirkamide (**56**) was produced by total synthesis, a large amountof compound was available to perform various activity assays (antibacterial, antifungal, glucosidase inhibitor, *N*-acetyl-glucosaminidase inhibitor, insecticidal and cytotoxic). In section the cytotoxicity test, conducted by Dr. Aurélien Carlier, and the insecticide test, conducted by Dr. Giselher Grabenweger (Agroscope, Switzerland) are discussed.

2.3.4.1. Brine Shrimp Toxicity Assay

The cytotoxicity of kirkamide (**56**) was evaluated using a brine shrimp assay. This assay has been widely used for the discovery of novel bioactive compounds, especially those possessing an antitumor activity.[87] A correlation was found between the ED_{50} values measured on the human epidermoid carcinoma cytotoxicity test with the LC_{50} values of the brine shrimp assay: the ED_{50} values were approximately ten times less than the IC_{50} values.[87] The activity of kirkamide (**56**) was determined and a LC_{50} value of 850 ng/mL with a standard deviation of ± 310 ng/mL was found. This result implies that kirkamide (**56**) possesses antitumor activity. In the light of the structural similarities of kirkamide and the anticancer agent cetoniacytone A (**54**), this result appears plausible.[51]

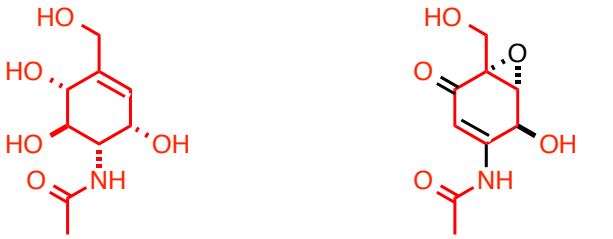

kirkamide (**56**) cetoniacytone A (**54**)

*Figure **9**: Structure of kirkamide (**56**) and cetoniacytone A (**54**). Common structural features with kirkamide (**56**) are highlighted in red.*

[87] J. L. McLaughlin, L. L. Rogers, J. E. Anderson, *Drug Inf. J.* **1998**, *32*, 513–524.

2.3.4.2. Insecticidal Activity of Kirkamide

The insecticidal activity of kirkamide (**56**) was determined on the pollen beetle *Meligethes aeneus*. Controlling the population of this insect is of importance due to the damage that they afflict to the structure of the Danish oilseed rape flowers.[88]

The mortality of the pollen beetle fed with 0.3% w/w of kirkamide (**56**) were found to be up to 90% after 14 days. Interestingly, validoxylamine A (**18**) a member of the C_7N aminocylitol family, was found to possess an insecticidal activity by inhibiting the degradation of trehalose.[89] A similar or related mechanism might be operative for kirkamide (**56**). Furthermore, structural similarities of the natural product kirkamide (**56**) with *N*-acetyl-D-glucosamine (**65**), which is the main component of the insect exosqueleton, also make kirkamide's insecticidal properties appear plausible.

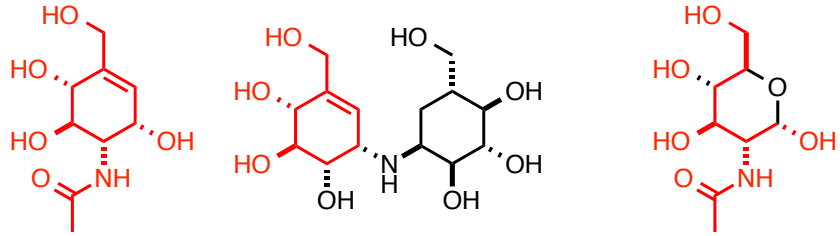

kirkamide (**56**) validoxylamine A (**18**) *N*-acetyl-D-glucosamine (**65**)

*Figure **10**: Structures of kirkamide (**56**), validoxylamine A (**18**) and N-acetyl-D-glucosamine (**65**). Common structural features with kirkamide (**56**) are highlighted in red.*

[88] L. M. Hansen, *Pest Manage. Sci.* **2003**, *59*, 1057–1059.
[89] Y. Kono, M. Takahashi, K. Matsushita, M. Nishina, Y. Kameda, E. Hori, *J. Insect Physiol.* **1994**, *40*, 455–461.

2.3.5. Streptol Glucoside

2.3.5.1. Isolation of Streptol Glucoside

During a biological activity screening of the nodulated plant *P. kirkii* leaves extract, we found a growth inhibition effect on lettuce seeds. We used this property to perform a bioassay-guided fractionation. The targeted compound exhibited similar chemical properties as kirkamide (**56**), and for this reason a Synergi Hydro HPLC column was chosen and the UV detector was set up at a wavelength of 190 nm. The separation of 88.6 mg of the crude extract from nodulated plants, which was already purified by an aminopropyl solid phase extraction (SPE), gave eight fractions and the biological activity of each of them was tested in the lettuce seed growth inhibition test. The fraction designated P_II_3 was shown to be the most biologically active in this assay, and was chosen for further separation (image **1**).

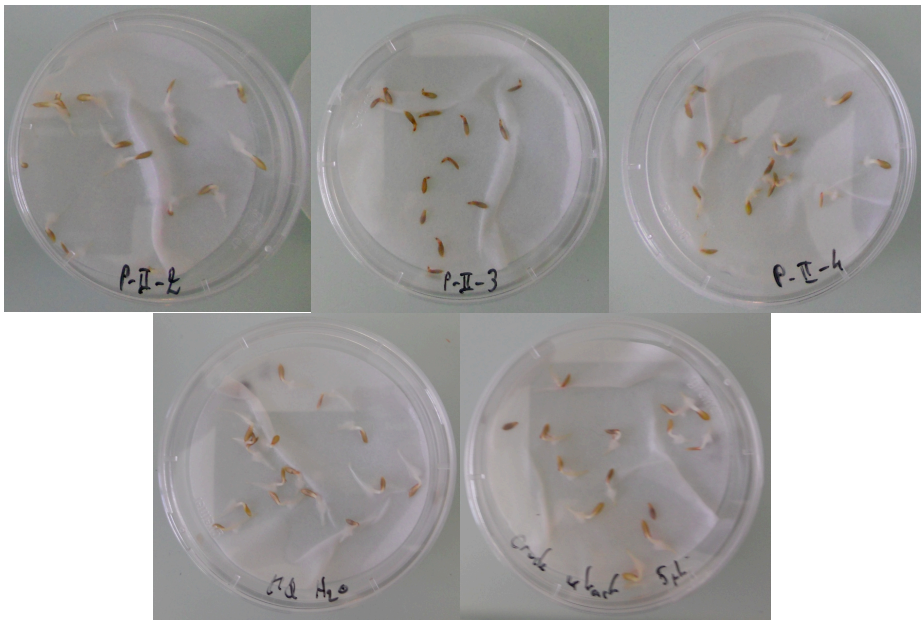

*Image **1**: Lettuce seeds incubated with HPLC fractions (P_II_2, P_II_3, P_II_4, control and crude extract) after one day.*

Fraction P_II_3_3 was then selected due to its high activity and by ^{1}H NMR analysis, a major component with the spectral characteristics of a cyclohexene structure was detected. Due to the small amount of compound obtained, we decided to repeat the isolation procedure and we purified the desired product in the fraction P_III_3_3_3. After structure elucidation (see below) we found that the isolated natural product was similar to streptol (**58**) and we chose to name the new compound streptol glucoside (**57**). Interestingly, we found also that a similar natural product, named A-79197-2 (**83**), was isolated from bacteria living on the leaves of the plant *Cucubalus sp*.[90]

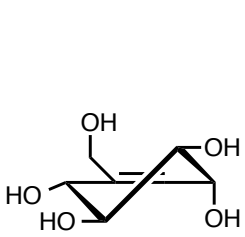

streptol (**58**)

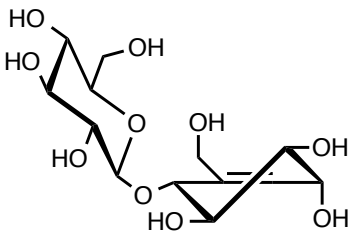

streptol glucoside (**57**)

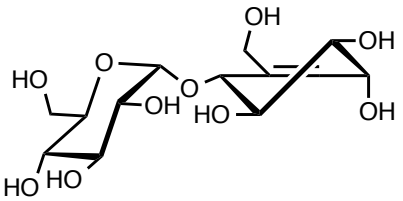

A-79197-2 (**83**)

[90] M. Kizuka, R. Enokita, K. Shibata, Y. Okamoto, Y. Inoue, T. Okazaki, *Actinomycetologica* **2002**, *16*, 14–16.

2.3.5.2. Structure Elucidation of Streptol Glucoside

The high resolution ESI-MS spectrum of streptol glucoside (**57**) in negative mode displayed an exact mass of *m/z* 337.1144 Da, which supports the molecular formula $C_{13}H_{21}O_{10}^-$ for the $[M–H]^-$ pseudo-molecular ion. ^1H and ^{13}C NMR spectroscopic data in DMSO-d_6 were used for the core structure characterization, and ^1H NMR spectroscopic data in D_2O were compared with those reported for streptol (**58**) in D_2O[62] to assign the relative configuration (table **3**).

The assignment of the carbocyclic core structure of the cyclohexene part was established using the ^1H ^{13}C HMBC correlations between H-2, H-5, H-7a and H-7b with C-6 and ^1H ^1H COSY relations between H-1 and H-2, H-2 and H-3, H-3 and H-4 and H-4 and H-5. Applying the same method, the carbon skeleton of the pyranoside was assigned based on ^1H ^1H COSY correlations between H-1' and H-2', H-2' and H-3', H-3' and H-4', H-4' and H-5', and H-5' and H-6'. Attachment of the pyranoside at position C-5 was confirmed by the observation of a ^1H ^{13}C HMBC correlation peak between H-1' and C-5. The relative configuration of the cyclohexene was assigned by comparing the *J*-coupling constants with those reported for streptol (**58**) in D_2O showing that both compounds possess H-2 is in the equatorial position, and H-3, H-4 and H-5 in the axial position. For the glucoside, the values of the *J*-coupling constants of the multiplets found in the region between 8.0 and 10.0 ppm for the couplings between H-1', H-2', H-3', H-4' and H-5' were characteristic for protons in axial-axial relations (Karplus curve).[91] Furthermore, the ^1H NMR chemical shifts of glucose in disaccharides, linked by an α– or β–glycosidic bond (table **4**), were compared with those of streptol glucoside (**57)** and confirmed the attachment of glucose by a β-glycosidic bond.[92]

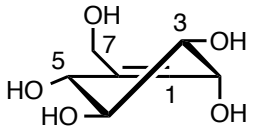

streptol (**58**)

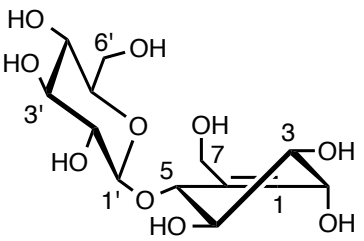

streptol glucoside (**57**)

[91] M. U. Roslund, P. Tähtinen, M. Niemitz, R. Sjöholm, *Carbohydr. Res.* **2008**, *343*, 101–112.
[92] P. E. Jansson, L. Kenne, I. Kolare, *Carbohydr. Res.* **1994**, *257*, 163–174.

Table **3**. NMR spectroscopic data (D_2O, 399.87 MHz for ^1H NMR and 100.55 MHz for ^{13}C NMR) of streptol (**58**).[62]

C no.	δ_H ($^3J_{H-H}$ in Hz)
1	5.67, dddd (5.5, 1.7, 1.6, 1.5)
2	4.10, ddd (5.5, 4.2, 0.6)
3	3.40, dd (10.7, 4.2)
4	3.52, dd (10.7, 7.8)
5	3.90, dddd (7.8, 1.7, 1.5, 0.8)
6	
7a	4.04, dddd (14.2, 1.5, 1.5, 0.6)
7b	4.00, ddd (14.2, 0.8, 0.7)

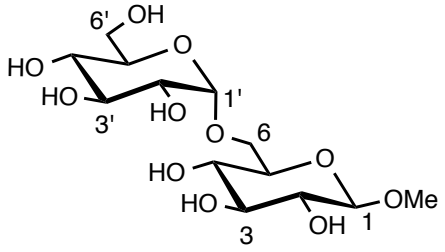

α-D-Glc-(1→6)-β-D-GlcOMe (**84**)

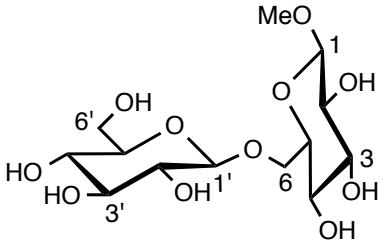

β-D-Glc-(1→6)-β-D-GlcOMe (**85**)

Table **4**. ^1H NMR spectroscopic data (D_2O, 400 MHz, in ppm) comparison of glycoside attached in α (**84**) or β (**85**) position with the glycoside of streptol glucoside (**57**).[92]

C no.	**α-D-Glc-(1→6)-β-D-GlcOMe**	**β-D-Glc-(1→6)-β-D-GlcOMe**	***streptol glucoside***
1'	4.96	4.52	4.63
2'	3.57	3.34	3.33
3'	3.73	3.51	3.51
4'	3.44	3.41	3.41
5'	3.73	3.46	3.52
6'a	3.76	3.74	3.72
6'b	3.86	3.92	3.91

Table **5**. NMR spectroscopic data (D_2O, 500 MHz for ^1H NMR) of streptol glucoside (**57**).

C no.	δ_H ($^3J_{H-H}$ in Hz)	COSY	NOESY
1	5.92, dd (5.4, 1.1)	2	2, 3, 7b
2	4.27, t (4.8)	1, 3	1, 3,
3	3.64, dd (10.5, 4.2)	2, 4	2, 4
4	3.89, d (10.7, 7.2)	3, 5	3, 5, 1’
5	4.26, d (8.3)	4	4, 1’
6			
7a	4.29, dd (13.0, 0.8)	7b	7b, 1’
7b	4.18, d (13.9)	7a	7a, 1’
1’	4.63, d (8.0)	2’	4, 5, 7, 2’, 3’, 4’
2’	3.33 dd (9.4, 8.0)	1’, 3’	1’, 3’, 4’
3’	3.51, t (9.3)	2’, 4’	1’, 2’
4’	3.41, t (9.4)	3’, 5’	1’, 2’, 6’a, 6’b
5’	3.52, ddd (9.9, 6.1, 2.3)	6’	6’a, 6’b
6’a	3.72, dd (12.4, 6.2)	5’, 6’b	4’, 6’b
6’b	3.91, dd (12.6, 2.2)	6’a	6’b, 5’

Table **6**. NMR spectroscopic data (DMSO-d_6, 500 MHz for ^{1}H NMR and 126 MHz for ^{13}C NMR) of streptol glucoside (**57**).

C no.	**δ_C, type**	**δ_H ($^3J_{H-H}$ in Hz)**	**COSY**	**HMBC[a]**
1	123.1, CH	5.69, d (5.3)	2, 5, 7a, 7b	3, 5, 7
2	65.5, CH	3.98, t (4.6)	1, 3	1, 3, 4, 6
3	70.7, CH	3.26, dd (10.1, 4.0)	2, 4	4
4	71.1, CH	3.68, d (10.1,7.0)	3, 5	3, 5
5	84.3, CH	3.88, d (6.9)	1, 4, 7a	1, 4, 6, 4’
6	140.6, C			
7a	61.2, CH_2	4.07, d (14.4)	7b	1, 6
7b		4.02, d (14.3)	1, 7a	1, 6
1’	104.2, CH	4.30, d (7.9)	2’	5
2’	73.6, CH	3.03 t (8.6)	1’, 3’	1’, 3’
3’	76.6, CH	3.18, t (9.5)	2’, 4’	4’
4’	70.2, CH	3.04, t (9.6)	3’, 5’	3’, 5’, 6’
5’	76.9, CH	3.21, ddd (9.2, 7.5, 1.8)	6’	
6’a	61.2, CH_2	3.72, dd (11.2, 1.4)	5’, 6’b	
6’b		3.40, dd (11.5, 7.1)	5’, 6’a	5’

[a] HMBC correlations are given from proton(s) stated to the indicated carbon atom.

2.4. Detection and Quantification of Kirkamide and Streptol Glucoside

2.4.1. Derivatization and Detection by GC-MS

The derivatization and GC-MS detection procedure was similar to a reported protocol with modifications regarding the use of *N*-methyl-*N*-(trimethylsilyl)trifluoroacetamide (MSTFA) as derivatization agent.[93,94] After derivatization, the sample was analyzed by GC-MS and two peaks possessing a retention time of 27.38 min and 27.73 min were detected. The first peak displayed a mass of 505 Da corresponding to kirkamide modified with four TMS groups, and fragmentation ions of 490 Da and 415 Da (figure **12**). The second compound displayed a mass of 577 Da corresponding to kirkamide modified with five TMS units (figure **11**) and a fragment observed at 562 Da (figure **13**).

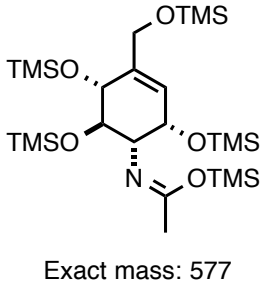

*Figure **11**: Proposed structure for the compound detected at 27.73 min.*

The masses of the two compounds with their specific degradation patterns were used as markers for the detection of kirkamide (**56**). In the extracts from the nodulated plants *Psychotria humilis*, *Psychotria verschuerenii, Psychotria punctata (P. punctata), Psychotria kirkii* and *Psychotria pumila*, at least one of the two compounds were successfully identified, corroborating the hypothesis of the production of kirkamide (**56**) by the bacteria living in obligate symbiosis with these plants.

[93] X. Wu, P. M. Flatt, H. Xu, T. Mahmud, *ChemBioChem* **2009**, *10*, 304–314.
[94] R. J. Molyneux, D. R. Gardner, L. F. James, S. M. Colegate, *J. Chromatogr. A* **2002**, *967*, 57–74.

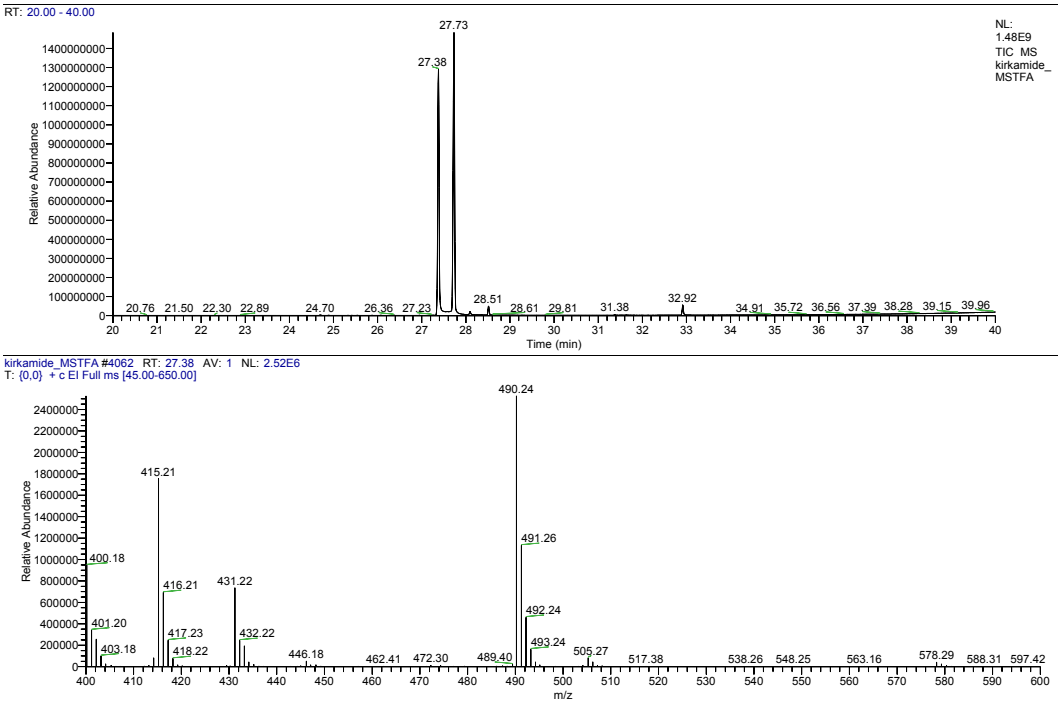

*Figure **12**: GC-MS chromatogram of kirkamide (**56**) after derivatization (top) and EI+ mass spectrum of the compound eluted at 27.38 min (excerpt: m/z =400 to m/z 600 Da).*

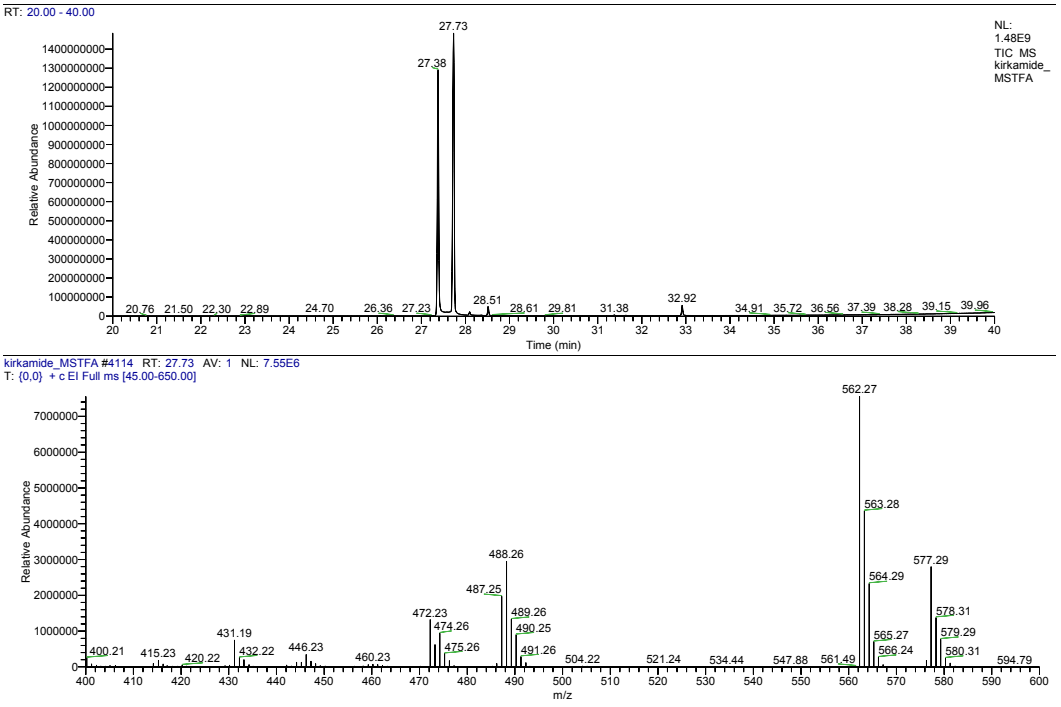

*Figure **13**: GC-MS chromatogram of kirkamide (**56**) after derivatization (top) and EI+ mass spectrum of the compound eluted at 27.73 min (excerpt: m/z =400 to m/z 600 Da).*

2.4.2. Quantification by ^{1}H NMR Spectroscopy

Kirkamide (**56**) and streptol glucoside (**57**) were found to possess a characteristic methylene proton with a chemical shift of around 6 ppm in the ^{1}H NMR spectrum. Additionally, during our isolation study, we determined the presence of asperuloside (**86**) in the *P. kirkii* extract, which was shown to give peaks in the same region of the ^{1}H NMR spectrum. This situation was ideal to determine the concentration of these three natural products quantitatively by a single ^{1}H NMR measurement. Maleic acid was chosen as the internal standard due to its solubility in D_2O and a characteristic peak with a chemical shift in the desired range.[95] Additionally, a precise amount of leave extracts from each plant was weighed in with an analytical balance for every measurement.

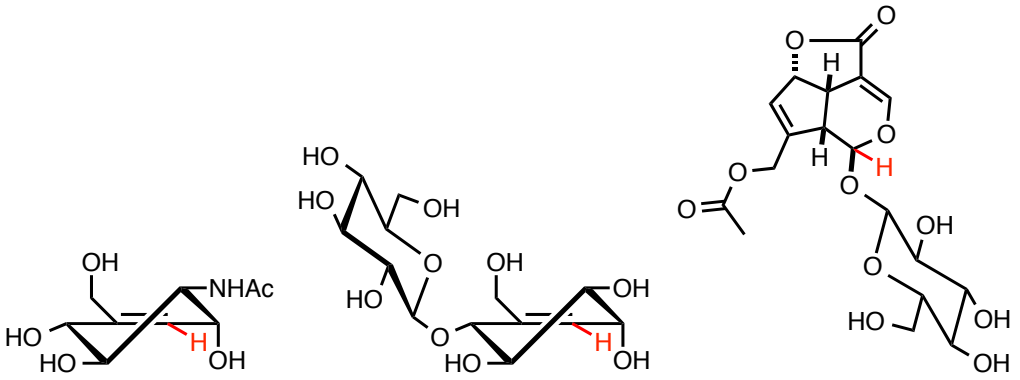

*Figure **14**: Natural products quantified by ^{1}H NMR, the protons highlighted in red were used for the measurement.*

The three natural products were quantified in the crude extracts from different parts of the plant *P. kirkii*. (table **7**). The leaves and shoot extracts were found to contain all three compounds. This result was expected due to the presence of the nodules on the leaves and since the iridoid **86** was known to accumulate in the aerial part of the plant.[96] We observed a higher concentration of kirkamide (**56**) and streptol glucoside (**57**) in the shoot tip, where the symbiontic bacteria are found in large numbers for the colonization of new leaves.[54] Furthermore, the detection of the two compounds in the root extract

[95] T. Rundlöf, M. Mathiasson, S. Bekiroglu, B. Hakkarainen, T. Bowden, T. Arvidsson, *J. Pharm. Biomed. Anal.* **2010**, *52*, 645–651.
[96] A. R. Trim, *Biochem. J.* **1952**, *50*, 319–326.

implied that the two compounds are up taking by the plant metabolism and travel up to the root of the plant.

The percentage of kirkamide (**56**), streptol glucoside (**57**) and asperuloside (**86**) present in the dried leaves was determined for the plants *P. kirkii* and *P. punctata.* The dried leaves of the two organisms were blended, the compounds were extracted and a portion of the crude extract was dissolved in a solution containing a known amount of maleic acid. The concentration of the natural products was calculated by comparison of their proton integration with the one of maleic acid. Kirkamide (**56**) was identified in both plants at a similar concentration, which is in agreement with the GC-MS measurements.

Table **7**. Quantification of kirkamide (**56**), streptol glucoside (**57**) and asperuloside (**86**) by ^{1}H NMR.

Extracts	Kirkamide [%]	Streptol glucoside [%]	Asperuloside [%]
P. kirkii leaves	0.72[a]	1.29[a]	2.18[a]
P. kirkii shoot	8.03[a]	6.81[a]	0.19[a]
P. kirkii root	5.04[a]	4.34[a]	-
P. kirkii soil	-	-	-
P. kirkii leaves	0.37[b]	0.60[b]	0.19[b]
P. punctata leaves	0.23[b]		0.07[b]

[a] The values indicated the percentage present in the crude extract; [b] The values indicated the percentage present in the dried leaves.

2.5. Conclusion

The analysis of the leaf extract of *Psychotria kirkii*, a plant living in an obligatory symbiosis with a bacterium forming nodules under the leaves of the host, led to the isolation of the two new natural products kirkamide (**56**) and streptol glucoside (**57**).

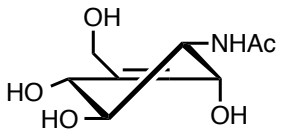

kirkamide (**56**)

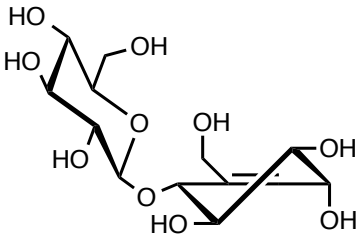

streptol glucoside (**57**)

Following a genome-driven ^{1}H NMR-guided fractionation a C_7N aminocyclitol, named kirkamide (**56**), was identified and the structure was elucidated by HRMS and NMR and confirmed by single crystal X-ray analysis. In order to obtain a larger amount of kirkamide (**56**) to understand its role in the symbiosis, a total synthetic route was developed to obtain the natural product in 11 steps from commercially available methyl-*N*-acteyl-D-glucosamine (**75**). The synthetic pathway proved its robustness allowing for a gram scale preparation at each step. Using this material, kirkamide (**56**) was shown to be cytotoxic in the brine shrimp assay and possessing insecticidal activity against the pollen beetle *Meligethes aeneus*. This last biological property of kirkamide is proposed to play a role in the symbiosis by protecting the plant against insects.

Applying a growth inhibition bioassay-guided fractionation against lettuce seeds, a compound similar to streptol (**58**) was identified and named streptol glucoside (**57**). HRMS and NMR data analyses were used for the structure elucidation of **57**. The role of streptol glucoside (**57**) in the symbiosis remains unclear and requires further investigation. A possible role of **57** could be the growth inhibition of other plant competitors or a bacterial defensive system against possible attacks from the host plant.

The last part of this chapter focus on the development of an analytical method towards the detection and quantification of the new natural products. Kirkamide (**56**) was detected by GC-MS after derivatization with MSTFA. Using this strategy, we were able to identify kirkamide in extracts from several plants in symbiosis as *Psychotria humilis*, *Psychotria verschuerenii, Psychotria punctata, Psychotria kirkii* and *Psychotria pumila*. The detection of **56** in another species showed that this phenomenon is not restricted at the plant *P. kirkii*.

The quantification of kirkamide (**56**), streptol glucoside (**57**) and asperuloside (**86**) was achieved in extracts from different parts of the plant *P. kirkii* and also from leaf extract of *P. punctata*. The determination of **56** in extracts from leaves, shoot and root indicate that the natural product travels to these different locations within plant.

3. Isolation and Biosynthesis Investigation of Fragin

3.1. Biosynthesis of Natural Products Possessing a Nitrogen-Nitrogen Bond

Only few natural products containing a nitrogen-nitrogen (N-N) bond have been reported with approximately 200 compounds isolated up to 2013. They are categorized in several classes such as azine, azo compound, azoxy, cinnoline, diazo, hydrazine, hydrazide, hydrazone, indazole, nitrosamine, *N*-nitrosohydroxylamine, *N*-*N* linked heterocycle, pyradazine, pyrazole, triazine and triazole.[97] An example for each class of compound is shown in figure **15** with the functional group highlighted in red.

The biosynthesis of some of the natural products belonging to the azoxy, diazo and hydrazide classes has been investigated with special interest in the mechanism of formation of the N-N bond.[98,99] In this chapter, the biosynthesis of these compounds will be presented using valanimycin (**87**), kutzneride 1 (**88**), kinamycin D (**89**) and azamerone (**90**) as main examples.

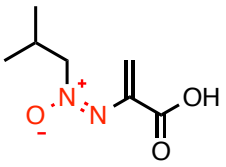

valanimycin (**87**)

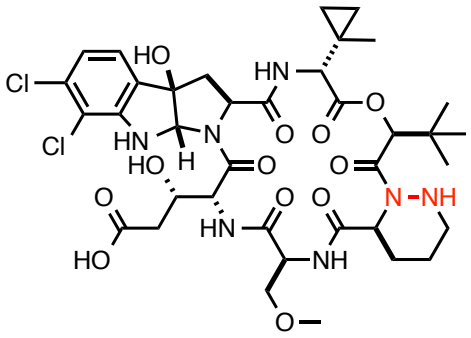

kutzneride 1 (**88**)

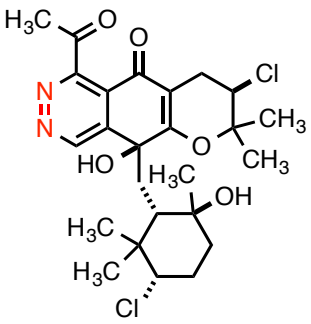

azamerone (**89**)

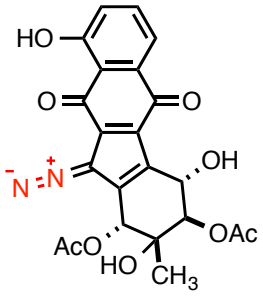

kinamycin D (**90**)

[97] L. M. Blair, J. Sperry, *J. Nat. Prod.* **2013**, *76*, 794–812.
[98] C. C. Nawrat, C. J. Moody, *Nat. Prod. Rep.* **2011**, *28*, 1426–1444.
[99] Le Goff, J. Ouazzani, *Bioorg. Med. Chem.* **2014**, *22*, 6529–6544.

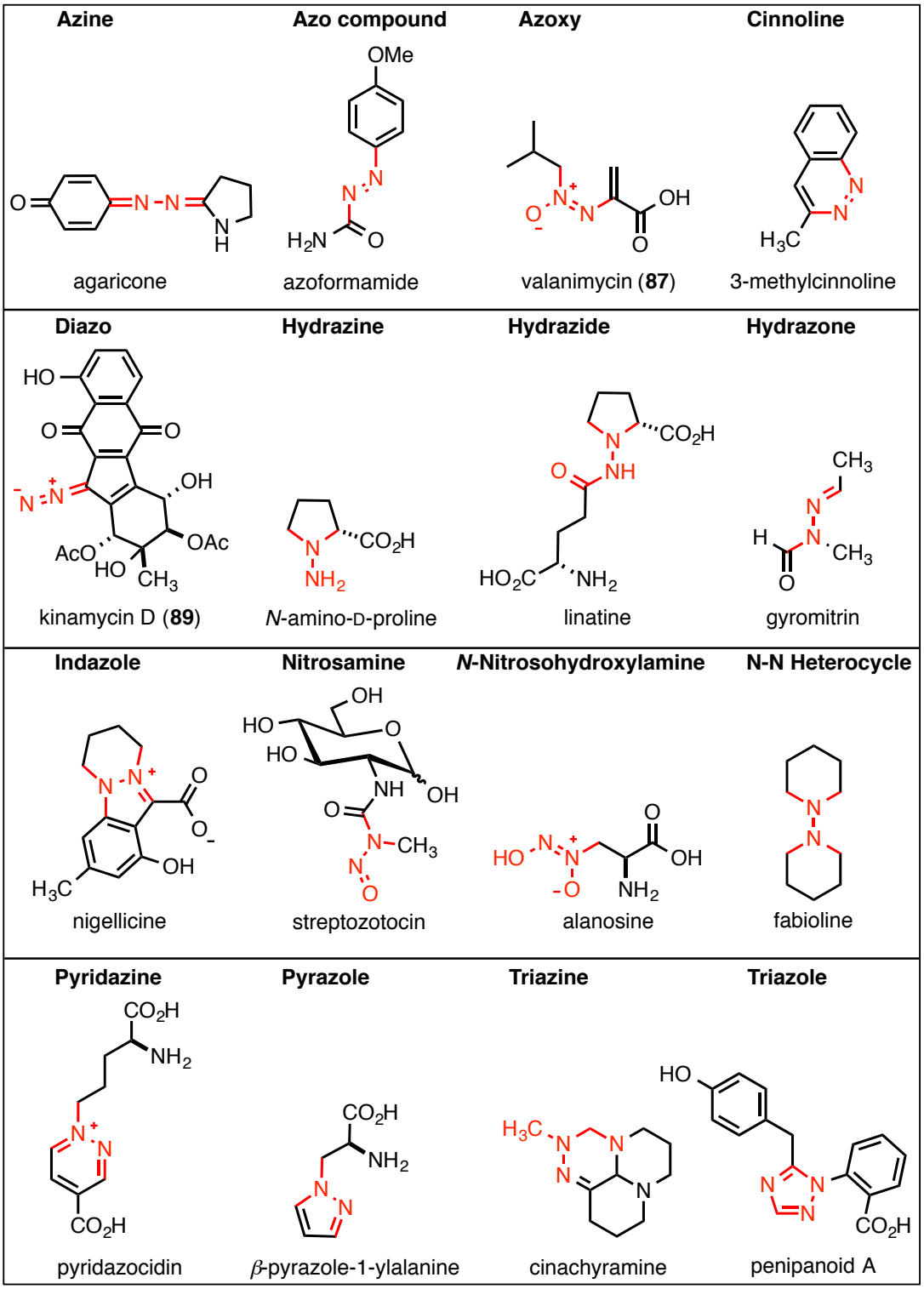

*Figure **15**: Examples of natural products containing a N-N bond.*

3.1.1. Biosynthesis of Azoxy Compounds

3.1.1.1. Valanimycin

An unstable azoxy compound, showing antibacterial and antitumor activity, was isolated from the bacterial culture of *Streptomyces viridifaciens* (*S. viridifaciens*). Part of the structure elucidation of valanimycin (**87**) was achieved by a combination of NMR and IR analyses. However, mass spectroscopy or elemental analysis could not be performed due to the fast degradation of the natural product.[100] The structure of **87** was confirmed then by the full characterization of its ammonium adduct.

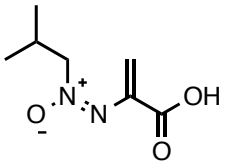

valanimycin (**87**)

Biosynthetic investigations of **87** was firstly achieved with isotopic labeling experiments leading and led to the discovery that valine (**91**), isobutylamine (**92**) and isobutylhydroxylamine (**93**) were precursors for the left part of the compound and serine (**94**) for the right part.[101,102]

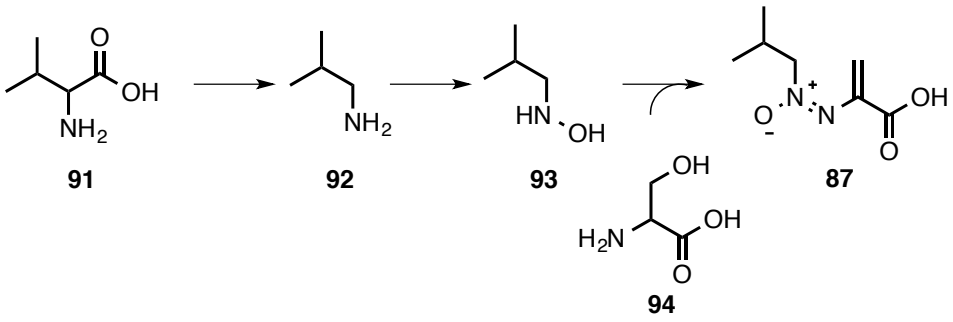

Scheme 7: Proposed biosynthetic pathway after feeding experiments with different isotopic labeled precursors.

[100] M. Yamato, H. Iinuma, H. Naganawa, Y. Yamagishi, M. Hamada, T. Masuda, H. Umezawa, Y. Abe, M. Hori, *J. Antibiot.* **1986**, *39*, 184–191.
[101] M. Yamato, T. Takeuchi, H. Umezawa, N. Sakata, H. Hayashi, M. Hori, *J. Antibiot.* **1986**, *39*, 1263–1269.
[102] R. J. Parry, Y. Li, F. L. Lii, *J. Am. Chem. Soc.* **1992**, *114*, 10062–10064.

Furthermore, the results from the feeding experiments indicated that the two nitrogens come from different sources; one from the amino acid serine (**94**) and the other one from valine (**91**). Additionally, the nitrogen bond formation was proposed to be the result of the reaction between **93** and **94**. It was found during *in vitro* assay that VlmH/VlmR enzymes (predicted as a two components flavin monooxygenase) from *S. viridifaciens* catalyzed the oxidation of the nitrogen atom of isobutylamine.[103]

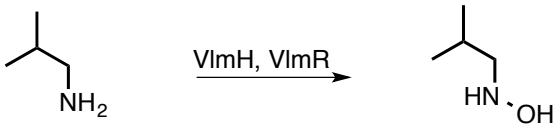

isobutylamine (**92**) isobutylhydroxylamine (**93**)

DNA sequencing and analysis of valanimycin genes allowed the function assignment of the different enzymes responsible for the production of the natural product. The gene responsible for valine decarboxylase (VlmD) producing isobutylamine (**92**) was determined and the enzymes isobutylamine *N*-hydroxylase (VlmH) and FAD reductase (VlmR) were identified.[104]

However, one gene responsible for a seryl tRNA synthetase (VlmL) was present in a cluster and its role in the biosynthesis was unclear.[104] This enzyme was purified and *in vitro* assay experiments performed using radiolabeled compounds showed the catalytic role of the protein towards the formation of seryl-tRNA.[105] Additionally, the reaction between seryl-tRNA and isobuthylhydroxylamine (**93**) was found to be an enzymatic process catalyzed by VlmA (scheme **8**). By taking into account these recent results a new biosynthesis was suggested including two proposed mechanisms for the formation of the N-N bond (scheme **9**).[106]

[103] R. J. Parry, W. Li, *Arch. Biochem. Biophys.* **1997**, *339*, 47–54.
[104] R. P. Garg, Y. Ma, J. C. Hoyt, R. J. Parry, *Mol. Microbiol.* **2002**, *46*, 505–517.
[105] R. P. Garg, J. M. Gonzalez, R. J. Parry, *J. Biol. Chem.* **2006**, *281*, 26785–26791.
[106] R. P. Garg, X. L. Qian, L. B. Alemany, S. Moran, R. J. Parry, *Proc. Natl. Acad. Sci. U. S. A.* **2008**, *105*, 6543–6547.

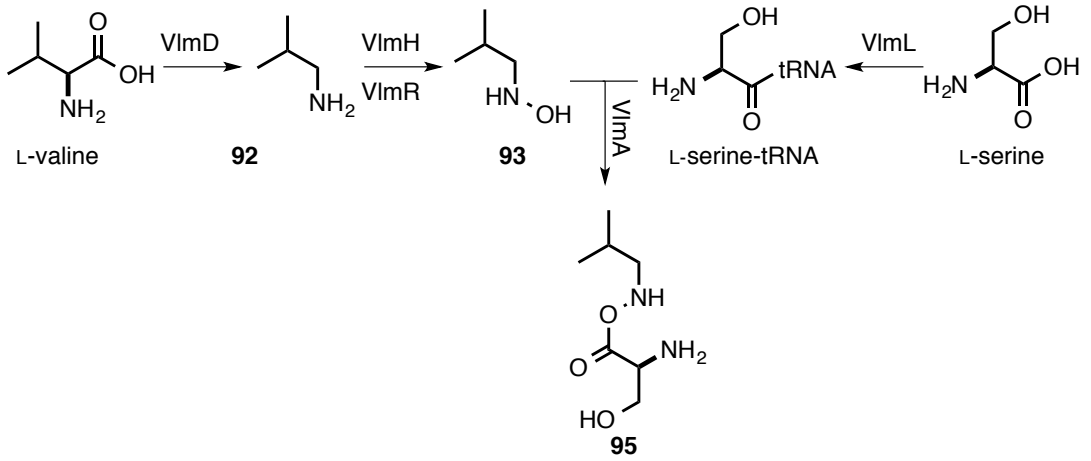

*Scheme **8**: Biosynthesis suggestion of the hydroxylamine intermediate **95**.*

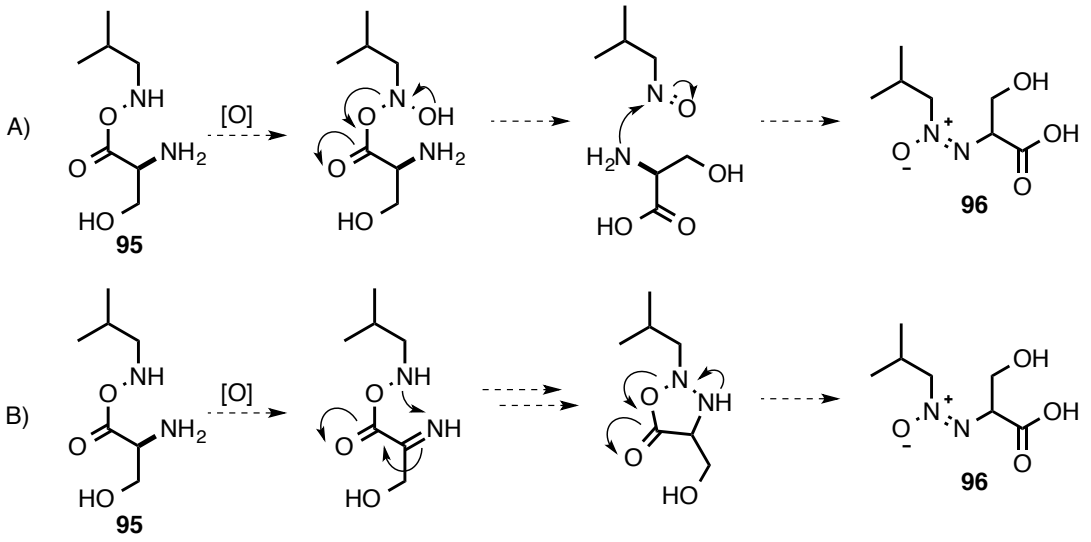

*Scheme **9**: Proposed mechanisms for the N-N bond formation. A) Mechanism involving the reaction of an amine and a nitroso. B) Proposed mechanism via imine formation.*

Finally, the dehydration of **96** into valanimycin (**87**) required two enzymes VlmJ and VlmK and the addition of ATP. It was therefore proposed that the last step undergoes *via* the addition of a phosphate, which triggered the reduction of **96** to **87** (scheme **10**).[107]

[107] R. P. Garg, L. B. Alemany, S. Moran, R. J. Parry, *J. Am. Chem. Soc.* **2009**, *131*, 9608–9609.

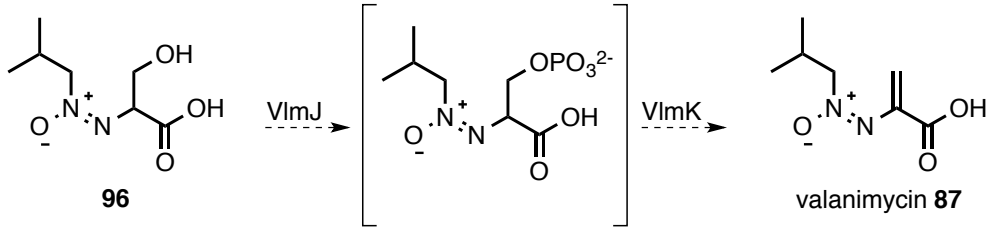

*Scheme **10**: Dehydration mechanism of **96** to the natural product **87**.*

3.1.1.2. Elaiomycin, Lyophillin and Malleobactin D

Similar biosynthetic pathways as valanimycin, including the reaction of two partners for the N-N bond formation, were proposed for other natural products as elaiomycin (**97**), lyophyllin (**98**) and malleobactin D (**99**).[108,109]

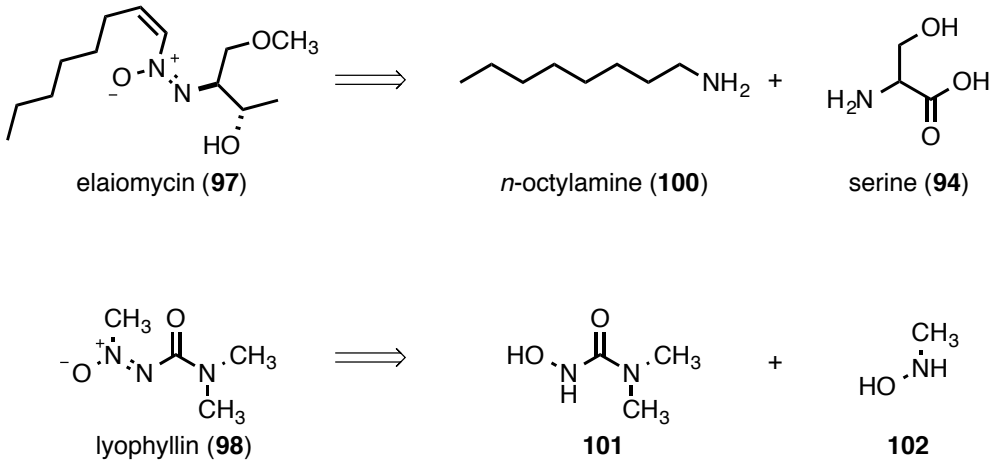

*Scheme **11**: The labeled precursors (**100**, **94**, **101** and **102**) were synthesized and the results of the feeding experiments indicated an isotopic enrichment of the natural products.*

[108] R. J. Parry, H. S. P. Rao, J. Mueller, *J. Am. Chem. Soc.* **1982**, *104*, 339–340; R. J. Parry, J. V. Mueller, *J. Am. Chem. Soc.* **1984**, *106*, 5764–5765; Y. Ye, K. Aulinger, N. Arnold, W. Spahl, W. Steglich, *Tetrahedron Lett.* **1997**, *38*, 8013– 8016.

[109] J. Franke, K. Ishida, M. Ishida-Ito, C. Hertweck, *Angew. Chem. Int. Ed. Engl.* **2013**, *52*, 8271–8275.

Malleobactin B (**103**), C (**104**) and D (**99**) were isolated from crude extracts of *Burkholderia thailandensis*. **99** was proposed to be the product of the reaction between malleobactins B (**103**) and C (**104**). These two natural products were incubated in physiological conditions and after several hours the formation of **99** was observed.[109]

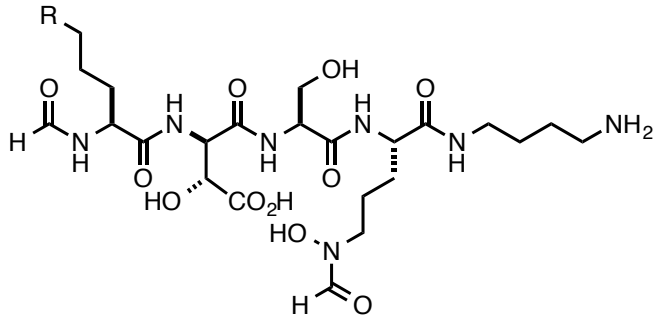

malleobactin B (**103**); R=NHOH
malleobactin C (**104**); R=NO

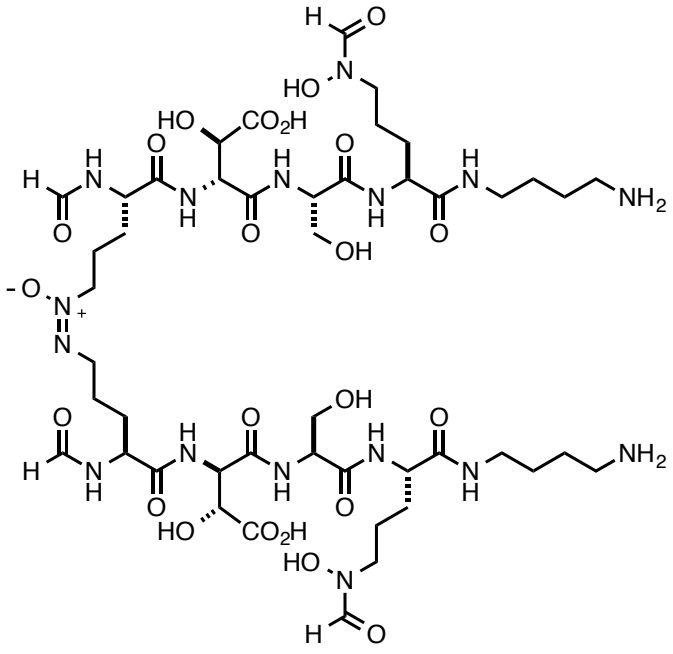

malleobactin D (**99**)

3.1.2. Biosynthesis of Hydrazide/Hydrazine

3.1.2.1. Kutzneride

Piperazic acid (**105**) is present in various cyclic peptides isolated from bacteria as in kutzneride 1 (**88**).[110] During the biosynthetic analysis of **88** important information was obtain about the N-N bond formation of **105**.

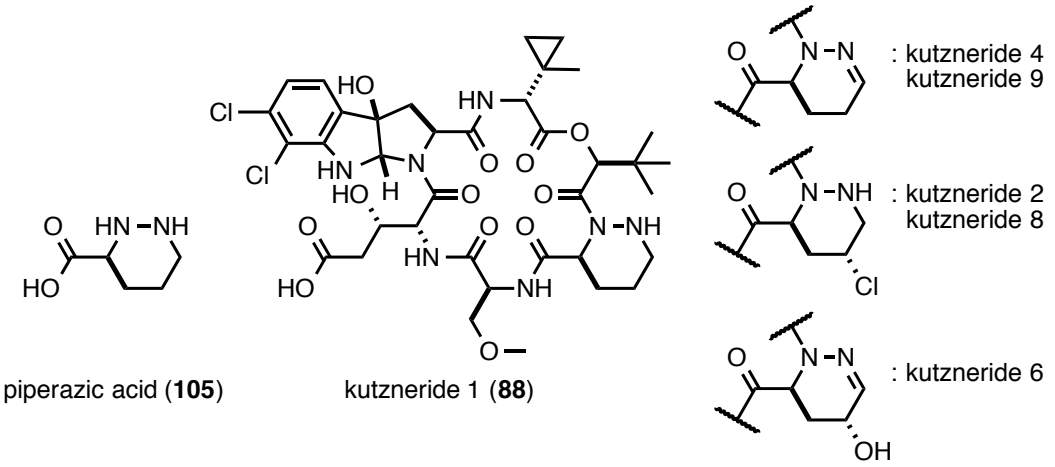

Nine kutznerides have been isolated from the actinomycete *Kutzneria* sp. 744 with variations in the piperazic acid moiety such as enamine, oxidation and chloride insertion.[111,112] The gene cluster of these compounds was identified and the function of the enzymes was assigned. A flavoprotein monooxygenase KtzI was found to show high similarities in their DNA with a lysine/ornithine *N*-monooxygenase from *Pseudomonas aeruginosa* and was predicted to be involved in the formation of **105**.[113] To test this hypothesis, the enzyme was produced by heterologous expression and evaluated with different substrates (L/D-Lys, L/D-Gln, L/D-Gln and L/D-Orn). Only L-ornithine (**106**) was significantly transformed to its *N*-oxidized form, which was detected by HPLC after Fmoc protection (scheme **12**). The confirmation of this compound as substrate was obtained by labeling experiment with $^{13}C_5$-Orn (**107**) and $^{13}C_5$-N^5-OH-Orn (**108**) resulting

[110] A. J. Oelke, D. J. France, T. Hofmann, G. Wuitschik, S. V. Ley, *Nat. Prod. Rep.* **2011**, *28*, 1445–1471.
[111] A. Broberg, A. Menkis, R. Vasiliauskas, *J. Nat. Prod.* **2006**, *69*, 97–102.
[112] A. Pohanka, A. Menkis, J. Levenfors, A. Broberg, *J. Nat. Prod.* **2006**, *69*, 1776–1781.
[113] D. G. Fujimori, S. Hrvatin, C. S. Neumann, M. Strieker, M. A. Marahiel, C. T. Walsh, *Proc. Natl. Acad. Sci. U. S. A.* **2007**, *104*, 16498–16503.

in the detection by $HRMS^2$ of the piperazic acid (**105**) containing the isotopically enriched carbon atoms (scheme **13**).[114]

L-ornithine (**106**)

*Scheme **12**: Enzymatic N-oxidation of L-Orn (**106**).*

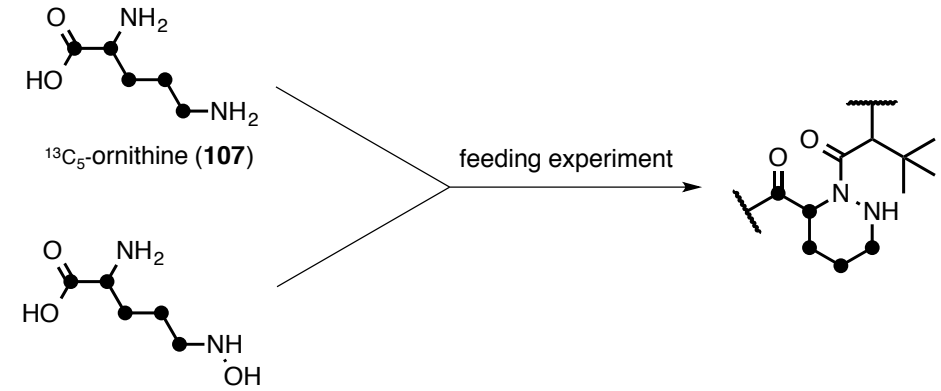

*Scheme **13**: Feeding experiment with isotopically labeled ornithine (**107**) and N^5-OH-ornithine (**108**).*

An hydroxylamine was proposed to play a key role in the formation of the N-N bond as it was found for the azoxy compound. The main difference would result in an intramolecular process for the case of the piperazic acid (**105**).

[114] C. S. Neumann, W. Jiang, J. R. Heemstra Jr., E. A. Gontang, R. Kolter, C. T. Walsh, *Chembiochem* **2012**, *13*, 972–976.

3.1.2.2. Monamycin D_1 and Polyoxypeptin A

Monamycin D_1 (**109**) and polyoxypeptin A (**110**) were isolated from different *Streptomyces* strains and were found to possess piperazic acids (**105**) in their core structure.[115,116] The biosynthesis of these natural products was investigated by feeding experiments with isotopic labeled ornithine and glutamic acid resulting mainly in the incorporation of glutamic acid (scheme **14**).[117,118] This result indicated that the biosynthesis of the piperazic acid (**105**) would take a different pathway as the one proposed for kutzneride 1 (**88**). However, the difficulties during the uptake of ornithine by the bacteria were advanced as an hypothesis to explain the lack of incorporation of this amino acid into the natural products.[114] Interestingly, two genes homologs as *ktzI* were found in the genome of the bacteria which produced polyoxypeptin.[119]

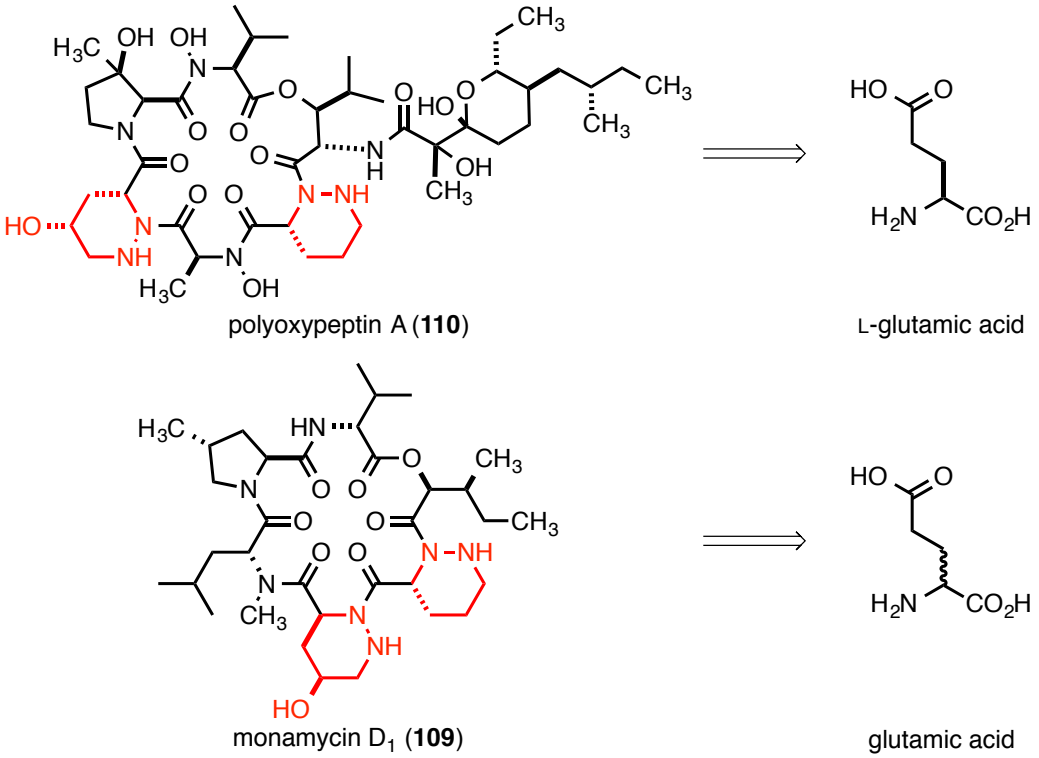

*Scheme **14**: Substrates predicted for the piperazic acid (**105**) moiety based on feeding experiments.*

[115] C. H. Hassall, K. E. Magnus, *Nature* **1959**, *184*, 1223–1224.
[116] K. Umezawa, K. Nakazawa, T. Uemura, Y. Ikeda, *Tetrahedron Lett.* **1998**, *39*, 1389–1392.
[117] V. Arroyo, M. J. Hall, C. H. Hassall, *J. Chem. Soc.* **1976**, 845–846.
[118] K. Umezawa, Y. Ikeda, O. Kawase, H. Naganawa, S. Kondo, *J. Chem. Soc., Perkin Trans. 1* **2001**, 1550–1553.
[119] Y. Du, Y. Wang, T. Huang, M. Tao, Z. Deng, S. Lin, *BMC Microbiol.* **2014**, *14*:30.

3.1.3. Biosynthesis of Pyridazine

3.1.3.1. Pyridazomycin

Pyridazomycin (**112**) was isolated in 1987 from the *Streptomyces violaceoniger* sp. *griseofuscus* strain Tü 2557.[120] Its biosynthesis was investigated by labeled amino acids feeding experiment. The results showed that ornithine (**106**) and glycine (**113**) were the initial substrates. Additionally, a nucleophilic attack from the amine of **113** to the proposed *N* oxidized **106** was suggested as the mechanism for the N-N bond formation.[121] It is interesting to note that the biosynthesis of pyridazomycin (**112**) and kutzneride 1 (**88**) required the oxidation of ornithine as a key step for the synthesis of the N-N bond.

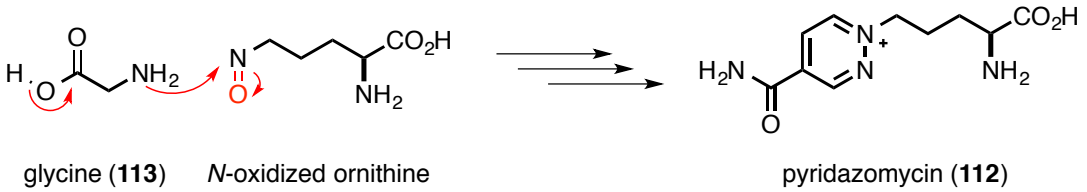

*Scheme **15**: Proposed mechanism for the formation of the N-N bond in pyridazomycin (**112**). Hypothetic oxidation of ornithine and the decarboxylation of glycine (**113**) are highlighted in red.*

3.1.3.2. Azamerone

The terpenoid azamerone (**90**) was isolated from the bacterium *Streptomyces* sp. CNQ-766 and the structure, which contained the unusual pyranophtalazinone ring, was elucidated by NMR and single crystal X-ray analysis.[122]

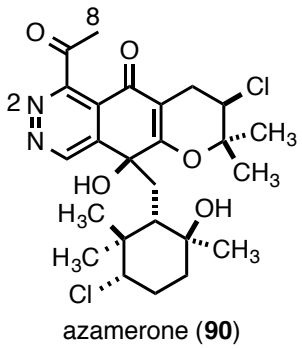

[120] R. Grote, Y. Chen, A. Zeeck, Z. X. Chen, H. Zähner, P. Mischnick-Lübbecke, W. A. König, *J. Antibiot.* **1988**, *41*, 595–601.
[121] H. Bockholt, J. M. Beale, J. Rohr, *Angew. Chem. Int. Ed. Engl.* **1994**, *33*, 1648–1651.
[122] J. Y. Cho, H. C. Kwon, P. G. Williams, P. R. Jensen, W. Fenical, *Org. Lett.* **2006**, *8*, 2471–2474.

The analysis of the gene cluster of azamerone (**90**) was achieved[123] and the natural products, SF2415A1 (**114**), SF2415A3 (**115**), SF2415B1 (**116**), SF2415B3 (**117**), A80915C (**118**) and A80915D (**119**), isolated from the culture of *Streptomyces aculeolatus*,[124] were proposed as biosynthetic precursors.[125]

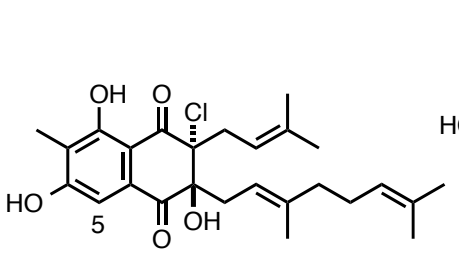

SF2415B1 (**116**)

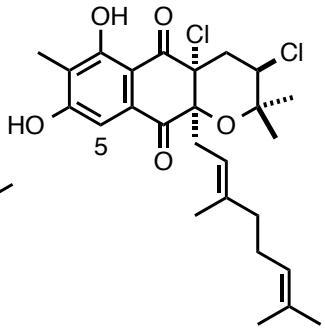

SF2415B3 (**117**)

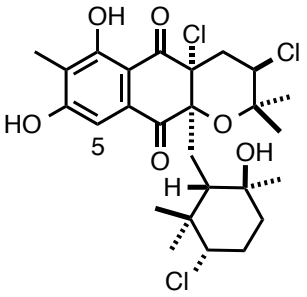

A80915C (**118**)

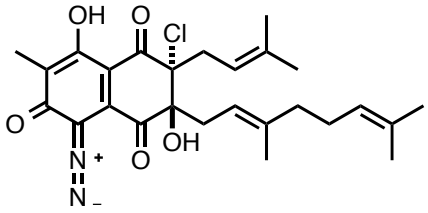

SF2415A1 (**114**)

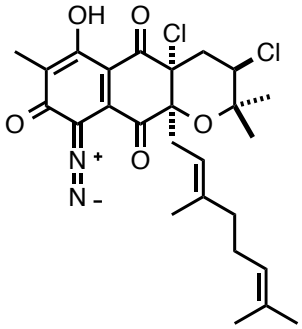

SF2415A3 (**115**)

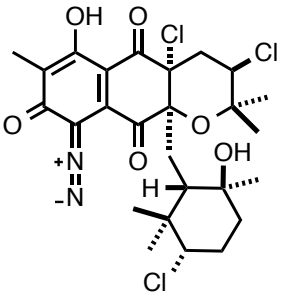

A80915D (**119**)

The compounds A80915C (**118**), A80915D (**119**) and SF2415A3 (**115**) were identified in the azamerone (**90**) producer bacterium strain. Feeding experiments with $Na^{15}NO_3$ and $Na^{15}NO_2$ indicated a specific isotopic enrichment only at N-2 for the natural products **115**, **119** and **90**. Furthermore, the compound **115** was biosynthetically obtained with isotopic labeled at N-2 and C-9 and the bacterium fed with the labeled natural product **115** produced azamerone (**90**) labeled at position N-2 and C-8

[123] J. M. Winter, M. C. Moffitt, E. Zazopoulos, J. B. McAlpine, P. C. Dorrestein, B. S. Moore, *J. Biol. Chem.* **2007**, *282*, 16362–16368.

[124] S. Gomi, S. Ohuchi, T. Sasaki, J. Itoh, M. Sezaki, *J. Antibiot.* **1987**, *40*, 740–749; T. Shomura, S. Gomi, M. Ito, J. Yoshida, E. Tanaka, S. Amano, H. Watabe, S. Ohuchi, J. Itoh, M. Sezaki, *J. Antibiot.* **1987**, *40*, 732–739; D. S. Fukuda, J. S. Mynderse, P. J. Baker, D. M. Berry, L. D. Boeck, R. C. Yao, F. P. Mertz, W. M. Nakatsukasa, J. Mabe, J. Ott, *J. Antibiot.* **1990**, *43*, 623–633; T. Henkel, A. Zeeck, *J. Antibiot.* **1991**, *44*, 665–669.

[125] J. M. Winter, A. L. Jansma, T. M. Handel, B. S. Moore, *Angew. Chem. Int. Ed. Engl.* **2009**, *48*, 767–770.

(scheme **16**).[125] A stepwise process *via* a diazo compound was proposed for the mechanism of formation of the N-N bond of the azamerone pyradizine.

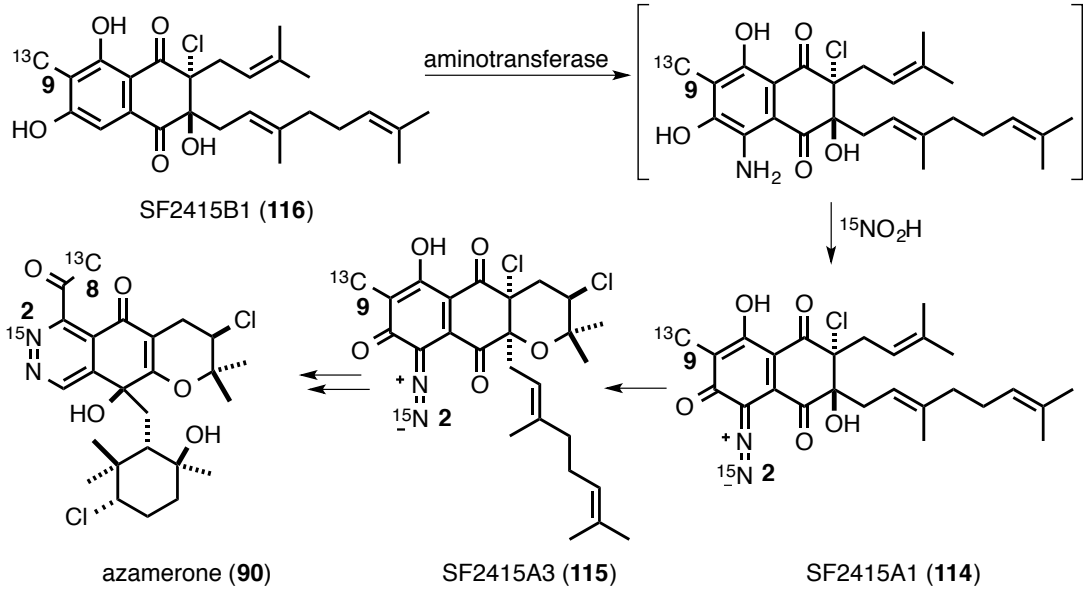

*Scheme **16**: Proposed mechanism, based on isotopic labeled experiments, for N-N bond formation in azamerone (**90**).*

3.1.4. Biosynthesis of Diazo Compounds

3.1.4.1. Kinamycins

Several natural products sharing similar core structure have been isolated from different bacteria and named kinamycins A–J (**120**–**129**).[126] The diazo functional group was initially assigned as cyano and the structure was finally elucidated in 1994 by the research groups of Gould and Dmitrienko.[127,128]

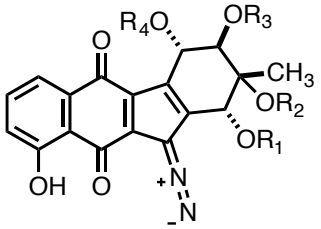

Table **8.** The natural products kinamycins.

Compound	R_1	R_2	R_3	R_4
kinamycin A (**120**)	H	Ac	Ac	Ac
kinamycin B (**121**)	H	Ac	H	H
kinamycin C (**122**)	Ac	H	Ac	Ac
kinamycin D (**123**)	Ac	H	Ac	H
kinamycin E (**124**)	Ac	H	H	H
kinamycin F (**125**)	H	H	H	H
kinamycin G (**126**)	Ac	C(O)*i*-Pr	Ac	Ac
kinamycin H (**127**)	C(O)*i*-Pr	H	Ac	Ac
kinamycin I (**128**)	C(O)*i*-Pr	H	C(O)*i*-Pr	Ac
kinamycin J (**129**)	Ac	Ac	Ac	Ac

[126] S. Itŏ, T. Matsuya, S. Omura, M. Otani, A. Nakagawa, *J. Antibiot.* **1970**, *23*, 315–317; T. Hata, S. Omura, Y. Iwai, A. Nakagawa, M. Otani, *J. Antibiot.* **1971**, *24*, 353–359; S. Omura, A. Nakagawa, H. Yamada, T. Hata, A. Furusaki, T. Watanabe, *Chem. Pharm. Bull.* **1971**, *19*, 2428–2430; S. Omura, A. Nakagawa, H. Yamada, T. Hata, A. Furusaki, *Chem. Pharm. Bull.* **1973**, *21*, 931–940; M. C. Cone, P. J. Seaton, K. A. Halley, S. J. Gould, *J. Antibiot.* **1989**, *42*, 179–188; P. J. Seaton, S. J. Gould, *J. Antibiot.* **1989**, *42*, 189–197; K. Isshiki, T. Sawa, H. Naganawa, N. Matsuda, S. Hattori, M. Hamada, T. Takeuchi, M. Oosono, M. Ishizuka, Z. Z. Yang, *J. Antibiot.* **1989**, *42*, 467–469; T. A. Smitka, R. Bonjouklian, T. J. Perun, A. H. Hunt, R. S. Foster, J. S. Mynderse, R. C. Yao, *J. Antibiot.* **1992**, *45*, 581–583.

[127] S. J. Gould, N. Tamayo, C. R. Melville, M. C. Cone, *J. Am. Chem. Soc.* **1994**, *116*, 2207–2208.

[128] S. Mithani, G. Weeratunga, N. J. Taylor, G. I. Dmitrienko, *J. Am. Chem. Soc.* **1994**, *116*, 2209–2210.

The biosynthesis of these natural products has been subject to extensive research.[129,130] Here, only the mechanism of the N-N bond formation will be discussed. The biosynthetic elucidation of kynamycin benefits from the isolation of a precursor named stealthin C (**130**) from the bacterial culture of *S. murayamaensis*. To confirm the role of **130** in the biosynthesis of kinamycin D (**123**), a deuterated labeled stealthin C was prepared. A feeding experiment with this precursor resulted in the production of labeled kinamycin D[131] and indicated that the N-N bond formation undergoes *via* a stepwise mechanism involving stealthin C (**130**). One hypothesis for the second nitrogen source was proposed to be nitric oxide or one of its derivatives.[132]

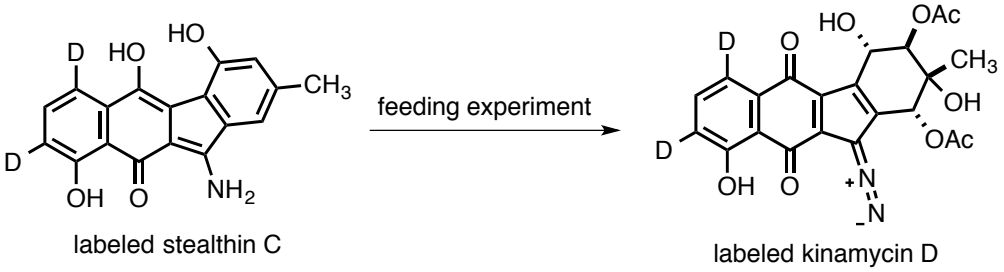

labeled stealthin C

labeled kinamycin D

*Scheme **17**: Labeled experiment demonstrating the involvement of stealthin C (**130**) in the biosynthesis of kinamycin D (**123**).*

[129] S. J. Gould, *Chem. Rev.* **1997**, *97*, 2499–2510.
[130] S. B. Herzon, C. M. Woo, *Nat. Prod. Rep.* **2012**, *29*, 87–118.
[131] S. J. Gould, C. R. Melville, M. C. Cone, J. Chen, J. R. Carney, *J. Org. Chem.* **1997**, *62*, 320–324.
[132] G. L. Abbott, PhD Thesis, the University of Waterloo, Waterloo, Ontario, Canada, **2011**.

3.1.4.2. Lomaiviticins

Lomaiviticins are natural products containing a core structure composed of a glycosylated kinamycin dimer. These natural products were found to possess potent antibiotic and anticancer properties, as example lomaiviticin A (**131**) is shown below.[133]

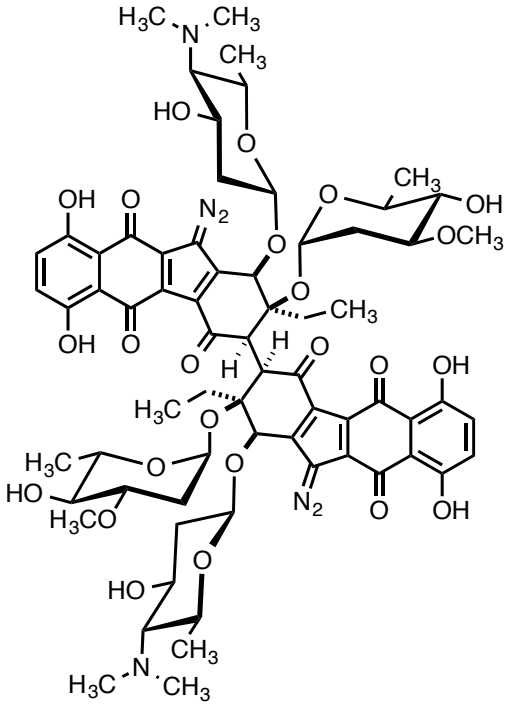

lomaiviticin A (**131**)

The gene cluster of lomaiviticin was discovered and sequenced from two different *Salinispora* strains.[134, 135] Comparing the genes involved in the biosynthesis of kinamycin[136] and those of lomaiviticin, a sub cluster (*lom29, 30, 32-35*), identified in both, was proposed as a good candidate for the diazo formation. The predicted gene functions are described in table **9** and interestingly, homologs were also found in the gene cluster of the hydrazide fosfazinomycin A (**132**).[135,137]

---

[133] H. He, W. D. Ding, V. S. Bernan, A. D. Richardson, C. M. Ireland, M. Greenstein, G. A. Ellestad, G. T. Carter, *J. Am. Chem. Soc.* **2001**, *123*, 5362–5363; C. M. Woo, N. E. Beizer, J. E. Janso, S. B. Herzon, *J. Am. Chem. Soc.* **2012**, *134*, 15285–15288.

[134] R. D. Kersten, A. L. Lane, M. Nett, T. K. S. Richter, B. M. Duggan, P. C. Dorrestein, B. S. Moore, *Chembiochem* **2013**, *14*, 955–962.

[135] J. E. Janso, B. A. Haltli, A. S. Eustáquio, K. Kulowski, A. J. Waldman, L. Zha, H. Nakamura, V. S. Bernan, H. He, G. T. Carter, F. E. Koehn, E. P. Balskus, *Tetrahedron* **2014**, *70*, 4156–4164.

[136] S. J. Gould, S. T. Hong, J. R. Carney, *J. Antibiot.* **1998**, *51*, 50–57.

[137] J. Gao, K.-S. Ju, X. Yu, J. E. Velásquez, S. Mukherjee, J. Lee, C. Zhao, B. S. Evans, J. R. Doroghazi, W. W. Metcalf, W. A. van der Donk *Angew. Chem.* **2013**, *126*, 1358–1361.

Table **9.** Predicted gene function for lomaiviticin diazo formation.

Genes	Predicted Function of the enzyme
lom29	Unknown
lom30	4Fe-4S ferrodoxin
lom32	Glutamine synthase
lom33	Amidase
lom34	Adenylosuccinate lyase
lom35	*N*-acetyltransferase

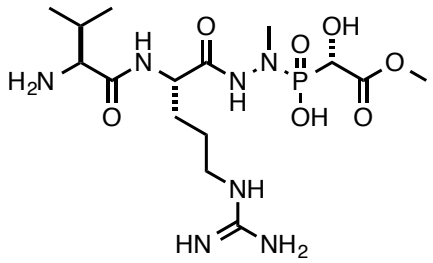

fosfazinomycin A (**132**)

Up to this date, the mechanism of N-N bond formation in natural products remains unclear. The examples presented above indicated that the insertion of the two nitrogens occurred *via* a stepwise mechanism, which can be intermolecular (e.g.: valanimycin (**87**)) or intramolecular (e.g.: azamerone (**90**)). In several natural products (**87**, **90**, **99** and **112**), a nucleophilic attack from an amine to a nitroso was proposed as the key step for the N-N bond formation.

3.1.5. Genomic Analysis of *Burkholderia cenocepacia H111*

To acquire a better understanding of the N-N bond formation in natural products, the identification of genes involved in the biosynthesis of these compounds is crucial. We analyzed the genome of the opportunistic pathogen *Burkholderia cenocepacia H111* (*B. cenocepacia H111*), isolated from a patient suffering from cystic fibrosis.[138] A gene cluster containing two nonribosomal peptide synthetases (NRPS) modules was identified and found to be responsible for the production of a natural product possessing an antifungal activity.[139] Using this biological property the gene cluster was named "ham" (H111 antifungal metabolite). Furthermore, the structure elucidation indicated the presence of N-N bond in the natural product and consequently we decided to investigate its biosynthesis.

[138] L. Eberl, *Int. J. Med. Microbiol.* **2006**, *296*, 103–110.
[139] A. Carlier, K. Agnoli, G. Pessi, A. Suppiger, C. Jenul, N. Schmid, B. Tümmler, M. Pinto-Carbo, L. Eberl, *Genome Announc.* **2014**, *2*, e00298–14.

3.2. Results and Discussion

This project was carried out in collaboration with Christian Jenul from the research group of Professor Leo Eberl at the Institute of Plant Biology, University of Zürich and Christophe Daeppen from the research group of Professor Karl Gademann. My contribution was the isolation, structure identification and biosynthesis proposal of fragin (**133**). I was also responsible for the analytical measurements involving HPLC and HPLC-MS. In this chapter the isolation and structure elucidation of **133** will be presented followed by biosynthetic proposals.

3.2.1. Isolation and Structure Elucidation of Fragin

The isolation of the natural compound produced by the NRPS gene cluster of *B. cenocepacia H111* and possessing an antifungal activity was carried out. Since we knew the biological activity of the compound a bioassay-guided fractionation was applied. The HPLC-MS spectra were compared between the supernatant of the wild type and the knockout strain (Δ*hamD*) and a compound eluting with a retention time of 20.4 min was exclusively found in the wild type extract (figure **16**). This compound (**133**) was isolated by RP-HPLC using a Gemini-NX column and its antifungal activity was confirmed.

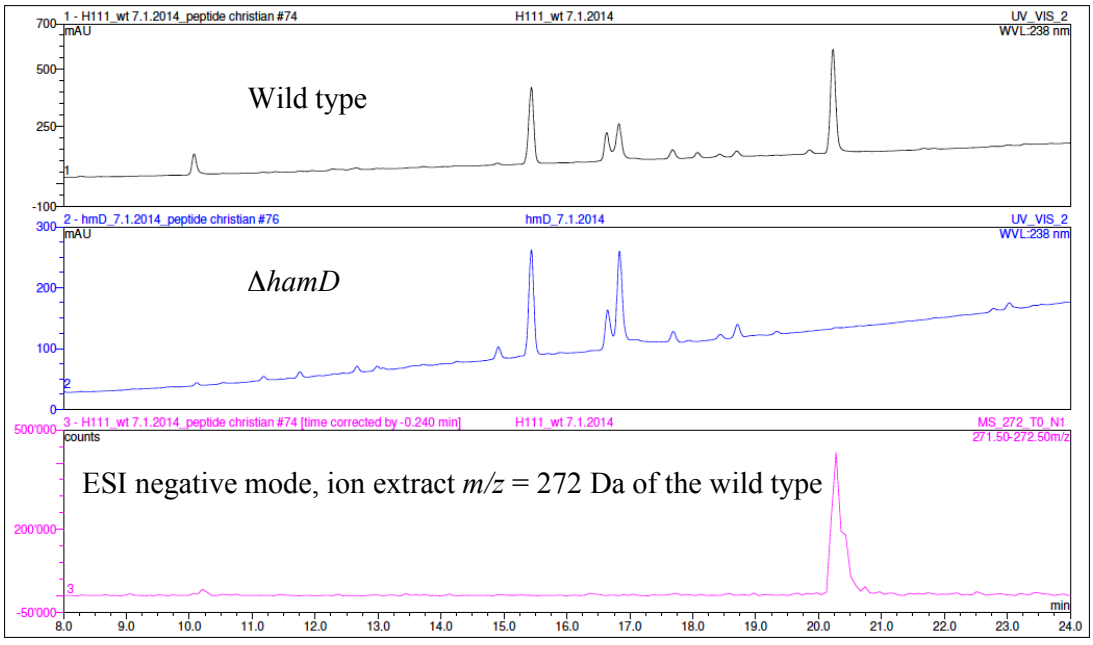

*Figure **16**: HPLC chromatograms of the wild type and ΔhamD extracts and mass chromatogram of the wild type extracted at 272 Da in negative mode.*

HPLC-MS analysis of the isolated compound showing a *m/z* = 274.2 Da (pos. mode) and a *m/z* = 272.2 Da (neg. mode) indicated a molecular mass of 273.2 Da. Additionally a major fragment (*m/z* = 244.2 Da, pos. mode) was found. The loss of 30 Da was attributed of a homolytic cleavage of fragin (**133**) generating nitric oxide (**134**) (figure **18**). The formation of positive and negative charge radical is a phenomenon, which has already been described for ESI-MS.[140]

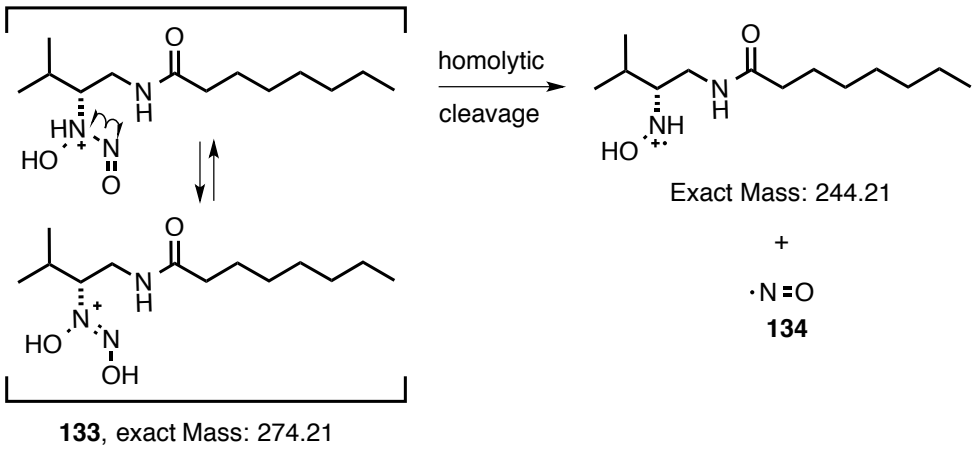

*Scheme **18**: Proposed mechanism of fragin (**133**) fragmentation in ESI-MS.*

The ^{1}H ^{1}H COSY correlations between H-1 to H-2, H-2 to H-3, H-3 to H-4 and H-4 to NH assigned the core structure of the left part of the compound and those between H-6 to H-7, H-7 to H-(8-11) and H-(8-11) to H-12 assigned the core structure of the right part. The presence of the *N*-nitrosohydroxylamine functional group was proposed due to the chemical shift of H-3 at 4.2 ppm and C-3 at 77.8 ppm indicating an electron-withdrawing group attached to C-3. A non-correlating deshielded proton at 11.72 ppm in addition with a ESI-MS fragment displaying a loss of 30 Da for **134** were further evidence for the presence of a *N*-nitrosohydroxylamine group.

[140] R. Vessecchi, A. E. M Crotti, T. Guaratini, P. Colepicolo, S. E. Galembeck, N. P. Lopes, *Mini-Rev. Org. Chem.* **2007**, *4*, 75–87.

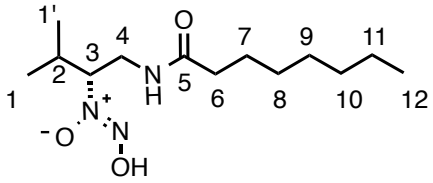

fragin (**133**)

Table **10**. ^{1}H-NMR Spectroscopic data ($CDCl_3$, 500 MHz) of fragin (**133**).

C/N no.	δ_C, type	δ_H ($^3J_{H-H}$ in Hz)	COSY
1+1'	19.2, CH_3	0.90, d (6.7)	2
	18.9, CH_3	1.07, d (6.8)	2
2	29.1, CH	2.25 - 2.17, m	1, 3
3	78.0, CH	4.20, td (9.2, 3.1)	2, 4a, 4b
NOH		11.72	
4	39.1, CH_2	3.86, ddd (14.4, 6.0, 3.1)	NH, 3, 4b
		3.60, ddd (14.4, 9.4, 6.1)	NH, 3, 4a
NH		5.69	4a, 4b
5	173.7, C		
6	36.7, CH_2	2.14, td (7.4, 1.8)	7
7	25.7, CH_2	1.61 - 1.52, m	6, 8-11
8 - 11	22.8 29.1, 29.3, 31.8, 4xCH_2	1.31 - 1.23, m	7, 12
12	14.2, CH_3	0.87, t (6.8)	8-11

Fragin (**133**) was identified with a single crystal X-ray analysis of our isolated natural product (figure **17**). **133** was isolated in 1967 from *Pseudomonas fragi* and was found to possess various biological activities as antifungal, growth inhibitor of lettuce seeds, antimicrobial, antiviral and antitumor.[141] The structure of fragin (**133**) was confirmed by a racemic total synthesis followed by an X-ray crystal structure analysis.[142,143] So far the absolute configuration remained unknown. To elucidate the absolute configuration of fragin (**133**), we developed an enantioselective total synthesis and after single crystal X-ray analysis the stereocenter of the natural product could be assigned. Additionally it was found that the single crystal X-ray analyses from the synthetic and isolated compound gave an identical result.

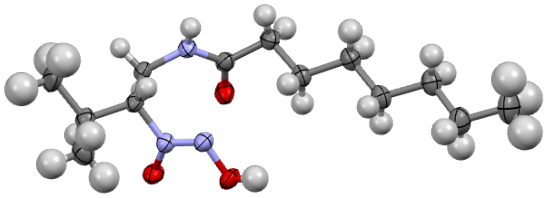

*Figure **17**: Single crystal X-ray analysis of fragin **133**.*

[141] A. Murayama, K. Hata, S. Tamura, *Agric. Biol. Chem.* **1969**, *33*, 1599–1605; A. Murayama, S. Tamura, *Agric. Biol. Chem.* **1970**, *34*, 122–129; A. Murayama, S. Tamura, *Agric. Biol. Chem.***1970**, *34*, 130–134.
[142] S. Tamura, A. Murayama, K. Kagei, *Agric. Biol. Chem.* **1967**, *31*, 996–997.
[143] R. Chang, W. Shin, *Acta Crystallogr., Sect. C: Cryst. Struct. Commun.* **1998**, *54*, 827–829.

3.2.2. Biosynthesis of Fragin

The function of the enzymes, involved in the biosynthesis of fragin (**133**), was predicted based on the DNA similarities that they shared with known proteins. Using this result a chemical reaction was assigned to each enzyme and their role in the biosynthesis of fragin (**133**) was proposed. To test these hypotheses, knockout strains were prepared and their metabolites pr

ofiles were analyzed by HPLC-MS.

Table **11**. Role of the ham gene cluster enzymes.

Enzymes	***Predicted Function***
HamA	β-Ketoacyl synthase
HamB	Dioxygenase
HamC	*N*-Oxygenase
HamD	NRPS complex
HamE	Unknown protein
HamF	NRPS condensation domain
HamG	Aminotransferase

3.2.2.1. Chemical Function of Enzymes

- **HamA: β-ketoacyl synthase**

The β-ketoacyl synthases (KS) are typically present in polyketide synthase (PKS) complexes and are responsible for the chain elongation of fatty acids.[144]

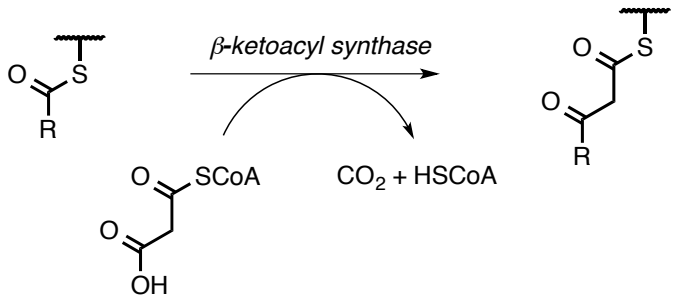

*Scheme **19** Reaction catalyzed by β-ketoacyl synthase.*

[144] Y. Chen, E. E. Kelly, R. P. Masluk, C. L. Nelson, D. C. Cantu, P. J. Reilly, *Protein Sci.* **2011**, *20*, 1659–1667.

- **HamB: dioxygenase, e. g.: acetylacetone dioxygenase**

The predicted function of the enzyme indicated similarities with several dioxygenases, as an example the acetylacetone dioxygenase (scheme **20**).[145] Therefore, we propose that HamB initiates an oxidative cleavage.

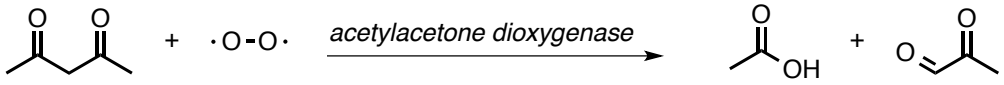

*Scheme **20**: Acetylacetone dioxygenase reaction.*

- **HamC: *N*-oxygenase, similarity with AurF**

The enzyme AurF was discovered during the study of aureothin biosynthesis and was found to oxidize *para*-aminobenzoic acid (PABA) (**135**) into *para*-nitrobenzoic acid (PNBA) (**136**).[146] An amine in *para* position was found to be important for the substrate recognition by the enzyme and a two-steps oxidation was suggested for the mechanism (scheme **21**).[147,148]

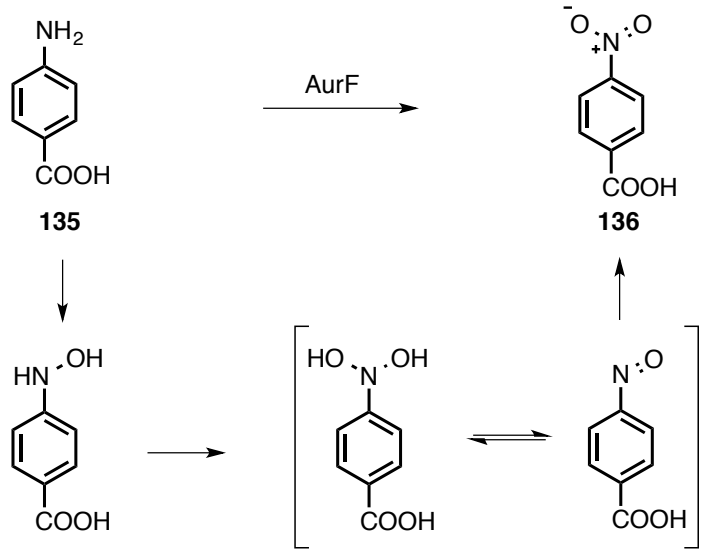

*Scheme **21**: Enzymatic oxidation of PABA (**135**) catalyzed by AurF.*

[145] I. Siewert, C. Limberg, *Angew. Chem., Int. Ed. Engl.* **2008**, *47*, 7953–7956.
[146] J. He, C. Hertweck, *Chem. Biol.* **2003**, *10*, 1225–1232.
[147] R. Winkler, M. E. A. Richter, U. Knüpfer, D. Merten, C. Hertweck, *Angew. Chem. Int., Ed. Engl.* **2006**, *45*, 8016–8018.
[148] R. Winkler, C. Hertweck, *Angew. Chem., Int. Ed.* **2005**, *44*, 4083–4087.

- **HamD: NRPS complex**

The NRPS enzyme complex was predicted to contain an adenylation (A), a peptidyl carrier protein (PCP) and a reductase (Red) domain. The A and PP domains are known for the attachment of amino acid to the NRPS complex and the R domain for the release of the product from the NRPS complex.

- **HamE: unknown protein**

The function of this enzyme could not be assigned by comparison with other proteins.

- **HamF: NRPS condensation domain**

The condensation domain of the NRPS complex catalyzed the formation of an amide bond from a fatty acid and an amino acid moiety.[149]

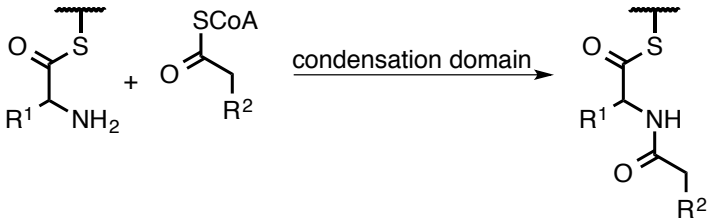

*Scheme **22**: Reaction of the NRPS condensation domain.*

- **HamG: Aminotransferase**

Aminotransferases transfer ketoacid to amino acid and consequently are responsible for the introduction of a new stereocenter.[150]

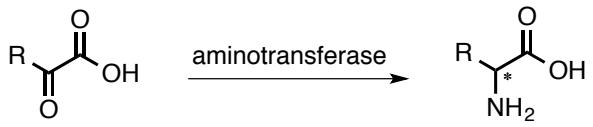

*Scheme **23**: Reaction catalyszed by aminotransferase.*

[149] C. Rausch, I. Hoof, T. Weber, W. Wohlleben, D. H. Huson, *BMC Evol. Biol.* **2007**, *7*:78.
[150] P. P. Taylor, D. P. Pantaleone, R. F. Senkpeil, I. G. Fotheringham, *Trends Biotechnol.* **1998**, *16*, 412–418.

3.2.2.2. Fragin Biosynthesis Proposal from L-Hydroxyleucine

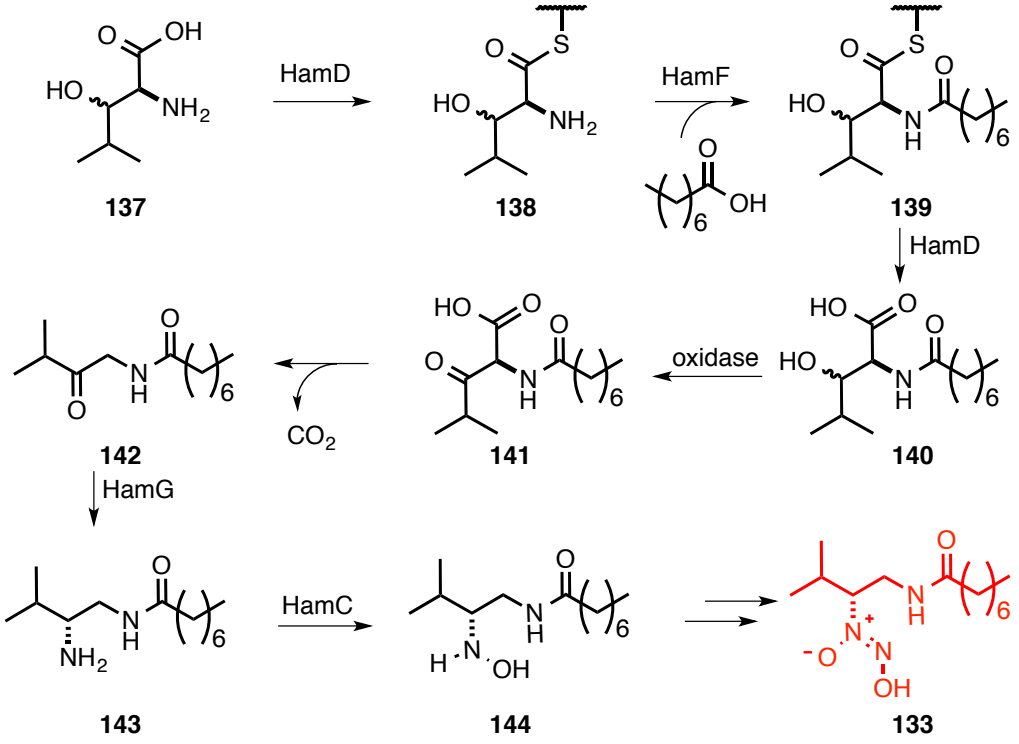

*Scheme **24**: Proposed biosynthesis with L-hydroxyleucine (**137**) as precursor.*

L-Hydroxyleucine (**137**) was chosen as the initial precursor of fragin biosynthesis and was proposed to react with HamD. The second step is the formation of the amide bond by the condensation domain of HamF. The release of **139** from the NRPS complex by the R domain of HamD followed by an oxidation of the hydroxyl to the ketone delivers the β-keto acid intermediate **141**. This unstable intermediate **141** is typically reported as an ideal substrate for a spontaneous decarboxylation.[151]

Next the aminotransferase, HamG, introduces the primary amine obtaining **143**. The last steps of the biosynthesis include the oxidation of the nitrogen to the hydroxylamine (**144**) by HamC followed by the introduction of the second nitrogen to obtain fragin (**133**). We proposed that the formation of the *N*-nitrosohydroxylamine to undergo *via* nucleophilic attack of the hydroxylamine **144** to an electrophilic source of N=O. (scheme **25**). The origin of the second nitrogen remained unclear and this question was the subject of the chapter 3.2.2.4.

[151] L. Du, L. Lou, *Nat. Prod. Rep.* **2010**, *27*, 255–278.

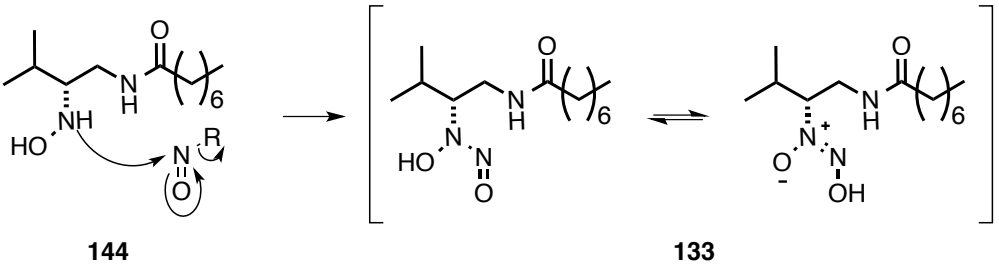

144 **133**

*Scheme **25**: Proposed mechanism for the N-N bond formation from the hydroxylamine **144** to fragin (**133**).*

Proposed Precursors Involved in the Biosynthesis of Fragin

In order to obtain evidence for the proposed biosynthetic pathway *via* L-hydroxyleucine (**137**), several suggested intermediates were synthesized and their retention time and MS fragmentation pattern were recorded by HPLC-MS. We used this information to detect the compounds in the bacterial extracts. With this approach the derivatives ketone **142**, amine **143**, hydroxylamine **144**, oxime **145**, nitroso **146** and nitro **147** were synthesized and their data were acquired by HPLC-MS (table **12**).

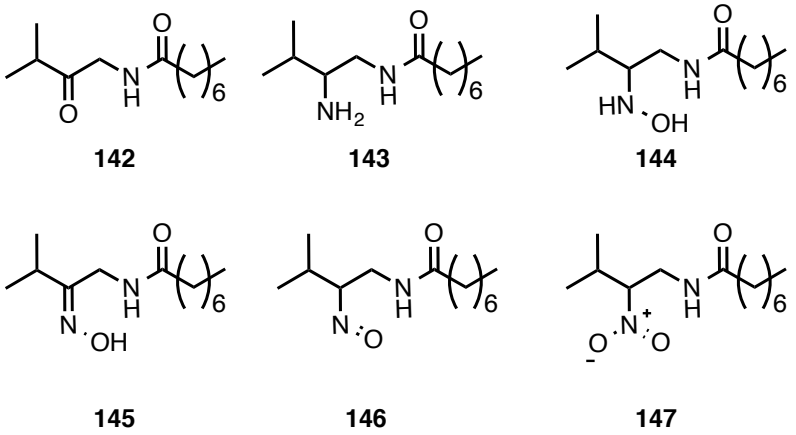

142 **143** **144**

145 **146** **147**

*Figure **18**: Synthetically prepared proposed intermediates involved in the biosynthesis of fragin (**133**).*

Table **12**. HPLC-MS Detection of Synthetic Intermediates.

Intermediates	**Retention Time [min]**	**MS [*m/z*]**
Amine **143**	11.6	229s
Hydroxylamine **144**	12.3	245
Oxime **145**	19.1	226/243
Ketone **142**	20.3	228
Nitro **147**	22.3	259/300
Nitroso **146**	28.4	243

The proposed biosynthetic precursors amine **143**, hydroxylamine **144** and oxime **145** were successfully identified in the extract from *B. cenocepacia H111*. However, the presence of the ketone **142**, displaying a *m/z* = 228 Da, could not be determined due to its overlap in retention time with fragin (**133**). Additionally the nitroso **146** and the nitro **147** could not be detected in this extract.

Knockout Experiments

Additional information about the function of the genes involved in the biosynthesis of fragin (1**33**) was obtained by the generation of several mutants. These strains were obtained by selectively removing a gene from the wild type strain. The nomenclature of the knockout strains is presented in the table **13**. We noticed the presence of fragin (**133**) in the extract of the mutant 869 implying than the enzyme HamB was not essential for the formation of the natural product fragin (**133**). To test if the knockout did not affect the other genes, a control experiment was executed where the gene *hamE* was inserted to the knockout strain Δ*hamE*. In this new strain 834 the production of fragin (**133**) was detected indicating that other genes are not affected. Unfortunately in the others knockout strains none of the proposed biosynthetic intermediates were found. This result indicates that fragin (**133**) is produced by another pathway. We deduced that the biosynthetic precursors stays attached to the NRPS domain and are released at a later stage (chapter 3.2.2.3).

Table **13**. Knockout strains from *B. cenocepacia H111*.

Strain	Gene mutated	Detection of fragin
811	None	yes
825	*hamD*	
826	*hamE*	
834	*hamE*[a]	yes
835	*hamG*	
841	*hamC*	
869	*hamB*	yes

[a] The gene hamE was reinserted to the knockout strain 826 as a control experiment.

3.2.2.3. Proposed Biosynthesis of Fragin from D-Valine

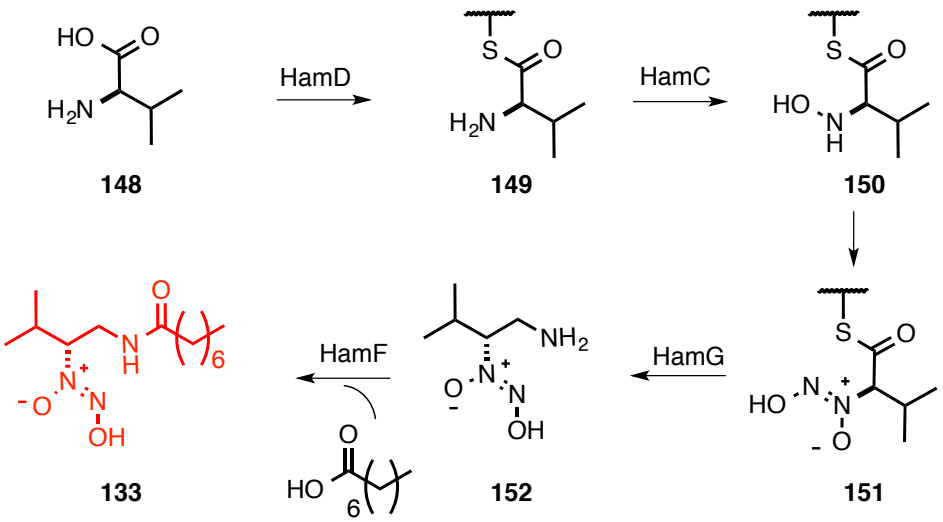

*Scheme **26**: Proposed biosynthesis of fragin (**133**) from D-valine (**149**).*

As the intermediates of the proposed biosynthesis from **137** were not detected in the knockout strains, it was deduced that the compounds **143**, **144** and **145**, identified in the wild type extract, were decomposition products of fragin (**133**).. A new biosynthetic pathway was proposed starting with the non-proteinogenic amino acid D-valine (**148**), which reacts first with HamD. Next the nitrogen atom of the amine **149** is oxidized by HamC to the hydroxylamine **150**, which reacts with a second source of nitrogen to form the *N*-nitrosohydroxylamine **151**. The release of **151** from the NRPS domain is catalyzed by the R domain of HamD giving an aldehyde, which is directly converted to the amine

152 by HamG. Similar mechanism of NRPS reductase was already proposed for the biosynthesis of the natural product myxochelin B (**153)** (scheme **27**).[152] The last step of the biosynthesis of **133** involves the amide bond formation by the condensation domain of HamF.

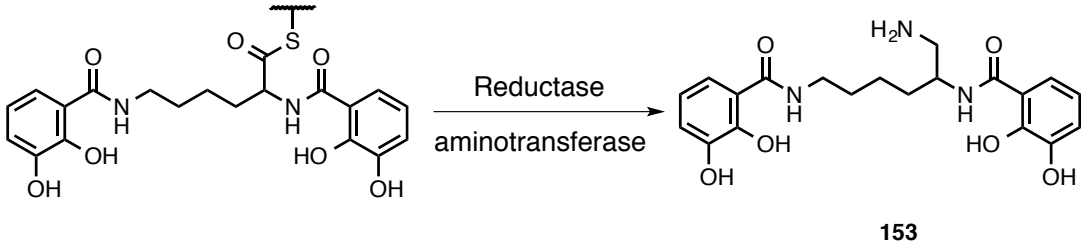

*Scheme **27**: Proposed release mechanism from the NRPS complex in the biosynthesis of myxochelin B (**153**).*

The validation of this proposal is currently investigated in our research groups. We are planning to perform feeding experiments with ^{15}N labeled D and L-valine in order to confirm the role of the amino acid in the biosynthesis of fragin (**133**).

[152] Y. Li, K. J. Weissman, R. Müller, *J. Am. Chem. Soc.* **2008**, *130*, 7554–7555.

3.2.2.4. Origin of the Nitrogen Atoms of the N-N Bond of Fragin

The mechanism of N-N bond formation in natural products remained unclear. Up to date no studies have been investigated the formation of *N*-nitrosohydroxylamine. In this work the predicted fragin precursors hydroxylamine **144** and nitroso **146** were synthesized and used as a model system to explore their reactivity and stability under various conditions.

Reactivity of the Hydroxylamine 144

In order to test the nucleophilic or electrophilic character of the hydroxylamine **144**, the compound was treated with five nitrogen-containing salts (figure **19**). Interestingly we found that the hydroxylamine **144** reacted with the salt $NaNO_2$ to give fragin (**133**).

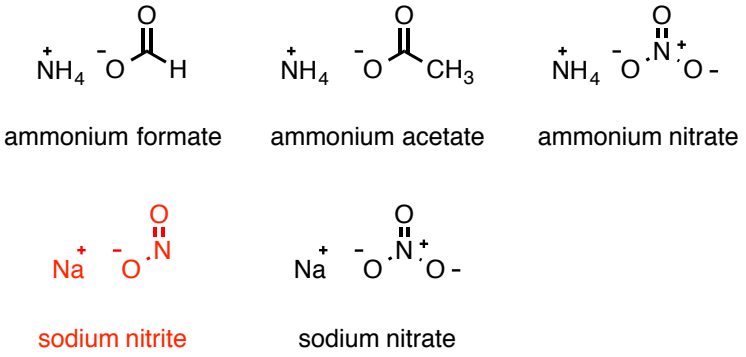

*Figure **19**: Possible source for the second nitrogen atom.*

This result was unexpected due to the absence of strong acidic condition, which is usually required for the synthesis of the nitrosonium ion (Scheme **28**). It is possible that the high concentration of $NaNO_2$ (65 µM) compared to the hydroxylamine **144** (0.9 µM) produced the nitrosonium ion in small amount, which reacted with **144**. This mechanism has to be further investigated but this result indicated that nitrite in presence with the hydroxylamine **144** can produce fragin (**133**).

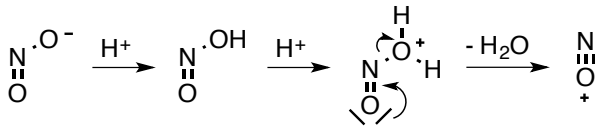

*Scheme **28**: Nitrosonium ion formation under acidic condition.*

Further reactions with **144** and $NaNO_2$, in buffer solutions fixed at a pH of 6.5 and 7.85, showed the formation of fragin (**133**) mainly in weak acidic conditions (pH = 6.5). The oxime **145** was detected at the major product during the reaction in basic buffer.

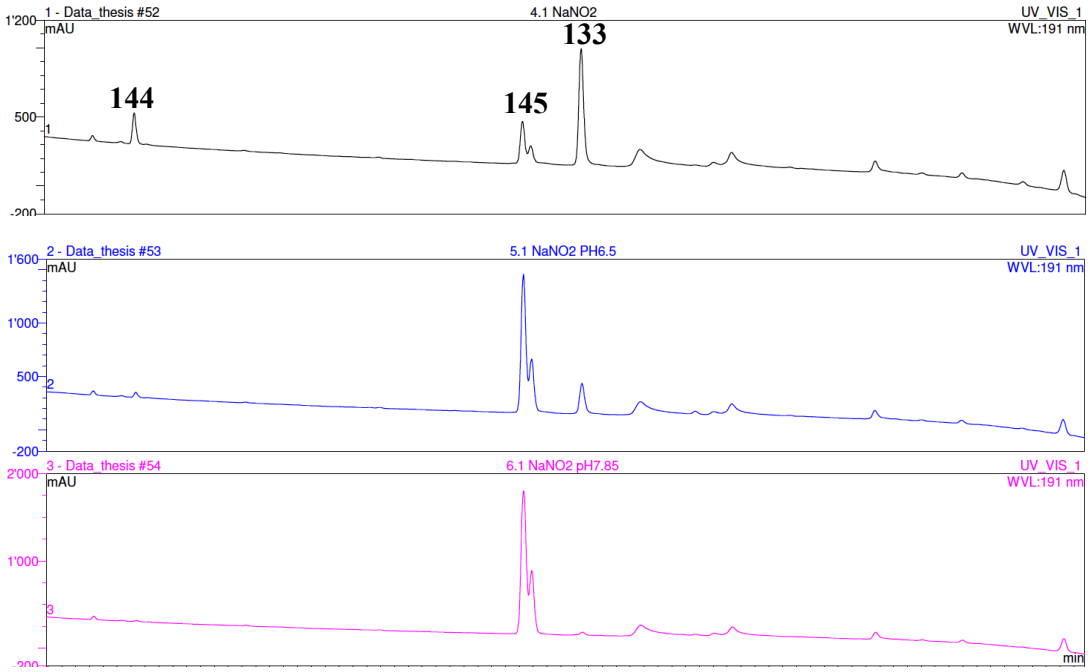

*Figure **20**: HPLC chromatograms of the reaction between $NaNO_2$ and the hydroxylamine **144**. From top to bottom the conditions used were without buffer, with buffer at pH 6.5 and with buffer at 7.85.*

To study in details the incorporation of the second nitrogen atom, a reaction with the hydroxylamine **144** and $Na^{15}NO_2$ was analyzed at three different time points; after the sample preparation, after 24 h and after 44 h. The incorporation of ^{15}N to fragin was confirmed by ESI-MS experiment where the pseudomolecular ion with a *m/z* = 275 Da was detected. Additionaly, the fragment with a *m/z* = 244 Da was detected indicating the loss of ^{15}NO showing that only one nitrogen was introduced to fragin (**133**). The results of the analysis over time showed the conversion of the labeled fragin (**133**) and the hydroxlamine **144** into the oxime **145** and the nitro **147** (figure **21**).

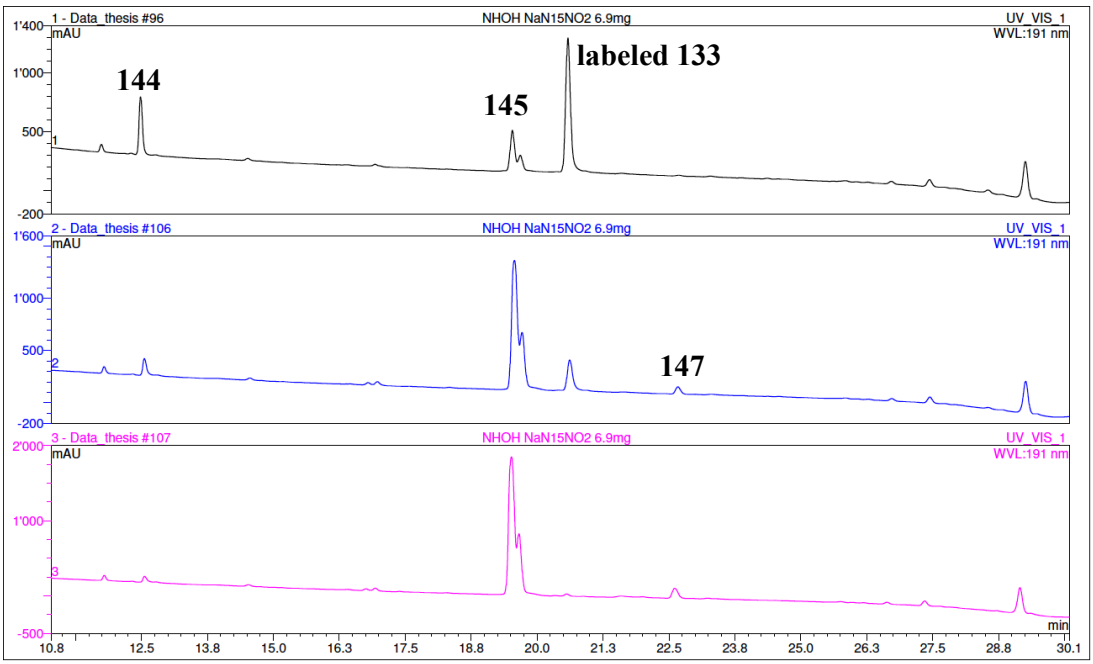

*Figure **21**: HPLC chromatograms of the reaction between $Na^{15}NO_2$ and hydroxylamine **144**. From top to bottom: after simple preparation and after 24 h and after 44 h.*

Prediction of Nitrite in *Burkholderia Cenocepacia* H111

Knowing that the hydroxylamine **144** in presence of sodium nitrite gave fragin (**133**), we decided to investigate if this reaction may occur spontaneously in the bacterium. For this reason we searched for a source of nitrite. Interestingly, recently it was reported that *B. cenocepacia* H111 possesses genes responsible for nitrate reduction and nitrate/nitrite transporters.[153] This implies that nitrate could be transformed to nitrite. The salts of the bacterial medium were analyzed and neither nitrate nor nitrite was added to the culture. However, the composition of a yeast extract, one component of the medium, was unknown and we decided to perform further tests.

To test the presence of nitrite in the yeast extract, the hydroxylamine **144** was mixed with the yeast extract but fragin **133** could not be detected. The concentration of nitrate/nitrite in yeast extract solutions at different concentration was measured using a stripes test developed for the detection of NO_3^- and NO_2^-. The results indicated the presence of nitrate in the yeast extract. With this information we can now propose that the

[153] M. Lardi, C. Aguilar, A. Pedrioli, U. Omasits, A. Suppiger, G. Cárcamo-Oyarce, N. Schmid, C. H. Ahrens, L. Eberl, G. Pessi, *Appl. Environ. Microbiol.* **2015**, DOI 10.1128/AEM.00694-15.

nitrate, from the yeast extract, is transformed by the bacteria into nitrite, which will be attacked by the hydroxylamine **144** to form fragin (**133**). To obtain evidence for this pathway *in vivo*, we are planning feeding experiments with $Na^{15}NO_2$ and $Na^{15}NO_3$ as it was performed for azamerone (**90**).[125]

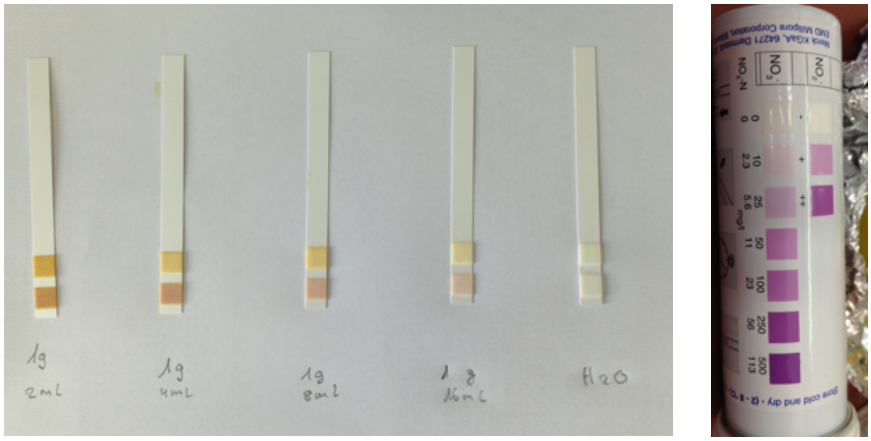

*Figure **22**: Stripes test detection done in various concentrations of aq. yeast extract soln. and with H_2O as a control. A purple coloration indicated the presence of the specific ion; at the top nitrite and at the bottom nitrate.*

3.3. Conclusion

A fundamental question consisting in the N-N bond formation by nature is addressed in this chapter by the biosynthetic study of the natural product fragin (**133**) possessing the unusual *N*-nitrosohydroxylamine functional group. The structure of **133** was elucidated and a gene cluster responsible for its biosynthesis was identified. The functions of seven enzymes involved in the production of **133** were predicted and based on this information, a biosynthetic pathway was proposed. To verify this route, mutant strains were produced and suggested biosynthetic intermediates were synthesized. Analysis of the mutant extracts indicated that the substrates were released only at a late stage of the biosynthesis. Additionally, evidence for a stepwise and spontaneous mechanism for the N-N bond formation was discovered. It was shown that the hydroxylamine **144** in presence of $NaNO_2$ could produce fragin (**133**) non-enzymatically.

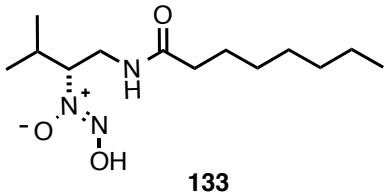

133

3.4. Outlook

The challenge of the biosynthetic elucidation of fragin (**133**) is the detection of its precursors. In the different mutant strains, no compounds were identified as potential precursors and we suspect that the biosynthetic intermediate(s) is/are released from the NRPS complex only at a late stage. To overcome this obstacle feeding experiments with proposed precursors would furnish crucial information. Additionally, *in vitro* assays using purified enzymes would unambiguously assign the role of each protein.

4. Cyanobacteria a Prolific Source of Natural Products

Cyanobacteria constitute some of the oldest organisms on Earth, their presence dating back over 2.8 billion years, and are considered as the first producers of oxygen.[154] To harvest light, cyanobacteria are equipped with chlorophyll, absorbing maximum of light at 430-440 nm and 670 nm, and a complementary set of pigments named phycobilisome, absorbing light with a maximum at 500 nm.[155] Additionally, cyanobacteria possess heterocysts, which consist of specialized cells that fixe and transform N_2 into NH_3.[156] An example of a cyanobacterium is presented at a macroscopic and microscopic level (figure **23**).

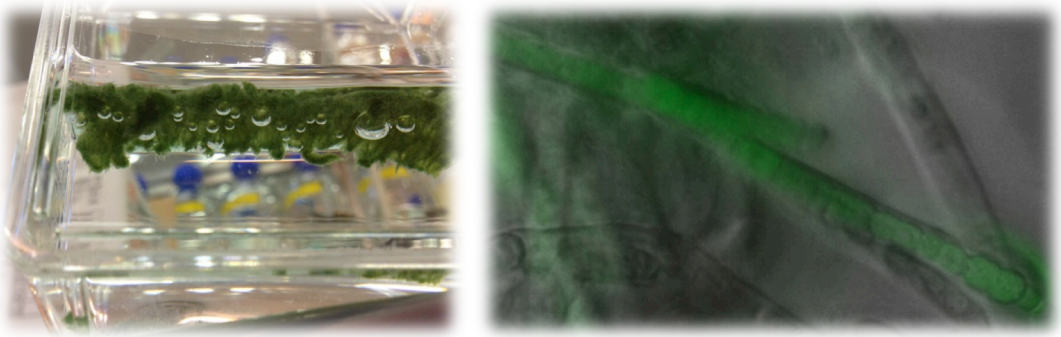

*Figure **23**: Pictures of the cyanobacterium Tolypothrix distorta var. symplocoides EAWAG 224a at a macroscopic and microscopic level (from left to right).*

Some cyanobacteria possess similar appearance to algae (figure **23,** left side) and it is therefore why they have been considered, for long time, as eukaryotic organisms and were called blue-green algae. In the 1970s, the analysis of cyanobacteria cellular properties showed that these organisms do not belong to the eukaryotic kingdom. Therefore a new classification and their integration to the Bacteriological code were proposed.[157]

---

[154] R. E. Kopp, J. L. Kirschvink, I. A. Hilburn, C. Z. Nash, *Proc. Natl. Acad. Sci. U. S. A.* **2005**, *102*, 11131–11136.

[155] Y. S. Deruyter, P. Fromme, Molecular structure of the photosynthetic apparatus. In *Cyanobacteria, Molecular Biology, Genomics, and Evolution* (Eds.: A. Herrero, E. Flores). Caister Academic Press, Norfolk, UK, **2008**, pp. 217–269.

[156] A. Herrero, A. M. Muro-Pastor, E. Flores, *J. Bacteriol.* **2001**, *183*, 411–425.

[157] R. Y. Stanier, W. R. Sistrom, T. A. Hansen, B. A. Whitton, R. W. Castenholz, N. Pfennig, V. N. Gorlenko, E. N. Kondratieva, K. E. Eimhjellen, R. Whittenbury, R. L. Gherna, H. G. Trüper, *Int. J. Syst. Bacteriol.* **1978**, *28*, 335–336; R. Rippka, J. Deruelles, J. B. Waterbury, M. Herdman, R. Y. Stanier, *J. Gen. Microbiol.* **1979**, *111*, 1–61.

Cyanobacteria are particularly interesting for the field of drug discovery due to biological activities and the various scaffolds of their secondary metabolites.[158] Among these natural products, peptides and their derivatives have been extensively reported.[159] Presented here is a collection of cyclic peptides with a particular attention on cyanobactins and cylic glycolipopeptides.

4.1. Cyclic Peptides

Cyclic peptides isolated from cyanobacteria have been investigated for their biological activities and for their biosynthesis. Interestingly, both non-ribosomal and ribosomal biosynthetic pathways were discovered to be responsible for the production of these compounds.[160] As an example, the hepatotoxic microcystins, produced by many cyanobacterial genera as *Microcystis*, *Anabaena*, *Planktothrix*, *Nostoc* and *Anabaena*, are cyclic peptides containing the unusual amino acid ADDA (figure **24**). The most study natural product from this class of compounds is microcystin-LR (**154**), which was found to be a common contaminant in drinking water. Due to its high toxicity the World Health Organization (WHO) determined a guideline value of 1 µg/L.[161] Additionally, genomic analysis of *M. aeruginosa* PCC 7806 indicated that the biosynthesis of **154** involved a nonribosomal peptide synthetase (NRPS) gene cluster.[162]

[158] A. Burja, B. Banaigs, E. Abou-Mansour, J. Grant Burgess, P. Wright, *Tetrahedron* **2001**, *57*, 9347–9377; K. Gademann, C. Portmann, *Curr. Org. Chem.* **2008**, *12*, 326–341; K. Gademann, *Chimia* **2011**, *65*, 416–419; K. Gademann, S. Sieber, *Chimia* **2011**, *65*, 835–838; J. K. Nunnery, E. Mevers, W. H. Gerwick, *Curr. Opin. Biotechnol.* **2010**, *21*, 787–793; G. E. Chlipala, S. Mo, J. Orjala, *Curr. Drug Targets* **2011**, *12*, 1654–1673; M. Costa, J. Costa-Rodrigues, M. H. Fernandes, P. Barros, V. Vasconcelos, R. Martins, *Mar. Drugs* **2012**, *10*, 2181–2207; F. Desriac, C. Jégou, E. Balnois, B. Brillet, P. Le Chevalier, Y. Fleury, *Mar. Drugs* **2013**, *11*, 3632–3660.

[159] A. Burja, B. Banaigs, E. Abou-Mansour, J. Grant Burgess, P. Wright, *Tetrahedron* **2001**, *57*, 9347–9377.

[160] M. Welker, H. von Döhren, *FEMS Microbiol. Rev*. **2006**, *30*, 530–563.

[161] M. Zhou, W.-W. Tu, J. Xu, *Toxicon* **2015**, *101*, 92–100.

[162] E. Dittmann, B. A. Neilan, M. Erhard, H. Von Döhren, T. Börner, *Mol. Microbiol.* **1997**, *26*, 779–787.

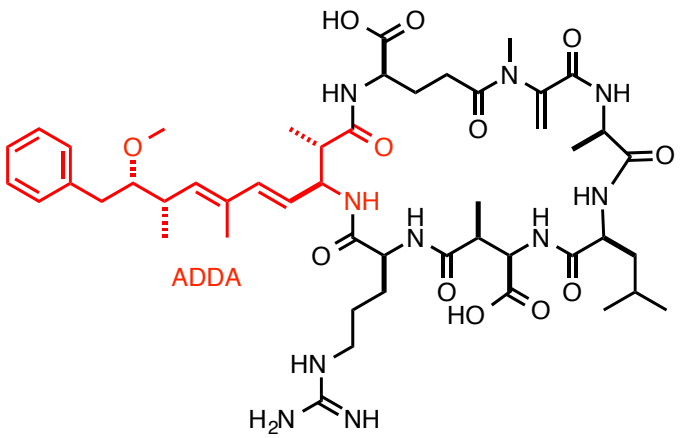

microcystin-LR (**154**)

*Figure **24**: Microcystin-LR (**154**) with its amino acid ADDA in red.*

4.1.1. Cyanobactins

The cyanobactin class of compounds was recently introduced to describe cyclic peptides containing a prenylated amino acid or a heterocyclic ring such as oxazole, oxazoline, thiazole or thiazoline.[163] The genome of the cyanobacterial symbiont *Prochloron didemni* was sequenced and it was found that the organism used a ribosomal biosynthetic pathway to obtain patellamide A (**155**) and C (**156**).[164] In this section, examples of cyanobactins produced *via* a ribosomal biosynthetic pathway will be presented.

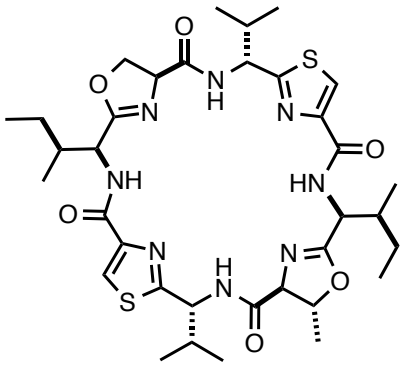

patellamide A (**155**)

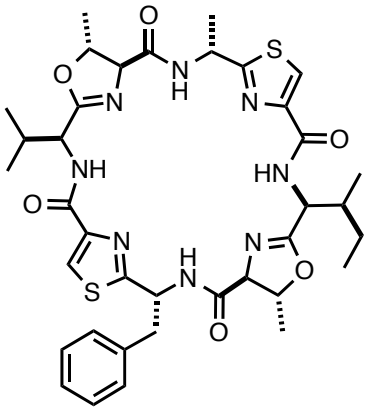

patellamide C (**156**)

[163] M. S. Donia, J. Ravel, E. W. Schmidt, *Nat. Chem. Biol.* **2008**, *4*, 341–343; E. W. Schmidt, M. S. Donia, in *Methods in Enzymology*, Elsevier, **2009**, pp. 575–596.

[164] E. W. Schmidt, J. T. Nelson, D. A. Rasko, S. Sudek, J. A. Eisen, M. G. Haygood, J. Ravel, *Proc. Natl. Acad. Sci. U. S. A.* **2005**, *102*, 7315–7320.

Cyanobactins from *Prochloron*/*Lissoclinum*

Cyanobactins have been isolated from the ascidian *Lissoclinum* sp. and it was proposed that the compounds were produced by the cyanobacterial symbiont *Prochloron* sp. This hypothesis was verified for patellamide A (**155**) and C (**156**) by Schmidt and coworkers with the identification of the biosynthetic gene cluster in the cyanobacterial genome.[164] Several natural products have been isolated from this system with variation in the number of amino acids (from 6 to 8) in their core structure. As examples the hexapeptide patellin 2 (**157**),[165] the cytoxic lissoclinamide 7 (**158**) [166] and the prenylated cyanobactin trunkamide A (**159**)[167] highlight the structure variety of the natural products isolated from the symbiotic system *Lissoclinum*/*Prochloron*. Interestingly the elucidation of the absolute configuration of trunkamide A (**159**) required several total syntheses.[168]

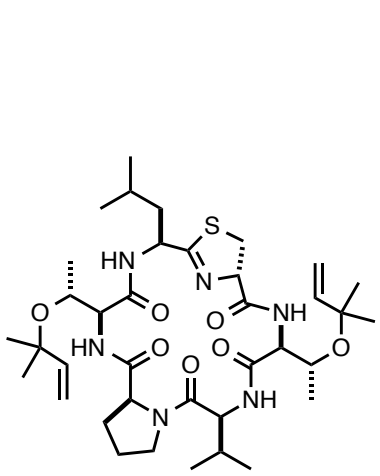

patellin 2 (**157**)

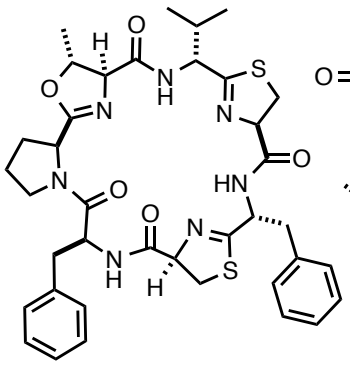

lissoclinamide 7 (**158**)

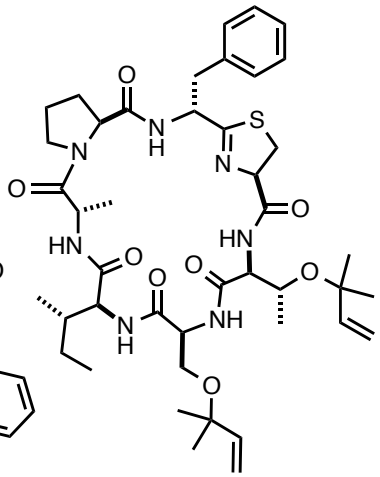

trunkamide A (**159**)

[165] T. M. Zabriskie, M. P. Foster, T. J. Stout, J. Clardy, C. M. Ireland, *J. Am. Chem. Soc.* **1990**, *112*, 8080–8084.

[166] J. M. Wasylyk, J. E. Biskupiak, C. E. Costello, C. M. Ireland, *J. Org. Chem.* **1983**, *48*, 4445–4449; B. M. Degnan, C. J. Hawkins, M. F. Lavin, E. J. McCaffrey, D. L. Parry, A. L. Van den Brenk, D. J. Watters, *J. Med. Chem.* **1989**, *32*, 1349–1354; C. J. Hawkins, M. F. Lavin, K. A. Marshall, A. L. van den Brenk, D. J. Watters, *J. Med. Chem.* **1990**, *33*, 1634–1638; L. A. Morris, J. J. K. van den Bosch, K. Versluis, G. S. Thompson, M. Jaspars, *Tetrahedron* **2000**, *56*, 8345–8353.

[167] A. R. Carroll, J. C. Coll, D. J. Bourne, J. K. MacLeod, T. M. Zabriskie, C. M. Ireland, B. F. Bowden, *Aust. J. Chem.* **1996**, *49*, 659–667.

[168] P. Wipf, Y. Uto, *J. Org. Chem.* **2000**, *65*, 1037–1049; B. McKeever, G. Pattenden, *Tetrahedron Lett.* **2001**, *42*, 2573–2577; J. M. Caba, I. M. Rodriguez, I. Manzanares, E. Giralt, F. Albericio, *J. Org. Chem.* **2001**, *66*, 7568–7574; B. McKeever, G. Pattenden, *Tetrahedron* **2003**, *59*, 2713–2727.

Cyanobactins from *Nostoc spongiaeforme* var. *tenue*

Tenuecyclamides A-D were isolated from the cyanobacterium *Nostoc spongiaeforme* var. *tenue* with an isolation yield of 0.05, 0.01, 0.02 and 0.06%, respectively. Tenuecyclamide C (**160**) was found to be the most potent of these compounds inhibiting the cellular division of sea urchins with an ED_{100} of 9.0 μM.

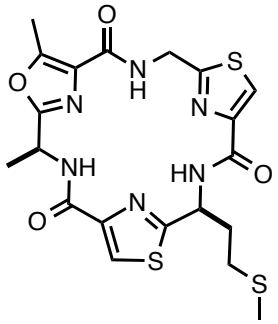

tenuecyclamide C (**160**)

Cyanobactins from *Trichodesmium erythraeum* IMS101

Genomic analysis of the cyanobacterium *Trichodesmium erythraeum* ISM101 led to the discovery of a new cyanobactin named trichamide (**161**). The structure elucidation of trichamide (**161**) was based on genetic and crude extract MS^2 analysis.[169] This example shows the potential of a genome mining approach.

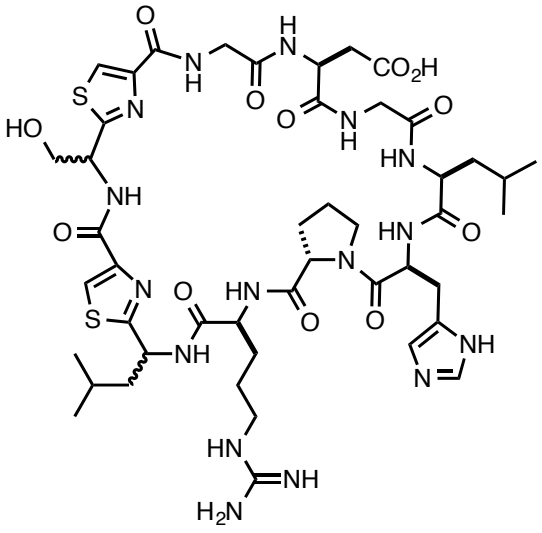

trichamide (**161**)

[169] S. Sudek, M. G. Haygood, D. T. A. Youssef, E. W. Schmidt, *Appl. Environ. Microbiol.* **2006**, *72*, 4382–4387.

Cyanobactins from *Lyngbya aestuarii* CCY9616.

The analysis of the *lyngbya aestuarii* CCY9616 genome led to the discovery of the gene cluster responsible for the production of lyngbyabactins A (**162**) and B (**163**). However, these compounds have not been isolated or detected from the crude extract of the cyanobacterium.[163]

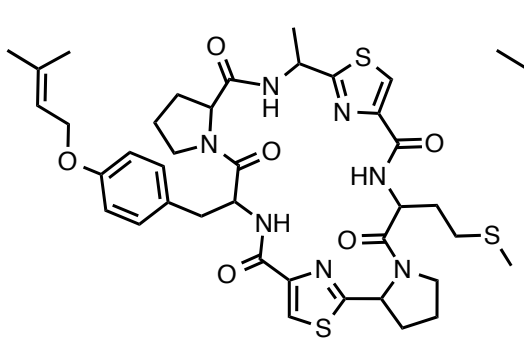

lyngbyabactin A (**162**)

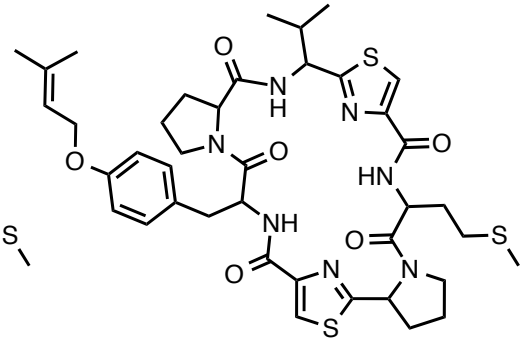

lyngbyabactin B (**163**)

Cyanobactins from *Microcystis aeruginosa*

Microcyclamides and aerucyclamides have been isolated from different species of *Microcystis aeruginosa*.[170,171,172,173] The gene cluster of microcyclamide was identified and the biosynthesis was proposed to undergo *via* a ribosomal pathway. During their biosynthetic investigations, Ziemert and coworkers discovered two new natural products, microcyclamides 7806A (**164**) and 7806B.[172] The same year, the structure of microcyclamide 7806A (**164**) was revised by NMR analysis and aerucyclamide C (**165**) degradation studies (scheme **29**).[173]

[170] K. Ishida, H. Nakagawa, M. Murakami, *J. Nat. Prod.* **2000**, *63*, 1315–1317.
[171] C. Portmann, J. F. Blom, K. Gademann, F. Jüttner, *J. Nat. Prod.* **2008**, *71*, 1193–1196.
[172] N. Ziemert, K. Ishida, P. Quillardet, C. Bouchier, C. Hertweck, N. T. de Marsac, E. Dittmann, *Appl. Environ. Microbiol.* **2008**, *74*, 1791–1797.
[173] C. Portmann, J. F. Blom, M. Kaiser, R. Brun, F. Jüttner, K. Gademann, *J. Nat. Prod.* **2008**, *71*, 1891–1896.

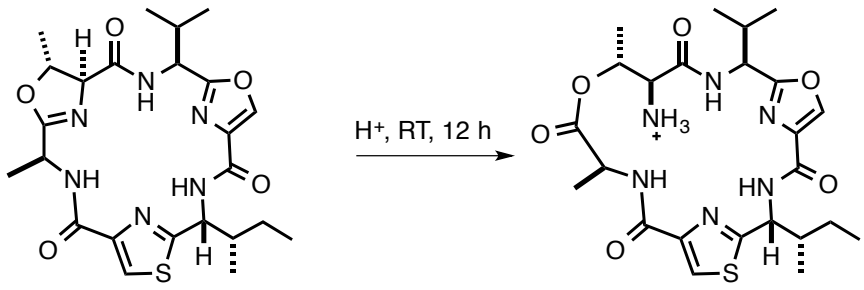

aerucyclamide C (**165**) microcyclamide 7806A (**164**)

*Scheme **29**: Conversion of aerucyclamide C (**165**) into microcyclamide 7806A (**164**) under acidic condition.*

Cyanobactin from *Anabaena* sp.

Another example of natural product isolated following a genome mining approach led the discovery of anacyclamide A 10 (**166**). The genomic analysis of the cyanobacterium *Anabaena* sp. 90 indicated the presence of a cluster of genes similar to the one of patellamides.[174] For this reason, it was proposed to include this compound, which possessed no modified and/or prenylated amino acid(s), into the cyanobactin class.[174]

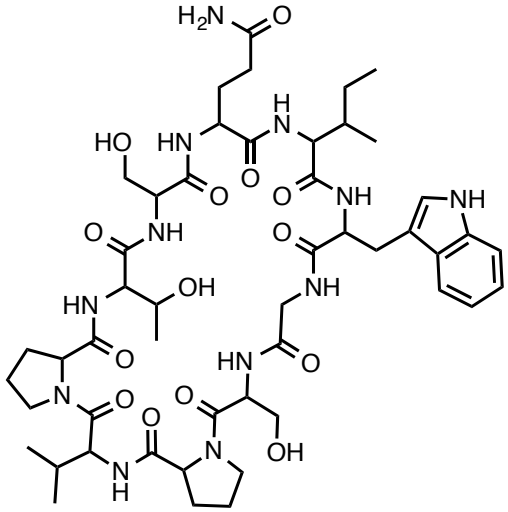

anacyclamide A10 (**166**)

[174] N. Leikoski, D. P. Fewer, J. Jokela, M. Wahlsten, L. Rouhiainen, K. Sivonen, *Appl. Environ. Microbiol.* **2010**, *76*, 701–709.

4.1.2. Glycolipopeptides

Hassallidins and balticidins are the only natural products, to our knowledge, that have been isolated from cyanobacteria and that contain the unique glycolipopeptide scaffolds.[175,176,177,178]

Hassallidin A (**167**) and B (**168**), produced by the cyanobacterium *Hassallia* sp., possess a macrolide core structure with one mannose molecule attached through a threonine side chain and a fatty acid forming an amide bond with the N-terminal of another threonine.[175,176] In hassallidin B (**168**), an additional rhamnose molecule is attached to one of the hydroxyl of the fatty acid. Both natural products were found to possess antifungal activity against several strains.[176] Recently, genomic analysis of *Anabaena* sp. 90 led to the discovery of hassallidins biosynthesis. During the course of this study, the natural product hassallidin D (**169**) was isolated and the structure was elucidated by MS and NMR analysis. The stereocenters configuration was assigned based on amino acids and genetic analysis. Furthermore, similar hassallidins' biosynthetic pathways were detected in several species such as *Aphanizomenon*, *Cylindrospermopsis raciborskii*, *Nostoc* and *Tolypothrix*. The presence of glycolipopeptides in these organisms was confirmed by HPLC-MS analysis.[177]

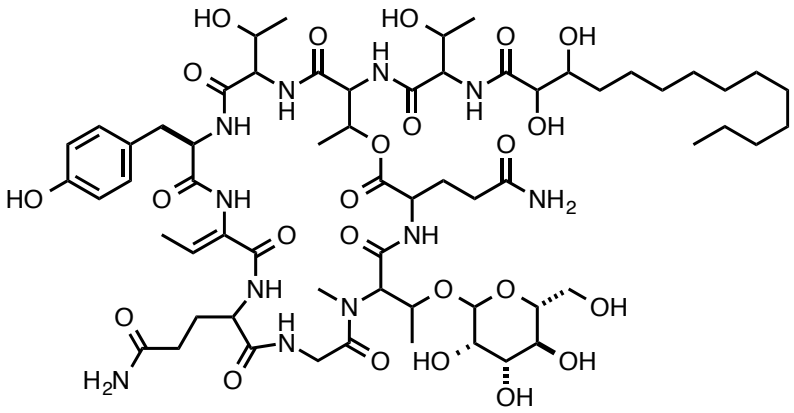

hassallidin A (**167**)

[175] T. Neuhof, P. Schmieder, K. Preussel, R. Dieckmann, H. Pham, F. Bartl, H. von Döhren, *J. Nat. Prod.* **2005**, *68*, 695–700.
[176] T. Neuhof, P. Schmieder, M. Seibold, K. Preussel, H. von Döhren, *Bioorg. Med. Chem. Lett.* **2006**, *16*, 4220–4222.
[177] J. Vestola, T. K. Shishido, J. Jokela, D. P. Fewer, O. Aitio, P. Permi, M. Wahlsten, H. Wang, L. Rouhiainen, K. Sivonen, *Proc. Natl. Acad. Sci. U. S. A.* **2014**, *111*, E1909–17.
[178] T.-H. Bui, V. Wray, M. Nimtz, T. Fossen, M. Preisitsch, G. Schröder, K. Wende, S. E. Heiden S. Mundt, *J. Nat. Prod.* **2014**, *77*, 1287–1296; T.-H. Bui, V. Wray, M. Nimtz, T. Fossen, M. Preisitsch, G. Schröder, K. Wende, S. E. Heiden, S. Mundt, *J. Nat. Prod.* **2015**, *78*, 345.

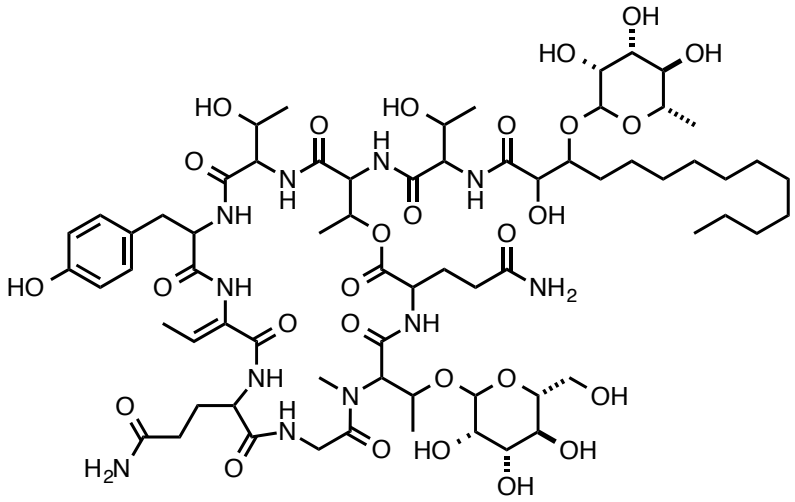

hassallidin B (**168**)

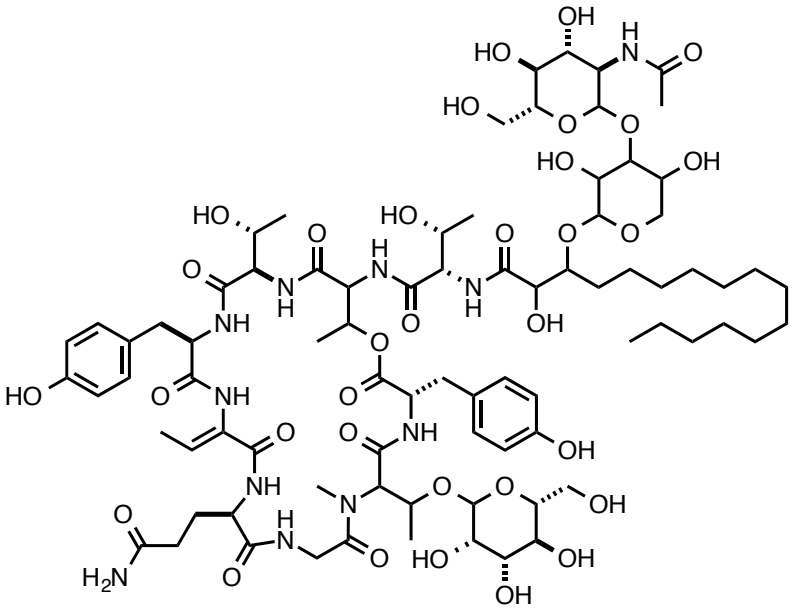

hassallidin D (**169**)

The antifungal compounds balticidins A-D (**170-173**) were isolated from the cyanobacterium *Anabaena cylindrical* strain Bio33 following a bioassay-guided fractionation. The main structural difference compared to hassallidins resides in a hydroxylated tyrosine and in the presence of a chloride attached to the fatty acid in the case of **170** and **171**. Furthermore, the sugars' composition was found to be different from hassallidins due to the presence of a disaccharide containing arabinose and galacturonic acid.[178]

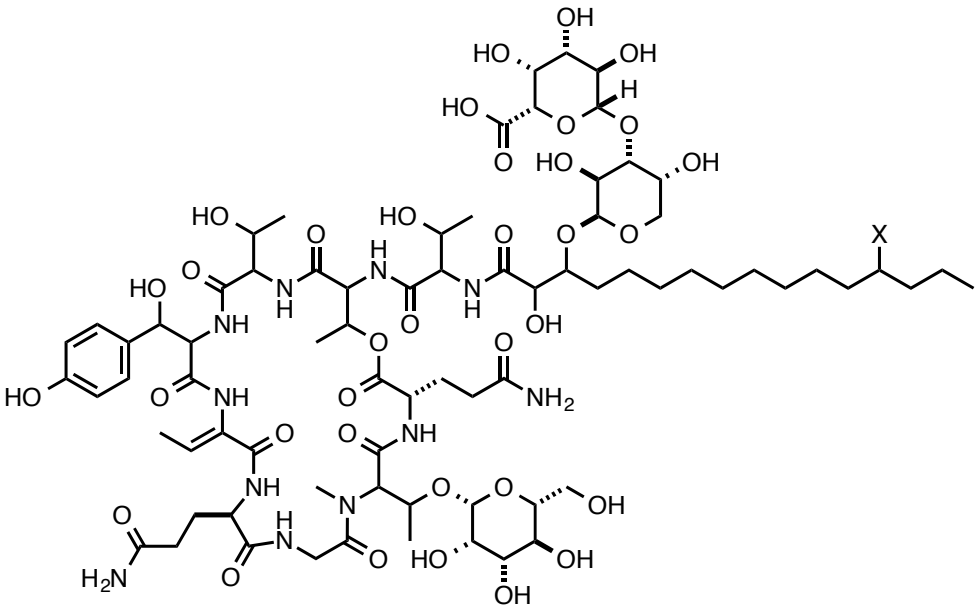

balticidin B (**171**); R = Cl
balticidin D (**173**); R = H

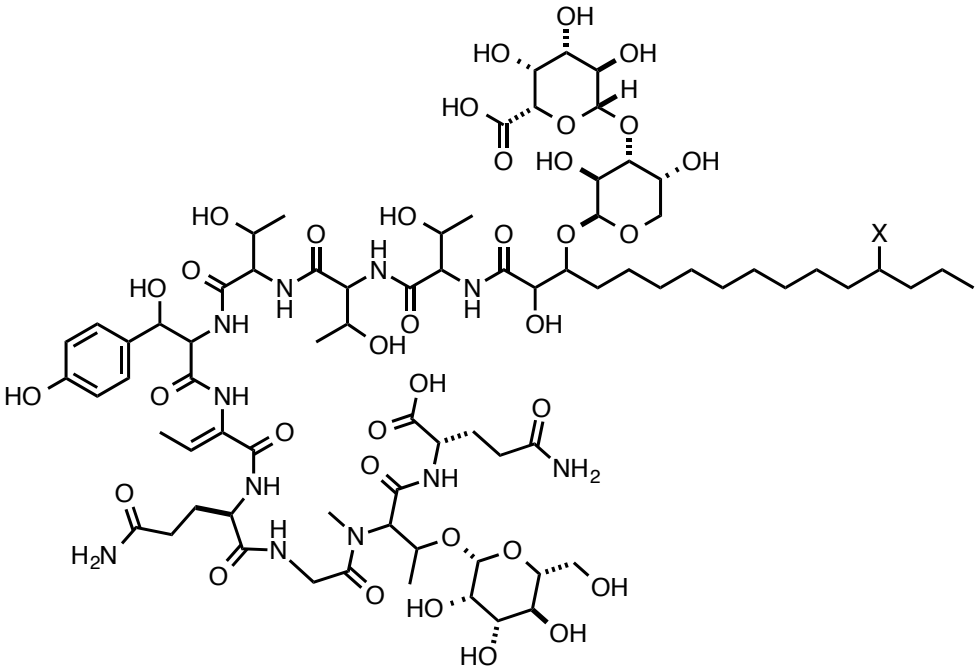

balticidin A (**170**); R = Cl
balticidin C (**172**); R = H

4.1.3. Cyclic Peptides Discovered by the Gademann Group

The search of new antimalarial natural products from cyanobacteria secondary metabolites have been of interest to our research group. We have access to more than 160 different cyanobacteria strains resulting in a collection with large chemical diversity (figure **25**). Previous results from Dr. Cyril Portmann and coworkers have led to the discovery of four new hexacyclopeptides (aerucyclamides A–D (**174, 175, 165** and **176**)) from the cyanobacterium strain *Microcystis aeruginosa* (*M. aeruginosa*) PCC 7806. It was found that the compounds possess a low micromolar and even submicromolar IC_{50} value against the parasite *Plasmodium falciparum* (*P. falciparum)* and a cytotoxicity of more than 100 µM (IC_{50} value against rat myoblast L6 cells, figure **26**).[171,173]

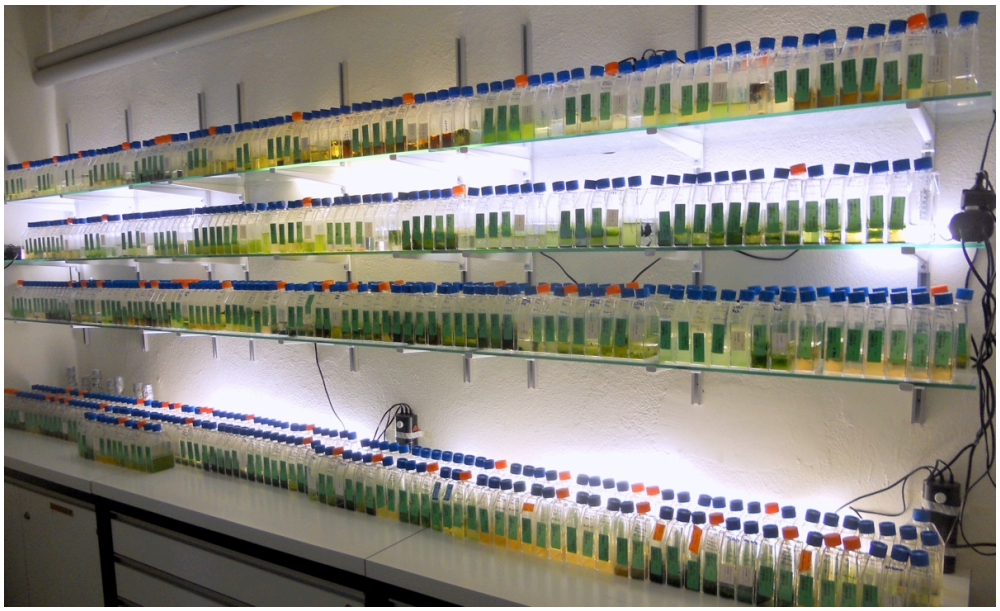

*Figure **25**: Cyanobacteria collection at the University of Basel.*

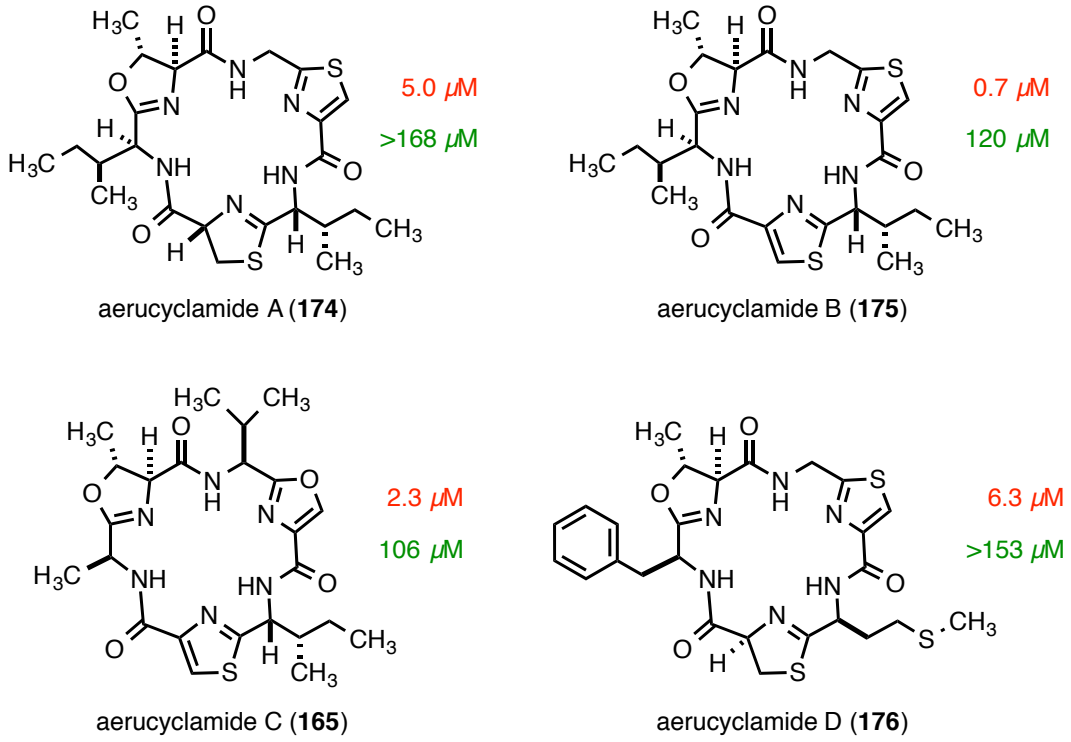

*Figure **26**: Structures of aerucyclamides A–D, the IC_{50} values against P. falciparum are indicated in red and in green, the cytotoxicity (IC_{50} against rat myoblast L6 cells).*

4.2. Results and discussion

In this chapter, the isolation and structure elucidation of the novel cyanobactins balgacyclamides A–C (**177-179**) and the isolation and preliminary structure elucidation towards two new glycolipopeptides are presented. There projects were carried out by M. Sc. Silvan Wirthensohn and by M. Sc. Darja Kolbin during their master thesis under my supervision.

4.2.1. Balgacyclamides from *M. aeruginosa* EAWAG 251[179]

Novel natural products, balgacyclamides A–C (**177-179**), sharing similar structure with aerucyclamides were detected in *M. aeruginosa* EAWAG 251 and isolated by Dr. Cyril Portmann. The core structure of these new natural products was determined by HRMS and NMR spectroscopy data analysis. Furthermore, balgacyclamide A (**177**) and balgacyclamide B (**178**) were found to possess an IC_{50} value of 9.0 µM and 8.2 µM, respectively, against the parasite *P. falciparum* and a cytotoxicity (IC_{50} against rat myoblast L6 cells) of more than 150 µM (figure **27**). However limited by the low isolation yield of 0.55, 0.15 and 0.80 mg per 15 L tank culture for balgacyclamide A (**177**), B (**178**) and C (**179**), the absolute configuration could not be determined and will be the subject of this chapter.

[179] C. Portmann, **S. Sieber**, S. Wirthensohn, J. F. Blom, L. Da Silva, E. Baudat, M. Kaiser, R. Brun, K. Gademann, *J. Nat. Prod.* **2014**, *77*, 557–562.

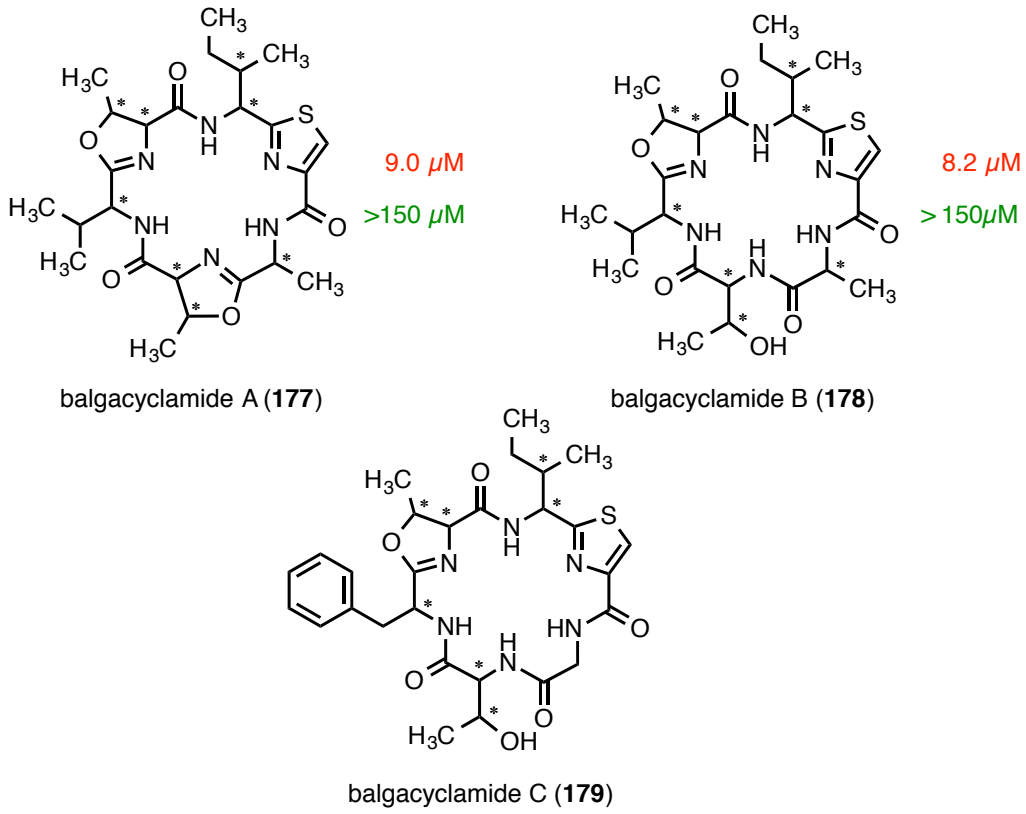

*Figure 27: Core structure of balgacyclamide A–C (**177–179**) with IC_{50} values against P. falciparum, indicated in red and in green the cytotoxicity (IC_{50} against rat myoblast L6 cells).*

4.2.1.1. Extraction and Isolation

The cyanobacterium *M. aeruginosa* EAWAG 251 was grown in a 20 L tank culture with constant aeration in order to ensure sufficient amount of material to complete the structure elucidation (the objective of this project). The cyanobacteria were harvested by removing the medium by centrifugation and then the compounds were extracted from the biomass by sonication in aqueous methanol solutions.

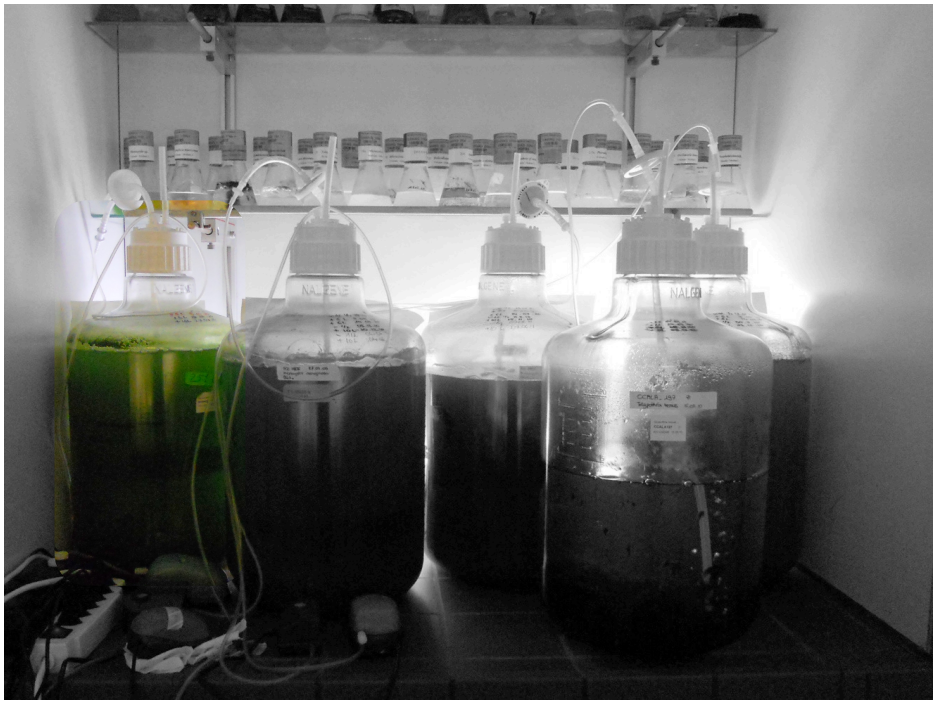

*Figure **28**: Cyanobacteria 20 L tank cultures, M. aeruginosa EAWAG 251 is highlighted on the left side of the picture.*

Balgacyclamides were isolated by RP-HPLC equipped with a semi-preparative Gemini-NX C_{18} column. The identity of the natural products was confirmed by comparing the retention time, the *m/z* and the ^{1}H-NMR spectra with previous results.

4.2.1.2. Ozonolysis and Hydrolysis

The strategy used for the stereochemistry determination was similar as the one reported for the aerucyclamides.[171, 173] The heterocycles of balgacyclamides (**177-179**) were opened by ozonolysis to prevent further epimerization of amino acids during hydrolysis.[180] The amide bonds were cleaved by heating the compounds in strong acidic condition and the mixture of amino acids obtained was separated in two equal aliquots to perform HPLC and GC analysis in parallel.

4.2.1.3. Marfey's Method for Amino Acids Analysis

To determine the absolute configuration of amino acids in balgacyclamides (**177-179**) Marfey's method was used. In this analytical method, the substrate reacts with a chiral reagent and the retention time of the product formed is compared by HPLC with analytical standards.[181] The design of the Marfey's reagent (**180**), containing a chromophore and functional groups with enhanced ionization properties, offers high UV sensitivity and MS detection. An example of the derivatization using the Marfey's reagent is shown for L-valine (**181**) in scheme **30**.

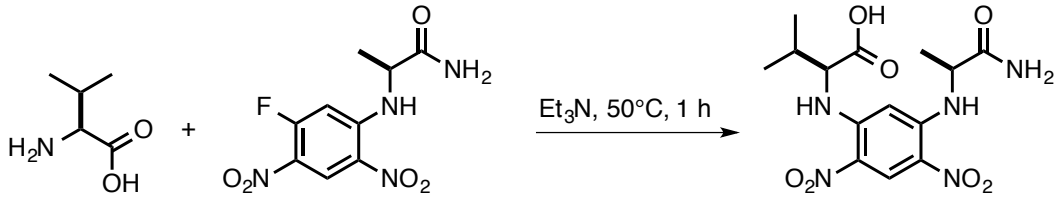

L-Val **181** Marfey's reagent **180**

*Scheme **30**: Reaction of L-valine (**181**) with Marfey's reagent (**180**).*

Following a reported protocol for the derivatization with Marfey's reagent (**180**) and HPLC analysis,[182] we could determined the amino acids configuration of the balgacyclamides A-C (**177-179**) with the exception of isoleucine. In this case, the separation between D-Ile and D-*allo*-Ile derivatives was not sufficient by HPLC. Additionally, a coinjection with L-Thr and L-*allo*-Thr was necessary to confirm the presence of L-Thr.

[180] L. A. McDonald, C. M. Ireland, *J. Nat. Prod.* **1992**, *55*, 376–379.
[181] P. Marfey, M. Ottesen, *Carlsberg Res. Commun.* **1984**, *49*, 585–590.
[182] S. Hess, *Methods Mol. Biol.* **2012**, *828*, 63–75.

4.2.1.4. TFA Derivatization and GC Analysis

To differentiate between D-Ile and D-*allo*-Ile, the amino acids were derivatized with freshly prepared trifluoroacetic anhydride (TFAA) and analyzed with a GC apparatus equipped with a chiral column. A coinjection confirmed the presence of D-*allo*-Ile in balgacyclamides A–C (**177**-**179**).

Combining the results obtained from amino acids analysis by HPLC and chiral GC the absolute configuration of the natural products was determined as D-Ala, L-Thr, L-Val and D-*allo*-Ile for balgacyclamide A (**177**), D-Ala, L-Thr, L-Val and D-*allo*-Ile for Balgacyclamide B (**178**) and L-Phe, L-Thr, Gly and D-*allo*-Ile for balgacyclamide C (**179**).[179]

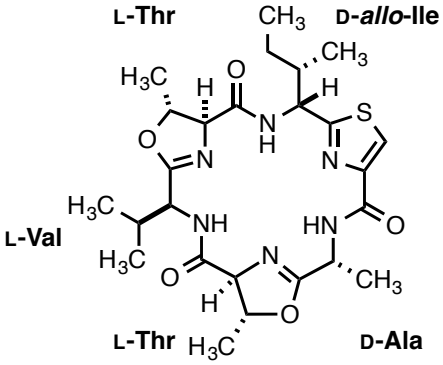

balgacyclamide A (**177**)

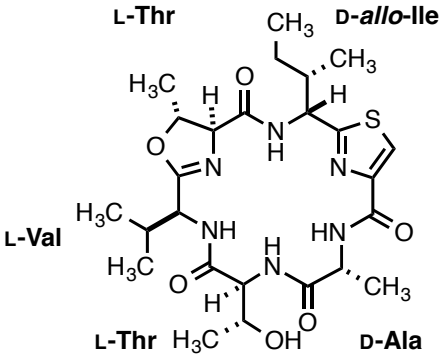

balgacyclamide B (**178**)

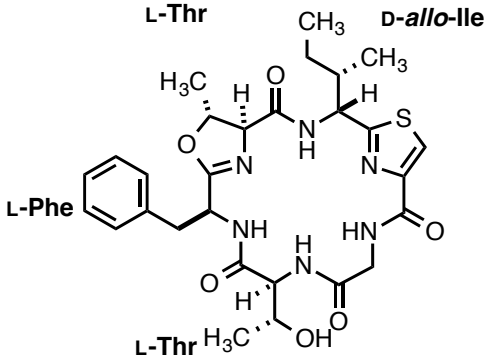

balgacyclamide C (**179**)

*Figure **29**: Balgacyclamides A–C (**177-179**) with the absolute configuration assigned.*

4.2.2. Conclusion

Baglacyclamides A–C (**177**–**179**) were isolated from the cyanobacterium *M. aeruginosa* and the absolute configuration of these natural products was elucidated. We showed that with only 0.1 mg of natural product, the amino acids configuration could be determined using Marfey's method and chiral-GC analysis.

Since balgacyclamides A–C (**177**–**179**) contain heterocycles in their core structure, we proposed to include them in the cyanobactin class of compounds. Furthermore, we proposed that their biosynthesis undergoes *via* a ribosomal pathway as for several compounds sharing similar structures.

Interestingly the non-proteinogenic amino acid D-*allo*-Ile was found in each balgacyclamide and was already reported for the aerucyclamides A–C (**174**, **175** and **165**). The formation of this non-proteinogenic amino acid was proposed to occur spontaneously and not enzymatically for lissoclinamide 7 (**158**)[183] and a similar mechanism can be envisaged for the balgacyclamides. Additionally, an interesting feature of D-*allo*-Ile is its position with respect to the thiazole/thiazoline. For **165**, **174**, **175**, **177**, **178** and **179**, D-*allo*-Ile is next to the fully unsaturated heterocycle.

Furthermore, balgacyclamide A (**177**) and B (**178**) exhibit promising antimalarial activity with good selectivity relative to their cytotoxicity.

[183] B. F. Milne, P. F. Long, A. Starcevic, D. Hranueli, M. Jaspars, *Org. Biomol. Chem.* **2006**, *4*, 631–638.

4.3. Glycolipopeptides from *Tolypothrix distorta* var. *symplocoides* EAWAG 224a

Based on a previous results on the evaluation of antiparasitic activity of several cyanobacteria strains, it was found that the crude extract of *Tolypothrix distorta* var. *symplocoides* (*T. distorta* var. *symplocoides*) EAWAG 224a exhibited micromolar activity against *Trypanosoma brucei rhodesiense* (*T. b. rhodesiense*), *Leishmania donovani* (*L. donovani*) and *P. falciparum* (Table **14**).[184]

Table **14**: Crude extract activity of EAWAG 224a.[a]

Tested against	**IC_{50} (µg/mL)**
T. b. rhodesiense	35.55
T. cruzi	>90
L. donovani	58.53
P. falciparum	9.61
Rat myoblast L6 Cells	>90

[a]: *T. distorta* var. *symplocoides* EAWAG 224a.

The result of the screening showed promising antimalarial activity for the cyanobacterium *T. distorta* var. *symplocoides* EAWAG 224a. Therefore, a bioassay-guided fractionation following by our efforts towards the structure elucidation was carried out and will be discussed in this chapter.

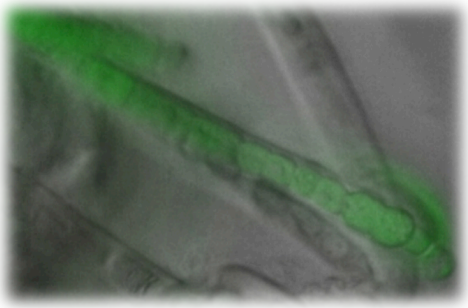

*Figure **30**: Microcscopic picture of T. distorta var. symplocoides EAWAG 224a.*

[184] C. Portmann, PhD thesis, École Polythechnique Fédéral de Lausanne (CH), **2008**, EPFL, Lausanne

4.3.1. Extraction

The cyanobacterium *T. tolypothrix distorta* var. *symplocoides* EAWAG 224a was grown in several 250 mL cultures equipped with vented caps. The biomass was collected by centrifugation and the compounds were extracted from the biomass by repeated sonications in aqueous methanol.

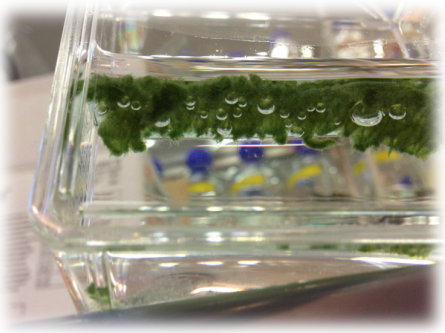

*Figure **31**: Picture of a T. distorta var. symplocoides EAWAG 224a 250 mL culture.*

4.3.2. Bioassay-guided Fractionation

The crude extract was separated by semi-preparative HPLC into 10 fractions. Each fraction was tested for its antimalarial activity. Fraction 4 (F4) was found to be the most potent with an IC_{50} value of 4.87 µg/mL (figure **32**).

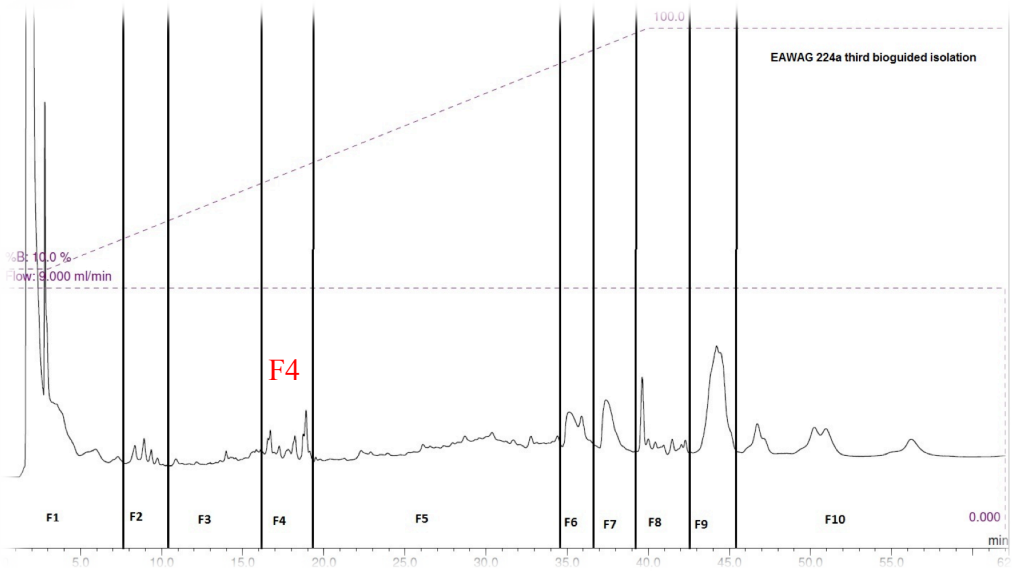

*Figure **32**: HPLC chromatogram of T. distorta var. symplocoides EAWAG 224a crude extract.*

F4 was further separated to obtain an active fraction composed of only three compounds. By repeating the extraction and isolation process with careful control of the temperature (35°C) during evaporation, one peak disappeared from the HPLC chromatogram. The missing compound was then proposed to be an artifact of isolation and we decided to focus our effort on the purification and structure characterization of the two other natural products.

4.3.3. Structure Elucidation Results

The first indication of the structure of the two unknown compounds was obtained during the analysis of the UV and mass spectra recorded during the HPLC separation. Absorption maxima were found for both compounds around 193, 223 and 276 nm, which is characteristic for peptide containg amide bonds (190 and 220 nm) and aromatic side chains (250-300 nm).[185] Furthermore, a *m/z* = 1634 Da for $[M+1]^+$ was detected for the first compound and a *m/z* = 1677 Da for $[M+1]^+$ for the second compound. A literature search of isolated peptides from *Tolypothrix sp.* with a molecular weight in the range of 1600–1700 Da revealed that recently, a compound similar to hassallidin A (**167**) was detected in *Tolypothrix sp*. extract.[175,177] Therefore it was proposed that the first and second isolated compounds were glycolipocyclopeptides, named GLCP-1 (**182**) and GLCP-2 (**183**), respectively, possessing a similar scaffold as **167**.

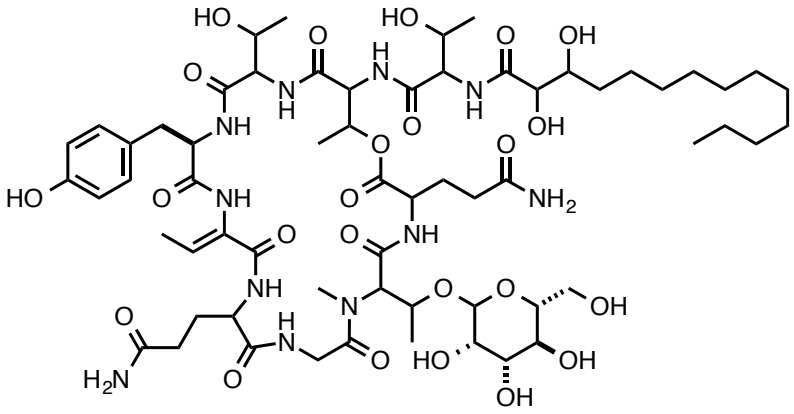

hassallidin A (**167**)

[185] M. R. Liyanage, K. Bakshi, D. B. Volkin, C. R. Middaugh, in *Methods Mol. Biol.,* Humana Press, Totowa, NJ, **2013**, pp. 225–236.

4.3.3.1. HRMS and HRMS^2 Analysis

The tandem mass spectrometry analyses for GLCP-1 (**182**) and GLCP-2 (**183**) were achieved by Dr. Nadine Bohni on a UHPLC-QTOFMS system. In both cases, the mass chosen for the experiment was the doubly charge pseudo-molecular ion $[M+2H]^{2+}$, which was 817.90078 Da for GLCP-1 (**182**) and 839.40274 Da for GLCP-2 (**183**). The different MS fragments from the two natural products, with their structure interpretation, are shown below (figures **33** and **34**).

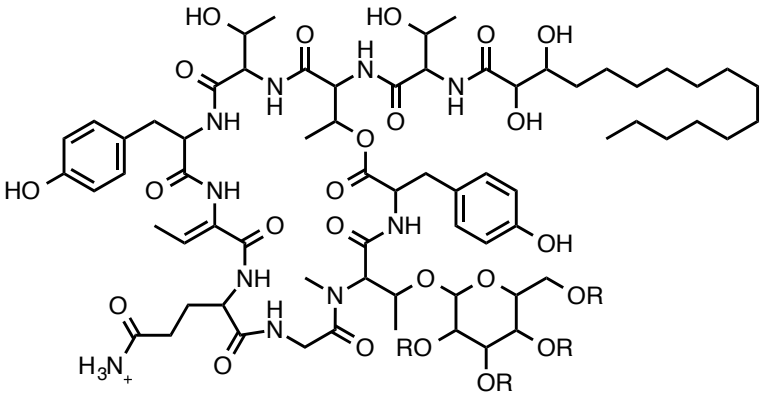

184 4R = 3H and 1$CONH_2$
Exact Mass: 1488.73558
Detected: 1488.72864
Δppm: 4.66

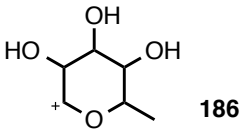

186
Exact Mass: 147.06519
Detected: 147.06323
Δppm: 13.4

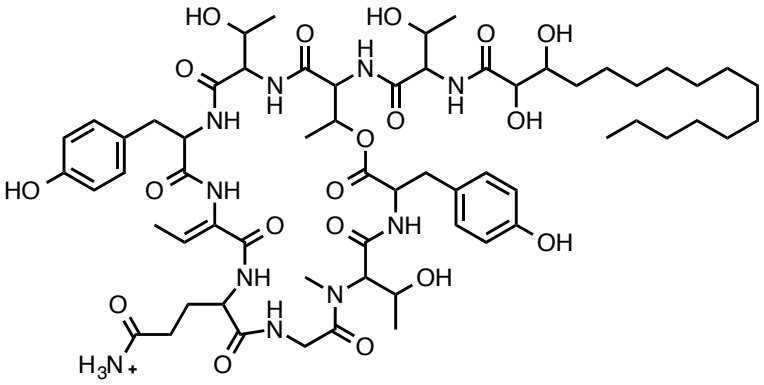

185 Exact Mass: 1283.67750
Detected: 1283.67950
Δppm: 1.56

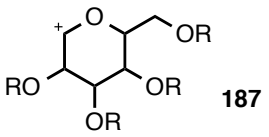

187
4R = 3H and 1$CONH_2$
Exact Mass: 206.06591
Detected: 206.06429
Δppm: 7.86

*Figure **33**: Fragments detected during HRMS^2 experiment of GLCP-1 (**182**), a proposed structure for each ion is shown.*

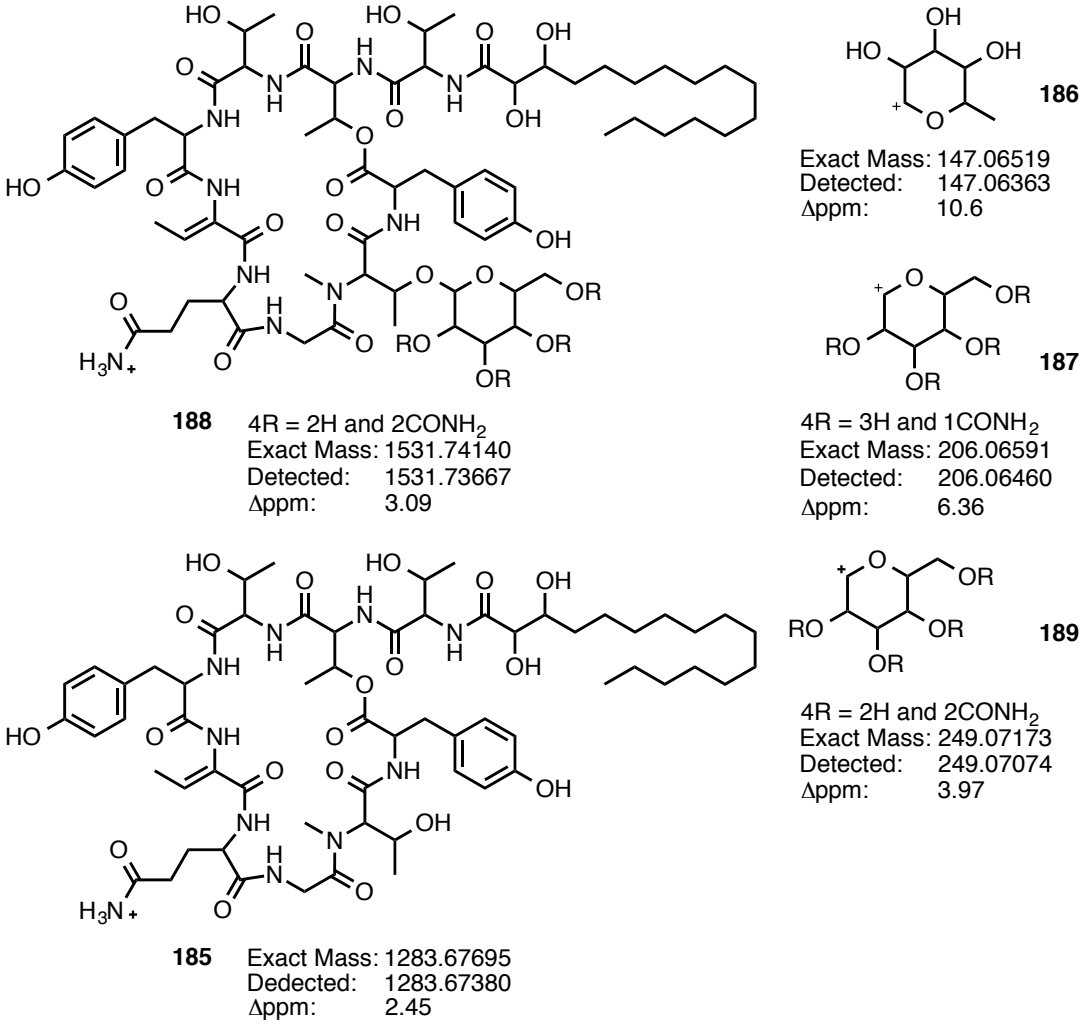

*Figure **34**: Fragments detected during HRMS^2 experiment of GLCP-2 (**183**), a proposed structure for each ion is shown.*

GLCP-1 (**182**) and GLCP-2 (**183**) displayed an exact mass of *m/z* 817.90078 Da and 839.40274 Da, respectively, which supports the molecular formula of $C_{75}H_{117}N_{11}O_{29}$ for the $[M+2H]^+$ pseudo-molecular ion of **182** and $C_{76}H_{118}N_{12}O_{30}$ for the $[M+2H]^+$ pseudo-molecular ion of **183**.

The core structure elucidation of GPLC-1 (**182**) and GPLC-2 (**183**) was deduced by comparing the fragment ion **185**, found in **182** and **183**, with the HRMS^2 available data on hassallidins[175–177] and balticidins.[178] We realized that the same ion was reported for

hassallidin D (**169**) and therefore we proposed that our natural products shared the same aglycone core structure **185** (figure **35**).

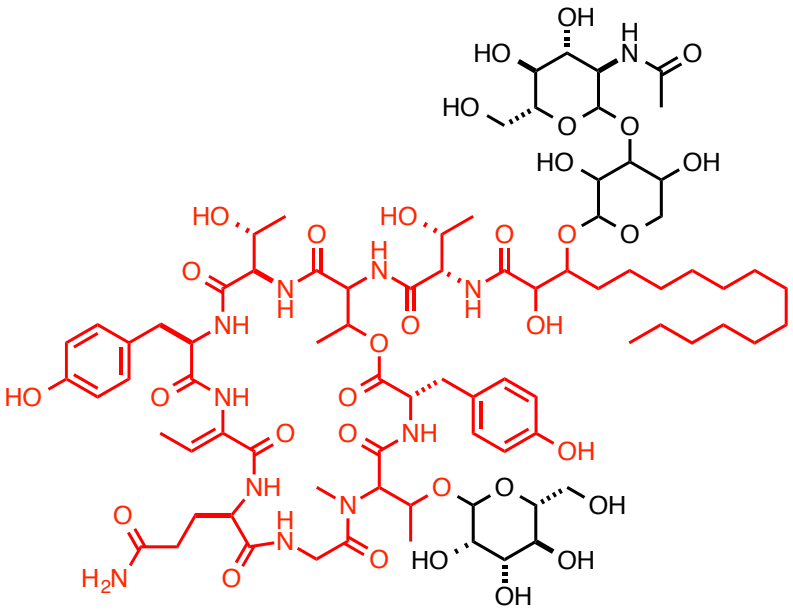

hassallidin D (**169**)

*Figure **35**: Structure of hassallidin D (**169**) with the assigned stereochemistry. The aglycone core structure **185** is highlighted in red.*

The presence of a deoxyhexose in GLCP-1 (**182**) and GLCP-2 (**183**) was supporting by the fragment ion **186**. Further evidence for this sugar was deduced by the ions **184** and **188**, which represent GLCP-1 (**182**) and GLCP-2 (**183**), respectively without a deoxyhexose.

The ion **187,** also detected in both compounds, was proposed to be a hexose possessing one carboxamide group. In the case of GLCP-2 (**183**) a hexose possessing two carboxamide groups was proposed to correspond to the fragment **189**. With these results it was deduced that GLCP-1 (**182**) possesses a hexose with one carboxamide group and GLCP-2 (**183**) possesses a hexose with two carboxamide groups.

Furthermore, an analysis of hassallidins and balticidins composition revealed that mannose was the carbohydrate attached to *N*-Me-Thr and that the deoxyhexose of hassallidin B (**168**) was identified as rhamnose (table **15**).[175–178] Taking into account these results, we propose that the carbohydrates in GLCP-1 (**182**) and GLCP-2 (**183**) are rhamnose and mannose.

Table **15**: Carbohydrates present in hassallidins and balticidins.

Glycolipopeptides	Attached to *N*-Me-Thr	Attached to OH of fatty acid
hassallidin A (**167**)	mannose	none
hassallidin B (**168**)	mannose	rhamnose
hassallidin C	n.d.	n.d.
hassallidin D (**169**)	mannose	pentopyranose-(3-1)-GlcNAc
balticidin A (**170**)	mannose	Ara(3-1)GalA
balticidin B (**171**)	mannose	Ara(3-1)GalA
balticidin C (**172**)	mannose	Ara(3-1)GalA
balticidin D (**173**)	mannose	Ara(3-1)GalA

n.d.: not determined; GlcNAc: *N*-acetyl-glucosamine; Ara: arabinose; GalA: galacturonic acid

4.3.3.2. Marfey's Method for Amino Acids Analysis

Marfey's and NMR analysis have been obtained only for GLCP-2 (**183**) and will be repeated for GLCP-1 (**182**). After isolation and hydrolysis of GLCP-2 (**183**) the amino acids configuration was determined by the Marfey's method described in chapter 4.2.1.3. The elucidation of *N*-Me-Thr required the synthesis of the three non-commercially available diastereoisomers (*N*-Me-D-Thr, *N*-Me-D-*allo*-Thr, *N*-Me-L-*allo*-Thr) using a reported procedure.[186] The results of the analysis indicated the presence of L-Tyr, D-Tyr, D-Glu, L-Thr (confirmed by coinjection with L-Thr), D-Thr, D-*allo*-Thr, Gly and *N*-Me-L-*allo*-Thr (confirmed by coinjection with *N*-Me-L-*allo*-Thr and *N*-Me-D-Thr).

The absence of glutamine was a result of its conversion to glutamic acid during the hydrolysis procedure as it was reported for balticidins.[178] Therefore the presence of D-Glu is an indication that GLCP-2 (**183**) possesses D-Gln and this result will be confirmed by $HRMS^2$ analysis of the aglycone core structure.

The amino acids composition was found to be identical to the one reported for hassallidin D (**169**). Considering this result, we propose to have the same amino acid sequence. Additionally, our result showed unambiguously the presence of *N*-Me-L-*allo*-Thr and we can reasonably by deduction assigned the absolute configuration of the unknown threonine in **169** to D-Thr.

[186] U. Groth, W. Halfbrodt, U. Schöllkopf, *Liebigs Ann. Chem.* **1992**, 351–355.

4.3.3.3. NMR Analysis

NMR spectroscopic data were recorded for GLCP-2 (**183**) in MeOD following the same procedure used for hassallidin D (**169**). It was found that both compounds were subject to hydrolysis and therefore the data are reported for the open form of the lactone.[177] The ^{1}H NMR and the ^{13}C chemical shifts obtained from HSQC measurments were compared for the aglycone core structure of **169** and strong similarities were found except for the part close to the carbohydrates (table **16**).

Table **16**: ^{1}H and ^{13}C chemical shift of GLCP-2 (**183**) and hassallidin D (**169**).

Substructure	**Position**	**δ_C (ppm)**		**δ_H (ppm)**	
		hassallidin D	**GLCP-2**	**hassallidin D**	**GLCP-2**
Dhh[1]	1	176.1			
	2	73.5	73.3	4.15	4.16
	3	75.8	76.7	4.05	3.99
	4	28.6	29.0	1.69	1.66
	5	26.0	26.3	1.36	1.36
	6-13	29.8-30.5	30.5	1.34-1.29	1.29
	14	32.8	32.8	1.28	1.28
	15	23.4	23.5	1.32	1.32
	16	14.1	14.2	0.89	0.89
Thr[2]	1	172.3		-	
	2	60.3	60.7	4.28	4.32
	3	67.8	68.1	4.13	4.15
	4	19.8	20.1	1.25	1.24
Thr[3]	1	174.1		-	
	2	59.7	60.7	4.38	4.32
	3	68.5	68.1	4.32	4.32
	4	19.8	20.0	1.23	1.23
Thr[4]	1	172.6		-	
	2	61.6	60.7	4.24	4.32
	3	67.9	68.1	4.07	4.07
	4	19.7	19.4	1.13	1.10
Tyr[5]	1	172.8		-	
	2	56.6	57.2	4.53	4.47
	3/3’	37.1	36.9	2.88/3.12	2.91/3.10
	4	128.7		-	
	5	131.3	131.2	7.05	7.04
	6	116.4	116.5	6.69	6.70
	7	157.5		-	
Dhb[6]	1	167.2		-	
	2	131.0		-	
	3	126.9		5.80	5.79
	4-CH_3	13.5	13.6	1.94	1.95

Substructure	Position	δ_C (ppm)		δ_H (ppm)	
		hassallidin D	GLCP-2	hassallidin D	GLCP-2
Gln^7	1	174.2		-	
	2	54.2	54.3	4.51	4.52
	3/3'	28.0	28.3	2.12/2.29	2.11/2.29
	4	32.2	32.8	2.44	2.44
	4-CO	178.2		-	
Gly^8	1	171.4		-	
	2	42.1	42.2	3.92/4.13	4.14/3.94
***N*-MeThr^9**	1	169.9		-	
	2	61.0	60.8	4.86	4.95
	3	69.6	70.4	4.31	4.33
	4	14.8	15.0	1.05	1.05
	NCH3	30.9	30.9	2.68	2.64
Tyr^{10}	1	173.7		-	
	2	54.2	54.7	4.75	4.74
	3/3'	37.8	37.8	2.73/3.11	2.71/3.13
	4	128.7		-	
	5/8	131.6	131.4	6.97	6.96
	6/9	116.4	116.6	6.72	6.68
	7	157.3			

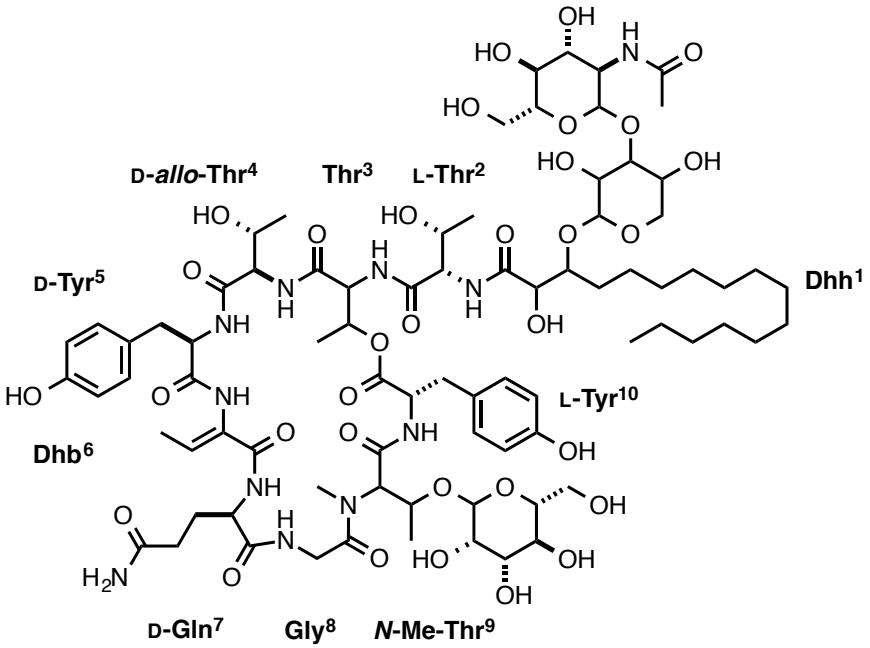

hassallidin D (**169**)

4.3.4. Conclusion

A bioassay-guided fractionation targeting antimalarial activity led to the isolation of two new natural products, GLCP-1 (**182**) and GLCP-2 (**183**). Their aglycone core structure is proposed to be the same as for hassallidin D (**169**) based on $HRMS^2$ analysis. Furthermore, applying marfey's method, the amino acids composition of GLCP-2 (**183**) was found to be identical to hassallidin D (**169**) and as both compounds exhibit strong similarities in their ^1H NMR data, the amino acid sequence of both natural products is proposed to be identical. Additionally, we determined for the first time, in this glycolipopeptide class of compounds, the absolute configuration of *N*-Me-L-allo-Thr.

The carbohydrates of GLCP-1 (**182**) and GLCP-2 (**183**) were determined by $HRMS^2$ analysis and identified as deoxyhexose and hexose containing functional groups. By comparison with hassallidins and balticidins, we propose that the natural products possess rhamnose as deoxyhexose and mannose as hexose. The presence of carboxamide has not been reported for this compound family but was observed in other natural products isolated from cyanobacteria such as banyaside A.[187]

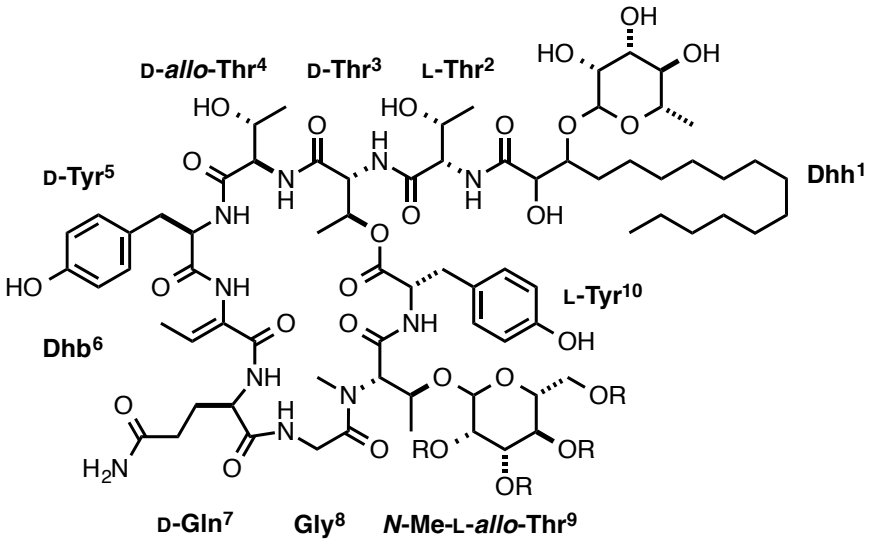

GLCP-2 (**183**)
4R = 2H and $2CONH_3$

[187] A. Pluotno, S. Carmeli, *Tetrahedron* **2005**, *61*, 575–583.

4.3.5. Outlook

As GLCP-1 (**182**) and GLCP-2 (**183**) possess strong similarities in their HPLC retention time and $HRMS^2$ data, we suggest that they have similar structures. This assumption will be tested by applying Marfey's derivatization method and NMR analysis of GLCP-1 (**182**). Furthermore, NMR spectroscopic data has to be acquired in an aprotic solvent such as DMSO-d_6 to confirm the amino acids sequence and the presence of glutamic acid as well as the identity of the carbohydrates. In parallel, the structure of the sugars and the fatty acid will be analyzed by GC-MS. Finally, the antimalarial activity of the natural products will be tested.

5. Conclusion

In this thesis, the potential of natural products as a source of knowledge is highlighted with three different examples. Firstly, secondary metabolites represent a rich and powerful source of new biologically active compounds. This field of study remains of high importance due the constant discovery of multidrug-resistant organisms. Secondly, natural products play an important role in the communication between living organisms. The study of this chemical language brings essential information towards our understanding of these interactions. Finally, the formation of compounds by living organisms represents a fascinating field of research and requires the detection and isolation of natural products involved in biosynthetic pathways.

P. kirkii is a plant living in obligatory symbiosis with the bacteria *B. kirkii* and the role of this microoganism on the plants' survival remains unclear. This question is addressed in the first part of this thesis by the analysis of the secondary metabolites produced by *B. kirkii*. The genomic analysis of the bacteria revealed the presence of a gene cluster responsible for the production of a putative C_7N aminocyclitol. The isolation of this predicted natural product was achieved using a ^{1}H-NMR-guided fractionation and the structure was elucidated by HRMS, NMR and single crystal X-ray analysis. To investigate the biological role of this new natural product, named kirkamide, a total synthesis was developed and optimized for gram scale preparation. Biological assays were carried out and revealed that kirkamide possesses a cytotoxic and insecticidale activity. Taking into account these results kirkamide was proposed to possess a protective role in the symbiosis. Furthermore, during the study of the secondary metabolites composition from this symbiotic system another new natural product, streptol glucoside, was isolated and its structure elucidated. Finally, the methods for the detection and quantification of these natural products were achieved by GC-MS and ^{1}H NMR.

A genome-driven bioassay-guided fractionation of the *B. cenocepacia* H111 extract led to the isolation of fragin, which possesses the unusual *N*-nitrosohydroxylamine functional group. The gene cluster of this compound was identified allowing the opportunity to study its biosynthesis and particularly the mechanism of the N-N bond formation, which remains unclear for all natural products. After the function assignment of the genes, a first biosynthetic pathway starting from L-hydroxyleucine was proposed. To test this hypothesis, predicted biosynthetic intermediates were synthesized and their presence in the crude extract was explored, which led to the detection of some of the proposed compounds. To obtain further evidence of their involvement in the biosynthesis, knockout strains were obtained and their molecular composition analyzed. Unfortunately, the intermediates were not found in these cultures leading to the conclusion that the compounds detected in the crude extract were degradation products of fragin. Furthermore, the gene cluster contained a NRPS domain, which could release the compound only at a later stage of the biosynthesis. On the base of this deduction, a second biosynthesis was proposed starting from D-valine and is currently being investigated. Additionally, the mechanism of N-N bond formation was investigated and a stepwise process involving a hydroxylamine compound and a nitrite ion is suggested.

The last chapter, separated into two parts, describes the discovery of new natural products from cyanobacteria possessing antimalarial activity. Balgacyclamides A–C are novel cyanobactins isolated from *Microcystis aeruginosa* EAWAG 251 culture. The absolute configuration was elucidated using chiral GC and Marfey's derivatization method followed by HPLC-MS measurement. Furthermore, balgacyclamides A and B were found to possess an antimalarial activity lower that 10 μM and a cytotoxicity of more than 150 μM. The second part of this chapter described the structure elucidation efforts of two new glycolipopeptides produced by *Tolpyothrix distorta* var. *symplocoides* EAWAG 224a. The natural products were isolated following a bioassay-guided fractionation and structural information was obtained by UV, HRMS fragmentation, amino acid analysis and NMR. These results indicated that the natural products shared the core structure of hassallidin D with variation in the attached carbohydrates.

6. Experimental Part

6.1.General Remarks

All reactions were performed in dry solvents under argon atmosphere unless stated otherwise. The anhydrous solvents were obtained by filtration and passing through activated anhydrous alumina columns (Innovative Technology solvent purification system) and from commercial suppliers without any purification. Syringes and stainless steel cannula were used to transfer air and moisture sensitive liquids and solutions. Analytical thin layer chromatography (Merck silica gel 60 F254 plates) was used to monitor reactions and the compounds were detected by UV light (254 nm and 350 nm) and by staining using ceric ammonium molybdate (CAM) solution followed by gentle heating with a heat gun. Flash chromatography was performed using SiliCycle silica gel 60 (230-400 Mesh) and R_f values of compounds are indicated. NMR experiments were performed at 298 K on a Bruker Avance III NMR spectrometer operating at 400 MHz proton frequency, Bruker Avance III NMR spectrometer operating at 500 MHz proton frequency and at 126 MHz carbon frequency, Bruker Avance III NMR spectrometer operating at 600.13 MHz proton frequency and Bruker Avance III NMR spectrometer operating at 600.13 MHz proton frequency equipped with a 1.7 mm TCI cryoprobe. The spectra were calibrating using the residual solvent proton and carbon signals (δ_H 2.50, δ_C 39.52 for DMSO-d_6, δ_H 7.26, δ_C 77.16 for $CDCl_3$, δ_H 5.32, δ_C 53.84 for CD_2Cl_2, δ_H 4.79 for D_2O and δ_H 3.31, δ_C 49.00 for CD_3OD). Melting points (Mp) were determined using a Büchi B-545 apparatus in open capillaries and are uncorrected. IR spectra were recorded on a Varian 800 FT-IR ATR spectrometer and data are reported in terms of frequency of absorption (ν, cm^{-1}). Optical rotations were recorded on a Jasco P-2000 digital polarimeter with a path length of 1 dm, using the 589.3 nm D-line of sodium. Concentrations (*c*) are quoted in g/100 mL. High-resolution masses (HRMS-ESI) were recorded by Dr. Heinz Nadig at the University of Basel on a Bruker max is 4G QTOF ESI mass spectrometer. Microwave reactions were performed using a Biotage® Initiator$^+$ system. HPLC purifications were performed on a UHPLC Dionex Ultimate 3000 system equipped with Ultimate 3000 pump, Ultimate 3000 autosampler, Ultimate 3000 thermostated column compartment and Ultimate 3000 photodiode array detector. HPLC-

MS analyses were performed on a Dionex HPLC system equipped with a P680 pump, an ASI-100 automated sample injector, a TCC-100 thermostated column compartment, a PDA-100 photodiode array detector and a MSQ-ESI mass spectrometric detector. Lyophilization was performed using a Christ Alpha 1-2 LD plus system.

6.2. The C_7N Aminocyclitol Kirkamide and Streptol Glucoside

6.2.1. Kirkamide

6.2.1.1. Isolation and Structure Elucidation of Kirkamide

Extraction Procedure

The leaves were collected from approximately 1 year-old *Psychotria kirkii* plants kept in the greenhouse of the Botanical Garden of the University of Zürich. Leaves were collected in the middle of the light cycle and washed with distilled water. About 10 g of leaf tissue were then grounded in liquid nitrogen and extracted by stirring the mixture in aq. MeOH soln. (80%, 2 x 100 mL) for 24 h. Extracts were concentrated under reduced pressure.

Isolation of Fraction P_TLC_IV_1_5_2_2

The extract from the leaves of *Psychotria kirkii* (160 mg) was subjected to ^{1}H NMR-guided fractionation using multiple semi-preparative Hydro RP-HPLC runs (Phenomenex Synergi Hydro-RP 10 µm; 150 x 10 mm) at a flow of 2 mL/min. The column was equilibrated for 5 min with 100% H_2O and the MeCN/H_2O gradient applied was changed from 0% to 0.5% and finally to 100% MeCN in 10 and 2 min, respectively. The column was then washed with MeCN for 5 min. The fraction P_TLC_IV_1_5_2_2 was shown to contain an inseparable mixture of kirkamide and sucrose eluting at 5.75 min.

Isolation of Kirkamide

The extract from the leaves of *Psychotria kirkii* (859 mg) was dissolved in MeOH (6 mL), *p*TsOH (400 mg) was added and the reaction was stirred overnight at RT. The reaction mixture was then evaporated under reduced pressure, dissolved in H_2O (600 µL), filtered and separated using multiple semi-preparative RP-HPLC runs (Phenomenex Synergi Hydro-RP 10 µm; 150 x 10 mm; 2 mL/min) and preparative RP-HPLC runs (Phenomenex Synergi Hydro-RP 10 µm; 250 x 21.2 mm; 7 mL/min). The preparative HPLC column was first equilibrated for 5 min with 100% H_2O, then the MeCN/H_2O gradient was changed from 0% to 0.5% and finally to 100% MeCN in 10 and 2 min

respectively. The column was washed with MeCN for 7 min. The elution conditions for the semi-preparative RP-HPLC were identical to those reported before. The compound was further purified using preparative TLC coated with Cu(II),[61] and finally by semi-preparative RP-HPLC using the same conditions as mentioned before to afford kirkamide (**56**) (1.31 mg) as a white solid. A single crystal was obtained by slow diffusion of Et_2O into a solution of kirkamide (**56**) in MeOH.

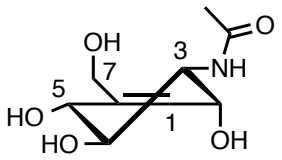

kirkamide (**56**)

Kirkamide (**56**): white solid: $[\alpha]_D$ = +21.6° (*c* 0.087, MeOH); R_f = 0.68 (Cu(II) coated TLC, *i*PrOH:H_2O 3:2); **IR (film)**: ν_{max} = 3310, 2953, 2923, 2853, 1653, 1647, 1636, 1558, 1541, 1458, 1376, 1310, 1099, 1074, 1061, 1045 cm^{-1}; **^{1}H NMR (500 MHz, DMSO-d_6)** δ = 7.36 (d, *J* = 8.1 Hz, 1H), 5.63 (dq *apparent pattern*, *J* = 4.8, 1.5 Hz, 1H), 4.01 (d, *J* = 14.8 Hz, 1H), 3.99 (m, 1H), 3.95 (d, *J* = 14.8 Hz, 1H), 3.79 (d, 7.1 Hz, 1H), 3.63 (ddd, *J* = 10.9, 8.1, 3.9 Hz, 1H), 3.56 (dd, *J* = 10.9, 7.1 Hz, 1H), 1.85 (s, 3H); **^{1}H NMR (500 MHz, D_2O)** δ = 5.86 (dq *apparent pattern*, *J* = 5.0, 1.5 Hz, 1H), 4.30 - 4.23 (m, 2H), 4.20 - 4.12 (m, 2H), 3.91 (dd, *J* = 11.5, 4.0 Hz, 1H), 3.72 (dd, *J* = 11.5, 7.9 Hz, 1H), 2.06 (s, 3H); **^{13}C-NMR (126 MHz, DMSO-d_6)** δ = 169.2, 142.5, 121.5, 72.9, 70.4, 64.3, 60.9, 53.1, 23.0; **HRMS (ESI)** calc. for $C_9H_{15}NO_5Na^+$ $[M+Na]^+$: 240.0842; found $[M+Na]^+$: 240.0844.

Crystallographic Data of Kirkamide

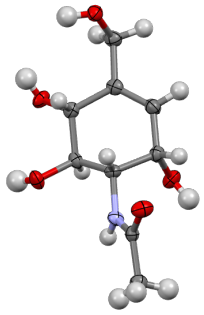

Formula	$C_9H_{15}N_1O_5$
Formula weight	217.22
Z, calculated density	4, 1.404 Mg · m^{-3}
F(000)	464
Description and size of crystal	colourless plate, 0.031 · 0.121 · 0.191
mm^3	
Absorption coefficient	0.978 mm^{-1}
Min/max transmission	0.84 / 0.97
Temperature	123K
Radiation(wavelength)	Cu K_α (λ = 1.54178 Å)
Crystal system, space group:	orthorhombic, P 2_1 2_1 2_1
a	7.3848(7) Å
b	11.2982(10) Å
c	12.3137(11) Å
α	90°
β	90°
γ	90°
V	1027.39(16) $Å^3$
Min/max Θ	5.313° / 68.379°
Number of collected reflections	12832
Number of independent reflections	1849 (merging r = 0.049)
Number of observed reflections	1736 (I>2.0σ(I))
Number of refined parameters	137
r	0.0256
rW	0.0303
Flack parameter	–0.03(15)
Goodness of fit	1.1028
CCDC	1054238

NMR Spectroscopic Data of Valienamine in DMSO-d_6

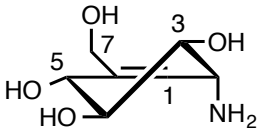

valienamine (**21**)

Valienamine (**21**) (1 mg) was obtained from Toronto Research Chemicals Inc., dissolved in DMSO-d_6 and then D_2O was added and evaporated in order to suppress the proton signals of the primary amine and the hydroxyl groups.

Table **17.** NMR Spectroscopic data (600 MHz, DMSO-d_6) of valienamine (**21**).

C no.	δ_C, type	δ_H (J in Hz)
1	115.9, CH	5.57, dq[a] (4.5, 1.4)
2	50.3, CH	3.82, t[a] (4.9)
3	67.9, CH	3.72, dd (9.7, 5.5)
4	72.8, CH	3.54, dd (9.7, 7.0)
5	71.8, CH	3.89, d (7.0)
6	147.4, C	
7a	62.0, CH_2	4.04, d (15.1)
7b		4.01, dq[a] (15.1, 1.6)

[a] Apparent splitting pattern.

6.2.1.2. Activity Assays of Kirkamide

Brine Shrimp Toxicity Assay

Experiment executed by Dr. Aurélien Carlier. Brine shrimp (*Artemia salina*) eggs purchased from Dohse Aquaristik (Zürich, Switzerland) were hatched in salt water (37 g/L) under constant illumination. Kirkamide (**56**) solution in methanol was added to the wells of 12-well microliter dishes and allowed to dry. Brine shrimp nauplii were then added to the wells with 2 mL salt water and incubated at 25°C under shaking. Nauplii survival was scored after 48 h incubation. The experiment was done in triplicate. LC_{50} value (± SD) was estimated at 0.85 ± 0.31 µg/mL by logistic regression using the "dose" function of the MASS package in R.[188]

Toxicity Assay on Pollen Beetles

Experiments executed by Dr. Giselher Grabenweger. Pollen beetles (*Meligethes aenus*) were collected in May and June 2014 in a pesticide-free field of oilseed rape in Reckenholz, Switzerland and kept in a climate chamber at 7°C on peat substrate until needed. For the assay, an aq. soln. of kirkamide (**56**) (0.3%, 100 µL), a soln. of a commercial insecticide (Audienz, Omya Agro, Switzerland, 0.4%, 100 µL) as a positive control or distilled water (100 µL) as a negative control was mixed with 100 mg of pure pollen (Bergland, Germany) in small petri dishes (55 mm diameter). Methanol and water were allowed to evaporate completely at room temperature. Petri dishes with dried feed were put into plastic boxes (100 x 80 x 130 mm), lined with filter paper and provided with a moist cotton plug as a water source. 20 pollen beetles were added per box. Boxes were closed with perforated lids and plugged with gauze to allow for gas exchange. Treatments were replicated 5 times and boxes with beetles were kept at 22°C and 75% humidity for the duration of the experiment. Mortality was assessed at 3, 7, 10 and 14 days after transfer. Mean pollen beetle mortality (± SD) in the kirkamide treatment was 20 ± 11.9, 48.3 ± 26.3, 67.7 ± 27.9 and 80.9 ± 28.3% at 3, 7, 10 and 14 dpi, respectively. The insecticide treatment reached 96.3 ± 8.5% mortality 3 dpi and 100% mortality after 7 dpi, respectively, while mean mortality in the distilled water control was 5.2 ± 3.6, 8.6 ±

[188] J. Carballo, Z. L. Hernández-Inda, P. Pérez, M. D. García-Grávalos, *BMC Biotechnol.* **2002**, *2*, 17–22.

6.5, 12.6 ± 7.9 and 16.7 ± 6.9% at 3, 7, 10 and 14 dpi, respectively. Pollen beetle mortality between the distilled water control and kirkamide treatment is significantly different at 10 and 14 dpi, while it is similar between kirkamide and the insecticide at the same observation dates (ANOVA, with Tamhane's τ post hoc testing).

6.2.1.3. Synthesis of Kirkamide

Synthesis First Generation

Synthesis of *N*-((3*R*,4*R*,5*S*,6*R*)-4,5-dihydroxy-6-(hydroxymethyl)-2-methoxytetrahydro-2*H*-pyran-3-yl)acetamide (75)[71]

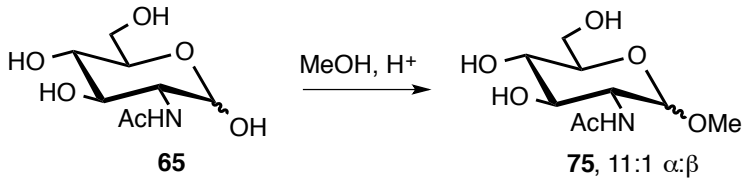

65 **75**, 11:1 α:β

Amberlite® IR-120 (H^+ form, 84.0 g), washed with MeOH, was added to a solution of *N*-acetyl-D-glucosamine (**65**) (35 g, 158 mmol) in MeOH (560 mL) and stirred 16 h at reflux. The hot mixture (60°C) was filtered, washed with MeOH (60°C, 2 x 300 mL) and evaporated under reduced pressure to afford the triol **75** (32.6 g, 11:1 α:β, 80%) as a white powder: $\mathbf{R}_f$ = 0.52 (CH_2Cl_2:MeOH 7:3). The product was used in the next step without further purification. The analytical data match those reported in the literature.[71]

Synthesis of *N*-((2*R*,4a*R*,6*S*,7*R*,8*R*,8a*S*)-8-hydroxy-6-methoxy-2-phenylhexahydropyrano[3,2-*d*][1,3]dioxin-7-yl)acetamide (190)[72]

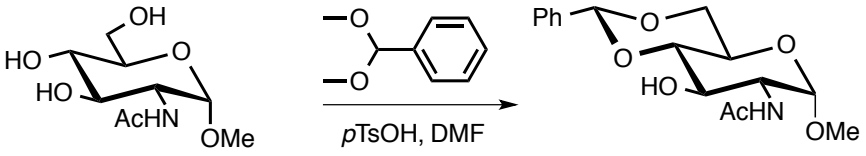

75 **190**

Benzaldehyde dimethyl acetal (156 mmol, 23.4 ml) and *p*TsOH (1.56 mmol, 296 mg) were added to a solution of the triol **75** (18.3 g, 77.8 mmol, 11:1 α:β) in DMF (150 mL) and the mixture was stirred at 70°C for 2.5 h. The orange solution was evaporated under reduced pressure, the residue was dissolved in CH_2Cl_2 (500 mL), a sat. aq. $NaHCO_3$ soln. (250 mL) was added and the precipitates were filtered. The crystallization was repeated by evaporating the organic layer under reduce pressure, dissolving the residue in CH_2Cl_2 (100 mL) and adding a sat. aq. $NaHCO_3$ soln. (100 mL). The solids were combined to afford the benzylidene **190** (24.4 g) as a white solid: $\mathbf{R}_f$ = 0.56

(CH_2Cl_2:MeOH 9:1). The product was used in the next step without further purification. The analytical data match those reported in the literature.[189]

Synthesis of *N*-((2*R*,4a*R*,6*S*,7*R*,8*R*,8a*S*)-8-(benzyloxy)-6-methoxy-2-phenylhexahydro pyrano[3,2-*d*][1,3]dioxin-7-yl)acetamide (67)[73]

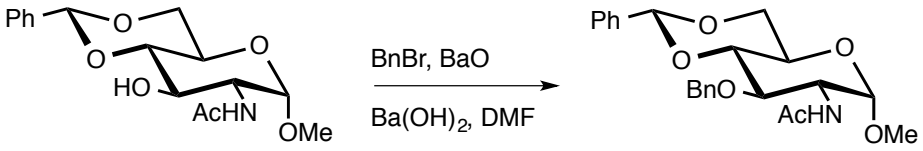

190 **67**

To a solution of the benzylidene **190** (30.0 g, 92.8 mmol) in DMF (200 mL), barium oxide (42.7 g, 278 mmol), barium hydroxyde octahydrate (13.3 g, 41.2 mmol) and benzyl bromide (16.2 mL, 135 mmol) were added sequentially and the solution was stirred for 2 h 40 at RT. The mixture was diluted with CH_2Cl_2 (1.2 L), the organic phase was washed with aq. HCl soln. (1 M, 400 mL), sat. aq. $NaHCO_3$ soln. (400 mL), washed with brine (3 x 400 ml), dried over Na_2SO_4 and concentrated under reduced pressure. Et_2O (50 mL) was added to the concentrated solution and the precipitates were filtered to afford the benzyl protected **67** (31.4 g) as a white solid. The product was used in the next step without further purification. The analytical data match those reported in the literature.[73]

Synthesis of *N*-((2*S*,3*R*,4*R*,5*S*,6*R*)-4-(benzyloxy)-5-hydroxy-6-(hydroxymethyl)-2-methoxytetrahydro-2*H*-pyran-3-yl)acetamide (68)[69]

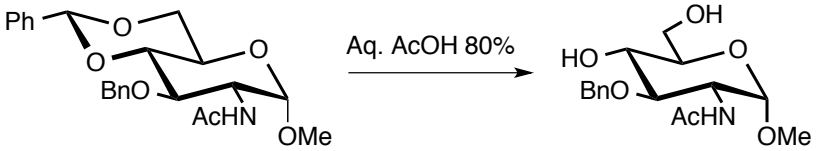

67 **68**

A solution of the benzyl protected pyranoside **67** (30 g) in aq. AcOH soln. (80%, 360 mL) was stirred for 1h at 70°C. The reaction mixture was evaporated under reduced pressure and the residue was washed with toluene (2 x 200 mL) and pentane (2 x 200

[189] J. Agarwal, R. K. Peddinti, *J. Org. Chem.* **2011**, *76*, 3502–3505.

mL) to afford the diol **68** (21.7 g) as a white solid. The product was used in the next step without further purification. The analytical data match those reported in the literature.[69]

Synthesis of ((2*R*,3*S*,4*R*,5*R*,6*S*)-5-acetamido-4-(benzyloxy)-3-hydroxy-6-methoxytetra-hydro-2*H*-pyran-2-yl)methyl 4-methylbenzenesulfonate (191)[69]

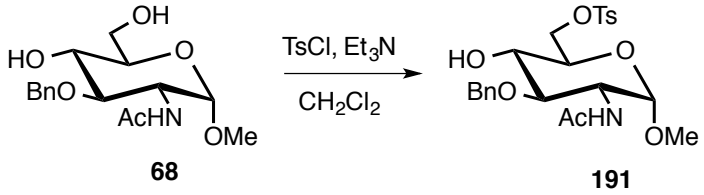

68 **191**

To a solution of the diol **68** (5 g) in CH_2Cl_2 (60 mL), 4-toluenesulfonyl chloride (5.86 g, 30.7 mmol) and freshly distilled Et_3N (6.65 mL) were added at 0°C. The solution was stirred for 3 h 20 at RT. The yellow reaction mixture was quenched with H_2O (40 mL) and extracted with CH_2Cl_2 (2 x 60 mL). The organic layer was washed with sat. aq. NH_4Cl soln. (3 x 60 mL) and with brine (3 x 60 mL), dried over Na_2SO_4 and evaporated under reduced pressure to afford the tosylated pyranoside **191** (7.37 g) as a yellow amorphous solid. The product was used in the next step without further purification. The analytical data match those reported in the literature.[69]

Synthesis of *N*-((2*S*,3*R*,4*R*,5*S*,6*S*)-4-(benzyloxy)-5-hydroxy-6-(iodomethyl)-2-methoxytetrahydro-2*H*-pyran-3-yl)acetamide (69)[69]

191 **69,** 36% over 5 steps

To a solution of the tosylated pyranoside **191** (7.29 g, 15.3 mmol) in DMF (60 mL), sodium iodide (11.4 g, 76.3 mmol) was added and the dark solution was stirred for 2 h at 100°C. The dark solution was evaporated under reduced pressure, dissolved in CH_2Cl_2 (60 mL), washed with sat. aq. Na_2SO_3 soln. (2 x 60 mL) and brine (3 x 60 mL), dried over Na_2SO_4, evaporated under reduced pressure and purified by column chromatography (EtOAc:Et_2O 1:1) to afford the iodide **69** (4.34 g, 36% over 5 steps) as a yellow solid:

R_f = 0.5 (EtOAc:Et_2O 1:1); **^{1}H NMR (500 MHz, $CDCl_3$)** δ 7.38 - 7.28 (m, 5H), 5.52 (d, *J* = 9.6 Hz, 1H), 4.72 (d, *J* = 11.6 Hz, 1H), 4.66 - 4.63 (m, 2H), 4.31 (ddd, *J* = 10.4, 9.5, 3.7 Hz, 1H), 3.61 - 3.54 (m, 2H), 3.49 (t, *J* = 9.0 Hz, 1H), 3.45 - 3.41 (m, 4H), 3.30 (dd, *J* = 10.6, 7.0 Hz, 1H), 1.94 (s, 3H); **^{13}C NMR (126 MHz, CD_3OD)** δ 169.94, 138.21, 128.88 (2C), 128.28, 128.24 (2C), 98.96, 80.30, 74.12, 74.02, 70.64, 55.55, 52.13, 23.66, 6.90; **Mp** 136-140 °C. The analytical data match those reported in the literature.[69]

Synthesis of *N*-((2*S*,3*R*,4*R*,5*S*)-4,5-bis(benzyloxy)-2-methoxy-6-methylenetetrahydro-2*H*-pyran-3-yl)acetamide (70)[69]

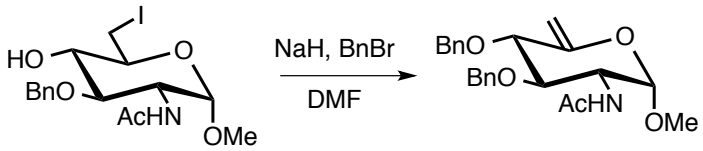

69 **70,** 74%

To a solution of sodium hydride (60% dispersion in mineral oil, 2.19 g, 54.7 mmol) in dry DMF (20 mL) at 0°C, a solution of the iodide **69** (4.33 g, 9.95 mmol) in DMF (60 mL) was added. The mixture was warmed to RT and benzyl bromide (1.3 mL, 10.9 mmol) was added. The reaction was monitored by ^{1}H NMR and was quenched after 2 h with MeOH (2 mL), the mixture was concentrated under reduced pressure, dissolved in EtOAc (130 mL), washed with brine (3 x 100 mL), dried over Na_2SO_4, evaporated under reduced pressure and purified by column chromatography (EtOAc:hexane 1:1 and finally eluted with CH_2Cl_2) to afford the olefin **70** (2.94 g, 74%) as a white solid; **R_f** = 0.5 (EtOAc:Et_2O 1:1); **$[\alpha]_D$** = +51.2° (*c* 0.53, $CHCl_3$); **IR (film)**: ν_{max} = 3293, 3086, 3066, 3032, 2928, 2914, 2871, 2836, 1651, 1553, 1497, 1453, 1401, 1376, 1355, 1319, 1292, 1210, 1134, 1096, 1075, 1051, 1030, 952 cm^{-1}; **^{1}H NMR (500 MHz, $CDCl_3$)** δ = 7.40 - 7.27 (m, 10H), 5.42 (d, *J* = 9.2 Hz, 1H), 4.86 - 4.83 (m, 2H), 4.80 - 4.77 (m, 2H), 4.74 - 4.70 (m, 2H), 4.64 (d, *J* = 12.0 Hz, 1H), 4.33 (td, *J* = 9.3, 3.3 Hz, 1H), 4.01 (dt, *J* = 8.2, 1.7 Hz, 1H), 3.64 (dd, *J* = 9.4, 8.3 Hz, 1H), 3.40 (s, 3H), 1.84 (s, 3H); **^{13}C-NMR (126 MHz, $CDCl_3$)** δ = 170.0, 153.8, 138.4, 137.8, 128.6 (2C), 128.6 (2C), 128.3 (2C), 128.0, 128.0 (2C), 127.9, 99.6, 97.7, 79.8, 78.6, 74.5, 74.0, 55.7, 51.8, 23.5; **Mp** 150 - 154°C; **HRMS (ESI)** calc. for $C_{23}H_{27}NNaO_5^+$ $[M+Na]^+$: 420.1781; found: $[M+Na]^+$ 420.1778. The analytical data match those reported in the literature.[69]

Second Generation Synthesis

Synthesis of *N*-((1*R*,3*S*,4*R*,5*R*,8*S*)-8-(benzyloxy)-3-methoxy-2,6-dioxabicyclo[3.2.1]oc -tan-4-yl)acetamide (77)

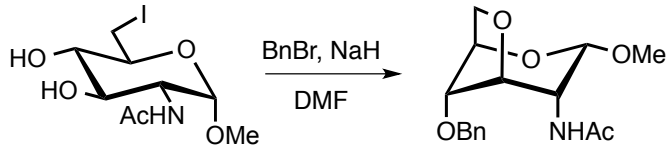

76 **77**

To a solution of the iodide **76** (15 mg, 43.0 µmol) in DMF (0.3 mL), benzyl bromide (11 µL, 91.3 µmol) was added at 0°C followed by a mixture sodium hydride (60% in mineral oil, 11.3 mg, 0.282 mmol) in DMF (0.1 mL). The reaction mixture was stirred for 2 h at RT and quenched with MeOH (0.2 mL). The reaction mixture was concentrated under reduced pressure, dissolved in EtOAc (10 mL), washed with brine (3 x 10 mL), dried over Na_2SO_4, evaporated under reduced pressure and purified by column chromatography (Et_2O:EtOAc 1:1, 1% Et_3N) to afford the bicyclic ether **77** as a yellowish oil: $\mathbf{R_f}$ = 0.2 (Et_2O:EtOAc 1:1, 1% Et_3N); $\mathbf{[\alpha]_D}$ = +39.5° (*c* 0.43, CH_2Cl_2); **IR (film)**: ν_{max} = 3417, 2952, 2928, 2891, 2852, 1674, 1515, 1454, 1438, 1369, 1313, 1275, 1220, 1194, 1168, 1117, 1091, 1063, 1037, 1010, 916 cm^{-1}; **^{1}H NMR (500 MHz, CD_2Cl_2)** δ = 7.51 - 7.29 (m, 5H), 6.65 (d, *J* = 9.9 Hz, 1H), 5.00 (d, *J* = 3.9 Hz, 1H), 4.78 (d, J = 11.4 Hz, 1H), 4.57 (d, *J* = 11.4 Hz, 1H), 4.46 (t, *J* = 2.7 Hz, 1H), 4.36 (dddt, *J* = 10.0, 4.5, 3.8, 0.7 Hz, 1H), 4.22 (t, *J* = 4.9 Hz, 1H), 4.20 (d, *J* = 10.6 Hz, 1H), 3.92 (ddd, *J* = 5.3, 2.6, 0.6 Hz, 1H), 3.91 (dd, *J* = 10.7, 3.1 Hz, 1H), 3.48 (s, 3H), 1.78 (s, 3H); **^{13}C-NMR (126 MHz, CD_2Cl_2)** δ = 169.4, 137.2, 128.6 (2C), 128.1, 127.6 (2C), 97.4, 77.8, 72.5, 72.3, 71.7, 69.0, 57.0, 50.1, 29.7 (unknown impurity), 23.1; **HRMS (ESI)** calc. for $C_{16}H_{21}NNaO_5^+$ $[M+Na]^+$: 330.1312; found: $[M+Na]^+$ 330.1315.

Synthesis of (3*S*,4*R*,5*R*,6*S*)-5-acetamido-6-methoxy-2-methylenetetrahydro-2*H*-pyran-3,4-diyl diacetate (76)

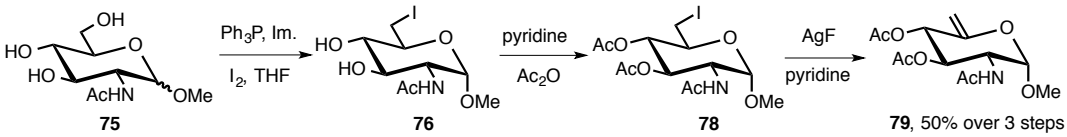

75 **76** **78** **79**, 50% over 3 steps

These compounds were prepared by using a modification of a published procedure.[75] To a solution of the triol **75** (13.55 g, 57.6 mmol, 11:1 α:β), triphenylphosphine (15.2 g, 58.1 mmol) and imidazole (7.26 g, 106 mmol) in THF (150 mL) at reflux, iodine (14.7 g, 58.1 mmol) in THF (60 mL) was added dropwise using a dropping funnel. After complete addition, the yellow solution was kept at reflux for 15 min, cooled to RT and evaporated under reduced pressure. The residue was dissolved in a mixture of EtOAc (700 mL) and sat. aq. $Na_2S_2O_3$ soln. (750 mL) and the layers were separated. The org. layer was extracted with H_2O (3 x 750 mL) and the combined aq. layers were evaporated under reduced pressure. The solid was suspended in EtOAc (60°C, 4 x 500 mL), filtered and evaporated under reduced pressure to afford a mixture of iodide **76** and imidazole. This mixture was used in the next step without further purification.

The crude residue was dissolved in pyridine (100 mL) and acetic anhydride (100 mL) and stirred for 24 h at RT. The reaction mixture was evaporated under reduced pressure, dissolved in EtOAc (500 mL), the org. layer was washed with sat. aq. $CuSO_4$ soln. (500 mL) and with brine (2 x 300 mL), dried over Na_2SO_4 and evaporated under reduced pressure to afford the acetylated pyranoside **78** as a white solid which was used in the next step without further purification.

Silver fluoride (10.0 g, 79 mmol) was added to a solution of the crude material in dry pyridine (100 mL), the mixture was stirred in the dark for 48 h and the reaction was monitored by ^{1}H NMR. The mixture was then diluted with EtOAc (1 L), the solids were filtered through a pad of celite and washed with EtOAc (500 mL). The org. layers were washed with aq. HCl soln. (1M, 2 x 500 mL), with brine (2 x 500 mL) until the solution was neutral (pH = 7), sat. aq. $CuSO_4$ soln. (500 mL) and brine (500 mL). Each aq. layer was extracted with EtOAc (100 mL), the org. layers were combined, dried over Na_2SO_4,

evaporated under reduced pressure and the residue was purified by column chromatography (Et_2O:EtOAc 1:9) to afford the olefin **79** (8.7 g, 50% over three steps) as a white solid: $\mathbf{R_f}$ = 0.43 (EtOAc); $\mathbf{[\alpha]_D}$ = +68.9° (*c* 0.48, $CHCl_3$); **IR (film)**: ν_{max} = 3279, 2940, 1741, 1665, 1550, 1434, 1373, 1217, 1099, 1046, 1016, 931 cm^{-1}; **^{1}H NMR (500 MHz, $CDCl_3$)** δ = 5.73 (d, *J* = 9.3 Hz, 1H), 5.49 (dt, *J* = 9.7, 2.1 Hz, 1H), 5.21 (dd, *J* = 10.6, 9.8 Hz, 1H), 4.78 (d, *J* = 3.4 Hz, 1H), 4.77 (t, *J* = 2.0 Hz, 1H), 4.55 (t, *J* = 1.8 Hz, 1H), 4.45 (ddd, *J* = 10.7, 9.5, 3.4 Hz, 1H), 3.43 (s, 3H), 2.12 (s, 3H), 2.03 (s, 3H), 1.96 (s, 3H); **^{13}C NMR (126 MHz, $CDCl_3$)** δ = 171.4, 170.0, 169.4, 150.4, 99.0, 97.4, 70.9, 69.2, 55.7, 52.1, 23.4, 20.9, 20.8; **Mp** 158 - 164°C; **HRMS (ESI)** calc. for $C_{13}H_{19}NO_7Na^+$ $[M+Na]^+$: 324.1054; found: $[M+Na]^+$ 324.1054.

A purified fraction of the iodide **76** was obtained by column chromatography (CH_2Cl_2:MeOH 95:5 to 85:15): $\mathbf{R_f}$ = 0.13 (CH_2Cl_2:MeOH 9:1); $\mathbf{[\alpha]_D}$ = +110.1° (*c* 2.00, MeOH); **IR (film)**: ν_{max} = 3302, 2929, 2908, 2836, 1617, 1554, 1473, 1442, 1422, 1374, 1321, 1195, 1122, 1041, 1026, 957, 943 cm^{-1}; **^{1}H NMR (500 MHz, CD_3OD)** δ = 4.64 (d, *J* = 3.6 Hz, 1H), 3.92 (dd, *J* = 10.7, 3.6 Hz, 1H), 3.63 (dd, *J* = 10.6, 8.4 Hz, 1H), 3.62 (dd, *J* = 10.5, 2.1 Hz, 1H), 3.43 (s, 3H), 3.39 (ddd, *J* = 9.5, 7.6, 2.1 Hz, 1H), 3.31 (dd, *J* = 10.6, 7.4 Hz, 1H), 3.20 (dd, *J* = 9.3, 8.9 Hz, 1H), 1.98 (s, 3H); **^{13}C-NMR (126 MHz, CD_3OD)** δ = 173.7, 99.9, 76.1, 72.5, 72.4, 55.8, 55.3, 22.6, 7.1; **Mp** 188 - 190°C; **HRMS (ESI)** calc. for $C_9H_{16}INO_5Na^+$ $[M+Na]^+$: 367.9965; found: $[M+Na]^+$ 367.9962.

A purified fraction of the acetylated pyranoside **78** was obtained by column chromatography (EtOAc): $\mathbf{R_f}$ = 0.43 (EtOAc); $\mathbf{[\alpha]_D}$ = +72.9° (*c* 0.15, MeOH); **IR (film)** : ν_{max} = 3324, 2952, 2937, 2922, 2905, 1737, 1657, 1542, 1519, 1434, 1372, 1240, 1223, 1200, 1121, 1076, 1034, 961, 929 cm^{-1}; **^{1}H NMR (500 MHz, $CDCl_3$)** δ = 5.68 (d, *J* = 9.5 Hz, 1H), 5.18 (dd, *J* = 10.8, 9.4 Hz, 1H), 4.90 (t, *J* = 9.6 Hz, 1H), 4.73 (d, *J* = 3.7 Hz, 1H), 4.33 (ddd, *J* = 10.7, 9.6, 3.7 Hz, 1H), 3.75 (ddd, *J* = 9.9, 8.9, 2.4 Hz, 1H), 3.47 (s, 3H), 3.28 (dd, *J* = 10.9, 2.5 Hz, 1H), 3.13 (dd, *J* = 10.9, 8.6 Hz, 1H), 2.05 (s, 3H), 2.01 (s, 3H), 1.95 (s, 3H); **^{13}C-NMR (126 MHz, $CDCl_3$)** δ = 171.4, 170.0, 169.6, 98.3, 72.1, 71.0, 69.5, 55.9, 52.1, 23.4, 20.9 (2C), 3.8; **Mp** 178 - 182°C; **HRMS (ESI)** calc. for $C_{13}H_{20}INO_7Na^+$ $[M+Na]^+$: 452.0177; found: $[M+Na]^+$ 452.0181.

Synthesis of *N*-((2*S*,3*R*,4*R*,5*S*)-4,5-bis(benzyloxy)-2-methoxy-6-methylenetetrahydro-2*H*-pyran-3-yl)acetamide (70)

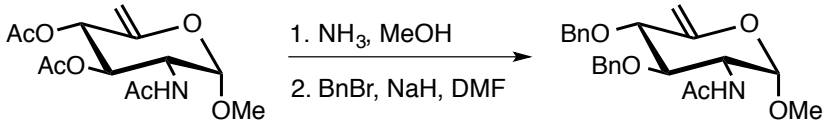

79 **70**, 36% over 2 steps

Using a modification of a published procedure,[75] NH_3 was bubbled through a solution of the acetylated pyranoside **78** (8.72 g, 28.9 mmol) in methanol (100 ml) for 3 h at RT. The solution was evaporated under reduced pressure, coevaporated with toluene, dissolved in DMF (100 mL) and added slowly to a solution of NaH (60% dispersion in mineral oil, 5.78 g, 145 mmol) in DMF (60 mL) at 0°C. After 1 h benzyl bromide (7.09 mL, 59.2 mmol) was added slowly *via* a syringe pump (0.5 mL/min) at 0°C and then the solution was stirred 16 h at RT. The reaction mixture was quenched with MeOH (20 mL), diluted with EtOAc (1 L), washed with brine (3 x 500 mL), dried over Na_2SO_4, evaporated under reduced pressure and the residue was purified by column chromatography (Et_2O:EtOAc 9:1 to 1:1) to afford the benzyl protected **70** (4.09 g, 36% over two steps) as a white solid: $\mathbf{R_f}$ = 0.5 (EtOAc:Et_2O 1:1); $\mathbf{[\alpha]_D}$ = +51.2° (*c* 0.53, $CHCl_3$); **IR (film)**: ν_{max} = 3293, 3086, 3066, 3032, 2928, 2914, 2871, 2836, 1651, 1553, 1497, 1453, 1401, 1376, 1355, 1319, 1292, 1210, 1134, 1096, 1075, 1051, 1030, 952 cm^{-1}; **^{1}H NMR (500 MHz, $CDCl_3$)** δ = 7.40 - 7.27 (m, 10H), 5.42 (d, *J* = 9.2 Hz, 1H), 4.86 - 4.83 (m, 2H), 4.80 - 4.77 (m, 2H), 4.74 - 4.70 (m, 2H), 4.64 (d, *J* = 12.0 Hz, 1H), 4.33 (td, *J* = 9.3, 3.3 Hz, 1H), 4.01 (dt, *J* = 8.2, 1.7 Hz, 1H), 3.64 (dd, *J* = 9.4, 8.3 Hz, 1H), 3.40 (s, 3H), 1.84 (s, 3H); **^{13}C-NMR (126 MHz, $CDCl_3$)** δ = 170.0, 153.8, 138.4, 137.8, 128.6 (2C), 128.6 (2C), 128.3 (2C), 128.0, 128.0 (2C), 127.9, 99.6, 97.7, 79.8, 78.6, 74.5, 74.0, 55.7, 51.8, 23.5; **Mp** 150 - 154°C; **HRMS (ESI)** calc. for $C_{23}H_{27}NO_5Na^+$ $[M+Na]^+$: 420.1781; found: $[M+Na]^+$ 420.1778. The analytical data match those reported in the literature.[69]

Synthesis of *N*-((1*R*,2*R*,3*S*,6*S*)-2,3-bis(benzyloxy)-6-((*tert*-butyldimethylsilyl)oxy)-4-oxocyclohexyl)acetamide (80)

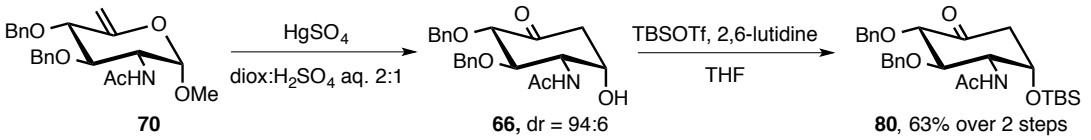

70 **66,** dr = 94:6 **80**, 63% over 2 steps

Using a modification of published procedures,[70,79] $HgSO_4$ (0.452 g, 1.52 mmol) was added to a solution of the benzyl protected olefin **70** (2.24 g, 5.64 mmol) in 1,4-dioxane (56 mL) and aq. H_2SO_4 soln. (5.5 mM, 28 mL) that have been degassed for 10 min with argon. The mixture was stirred at 60°C in the microwave for 15 min, diluted with CH_2Cl_2 (600 mL), washed with brine (2 x 400 mL), dried over Na_2SO_4 and evaporated under reduced pressure. The solids were washed with Et_2O to afford **66** (1.74 g) as a white powder.

Using a modification of a published procedure,[80] the residue was dissolved in THF (160 mL), freshly distilled 2,6-lutidine (2.461 mL, 21.1 mmol) was added at 0°C and the reaction was stirred 30 min at 0°C. Then, TBSOTf (1.272 mL, 5.53 mmol) was added *via* a syringe pump (0.06 mL/h) and the reaction mixture was stirred for 1 h. The reaction mixture was diluted with CH_2Cl_2 (500 mL), washed with sat. aq. Na_2CO_3 soln. (500 mL), with sat. aq. $CuSO_4$ soln. (2 x 400 mL) and with brine (400 mL), dried over Na_2SO_4 and evaporated under reduced pressure. The residue was purified by column chromatography (Et_2O:pentane 7:3) to afford the TBS-protected cyclohexanone **80** (1.76 g, 63% over two steps) as a white solid: $\mathbf{R_f}$ = 0.63 (EtOAc:Et_2O 1:1); $\mathbf{[\alpha]_D}$ = +33.3° (*c* 0.27, $CHCl_3$); **IR (film)**: ν_{max} = 3439, 3312, 3064, 3033, 2955, 2928, 2888, 2857, 1736, 1656, 1548, 1539, 1519, 1498, 1471, 1463, 1455, 1373, 1255, 1137, 1098, 1047, 1028, 933 cm^{-1}; **^{1}H NMR (500 MHz, $CDCl_3$)** δ = 7.45 - 7.42 (m, 2H), 7.40 - 7.29 (m, 8H), 4.98 (d, *J* = 11.7 Hz, 1H), 4.89 (d, *J* = 12.1 Hz, 1H), 4.84 (d, *J* = 7.5 Hz, 1H), 4.66 (d, *J* = 12.1 Hz, 1H), 4.61 (d, *J* = 11.7 Hz, 1H), 4.23 (dt, *J* = 3.3, 2.7 Hz, 1H), 4.14 - 4.09 (m, 2H), 3.78 (dd, *J* = 10.3, 9.3 Hz, 1H), 2.56 (ddd, *J* = 14.0, 2.6, 0.6 Hz, 1H), 2.44 (dd, *J* = 14.2, 3.7 Hz, 1H), 1.72 (s, 3H), 0.79 (s, 9H), 0.00 (s, 3H), –0.11 (s, 3H); **^{13}C NMR (126 MHz, $CDCl_3$)** δ = 203.8, 169.8, 138.2, 137.7, 129.4 (2C), 128.9 (2C), 128.6 (2C), 128.4, 128.3 (2C), 128.1,

86.7, 77.4, 74.6, 73.7, 68.5, 54.9, 45.7, 25.7 (3C), 23.4, 18.0, –4.7, –5.0; **Mp** 101-104°C; **HRMS (ESI)** calc. for $C_{28}H_{39}NO_5SiNa^+$ $[M+Na]^+$: 520.2490; found: $[M+Na]^+$ 520.2483.

Synthesis of (3*R*,4*S*,5*R*,6*R*)-4-acetamido-5,6-bis(benzyloxy)-3-((*tert*-butyldimethylsilyl)oxy)cyclohex-1-en-1-yl trifluoromethanesulfonate (81)

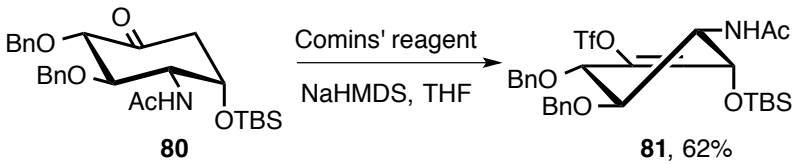

80 **81**, 62%

The compound was prepared by using a modification of a published procedure.[81] To a solution of the TBS-protected cyclohexanone **80** (900 mg, 1.81 mmol) in THF (40 mL) at –78°C Comins' reagent (1.8 g, 4.4 mmol) in THF (40 mL) was added. NaHMDS (2M in THF, 1.9 mL, 3.8 mmol) was added slowly *via* a syringe pump (1.3 mL/h) to the reaction mixture at –78°C. The orange solution was stirred for 5 min, quenched with aq. NaOH soln. (1M, 40 ml) and warmed to RT. The mixture was diluted with EtOAc (400 mL), washed with aq. NaOH soln. (1M, 400 mL), with brine (2 x 200 mL), the org. layer was dried over Na_2SO_4, evaporated under reduced pressure and purified by column chromatography (Et_2O:pentane 1:1 to Et_2O, 1% Et_3N) to afford the enol triflate **81** (699 mg, 62%) as a yellowish oil: $\mathbf{R_f}$ = 0.63 (Et_2O, 1% Et_3N); $\mathbf{[\alpha]_D}$ = +9.1° (*c* 1, $CHCl_3$); **IR (film)** : ν_{max} = 3442, 3433, 3323, 3068, 3032, 2954, 2930, 2886, 2859, 1678, 1516, 1472, 1456, 1423, 1365, 1247, 1210, 1142, 1086, 1043, 985, 937 cm^{-1}; **^{1}H NMR (500 MHz, $CDCl_3$)** δ = 7.42 - 7.29 (m, 10H), 5.76 (dd, *J* = 4.1, 0.8 Hz, 1H), 5.42 (d, *J* = 8.2 Hz, 1H), 4.69 (d, *J* = 10.7 Hz, 1H), 4.68 (d, *J* = 11.8 Hz, 1H), 4.59 (d, *J* = 10.8 Hz, 1H), 4.58 (d, *J* = 11.9 Hz, 1H), 4.55 (t, *J* = 4.1 Hz, 1H), 4.28 (td, *J* = 8.1, 4.4 Hz, 1H), 4.16 (d, *J* = 4.9 Hz, 1H), 4.03 (dd, *J* = 7.8, 4.9 Hz, 1H), 1.78 (s, 3H), 0.85 (s, 9H), 0.07 (s, 3H), 0.02 (s, 3H); **^{13}C NMR (126 MHz, $CDCl_3$)** δ = 170.0, 147.3, 137.6, 136.9, 128.9 (2C), 128.7 (2C), 128.6 (4C), 128.4, 128.4, 121.5, 118.6 (q, *J* = 319.9 Hz), 77.0, 75.3, 74.5, 73.6, 65.1, 49.9, 25.8 (3C), 23.4, 18.1, –4.7, –4.9; **HRMS (ESI)** calc. for $C_{29}H_{38}F_3NO_7SSiNa^+$ $[M+Na]^+$: 652.1983; found: $[M+Na]^+$ 652.1978.

Synthesis of *N*-((1*S*,2*R*,5*S*,6*R*)-5,6-bis(benzyloxy)-2-((*tert*-butyldimethylsilyl)oxy)-4-(hydroxylmethyl)cyclohex-3-en-1-yl)acetamide (82)

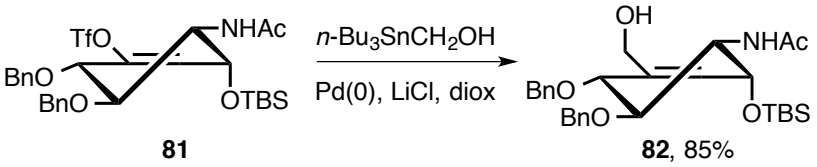

81 **82**, 85%

Using a modification of a published procedure,[82] a solution of the enol triflate **81** (1.54 g, 2.45 mmol), *n*-Bu_3SnCH_2OH (3.01 g, 9.38 mmol)[190] and LiCl (3.92 g, 92.4 mmol) in dioxane (60 mL) was degassed with argon for 10 min and $Pd(PPh_3)_4$ (283 mg, 0.245 mmol) was added. The reaction mixture was heated to 105°C in a microwave oven for 1 h. The mixture was cooled to RT, diluted with CH_2Cl_2 (600 mL), washed with brine (2 x 400 mL), dried over Na_2SO_4, evaporated under reduced pressure and the residue was purified by column chromatography (Et_2O to Et_2O:EtOAc 1:1) to afford the alcohol **82** (1.06 g, 85%) as a yellowish oil: $\mathbf{R}_f$ = 0.2 (Et_2O); $\mathbf{[\alpha]_D}$ = +30.7° (*c* 0.26, $CHCl_3$); **IR (film)**: ν_{max} = 3429, 3362, 3334, 3087, 3065, 3032, 2953, 2929, 2884, 2857, 1656, 1523, 1498, 1461, 1369, 1304, 1254, 1210, 1078, 1028, 1006, 938 cm^{-1}; **^{1}H NMR (500 MHz, $CDCl_3$)** δ = 7.40 - 7.29 (m, 10H), 5.69 (ddd, *J* = 3.7, 2.4, 1.1 Hz, 1H), 5.54 (d, *J* = 8.7 Hz, 1H), 4.77 (d, *J* = 11.8 Hz, 1H), 4.73 (d, *J* = 11.0 Hz, 1H), 4.69 (d, *J* = 11.8 Hz, 1H), 4.58 (d, *J* = 11.0 Hz, 1H), 4.38 (t, *J* = 3.8 Hz, 1H), 4.29 (td, *J* = 8.4, 4.5 Hz, 1H), 4.14 - 4.09 (m, 3H), 4.01 (dd, *J* = 8.1, 5.4 Hz, 1H), 1.83 (dd, *J* = 7.3, 5.1 Hz, 1H), 1.80 (s, 3H), 0.86 (s, 9H), 0.07 (s, 3H), 0.03 (s, 3H); **^{13}C NMR (126 MHz, $CDCl_3$)** δ = 169.9, 139.0, 138.2, 137.7, 128.8 (4C), 128.5 (2C), 128.4 (2C), 128.3, 128.2, 126.8, 78.3, 76.0, 73.9, 73.5, 66.3, 64.3, 50.3, 25.9 (3C), 23.56, 18.21, –4.36, –4.80; **HRMS (ESI)** calc. for $C_{29}H_{41}NO_5SiNa^+$ $[M+Na]^+$: 534.2646; found: $[M+Na]^+$ 534.2640.

[190] R. L. Danheiser, K. R. Romines, H. Koyama, S. K. Gee, C. R. Johnson, J. R. Medich, *Org. Synth.* **1998**, *9*, 704–708.

Synthesis of N-((1R,2R,5S,6R)-5,6-bis(benzyloxy)-2-hydroxy-4-(hydroxymethyl)cyclohex-3-en-1-yl)acetamide (192)

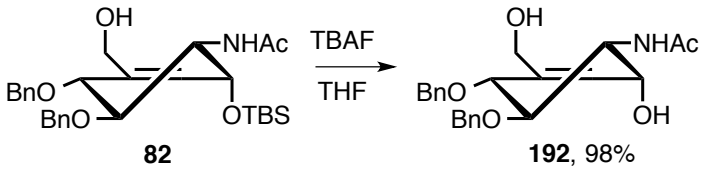

Using a modification of a published procedure,[191] TBAF (1M in THF, 2.97 mL, 2.97 mmol) was added to a solution of the protected alcohol **82** (1.38 g, 2.7 mmol) in THF (100 mL) at 0°C. The reaction mixture was stirred for 3 h at RT and then evaporated under reduced pressure. The residue was purified by column chromatography (EtOAc to EtOAc:MeOH 9:1) to afford the diol **192** (1.05 g, 98%) as a white amorphous solid: $\mathbf{R_f}$ = 0.33 (EtOAc:MeOH 9:1); $\mathbf{[\alpha]_D}$ = –27.8° (*c* 0.26, MeOH); **IR (film)**: ν_{max} = 3282, 2908, 2860, 1655, 1626, 1556, 1544, 1133, 1068, 1028 cm^{-1}; **^{1}H NMR (500 MHz, CD_3OD)** δ = 7.34 - 7.25 (m, 10H), 5.87 - 5.85 (m, 1H), 4.74 (s, 2H), 4.71 (d, *J* = 11.1 Hz, 1H), 4.68 (d, *J* = 11.1 Hz, 1H), 4.26 - 4.22 (m, 2H), 4.19 (d, *J* = 6.6 Hz, 1H), 4.18 - 4.15 (m, 1H), 4.13 (d, *J* = 13.9 Hz, 1H), 4.00 - 3.95 (m, 1H), 1.92 (s, 3H); **^{13}C NMR (126 MHz, CD_3OD)** = 173.4, 142.3, 140.0, 139.8, 129.4 (2C), 129.4 (2C), 129.1 (2C), 128.8 (3C), 128.7, 125.3, 79.9, 78.9, 74.9, 74.7, 66.4, 63.1, 53.0, 22.9; **HRMS (ESI)** calc. for $C_{23}H_{27}NO_5Na^+$ $[M+Na]^+$: 420.1781; found: $[M+Na]^+$ 420.1777.

[191] L. Song, E. N. Duesler, P. S. Mariano, *J. Org. Chem.* **2004**, *69*, 7284–7293.

Synthesis of *N*-((1*R*,2*R*,5*S*,6*R*)-2,5,6-trihydroxy-4-(hydroxymethyl)cyclohex-3-en-1-yl)acetamide, Kirkamide (56)

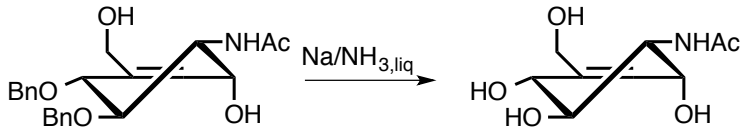

192 **56**, 59%

Using a modification of a published procedure,[192] NH_3 (8 mL) was condensed in a solution of THF (1 mL) at –78°C and sodium (30 mg, 1.29 mmol) was added. To the blue mixture a solution of the diol **192** (40 mg, 0.101 mmol) in THF (4 mL) was added and stirred for 30 min. More sodium (30 mg, 1.29 mmol) was added as soon as the blue color disappeared. After 30 min of remaining color, the reaction mixture was quenched with MeOH (1 mL), stirred for 30 min, water (1 mL) was added and the reaction mixture was warmed to RT. The solution was evaporated under reduced pressure, purified by a column loaded with Amberlite® IR-120 (H^+ form), by column chromatography (CH_2Cl_2:MeOH 8:2) and crystallization (Et_2O:MeOH) to afford kirkamide (**56**) (12.8 mg, 59%) as a white solid: $\mathbf{R}_f$ = 0.13 (CH_2Cl_2:MeOH 8:2). The analytical data were in good agreement with those reported for isolated product. The chemical shifts of the OH protons could be assigned.

[192] X. Lu, G. Arthur, R. Bittman, *Org. Lett.* **2005**, *7*, 1645–1648.

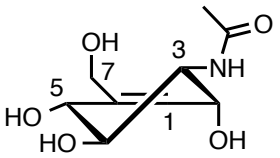

kirkamide (**56**)

Table **18.** NMR spectroscopic data (500 MHz, DMSO-d_6) of the synthetic kirkamide (**56**).

C/N/O no.	**δ_C, type**	**δ_H ($^3J_{H\text{-}H}$ in Hz)**
1	121.5, CH	5.63, dq[a] (4.8, 1.5)
2	64.3, CH	3.98, m
OH(1)		4.80, d (5.5)
3	53.1, CH	3.63, ddd (10.9, 8.1, 3.9)
NH		7.35, d (8.1)
4	70.4, CH	3.55, ddd (10.9, 7.1, 5.2)
OH(2)		4.55, d (5.2)
5	72.9, CH	3.79, ddd[a] (7.1, 6.1, 0.8)
OH(3)		4.97, d (6.1)
6	142.5, C	
7a	60.9, CH_2	3.98, m
7b		3.98, m
OH(4)		4.63, t (5.6)
8	169.3, C	
9	23.0, CH_3	1.85, s

[a] Apparent splitting pattern.

Crystallographic Data of TBS Protected Cyclohexanone 80

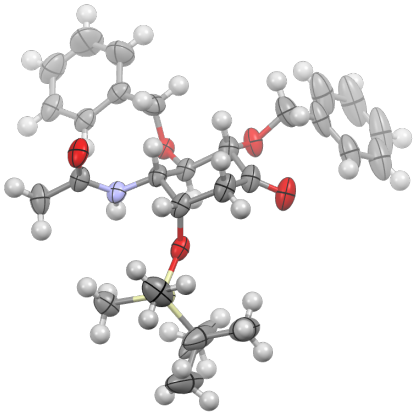

Table 1. Crystal data for **80**

Formula	$C_{28}H_{39}NO_5Si$
Formula weight	497.71
Z, calculated density	6, 1.179 Mg · m^{-3}
F(000)	1608.001
Description and size of crystal	colourless needle, 0.020 · 0.040 · 0.210
mm^3	
absorption coefficient	1.028 mm^{-1}
min/max transmission	0.98 / 0.98
Temperature	123K
Radiation(wavelength)	Cu K_α (λ = 1.54178 Å)
Crystal system, space group	hexagonal, P 6_5
a	12.8301(10) Å
b	12.8301(10) Å
c	29.514(3) Å
α	90°
β	90°
γ	120°
V	4207.4(4) $Å^3$
min/max Θ	3.978° / 69.031°
number of collected reflections	29531
number of independent reflections	5119 (merging r = 0.039)
number of observed reflections	4252 (I>2.0σ(I))
number of refined parameters	393
r	0.0403
rW	0.0551
Goodness of fit	1.1114
Flack parameter	0.01 (4)

6.2.2. Streptol Glucoside

6.2.2.1. Isolation and Structure Elucidation

Bioassay-Guided-Fractionation of Streptol Glucoside

The extract from the leaves of *Psychotria kirkii* (88.6 mg) that was purified with a aminopropyl SPE, was dissolved in H_2O (2.2 mL), filtered and separated using semi-preparative HPLC runs (Phenomenex Synergi Hydro-RP 10 µm; 150 x 10 mm at a flow of 2 mL/min). The column was equilibrated for 10 min with 100% H_2O and the MeCN/H_2O applied gradient was changed from 0% to 1.0% and finally to 100% MeCN in 20 and 10 min, respectively. The column was then washed with MeCN for 10 min. The activities of the fractions were tested in the lettuce seeds growth-inhibition assay described in a section below (table **19**). The most potent fraction (P_II_3) was chosen for further separation using the same analytical method affording a fraction containing streptol glucoside (**57**) (0.6 mg) as a white solid with a retention time of 7 min. The HPLC separation procedure was repeated on a crude extract of the leaves of *Psychotria kirkii* (1.23 g) to afford streptol glucoside (**57**) (1.13 mg).

Streptol glucoside (**57**) as a white solid; **HRMS (ESI)** calc. for $C_{13}H_{21}O_{10}^-$ $[M–H]^-$: 337.1140; found $[M–H]^-$, 337.1144.

Table **19.** Bioassay-guided fractionation of streptol glucoside (**57**).

Fraction	Weight [mg]	Amount tested [mg]	Activity
P_II_1	36.71	0.87	-
P_II_2	31.32	0.53	+
P_II_3	2.09	0.56	++
P_II_4	0.59	0.25	-
P_II_5	1.18	0.40	-
P_II_6	0.09	0.02	-
P_II_7	6.32	0.64	-
P_II_8	1.38	0.07	-

+: active, ++: very active, -: no effect could be detected.

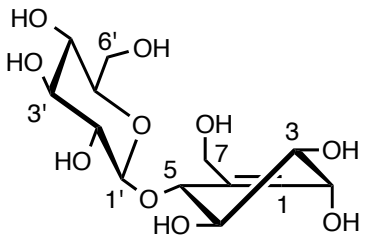

streptol glucoside (**57**)

Table 20. NMR Spectroscopic data (500 MHz, D_2O) of streptol glucoside (**57**).

C no.	δ_H ($^3J_{H\text{-}H}$ in Hz)	COSY	*NOESY*
1	5.92, dd (5.4, 1.1)	2	*2, 3, 7b*
2	4.27, t (4.8)	1, 3	*1, 3,*
3	3.64, dd (10.5, 4.2)	2 4	*2, 4*
4	3.89, d (10.7, 7.2)	3, 5	*3, 5, 1'*
5	4.26, d (8.3)	4	*4, 1'*
6			
7a	4.29, dd (13.0, 0.8)	7b	*7b, 1'*
7b	4.18, d (13.9)	7a	*7a, 1'*
1'	4.63, d (8.0)	2'	*4, 5, 7, 2', 3', 4'*
2'	3.33 dd (9.4, 8.0)	1', 3'	*1', 3', 4'*
3'	3.51, t (9.3)	2', 4'	*1', 2'*
4'	3.41, t (9.4)	3', 5'	*1', 2', 6'a, 6'b*
5'	3.52, ddd (9.9, 6.1, 2.3)	6'	*6'a, 6'b*
6'a	3.72, dd (12.4, 6.2)	5', 6'b	*4', 6'b*
6'b	3.91, dd (12.6, 2.2)	6'a	*6'b, 5'*

Table 21. NMR Spectroscopic data (500 MHz, DMSO-d_6) of streptol glucoside (**57**).

C no.	δ_C, type	δ_H ($^3J_{H-H}$ in Hz)	COSY	HMBC[a]
1	123.1, CH	5.69, d (5.3)	2, 5, 7a, 7b	3, 5, 7
2	65.5, CH	3.98, t (4.6)	1, 3	1, 3, 4, 6
3	70.7, CH	3.26, dd (10.1, 4.0)	2, 4	4
4	71.1, CH	3.68, d (10.1,7.0)	3, 5	3, 5
5	84.3, CH	3.88, d (6.9)	1, 4, 7a	1, 4, 6, 4’
6	140.0, C			
7a	61.2, CH_2	4.07, d (14.4)	7b	1, 6
7b		4.02, d (14.3)	1, 7a	1, 6
1’	104.2, CH	4.3, d (7.9)	2’	5
2’	73.6, CH	3.03 t (8.6)	1’, 3’	1’, 3’
3’	76.6, CH	3.18, t (9.5)	2’, 4’	4’
4’	70.2, CH	3.04, t (9.6)	3’, 5’	3’, 5’, 6’
5’	76.9, CH	3.21, ddd (9.2, 7.5, 1.8)	6’	
6’a	61.2, CH_2	3.72, dd (11.2,1.4)	5’, 6’b	
6’b		3.40, dd (11.5, 7.1)	5’, 6’a	5’

[a] HMBC correlations are given from proton(s) stated to the indicated carbon atom.

Biological Assay

Growth Inhibition Assay of Lettuce Seeds

The HPLC fractions (0.1 – 0.9 mg) were placed in a Petri dish (50 mm diameter) equipped with a filter paper (Whatman), H_2O (1 mL) and lettuce seeds (Krachsalat Grazer Krauthäuptel 3, Migros, Switzerland) were added and the Petri dish sealed with Parafilm was incubated in the dark for one day. The control experiment was done in the same conditions by adding only H_2O (1 mL) and in the positive control the crude extract of *Psychotria kirkii* was used.

6.2.3. Detection and Quantification of Kirkamide and Streptol Glucoside

6.2.3.1. Detection of Kirkamide by GC-MS

Whole leaves of several plants were grounded to a powder, macerated in methanol for 24 h, filtered and dried. Part of the extract was dissolved in water (500 µL), filtered, transferred into a HPLC vial and dried by lyophilization. MSTFA (Sigma) was added, the mixture was stirred for 30 min at 70°C, pyridine (dry, same volume as MSTFA) was added, and the reaction was filtered. Samples of 5 µL were analyzed on a Thermo Scientific™ TRACE™ 1300 Series gas chromatograph equipped with a Thermo Scientific™ ISQ™ Series Single Quadrupole mass spectrometer using a HP-Ultra-1 column (Agilent Technologies, 25 m x 0.200 mm, 0.35 µm). The GC runs were performed using an initial temperature of 40°C (kept for 1 min) a ramp of 7 °C/min and a final temperature of 330°C (kept for 10 min). As a control, derivatization and GC analysis was also carried out with synthetic kirkamide and the data were used as analytical standard.

6.2.3.2. Quantification by ^{1}H NMR Spectroscopy

A solution of maleic acid as internal standard (Sigma Aldrich, TraceCERT®) was prepared at a concentration of 0.52 µmol/mL in D_2O (99.9% deuterated) and the NMR experiments were performed on a Bruker Avance III NMR spectrometer operating at 500 MHz proton frequency.

The protons chosen for maleic acid displayed a chemical shift between 6.30 - 6.20 ppm, for asperuloside (**86**) between 5.997 - 5.981 ppm, for streptol glucoside (**57**) between 5.966 - 5.941 ppm and for kirkamide (**56**) between 5.887–5.874 ppm. The delay times were determined for these protons and values of 7.5 sec for maleic acid, 1.4 sec for asperuloside (**86**), 1.7 sec for streptol glucoside (**57**) and 2.2 sec for kirkamide (**56**) were found. The quantitative ^{1}H NMR measurements were operating with a relaxation delay (D1) of 40 sec, a number of scans (ns) of 128 or 256, a spectral width (sw) of 1.2 ppm and a transmitter offset (O1) of 6 ppm. The water peak at 4.79 ppm was used as the reference for calibration of the maleic acid peak based on a second ^{1}H NMR spectrum recorded for every measurement. The concentrations of asperuloside (**86**), streptol glucoside (**57**) and kirkamide (**56**) were calculated by comparing their peak integration

with the one measured for maleic acid. For the determination of kirkamide (**56**) in the *P. kirkii* leaves extract a mixing experiment was carried out by spiking with 40 µg of synthetic kirkamide (**56**). The leaves extracts, prepared as described for the GC measurement, were weighted using an analytical balance.

Dried leaves from *Psychotria kirkii* (1.0507 g) were ground to small pieces in a mortar with liquid nitrogen. The green powder was stirred in an aq. soln. of MeOH (80%, 100 mL) at rt for 18 h and in an aq. soln. of MeOH (50%, 100 mL) at RT for 18 h. The solutions were filtered, combined, evaporated under reduced pressure and dried by lyophilization to afford the crude extract (372 mg) as a green powder. A portion of the crude extract (9.75 mg) was used for NMR measurement. The integration of kirkamide was corrected by removing a part of a peak, from an unknown compound, possessing a ddd multiplet pattern and a spectra was recorded with co-addition of kirkamide (40 µg) to confirm the result.

The same procedure was applied on the leaves of *Psychotria punctata* (548.0 mg) using different volumes for extraction, 50 mL instead of 100 mL. A portion (17.23 mg) of the crude extract (191.4 mg) was used for the NMR measurement.

Similar procedures were used for the quantification of the natural products in the different parts of the plant. The different extracts were weighed and suspended in a solution of maleic acid (0.52 µmol/mL) in D_2O (500 µL).

6.3. Experimental Fragin

6.3.1. Isolation and Structure Elucidation of Fragin

Genome-driven Bioassay-Guided Fractionation of Fragin

After a comparison of the extracts from *B. cenocepacia* H111 and the mutant *ΔhamD* fragin (**133**) was chosen for the separation and the antifungal activity was tested. The separation was achieved by HPLC using a reversed phase column (Phenomenex Gemini-NX 5 µm; 250 x 4.6 mm with flow of 1 mL/min). The column was equilibrated for 5 min with 20% MeCN/H_2O and the MeCN/H_2O applied gradient was changed from 20% to 80% and finally to 100% MeCN in 15 and 1 min, respectively. The column was then washed with MeCN for 8 min. A peak at 14.8 min**,** identified only in the wild type strain, was isolated and the antifungal activity was tested. The procedure was repeated using multiple HPLC runs with the same conditions described above and fragin (1.4 mg) was obtained as a white solid. NMR experiments were performed in $CDCl_3$ that was filtered through aluminum oxide (activated, basic). By dissolving fragin (1.4 mg) in warm toluene (40°C) and cooling slowly to RT, a single crystal was obtained. Using a similar procedure, Christophe Daeppen obtained a single crystal of synthetic fragin (**133**) where the absolution configuration could be determined by X-ray crystallography structure analysis. The conformations of the synthetic and isolated products were found to be identical due to the negative values for the optical rotation obtained in both cases as well as the same single crystal X-ray structure.

Fragin (**133**): white solid; **MS (ESI)** $[M+H]^+$: 244.2 and 274.2; $[M–H]^–$: 272.2; $\mathbf{[\alpha]_D}$ –12.5° (*c* 0.1, MeOH); ^{1}**HNMR** (500 MHz, $CDCl_3$) δ 11.72 (s, 1H), 5.69 (s, 1H), 4.20 (td, *J* = 9.2, 3.1 Hz, 1H), 3.86 (ddd, *J* = 14.4, 6.0, 3.1 Hz, 1H), 3.60 (ddd, *J* = 14.4, 9.4, 6.1 Hz, 1H), 2.25 - 2.17 (m, 1H), 2.14 (td, *J* = 7.4, 1.8 Hz, 2H), 1.61 - 152 (m, 9H), 1.31 - 1.23 (m, 8H), 1.07 (d, *J* = 6.8 Hz, 3H), 0.90 (d, *J* = 6.7 Hz, 3H), 0.87 (t, *J* = 6.8 Hz, 3H); ^{13}**C NMR** (126 MHz, $CDCl_3$) δ 173.7, 78.0, 39.1, 36.7, 31.8, 29.3, 29.1, 29.1, 25.7, 22.7, 19.2, 18.9,14.2

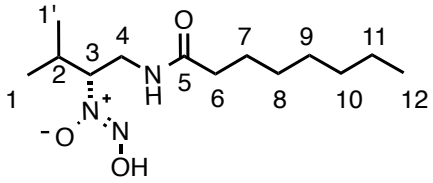

fragin (**133**)

Table **22**. NMR spectroscopic data ($CDCl_3$, 500 MHz) of fragin (**133**).

C/N no.	δ_C, type	δ_H ($^3J_{H-H}$ in Hz)	COSY
1+1'	18.9, CH_3	0.90, d (6.7)	2
	19.2, CH_3	0.87, d (6.8)	2
2	29.1, CH	2.25 - 2.17, m	1, 3
3	78.0, CH	4.20, td (9.2, 3.1)	2, 4a, 4b
NOH		11.72	
4	39.1, CH_2	3.86, ddd (14.4, 6.0, 3.1)	NH, 3, 4b
		3.60, ddd (14.4, 9.4, 6.1)	NH, 3, 4a
NH		5.69	4a, 4b
5	C		
6	36.7, CH_2	2.14, td (7.4, 1.8)	7
7	25.7, CH_2	1.61 - 1.52, m	6, 8-11
8 - 11	22.7, 29.1, 29.3, 31.8 (4x, CH_2)	1.31 - 1.23, m	7, 12
12	14.2, CH_3	0.87, t (6.8)	8-11

Crystallographic Data of Fragin

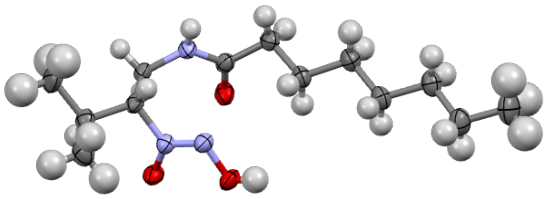

Formula	$C_{13}H_{27}N_3O_3$
Formula weight	273.38
Z, calculated density	4, 1.145 Mg · m^{-3}
F(000)	600
Description and size of crystal	colourless block, 0.050 · 0.110 · 0.190
mm^3	
Absorption coefficient	0.660 mm^{-1}
Min/max transmission	0.93 / 0.97
Temperature	123K
Radiation(wavelength)	Cu K_α (λ = 1.54178 Å)
Crystal system, space group	orthorhombic, P 2_1 2_1 2_1
a	5.6786(4) Å
b	9.1130(6) Å
c	30.633(2) Å
α	90°
β	90°
γ	90°
V	1585.26(19) $Å^3$
Min/max Θ	5.063° / 68.828°
Number of collected reflections	19332
Number of independent reflections	2887 (merging r = 0.036)
Number of observed reflections	2847 (I>2.0σ(I))
Number of refined parameters	173
r	0.0290
rW	0.0241
Goodness of fit	0.9594
Flack	0.08(6)

6.3.2. Biosynthetic Investigations

General HPLC-MS Analysis

The solvent system used was composed of MeCN and H_2O both containing 0.1% of formic acid. The separation was achieved by HPLC using a reversed phase column (Phenomenex Gemini-NX 5 µm; 250 x 4.6 mm with a flow of 1 mL/min). The column was equilibrated for 5 min with 2% MeCN/H_2O and the MeCN/H_2O applied gradient was changed from 2% to 100% in 25 min. The column was then washed with MeCN for 7 min. For the experiments involving salts, during 10 min after injection the flow was redirected to a waste channel before the UV and MS detectors to avoid salt contamination of the MS. The mass chromatograms were recorded in positive and negative ion modes and after each sample at least one wash run was performed.

HPLC Analysis of Synthetic Intermediates

Intermediates were synthesized by Christophe Daeppen on the basis of a suggested fragin (**133**) biosynthesis and they were used as analytical standards for HPLC-MS (ESI + mode) measurements. The amine **143** was detected at 11.6 min with a *m/z* of 229 Da, the hydroxylamine **144** at 12.3 min with a *m/z* = 245 Da, the oxime **145** at 19.1 with a *m/z* = 243 Da, fragin **133** at 20.3 min with a *m/z* = 244 Da and 274 Da, the ketone **142** at 20.3 min with a *m/z* = 228, the nitro **147** at 22.3 with a *m/z* = 300 Da and the nitroso **146** at 28.4 min with a *m/z* = 243 Da.

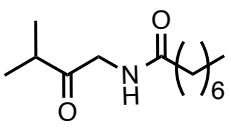

142

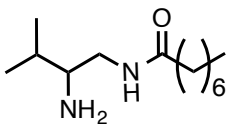

143

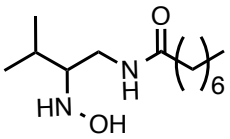

144

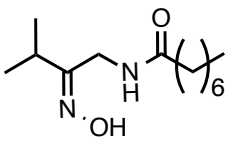

145

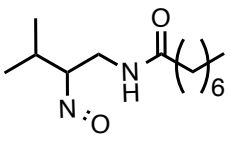

146

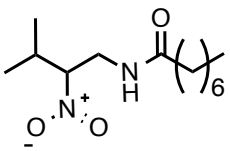

147

Reactivity of the Hydroxylamine 144 with Various Salts

To a solution of the hydroxylamine **144** (0.5 μM, 1.5 mL) in aq. MeOH (50%) a selected salt was added obtaining a final molarity of 67 μM and the solution was filtered. The salts used for the test were NH_4OOCH, NH_4NO_3, $NaNO_3$, $NaNO_2$ and NH_4OAc.

Reactivity of the Hydroxylamine 144 in Various Conditions

For each experiment a solution of the hydroxylamine **144** (0.9 μM) in MeOH was used. Aq. phosphate buffer (10 mM) solns. at different pH (6.5 and 7.85) were prepared and yeast extract was obtained from Sigma Aldrich. The reactivity of the hydroxylamine **144** was tested in different conditions, which are listed in table (**23**).

Table **23**. Reactivity of the hydroxylamine **144** in various conditions.

Experiments	**1**	**2**	**3**	**4**	**5**	**6**	**7**	**8**	**9**
144 (0.9 μM, mL)	0.5	0.5	0.5	0.5	0.5	0.5	0.5	0.5	0.5
H_2O (mL)	0.5	0.5							
Buffer (pH = 6.5, mL)			0.5						
Buffer (pH = 7.85, mL)				0.5					0.5
$NaNO_2$ (mg)		6.9	6.9	6.9					
Yeast extract (mg)					1.4	5			

Synthesis of ^{15}N-labeled Fragin

To a solution of the hydroxylamine **144** (1.4 μM, 0.5 mL) in MeOH $Na^{15}NO_2$ and water (0.5 mL) were added. The solution was filtered and analyzed by HPLC-MS (ESI positive mode). Three data points were recorded: after the preparation of the sample, after 24 h and after 44 h.

Detection of Nitrate/Nitrite

To detect nitrate and nitrite Merckoquant® test stripes (Merck) were used. A pink color at the top indicated the presence of nitrite and at the bottom the presence of nitrate. Solutions of yeast extract were prepared by dissolving 1 g in 2, 4, 8 and 16 mL of water and as a negative control water was chosen.

6.4. Cyclic Peptides Isolated from Cyanobacteria

6.4.1. Balgacyclamides

6.4.1.1.Extraction and Isolation

M. aeruginosa EAWAG 251 was obtained from the EAWAG (Swiss Federal Institute of Aquatic Science and Technology) Culture Collection of Cyanobacteria, currently at the University of Basel. This strain is identical as the *M. aeruginosa* PCC 7820 from the Pasteur Culture Collection of Cyanobacteria, Paris, France. The strain was grown in a 20 L batch reactor (Zehnder medium[193]) with continuous aeration and a light/dark cycle of 12:12 h. The biomass was isolated by centrifugation and subsequently kept frozen until extraction.

The biomass was extracted with 100% MeOH and then twice with 60% MeOH. The extract was separated from the biomass by centrifugation. MeOH was removed from the combined extracts by evaporation under reduced pressure and the mixture was then dried by lyophilization. The resulting powder was dissolved in 80% MeOH and centrifuged to remove remaining particles. The solutions were then sequentially loaded to a C_{18} SPE column (Supelco Discovery DSC-18, 10 g, conditioned with 10% aqueous MeOH), and eluted with 30%, 60%, 80%, and 100% aqueous MeOH solutions. MeOH was removed from the combined extract by evaporation under reduced pressure and the mixture was then dried by lyophilization. The resulting oil from the 80% MeOH fraction was redissolved in 80% MeOH, and the compounds were isolated using multiple C_{18} RP-HPLC runs (Phenomenex Gemini C_{18} 5 µm; 150 × 10 mm). The gradient MeOH/H_2O at a flow of 5 mL/min was 35% MeOH to 100% over 30 min. The column was then washed for 10 min with 100% MeOH and stabilized for the next cycle during 10 min with 35% MeOH. MeOH was removed under reduced pressure and the compounds were then dried with a stream of N_2. Balgacyclamides A, B and C eluted at 17.4, 13.2 and 14.3 min respectively. Balgacyclamide B and C were further purified by HPLC using multiple runs on an analytical column C_{18} RP-HPLC (Phenomenex Gemini C_{18} 5 µm; 150 × 4.6 mm). The gradient MeCN/H_2O at a flow of 1 mL/min was 30% MeCN to 100% over 60 min. The column was then washed for 10 min with 100% MeCN and stabilized for the next

[193] P. Mian, J. Heilmann, H. R. Bürgi, O. Sticher, *Pharm. Biol.* **2003**, *41*, 243–247.

cycle in 10 min with 30% MeCN. Balgacyclamide B and C eluted at 10.0 and 11.2 min respectively. The compounds were dried as described above. The isolation yields of the balgacyclamides A (**177**), B (**178**) and C (**179**) were 0.55 mg, 0.15 mg and 0.80 mg per 15 liters of culture, respectively.

6.4.1.2. Structure Elucidation

Ozonolysis

Each compound (0.1 mg, 0.2 μmol) was dissolved in dry CH_2Cl_2 (0.3 mL), ozonized at RT for 5 min and the solvent was removed under a stream of N_2.

Hydrolysis

Each ozonized compound was hydrolyzed in a closed microwave tube by adding freshly prepared aq. HCl soln. (6 M, 0.5 mL) and the reaction was let at 108 °C for 20 h. The solvent was concentrated by with a gentle stream of N_2 and removed by lyophilization and then the residue was dissolved in H_2O (0.06 mL).

Marfey's Derivatiziation and Analysis[181]

Half of the solution of the hydrolyzed compounds was treated with a FDAA soln. (1% in acetone, 0.03 mL) and an aq. Et_3N soln. (6%, 0.03 mL), the reaction was let at 50°C for 1 h in a closed HPLC vial. The reaction was quenched with an aq. acetic acid soln. (5%, 0.03 mL) and the solvent was removed by lyophilization. The residue was solved in MeOH (0.03 mL) and analyzed by RP-HPLC using an Agilent Zorbax SB-C18 (3.55 μm 150 x 2.1 mm). The mobile phases were A, an aq. acetic acid soln. (5%), and B, MeCN/MeOH (9:1) mixture. The column was stabilized for 20 min with 5% of B, then the gradient went from 5-50% in 50 min and the column was washed with 100% of B for 20 min. The flow was set at 0.25 mL/min and the temperature of the column oven at 50°C.

By comparison of the retention times of the derivatized commercially available amino acids the configuration can be determined except for isoleucine. The retention times (min) for the derivatized standard amino acids were: L-Ala 28.25; D-Ala 32.21; L-Val 35.89; D-Val 40.64; L-Phe 41.01; D-Phe 46.39; L-Thr 21.09; L-*allo*-Thr 22.22; D-

allo-Thr 24.73; D-Thr 28.89; L-Ile 40.47; L-*allo*-Ile 40.45; D-Ile 47.38 and D-*allo*-Ile 47.46.

TFA Derivatization and GC Analysis

The hydrolyzed compound solution (0.03 mL) was transferred to a GC vial and the solvent was evaporated. The residue was treated with trifluoroacetic acid anhydride (0.03 mL) at RT for 12 h and quenched with MeOH (0.03 mL). The configuration of isoleucine was determined after analyses on a chiral GC column (Permabond-L-Chirasil-Val; 25 m, 0.25 mm, Marcherey-Nagel, Düren, Germany) with the following conditions: 2 min at 80 °C, 80 to 180 °C at rate of 8 °C min^{-1} and 10 min at 180 °C with a split ratio 10:1, at a flow of 1mL/min and a FID detector at 250 °C.

The four commercially available stereoisomers of isoleucine were derivatized with the same method as presented above and the retention times (min) were: D-*allo*-Ile 6.20, L-*allo*-Ile 6.35, D-Ile 6.39 and L-Ile 6.45.

Absolute Configuration

Balgacyclamide A (**177**): from ozonolysis−hydrolysis−Marfey D-Ala, L-Thr (confirmed by a co-injection with L-*allo*-Thr), L-Val and D-Ile or D-*allo*-Ile and from ozonolysis−hydrolysis−TFA D-*allo*-Ile (confirmed by a co-injection with D-Ile).

Balgacyclamide B (**178**): from ozonolysis−hydrolysis−Marfey D-Ala, L-Thr, L-Val and D-Ile or D-*allo*-Ile and from ozonolysis−hydrolysis−TFA D-*allo*-Ile (confirmed by a co-injection with D-Ile).

Balgacyclamide C (**179**): from ozonolysis−hydrolysis−Marfey L-Thr, L-Phe and D-Ile or D-*allo*-Ile and from ozonolysis−hydrolysis−TFA D-*allo*-Ile (confirmed by a co-injection with D-Ile).

6.4.1.3. Activity Assays

Plasmodium falciparum, *Trypanosoma b. rhodesiense* and cytotoxicity *in vitro* assay were performed according to procedures previously described.[173]

6.4.2.Glycolipopeptides

6.4.2.1.Extraction and Isolation

Sources and Cultivation of *M. aeruginosa* EAWAG 251

The cyanobacteria strain *Tolypothrix distorta var. symplocoides* EAWAG 224a was obtained from the EAWAG (Swiss Federal Institute of Aquatic Science and Technology) Culture Collection of Cyanobacteria, currently at the University of Basel. The cyanobacteria cultures were grown in 250 mL culture flasks, 20 L tank (EAWAG 224a_VI) and a 500 mL Erlenmeyer in Z2 medium with continuous aeration and a light/dark cycle of 12:12 h.[193] The biomass was isolated by centrifugation.

Extraction and Isolation

The biomass of EAWAG 224a culture was collected by centrifugation at 9000 G for 30 min, followed by decantation of the media. For the extraction MeOH (100 mL) was added to the residual biomass and a sonification (3 x 3 min), a centrifugation at 9000 G for 30 min and filtration over a Büchner filter were performed. This procedure was repeated with MeOH (100 mL) and with an aq. MeOH soln. (40%, 2 x 100 mL). The combined filtrates were evaporated under reduced pressure at 35°C and lyophilized to yield a green crude extract.

The crude extract (90.3 mg) was dissolved in an. aq. MeOH soln. (60%) and eluted with an aq. MeOH soln. (80%) through a RP-SPE column (Supleco Discovery DSC-18, 500 mg) that was washed with MeOH and H_2O and conditioned with an aq. MeOH soln. (80%). The filtrate was evaporated under reduced pressure at 30°C and resuspended in an aq. MeOH soln. (60%). The green liquid was centrifuged (Eppendorf Centrifuge 5415D) for 5 min at 9000 G, filtered and transferred into a HPLC vial. The extract was purified by HPLC using a RP preparative column (Phenomenex Gemini-NX 5 µm; 75 x 21.1 mm, flow of 9 mL/min). The column was equilibrated for 5 min with 10% MeCN, then the MeCN/H_2O gradient was changed from 10% to 60% to 100% MeCN respectively in 25 to 3 min and the column was then washed with MeCN for 14 min. Multiple HPLC runs were conducted to obtain the fraction VIII_F5 (eluted between 18.4 min to 19.3 min, 0.72

mg), which was chosen for further separation. All fractions were evaporated under reduced pressure at 35°C.

The fraction VIII_F5 (0.72 mg) was dissolved in an aq. MeOH soln. (60%), filtered and transferred into an HPLC vial. The sample was purified by HPLC using an analytical column (Phenomenex Synergi Hydro-RP 4 µm; 150 x 4.6 mm, flow of 1 mL/min). The column was equilibrated for 5 min with 40% MeCN, then the MeCN/H_2O gradient was changed from 40% to 50% to 100% MeCN in respectively 35 to 2 min and the column was then washed with MeCN for 9 min. Multiple HPLC runs were conducted to obtain the fractions GLCP-1 (**182**) (eluted between 13.2 min to 13.5 min, 0.29 mg) and GLCP-2 (**183**) (eluted between 13.8 min to 14.5 min, 28.45 mg, 0.4 mg), which were lyophilized.

6.4.2.2. Structure Elucidation

Synthesis *N*-methylated Threonines

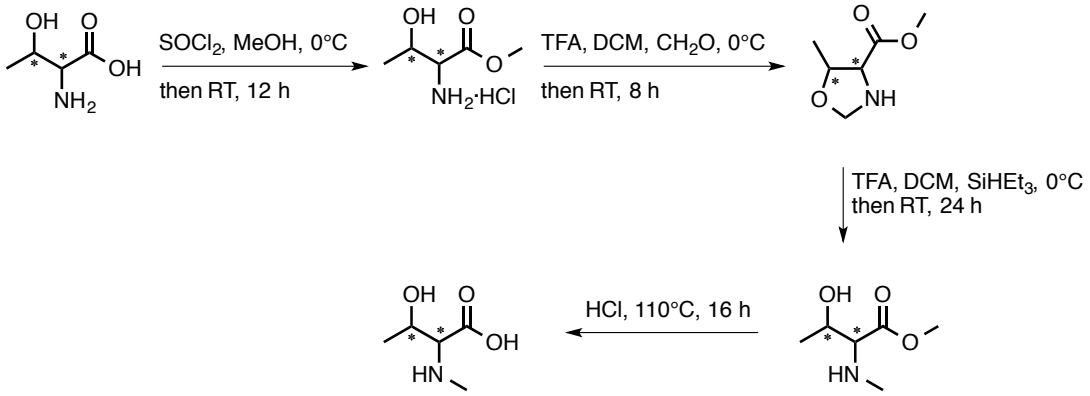

General procedure[186]

The synthesis route was identical for the three non-proteinogenic threonines and here is described, as an example, the procedure for D-threonine (**193**).

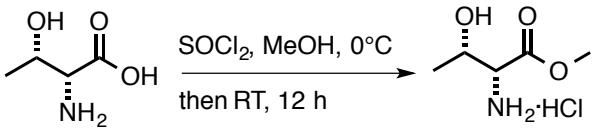

193 **194**

$SOCl_2$ (0.26 mL, 426 mg, 3.58 mmol) was added to MeOH (1 mL, 24.7 mmol) cooled at 0°C and the mixture was stirred at 0°C for 30 min. D-Threonine (**193**) (100 mg, 0.83 mmol) was added to the reaction in one portion and after 10 min the mixture was

warmed at RT, stirred for 12 h and evaporated under reduced pressure to give D-threonine methylester hydrochloride (**194**). The compound was used in the next step without any further purification.

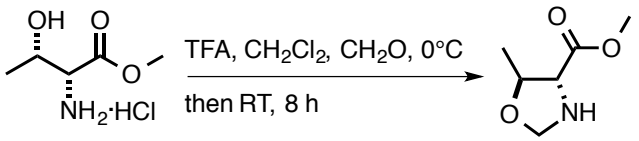

194 **195**

D-Threonine methylester hydrochloride (**194**) was dissolved in CH_2Cl_2 (12.5 mL) and cooled at 0°C in an ice bath for 20 min. An aq. TFA soln. (0.1 M, 12.5 mL, 1.25 mmol) was added to the solution and the biphasic mixture was stirred vigorously for 15 min at 0°C. An aq. formaldehyde soln. (37%, 77.5 µL, 1.04 mmol) was added dropwise to the mixture. After 10 min the mixture was stirred for 8 h at RT. The reaction mixture was neutralized with a sat. aq. $NaHCO_3$ soln. extracted with CH_2Cl_2 (4 x 15 mL), the organic layers were combined, dried over $NaSO_4$ and evaporated under reduced pressure to yield the oxazolidine **195**. The compound was used in the next step without any further purification.

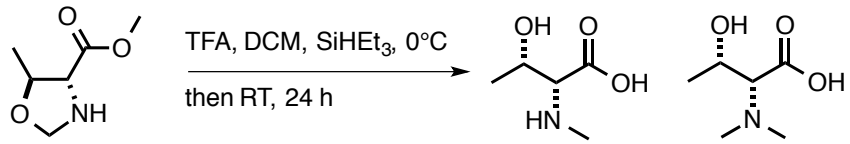

195 **196** **197**

To a solution of the crude oxazolidine **195** (52.45 mg) in CH_2Cl_2 (4.9 mL) at 0°C, TFA (4.9 mL, 66.2 mmol) cooled at 0°C was added followed by a dropwise addition of triethylsilane (0.49 mL, 3.04 mmol) and after 10 min the reaction was stirred for 24 h at RT. The mixture was evaporated under reduced pressure. The yellow oil was resuspended in an aq. HCl soln. (1 M) and extracted with pentane. The aq. layer was collected and evaporated under reduced pressure giving an oil which was then directly used for the following hydrolysis in an aq. HCl soln. (6 M, 1 mL) at 110°C for 16 h. The solvent was evaporated under reduced pressure yielding a 2:1 mixture (41.5 mg), interpreted from NMR analysis, of *N*-Me-D-threonine **196** (27.6 mg, 0.207 mmol, 5.8 % over 4 steps) with *N,N*-dimethyl-D-threonine **197** (13. 8 mg, 0.094 mmol, 2.6% over 4 steps). The analytical data were in agreement with those reported.[180]

Hydrolysis

GLCP-2 (**183**) (150 µg) was transferred into a microwave tube with MeOH and the solvent was evaporated under reduced pressure at 40°C. A freshly prepared aq. HCl soln. (6 M, 275 µL) was added and the reaction was degassed with argon. Then the reaction was stirred at 108°C for 24 h. The solvent was removed under a gentle stream of N_2 at 40°C. The residue was dissolved in H_2O (0.5 mL), transferred into a vial and dried by lyophilisation.

Marfey's Derivatization and Analysis of GLCP-2

The procedure of the Marfey's derivatization was identical as the one described for the structure analysis of the balgacyclamides.

The retention times of the derivatized standard amino acids were compared to the values observed for the derivatized amino acid from GPLC-2 (**183**) confirming the presence of L-tyrosine, D-tyrosine, D-glutamic acid, L-threonine (confirmed by coinjection with L-threonine), D-threonine, D-*allo*-threonine, glycine and *N*-Me-L-*allo*-threonine (confirmed by coinjection with *N*-Me-L-*allo*-threonine and *N*-Me-D-threonine). The retention times (min) for the derivatized standard amino acids were: L-Tyr 24.33/48.92[194]; D-Tyr 25.19/54.09[194]; L-Gln 20.09; D-Gln 21.65; L-Glu 25.67; D-Glu 22.27; L-Thr 19.99; D-Thr 26.58; L-*allo*-Thr 21.10; D-*allo*-Thr 23.90; Gly 22.51; *N*-Me-L-Thr 22.24; *N*-Me-D-Thr 24.97; *N*-Me-L-*allo*-Thr 28.54; *N*-Me-D-*allo*-Thr 29.25

NMR Spectroscopy Analysis of GLCP-2

GLCP-2 (**183**) (0.4 mg) was dissolved in CD_3OD (35 µL) and transferred into a NMR capillary tube (1.7 mm). NMR experiments (^{1}H-NMR, COSY, TOCSY, NOESY and HSQC) were measured on 600.13 MHz equipped with a 1.7 mm TCI cryoprobe.

Activity Assays

Plasmodium falciparum, *Trypanosoma b. rhodesiense* and cytotoxicity *in vitro* assay were performed according to procedures previously described.[173]

[194] The value are for threnonine containing two Marfey's reagent

7.Appendices

NMR Spectra Isolated Kirkamide

^{1}H NMR Spectrum of isolated kirkamide (**56**) in DMSO-d_6 (500 MHz).

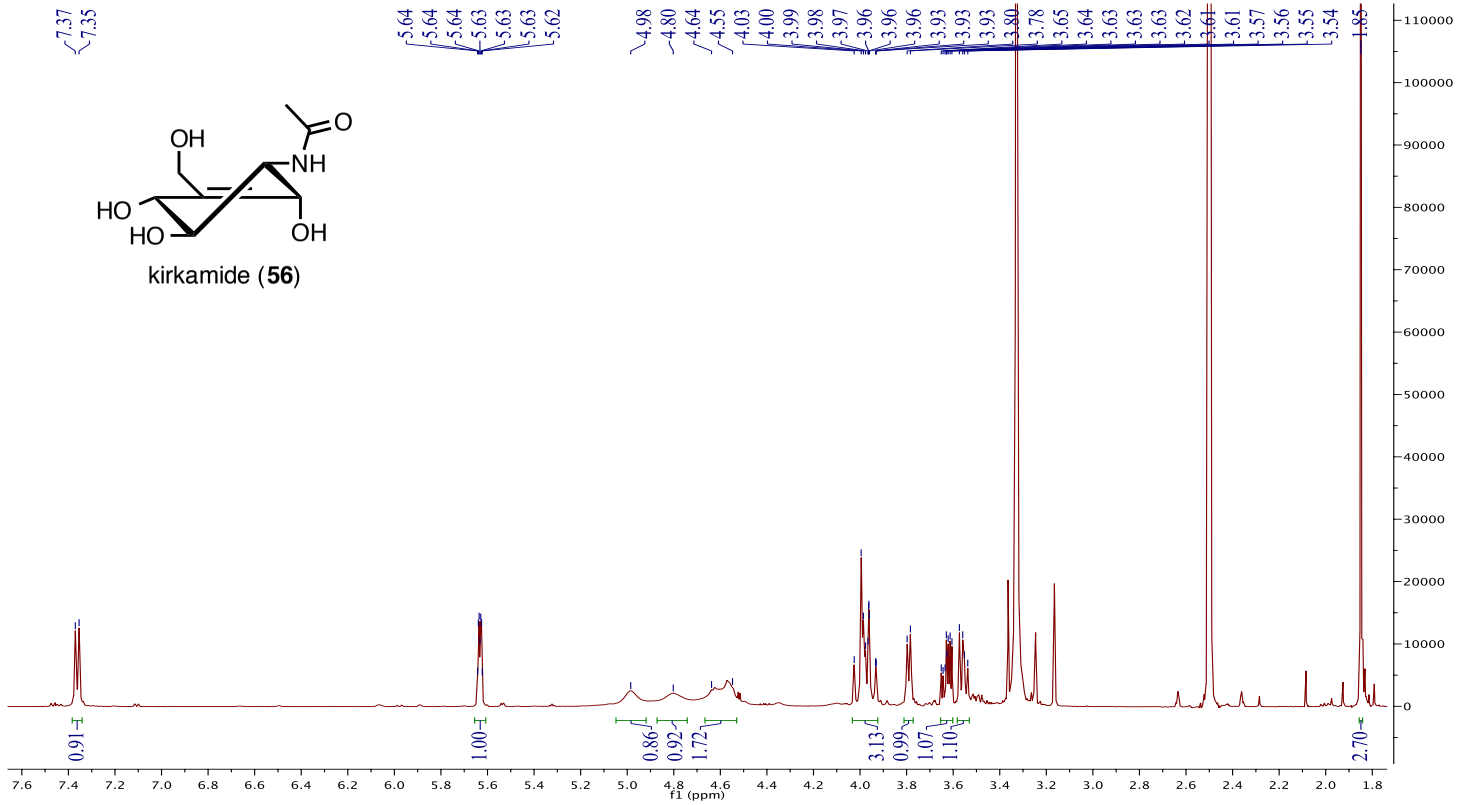

^{1}H-^{1}H COSY NMR Spectrum of isolated kirkamide (**56**) in DMSO-d_6 (500 MHz).

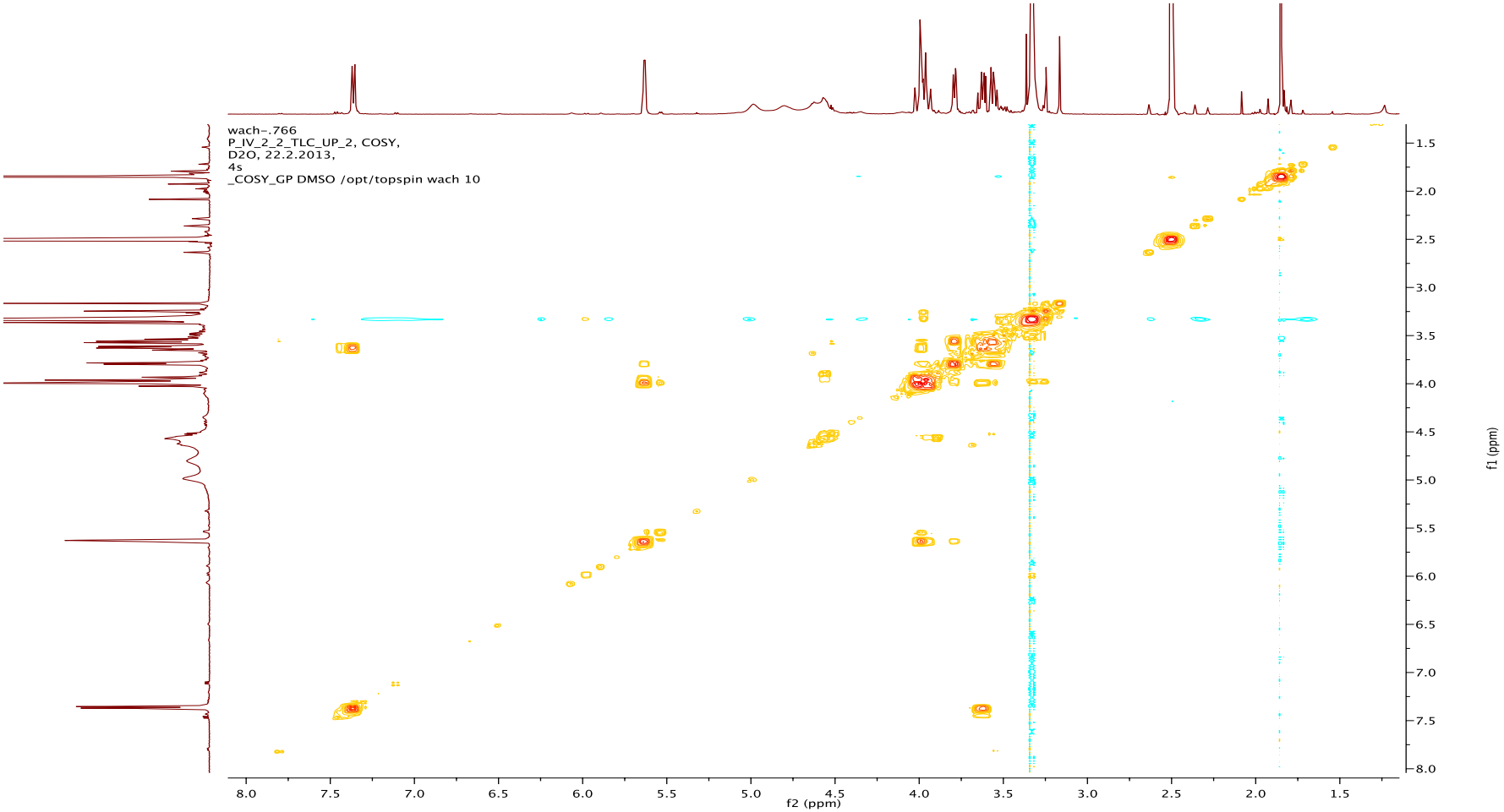

^{1}H-^{13}C gHMQC NMR Spectrum of isolated kirkamide (**56**) in DMSO-d_6 (500 MHz).

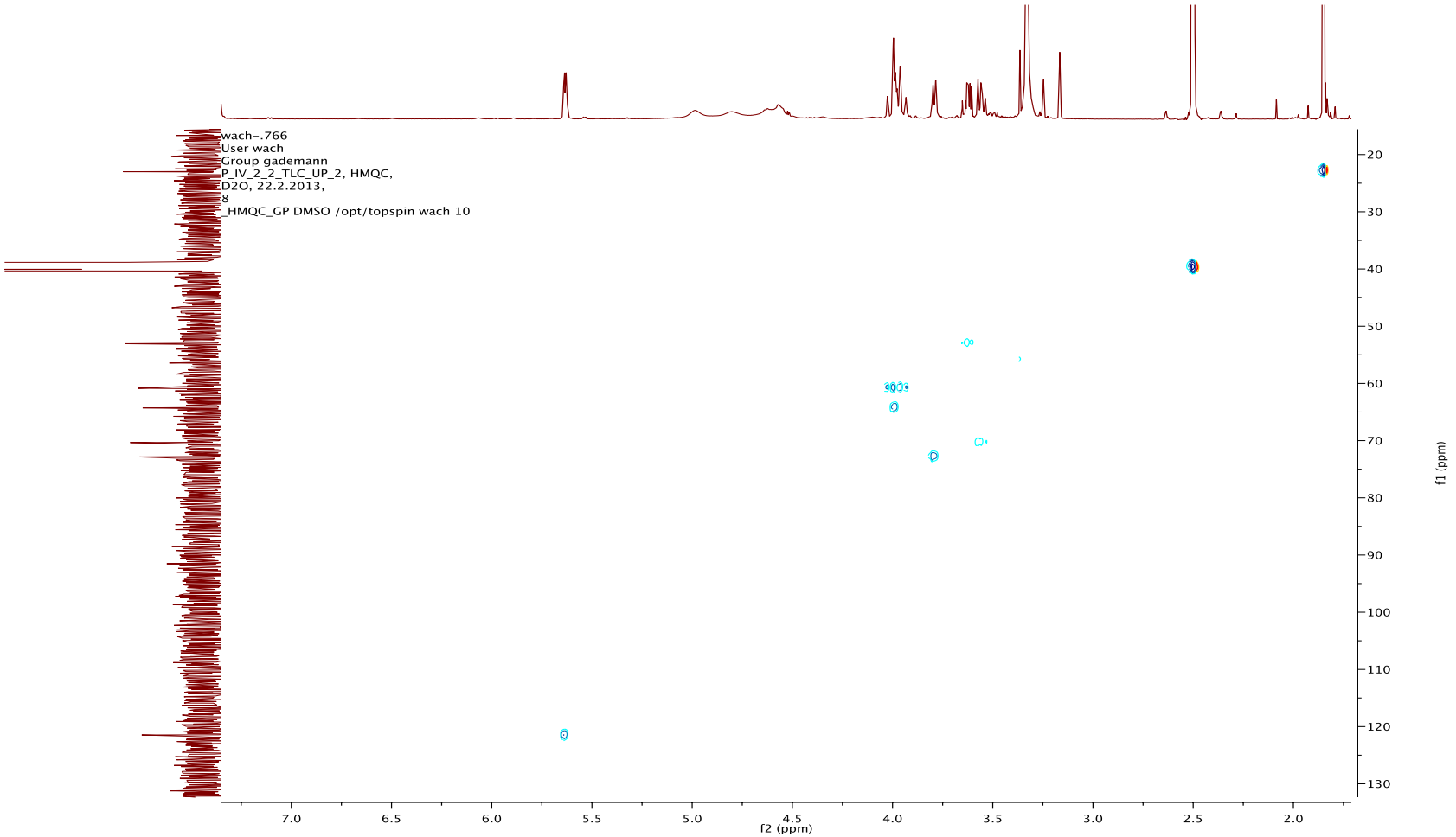

^{1}H-^{13}C gHMBC NMR Spectrum of isolated kirkamide (**56**) in DMSO-d_6 (500 MHz).

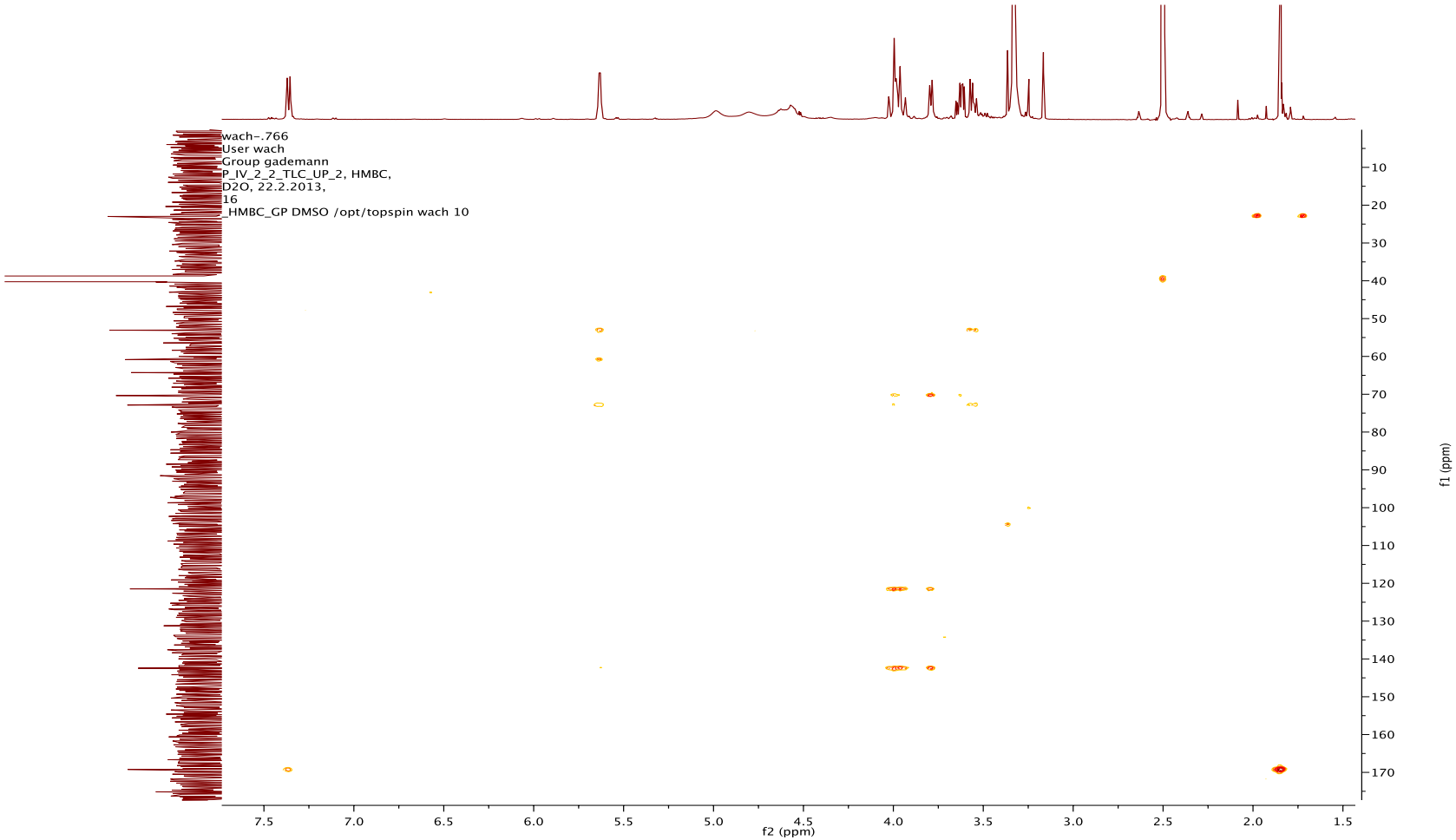

^{1}H-^{1}H NOESY NMR Spectrum of isolated kirkamide (**56**) in DMSO-d_6 (500 MHz).

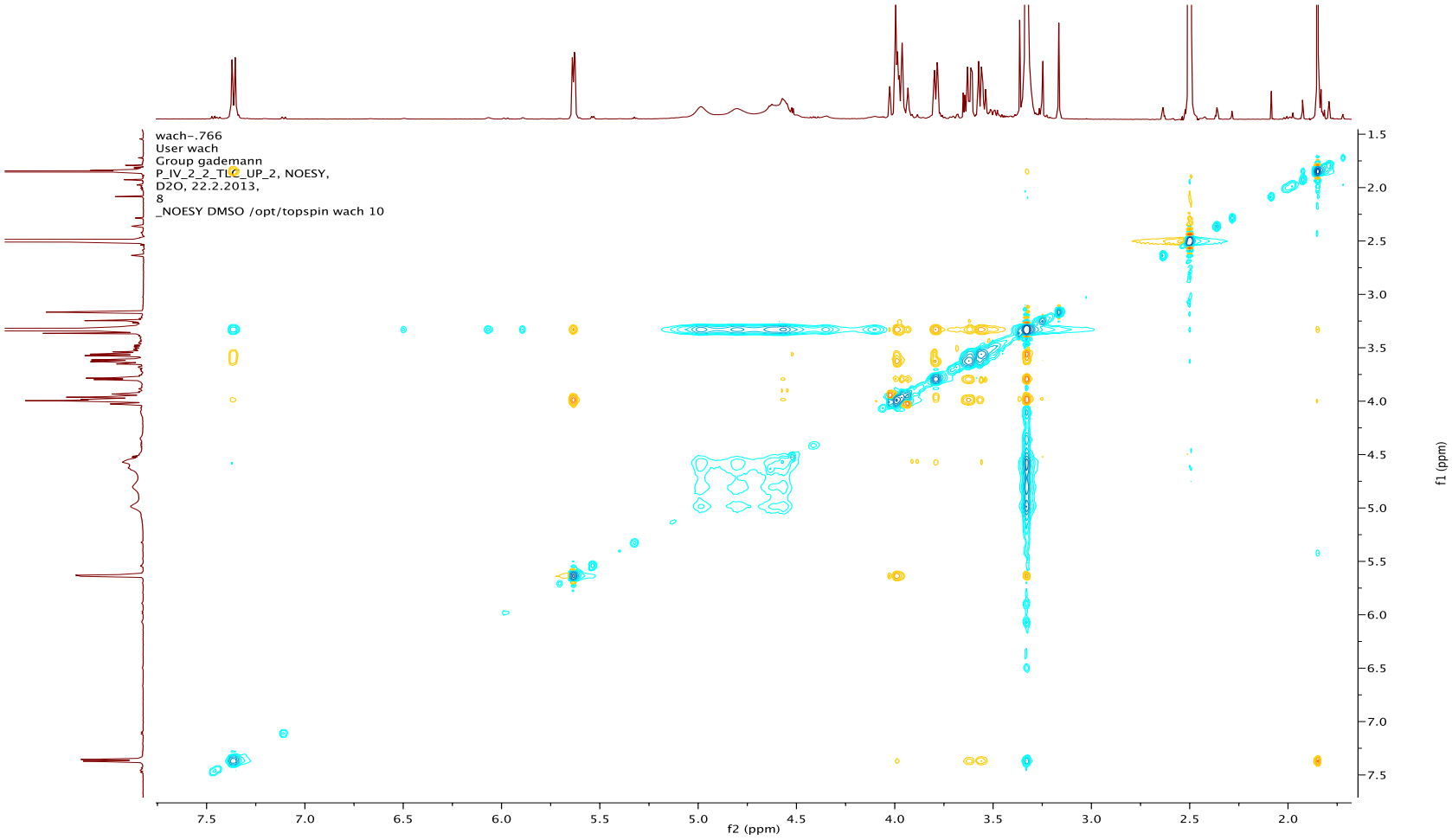

^{13}C NMR Spectrum of isolated kirkamide (**56**) in DMSO-d_6 (400 MHz).

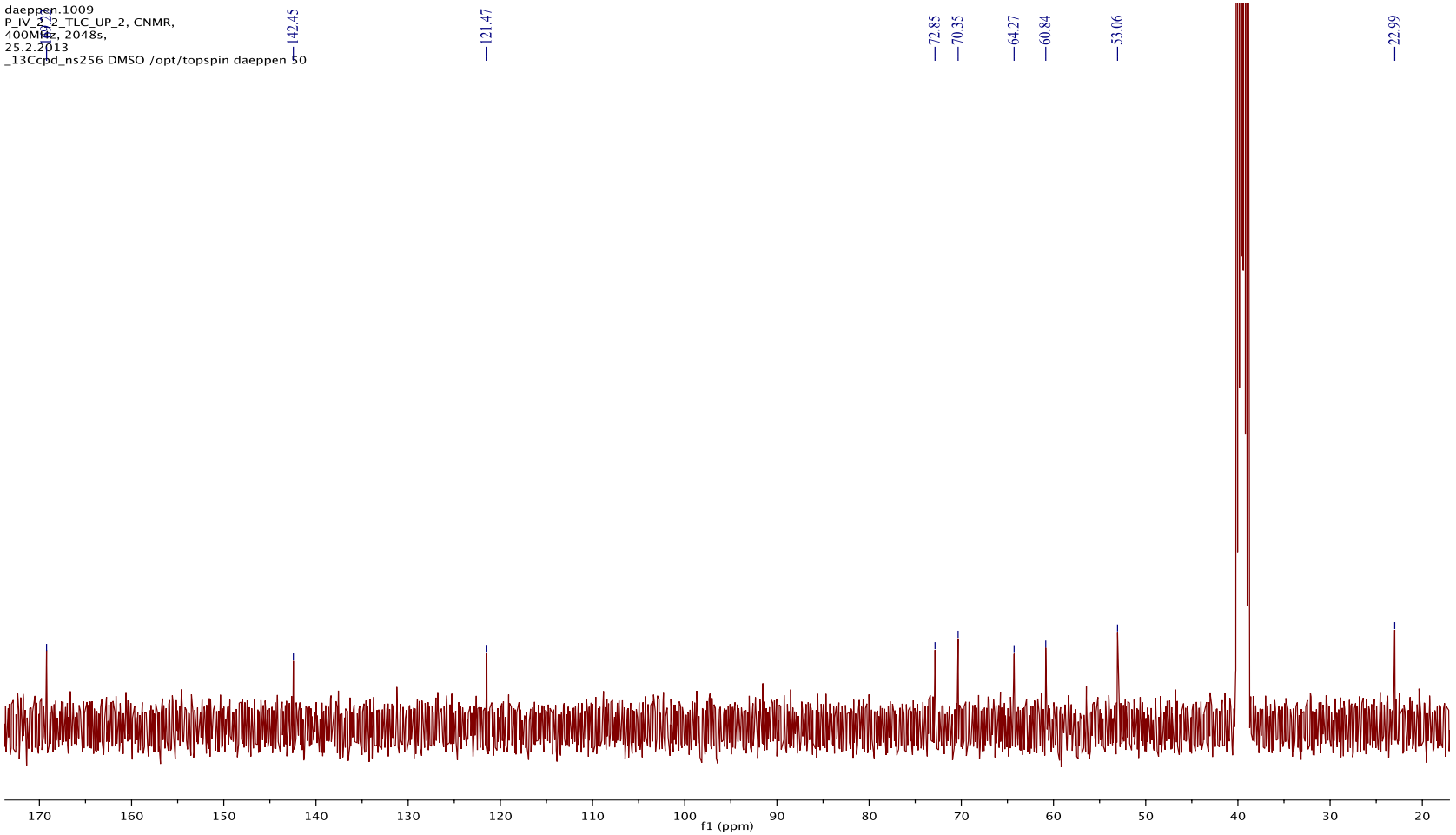

^{1}H NMR Spectrum of isolated kirkamide (**56**) in D_2O (500 MHz).

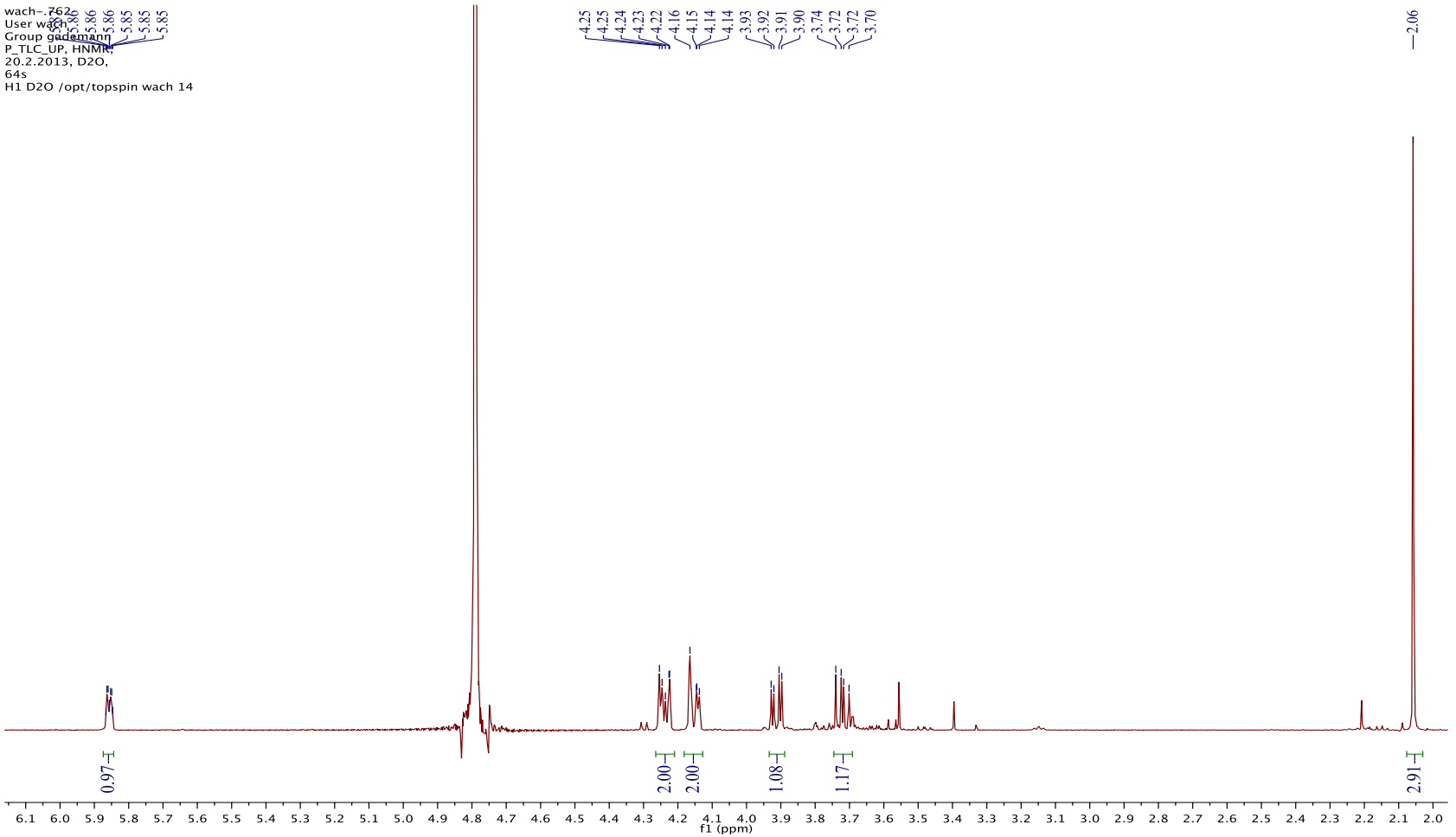

^{1}H NMR Spectra comparison of sucrose (bio sugar: COOP, Switzerland) and the mix fraction containing sucrose with kirkamide (**56**) in D_2O.

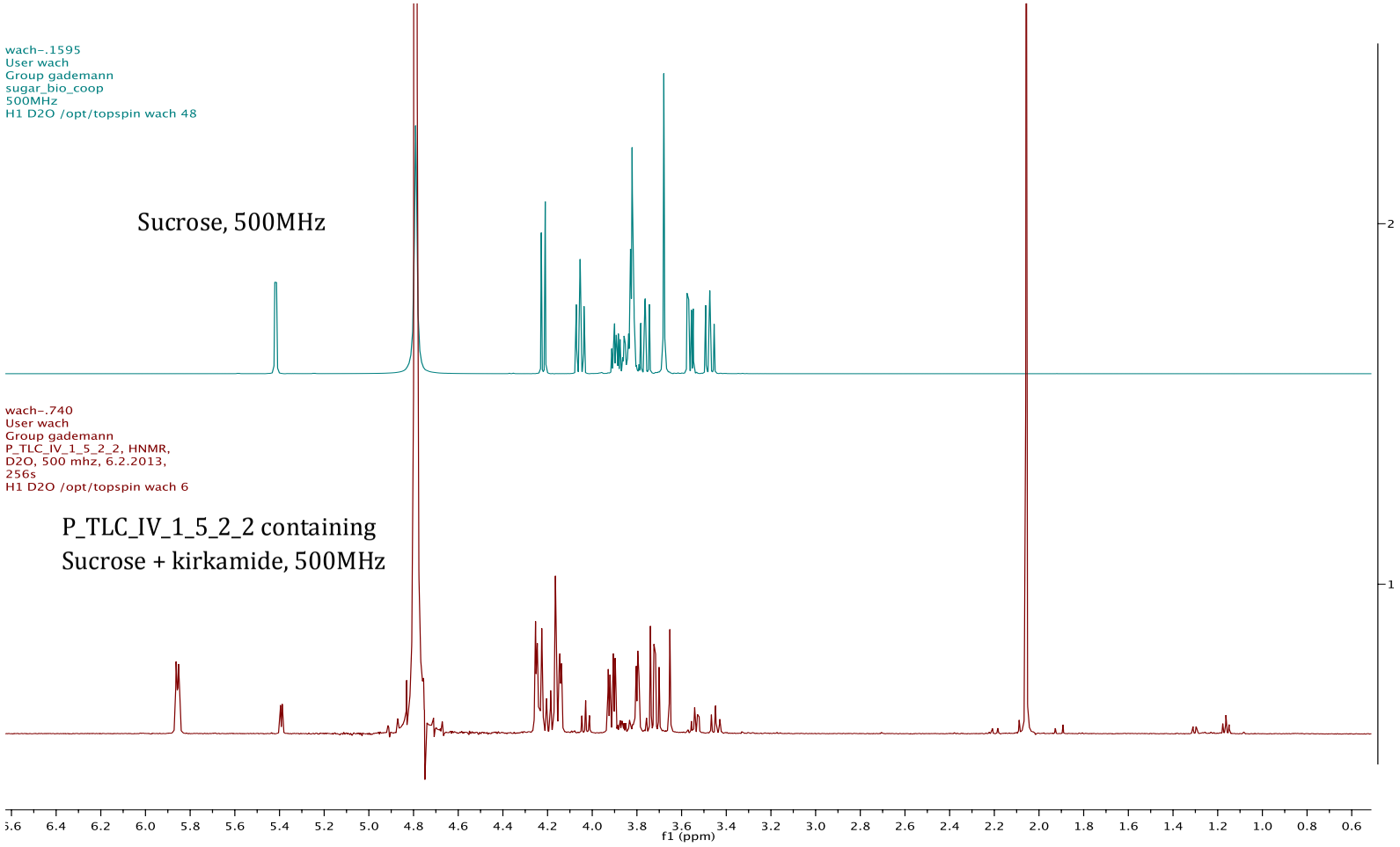

^{1}H NMR of isolated kirkamide (**56**) (650 ng, 3 nmol) in DMSO-d_6 using capillary tube (1.7 mm) and 600 MHz NMR equipped with a Cryo Probe.

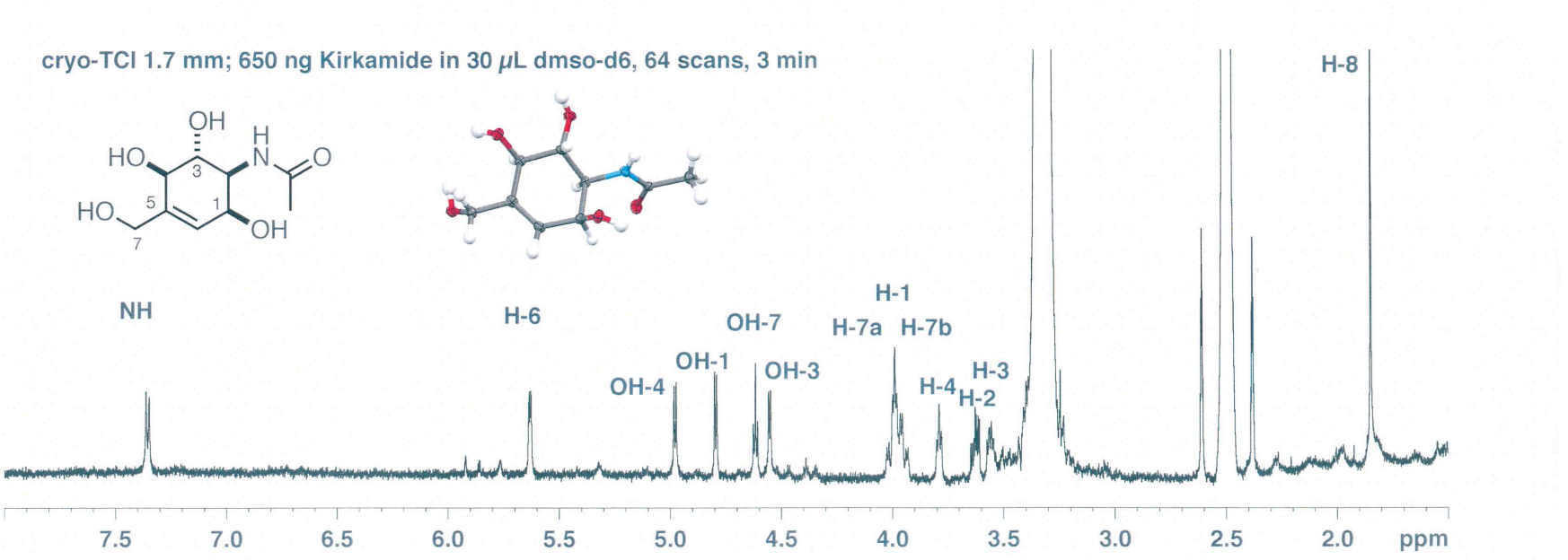

NMR Spectra of Valienamine (21) in DMSO-d_6

^{1}H NMR Spectrum of valienamine (**21**) in DMSO-d_6 (600 MHz).

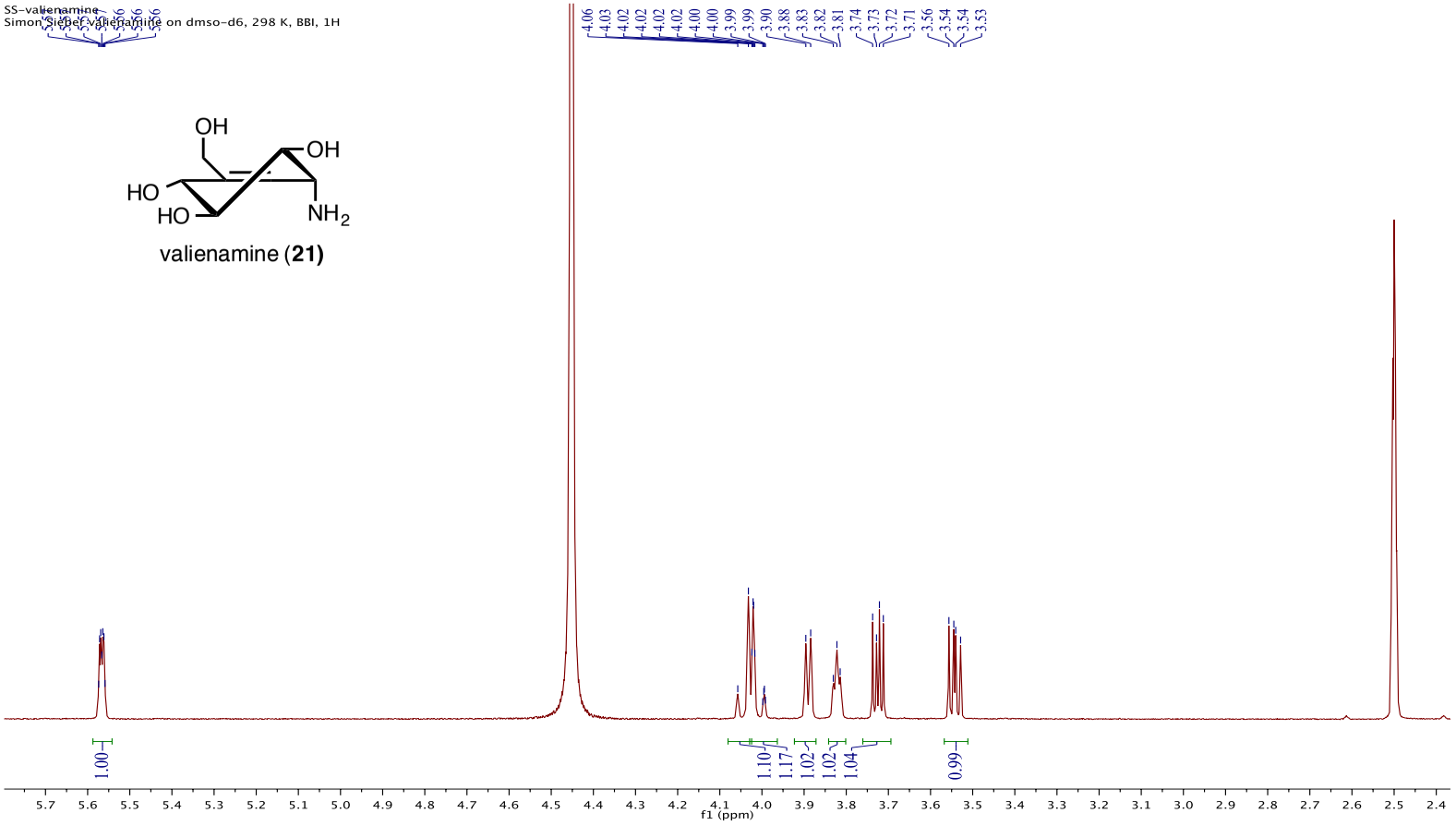

^{1}H-^{1}H COSY Spectrum of valienamine (**21**) in DMSO-d_6 (600 MHz).

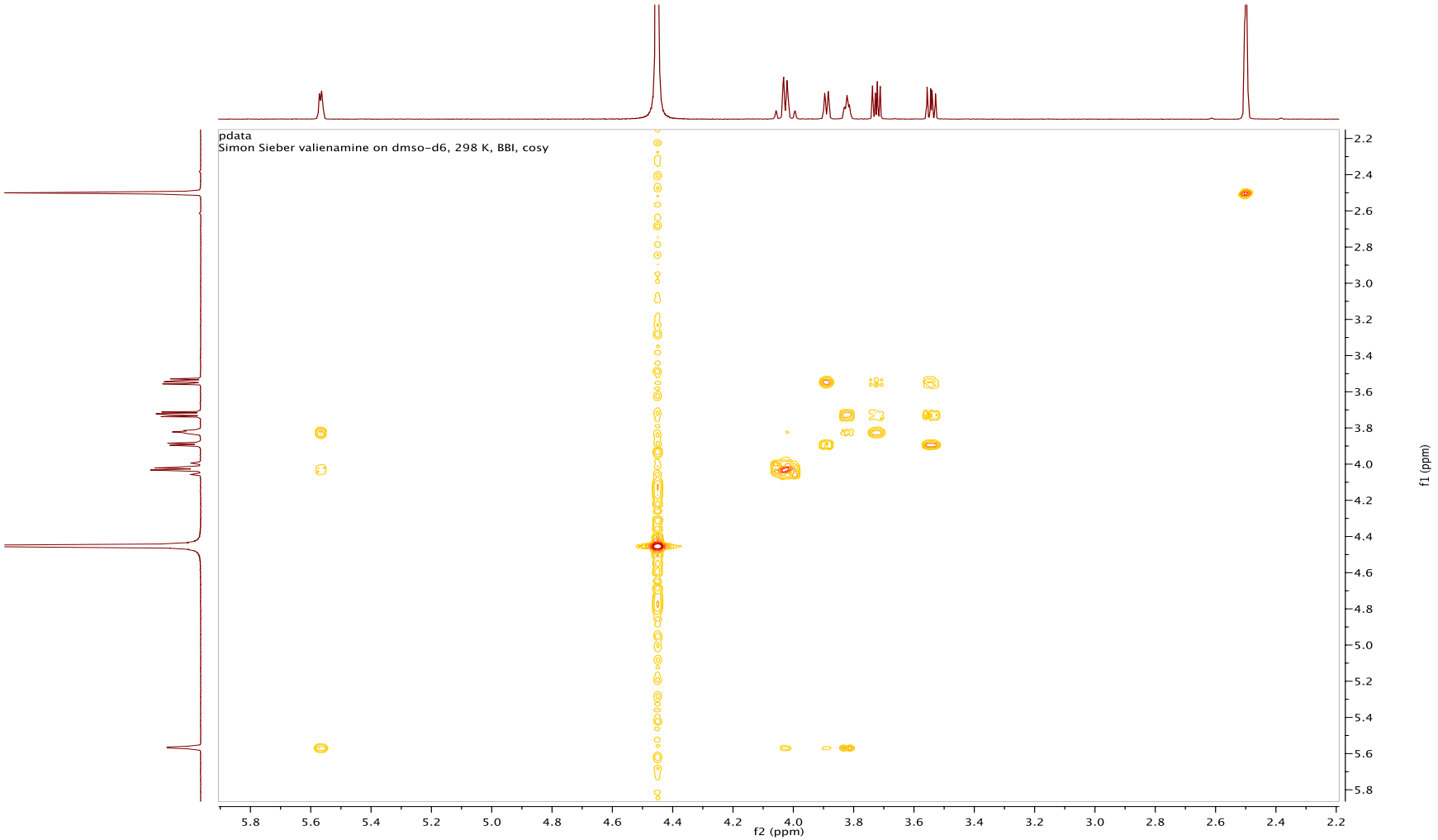

^{1}H-^{13}C HMQC Spectrum of valienamine (**21**) in DMSO-d_6 (600 MHz).

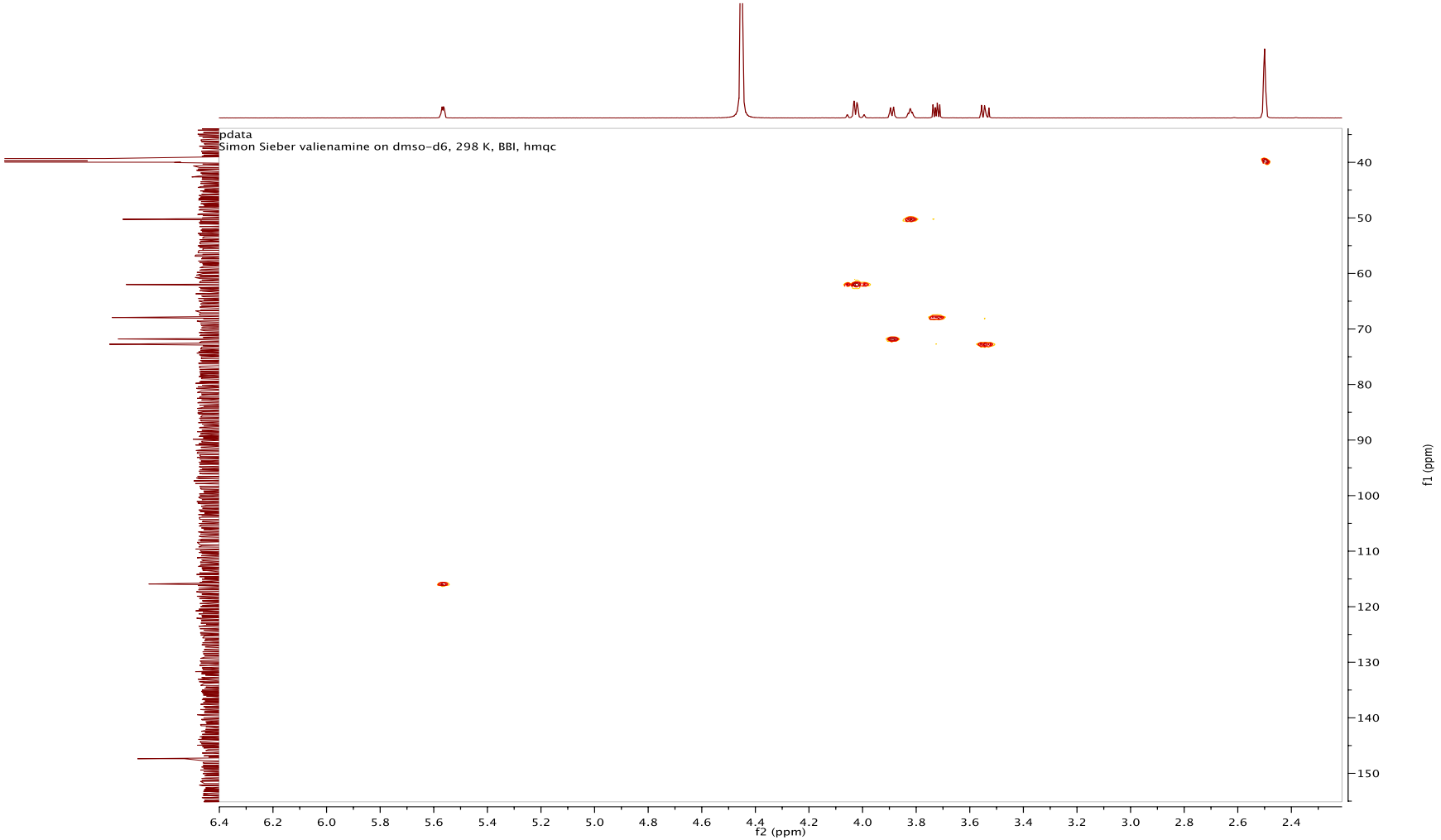

^{1}H-^{13}C HMBC Spectrum of valienamine (**21**) in DMSO-d_6 (600 MHz).

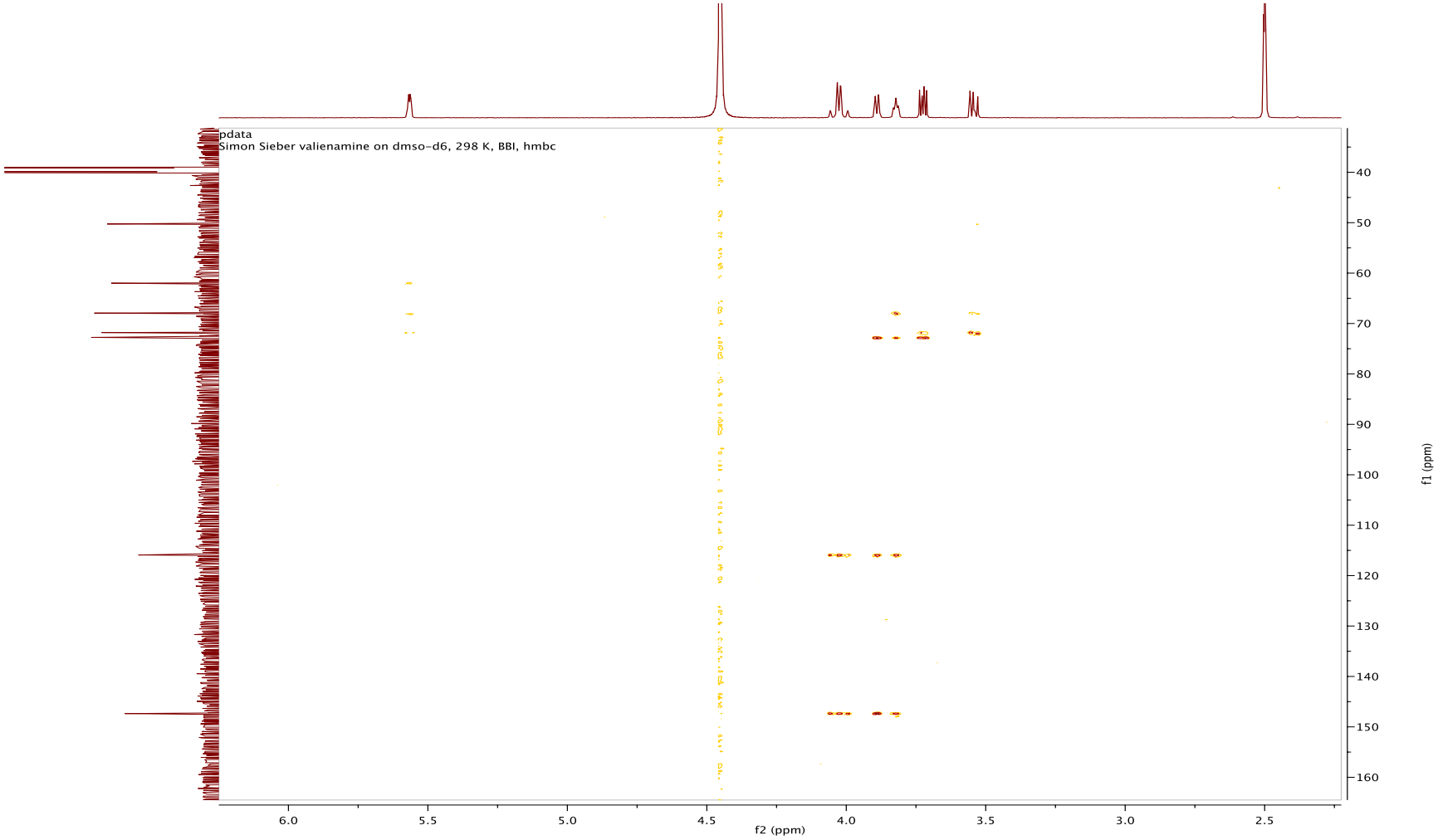

^{13}C NMR Spectrum of valienamine (**21**) in DMSO-d_6.

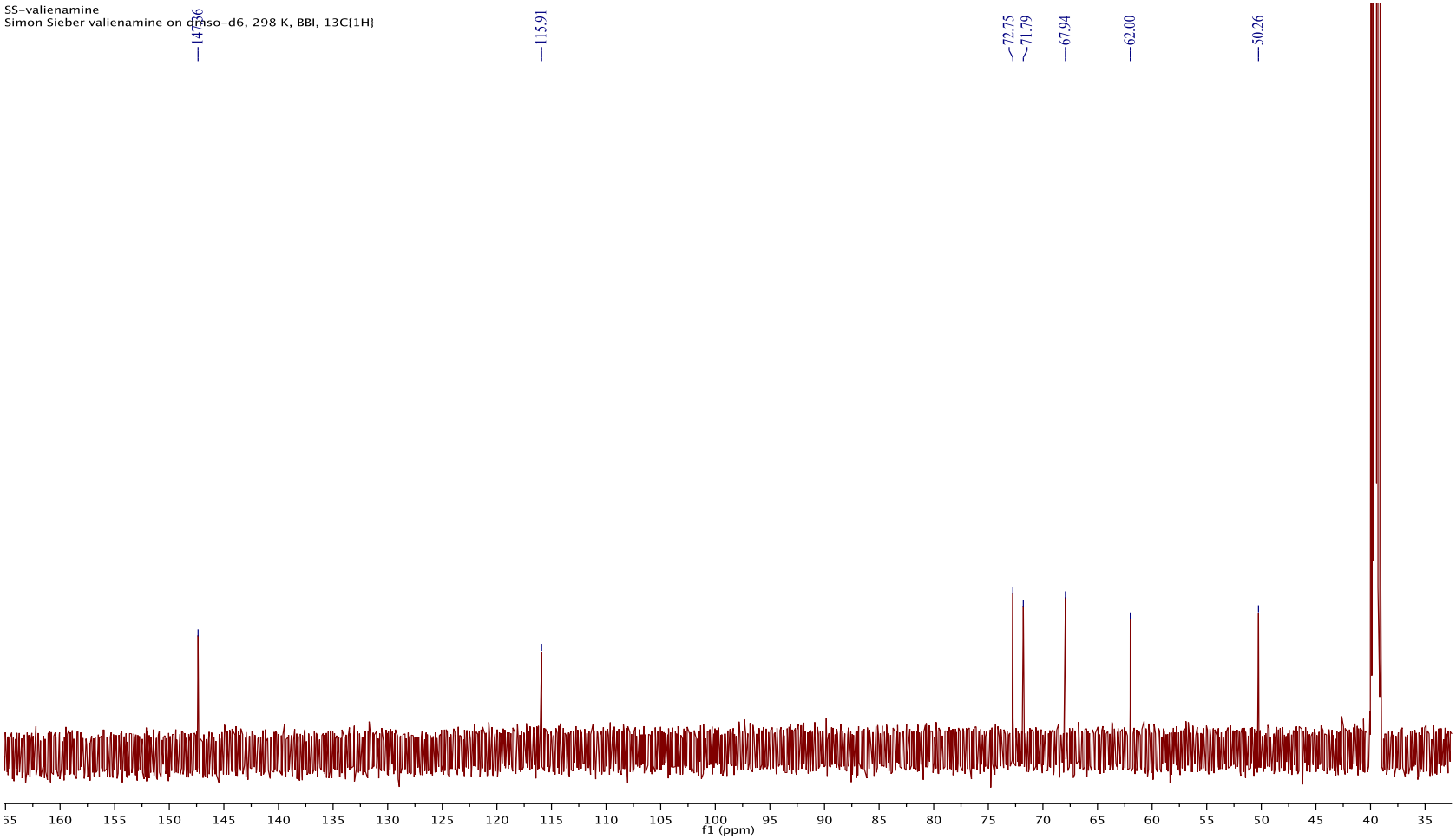

^{1}H NMR Spectra comparison of the isolated and synthetic kirkamide (**56**) in D_2O.

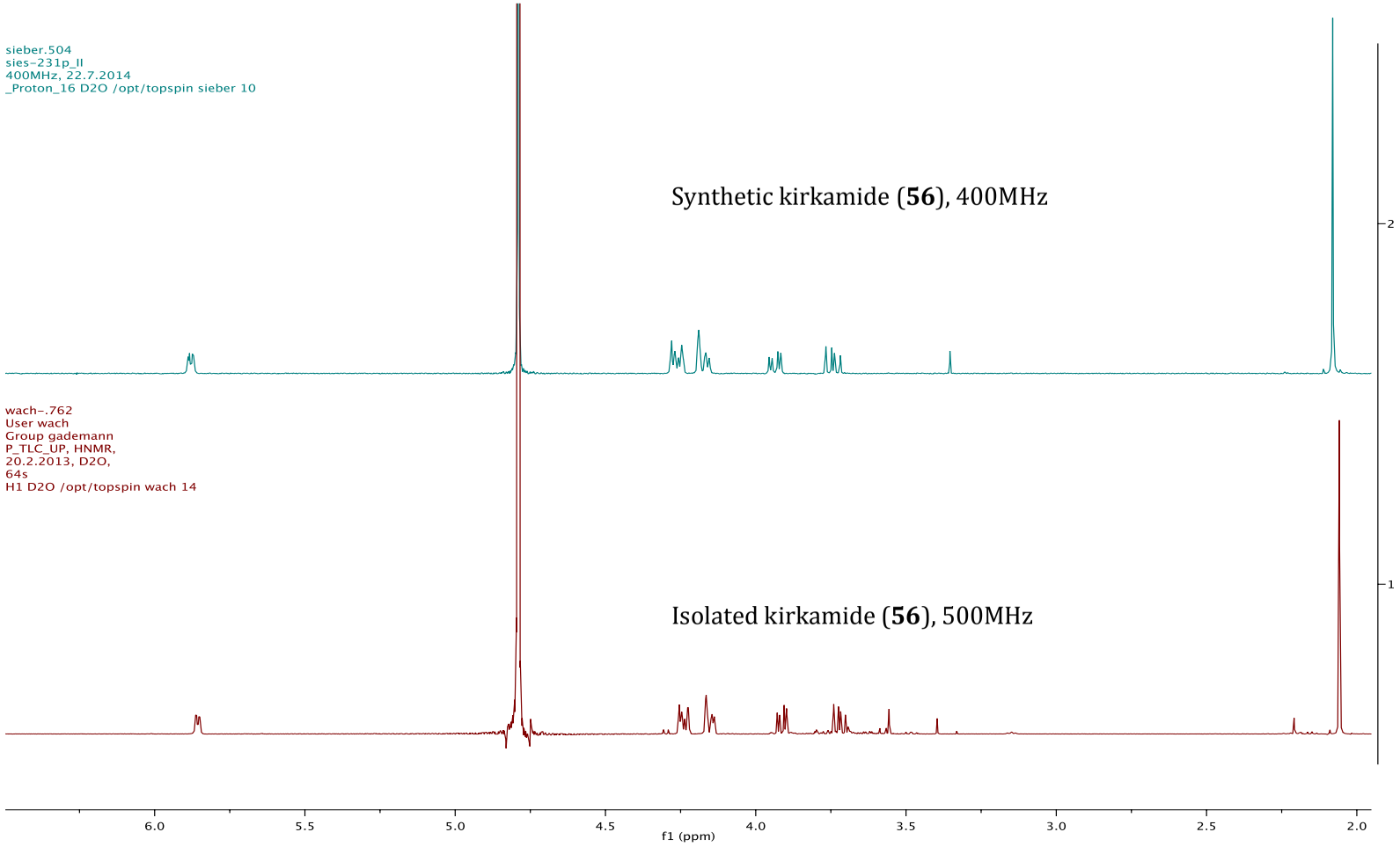

NMR Spectra of the Kirkamide Synthetic Part

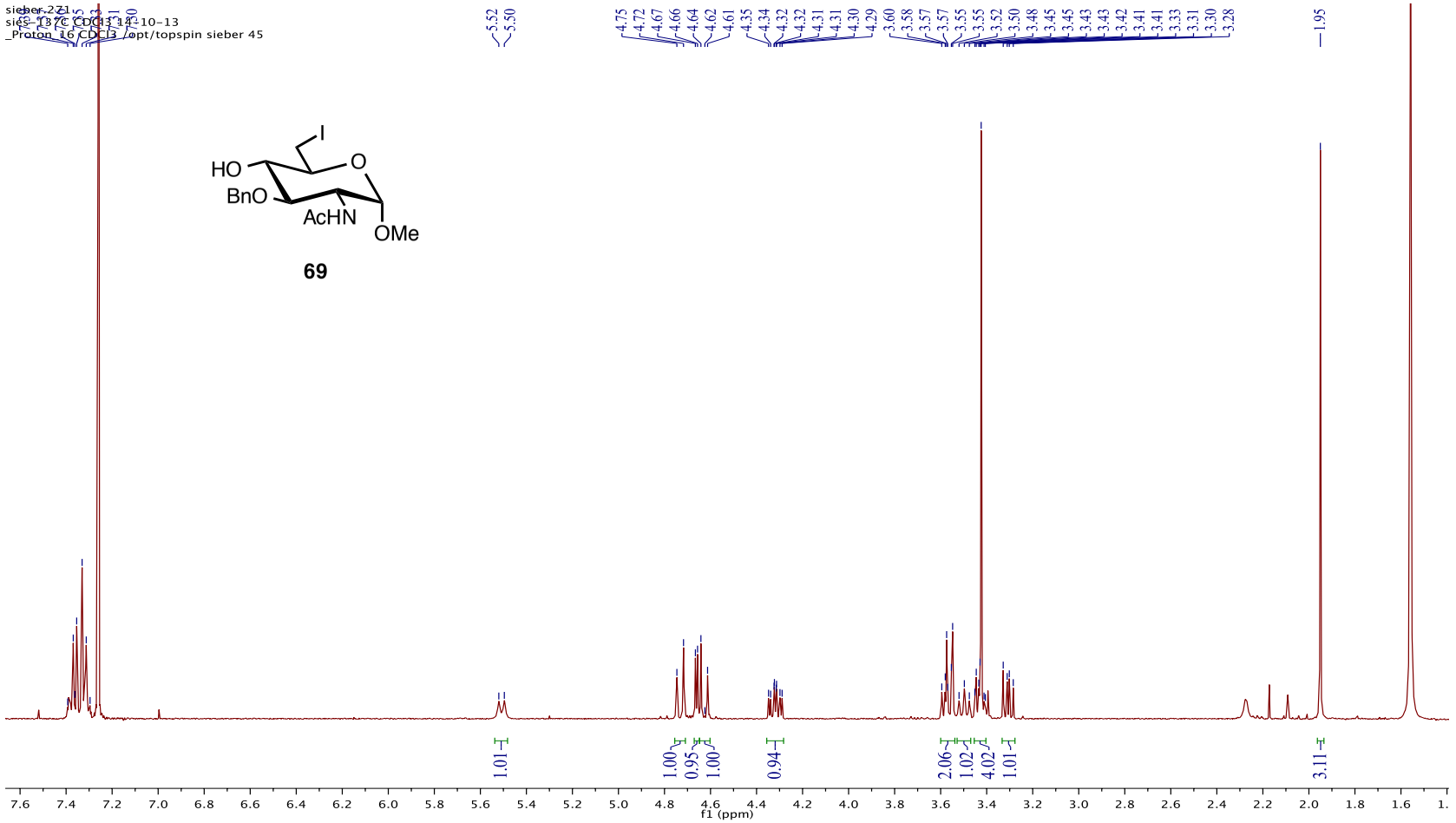

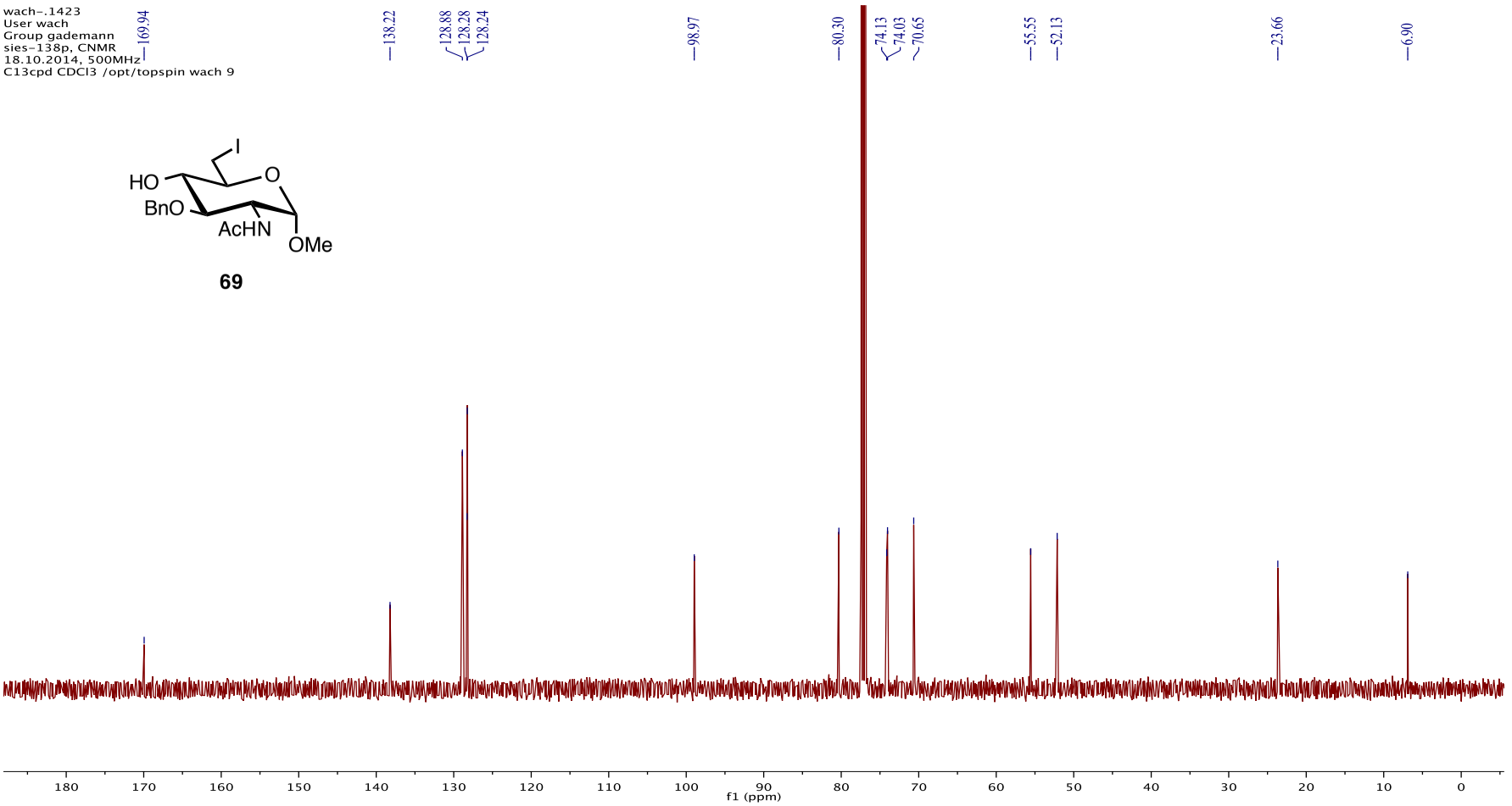
wach-.1423
User wach
Group gademann
sies-138p, CNMR
18.10.2014, 500MHz
C13cpd CDCl3 /opt/topspin wach 9
169.94
138.22
128.88
128.28
128.24
98.97
80.30
74.13
74.03
70.65
55.55
52.13
23.66
6.90
HO
BnO
AcHN
OMe
I
O
69
180
170
160
150
140
130
120
110
100
90
80
70
60
50
40
30
20
10
0
f1 (ppm)

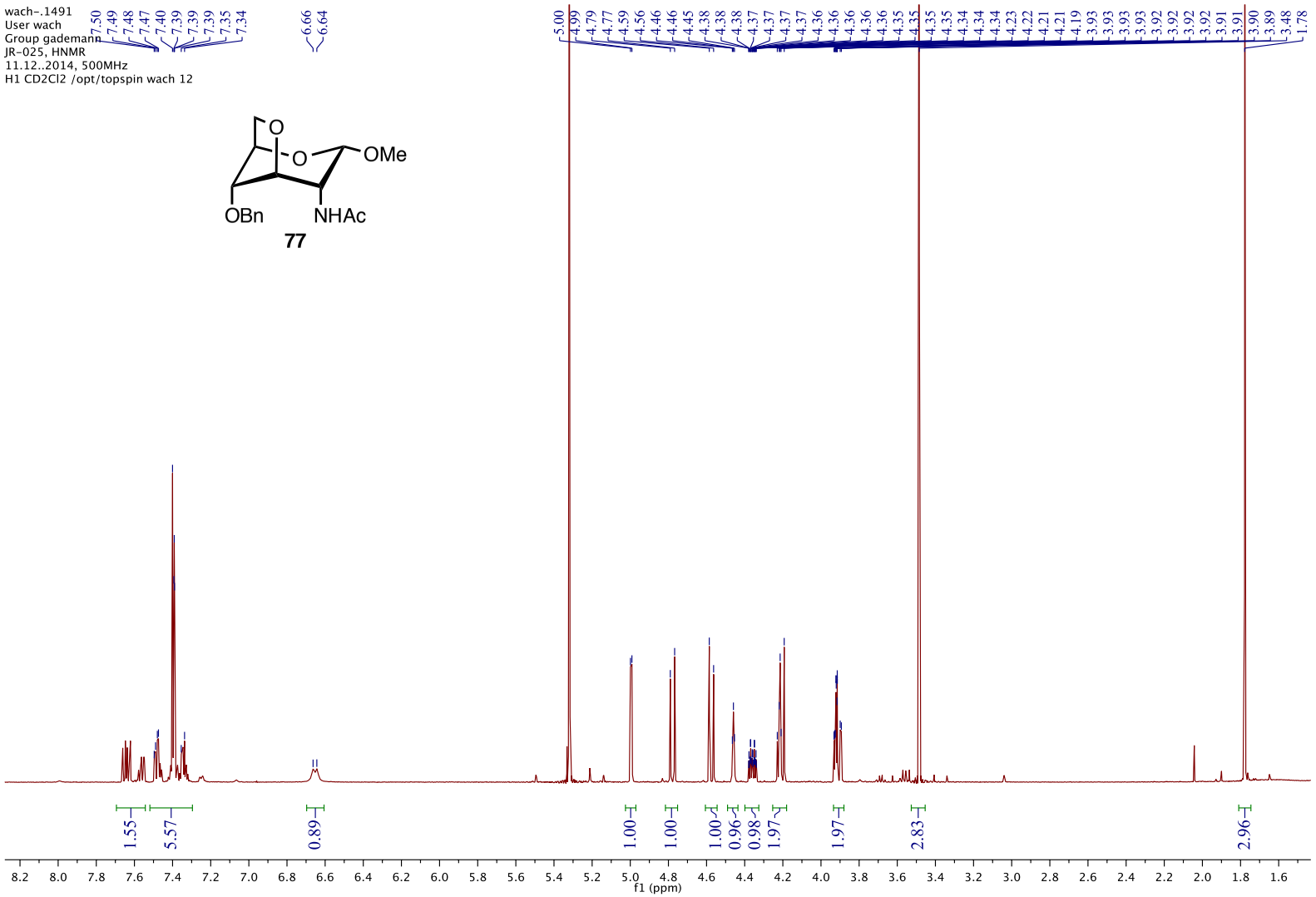
wach-.1491
User wach
Group gademann
JR-025, HNMR
11.12..2014, 500MHz
H1 CD2Cl2 /opt/topspin wach 12
O
O
OMe
OBn
NHAc
77
f1 (ppm)

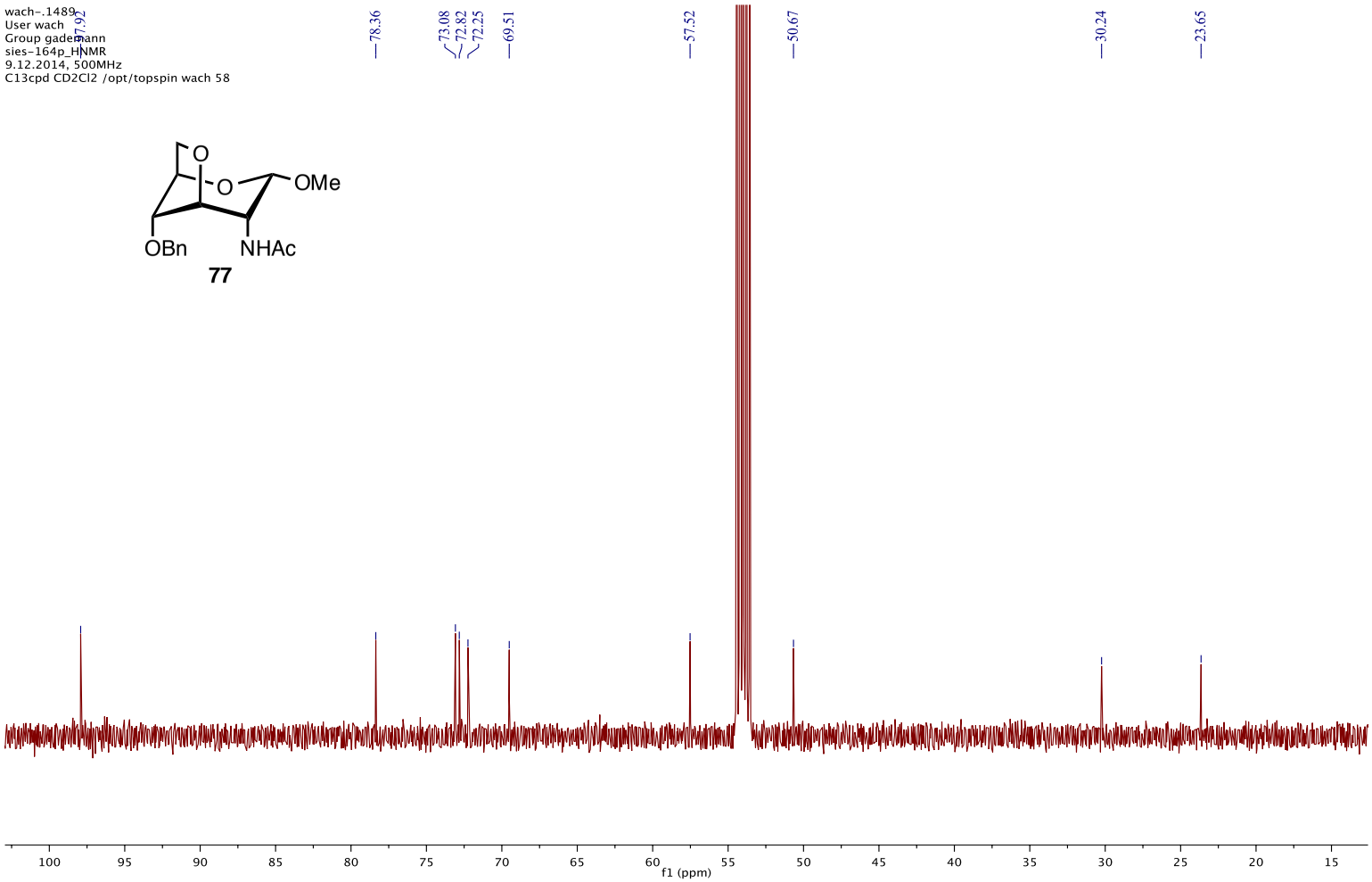
wach-.1489
User wach
Group gademann
sies-164p_HNMR
9.12.2014, 500MHz
C13cpd CD2Cl2 /opt/topspin wach 58
97.92
78.36
73.08
72.82
72.25
69.51
57.52
50.67
30.24
23.65
O
O
OMe
OBn
NHAc
77
100
95
90
85
80
75
70
65
60
55
50
45
40
35
30
25
20
15
f1 (ppm)

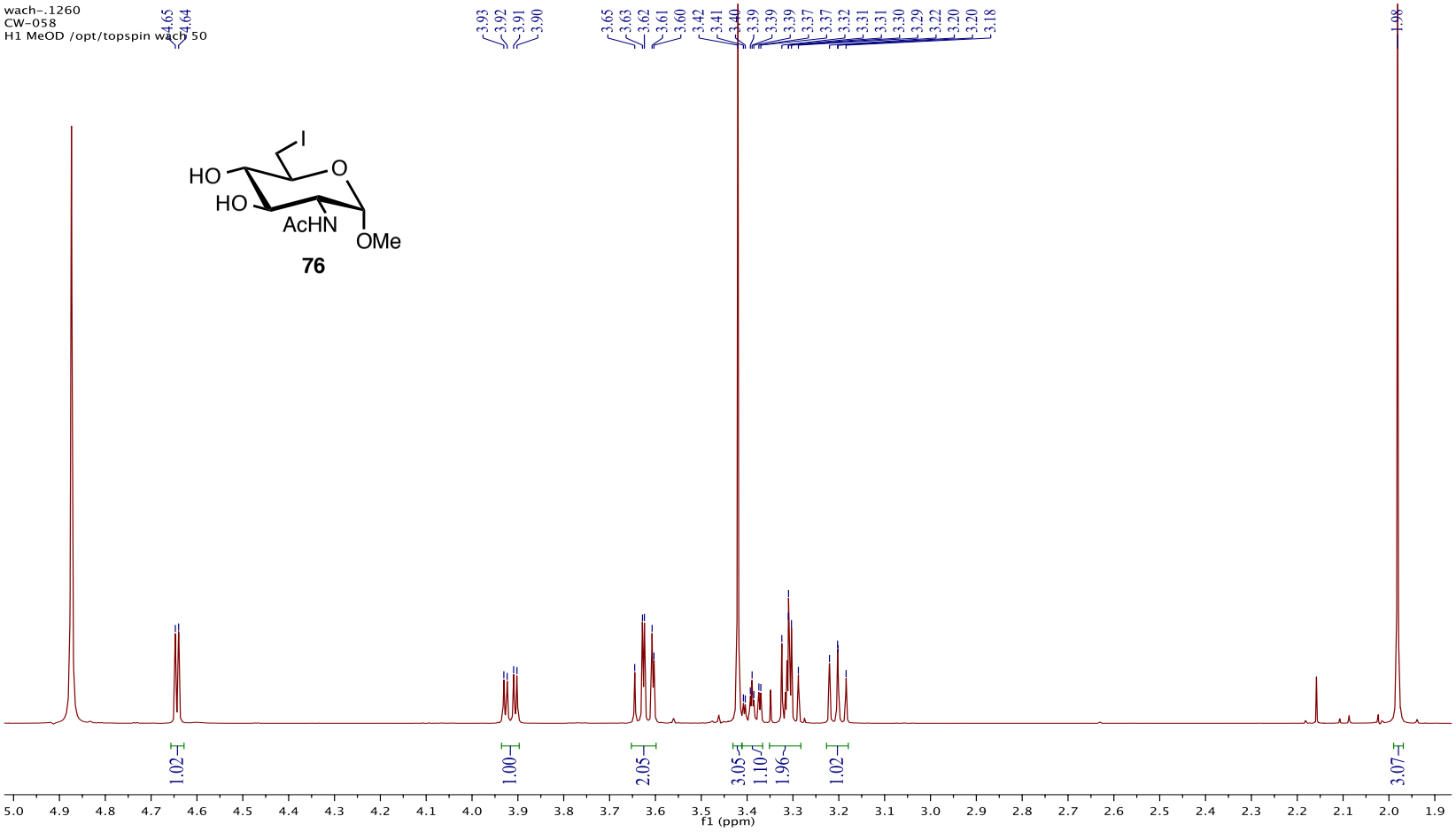
wach~.1260
CW-058
H1 MeOD /opt/topspin wach 50
4.65
4.64
3.93
3.92
3.91
3.90
3.65
3.63
3.62
3.61
3.60
3.42
3.41
3.40
3.39
3.39
3.39
3.37
3.37
3.32
3.31
3.31
3.30
3.29
3.22
3.20
3.20
3.18
1.98
HO
HO
AcHN
O
I
OMe
76
1.02
1.00
2.05
3.05
1.10
1.96
1.02
3.07
5.0 4.9 4.8 4.7 4.6 4.5 4.4 4.3 4.2 4.1 4.0 3.9 3.8 3.7 3.6 3.5 3.4 3.3 3.2 3.1 3.0 2.9 2.8 2.7 2.6 2.5 2.4 2.3 2.2 2.1 2.0 1.9
f1 (ppm)

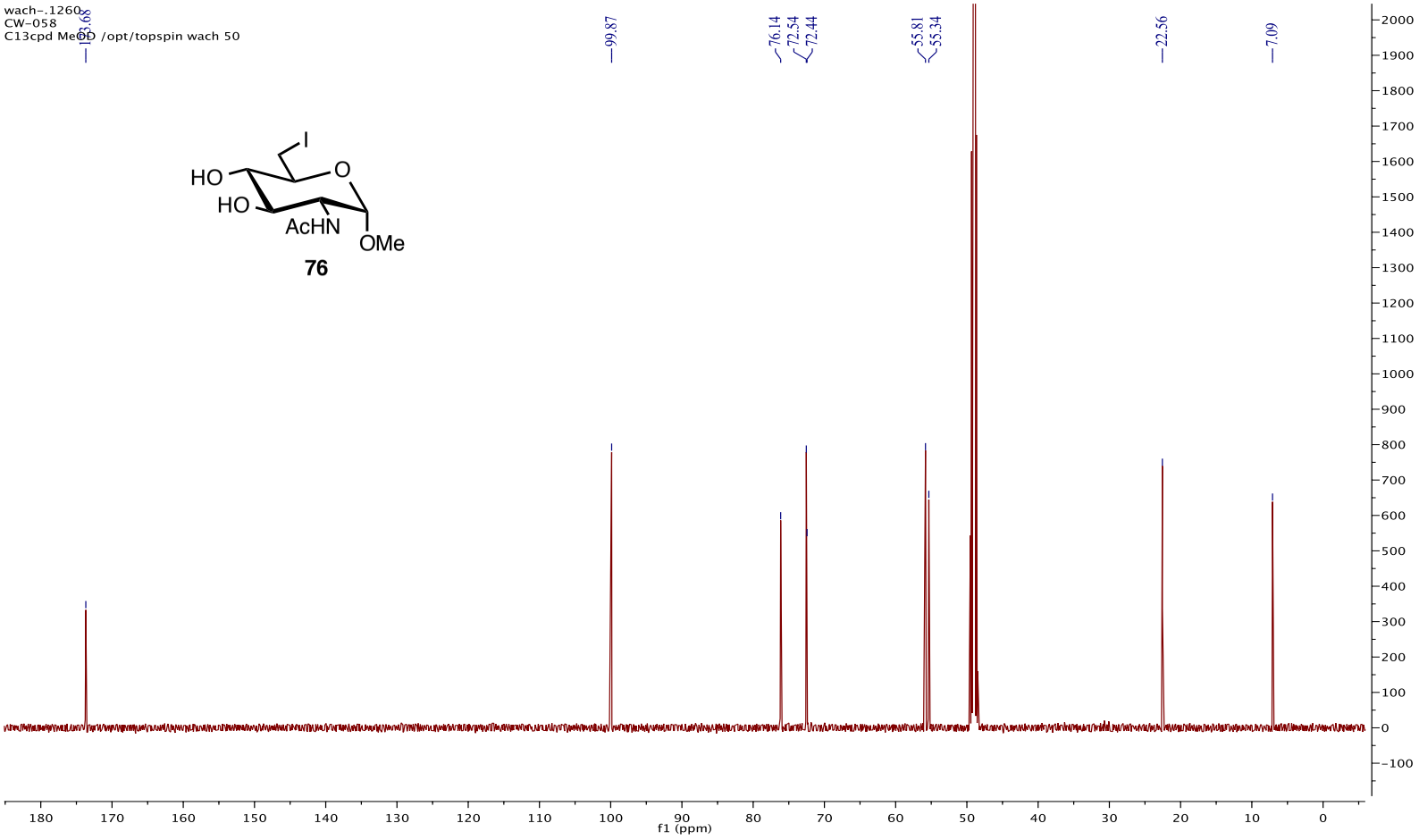
wach-.1260
CW-058
C13cpd MeOD /opt/topspin wach 50
168.68
99.87
76.14
72.54
72.44
55.81
55.34
22.56
7.09
HO
HO
AcHN
O
I
OMe
f1 (ppm)

76

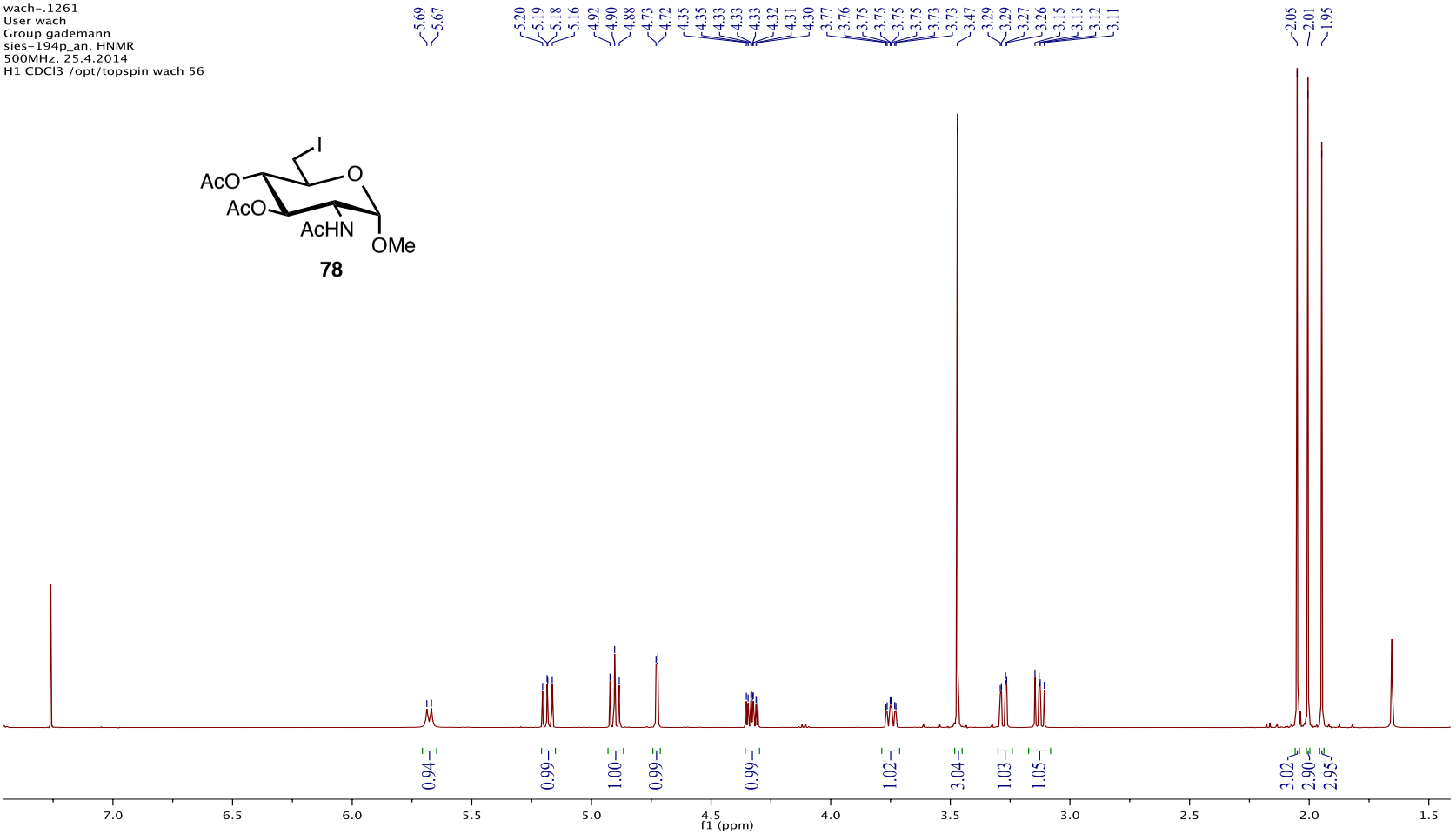
wach-.1261
User wach
Group gademann
sies-194p_an, HNMR
500MHz, 25.4.2014
H1 CDCl3 /opt/topspin wach 56
AcO
AcO
AcHN
OMe
I
O
78
5.69
5.67
5.20
5.19
5.18
5.16
4.92
4.90
4.88
4.73
4.72
4.35
4.33
4.33
4.33
4.32
4.31
4.30
3.77
3.76
3.75
3.75
3.75
3.75
3.73
3.73
3.47
3.29
3.29
3.27
3.26
3.15
3.13
3.12
3.11
2.05
2.01
1.95
0.94
0.99
1.00
0.99
0.99
1.02
3.04
1.03
1.05
3.02
2.90
2.95
7.0
6.5
6.0
5.5
5.0
4.5
4.0
3.5
3.0
2.5
2.0
1.5
f1 (ppm)

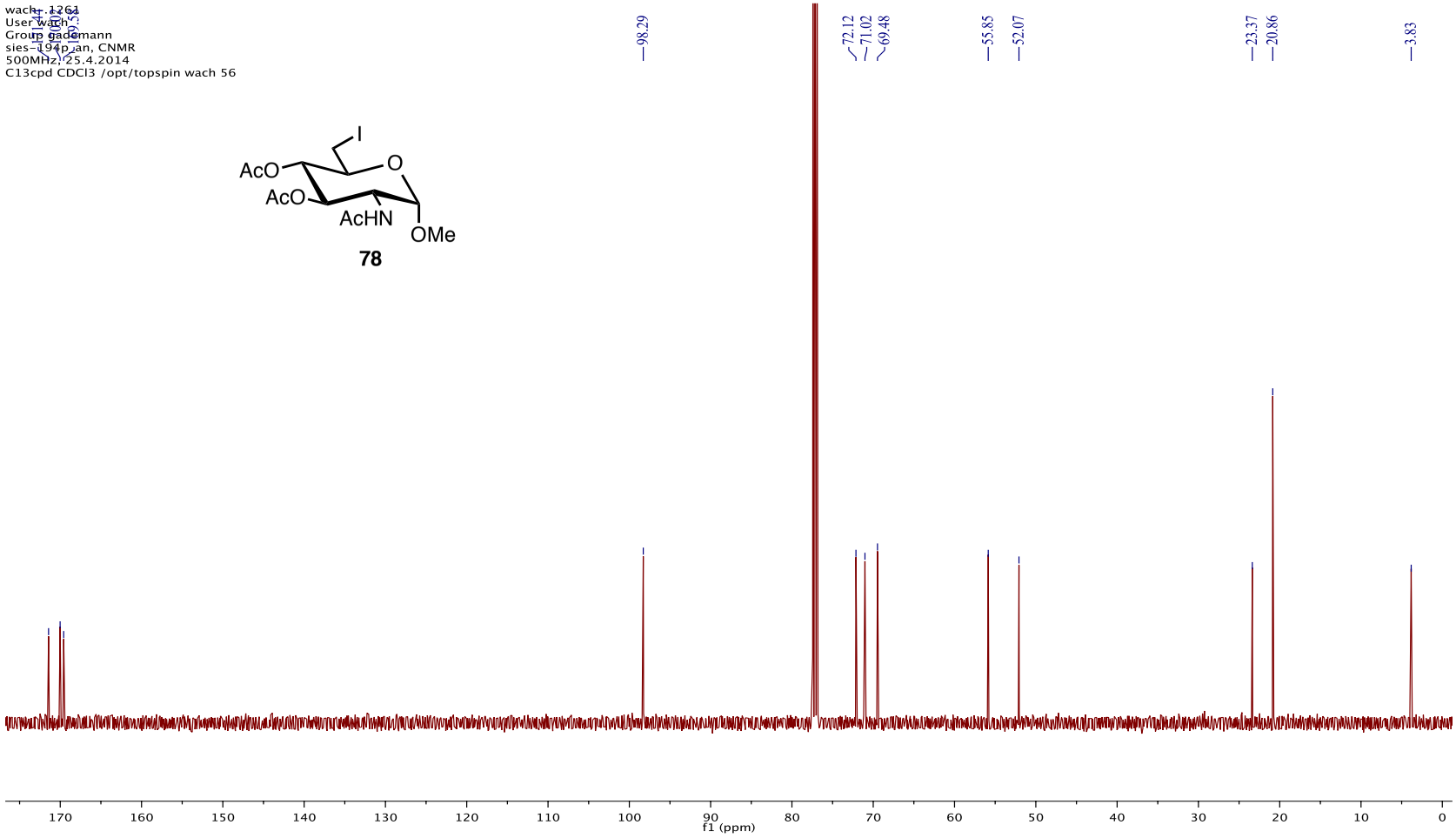
wach-1261
User wach
Group gademann
sies-194p.jan, CNMR
500MHz, 25.4.2014
C13cpd CDCl3 /opt/topspin wach 56
98.29
72.12
71.02
69.48
55.85
52.07
23.37
20.86
3.83
I
O
AcO
AcO
AcHN
OMe
78
170
160
150
140
130
120
110
100
90
80
70
60
50
40
30
20
10
0
f1 (ppm)

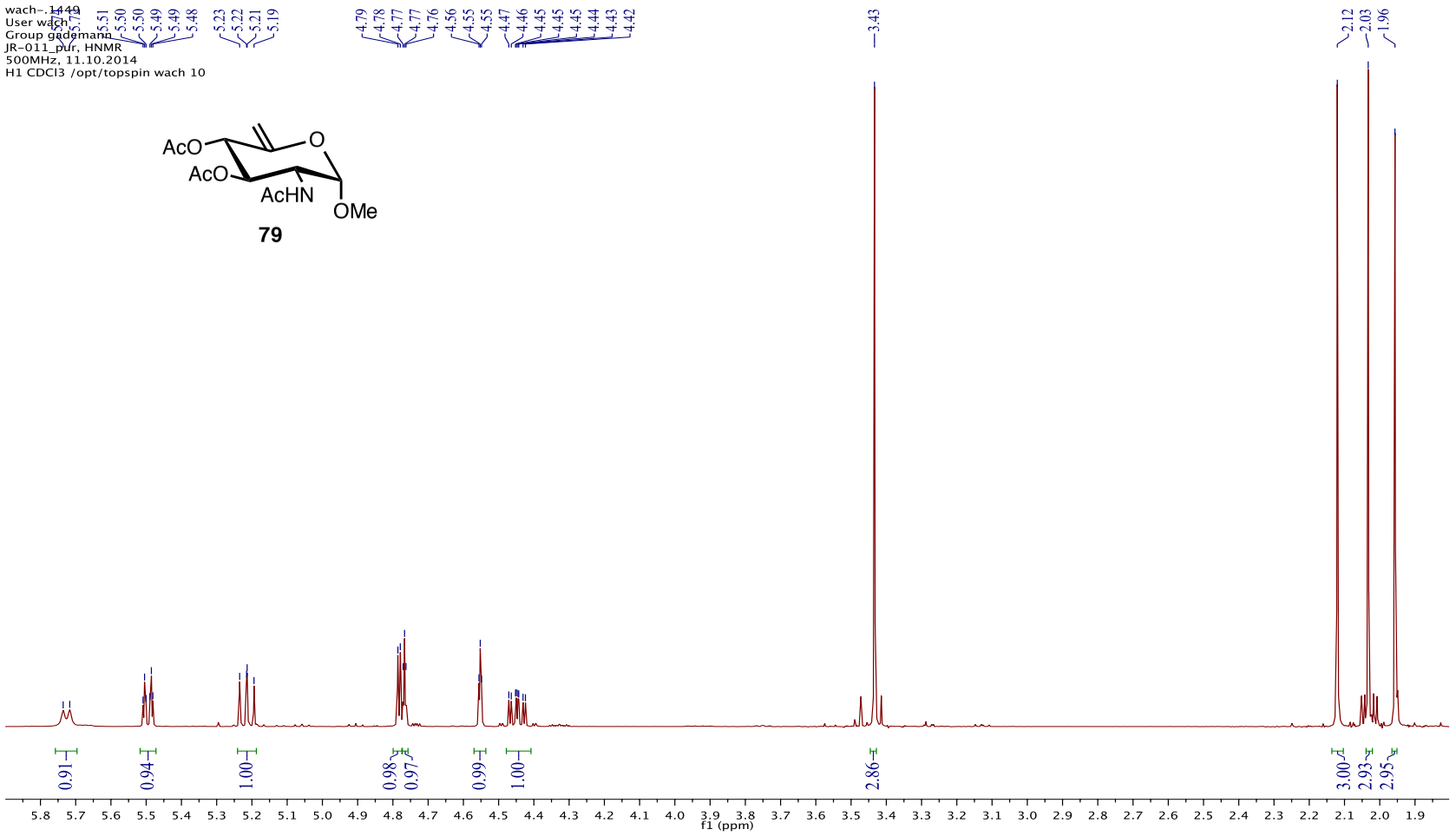
wach-1449
User wach
Group gademann
JR-011_pur, HNMR
500MHz, 11.10.2014
H1 CDCl3 /opt/topspin wach 10
AcO
AcO
AcHN
O
OMe
79
f1 (ppm)

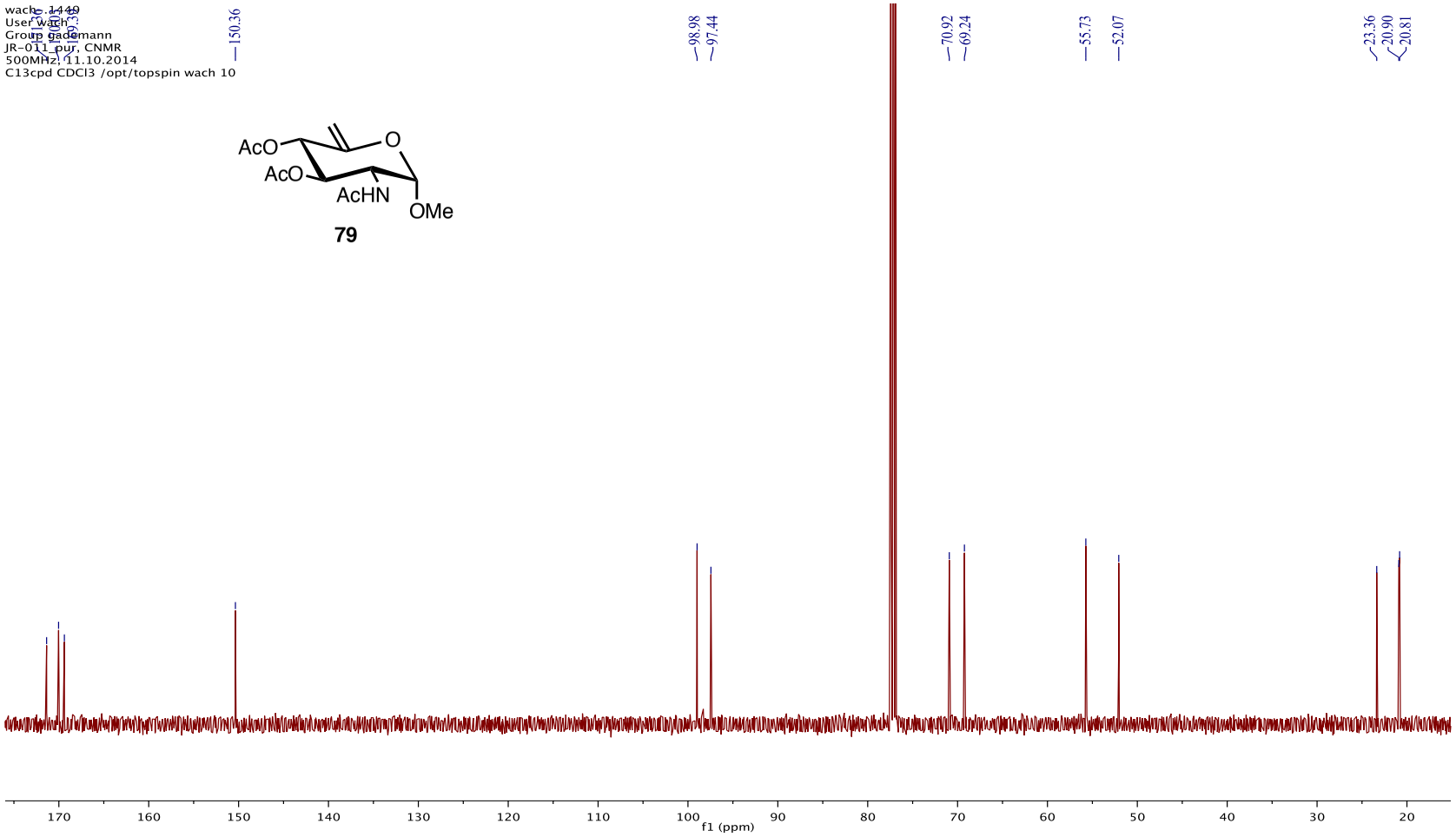
wach-1449
User wach
Group gademann
JR-011_pur, CNMR
500MHz, 11.10.2014
C13cpd CDCl3 /opt/topspin wach 10
169.73
169.38
169.13
150.36
98.98
97.44
70.92
69.24
55.73
52.07
23.36
20.90
20.81
AcO
AcO
AcHN
O
OMe
79
170
160
150
140
130
120
110
100
90
80
70
60
50
40
30
20
f1 (ppm)

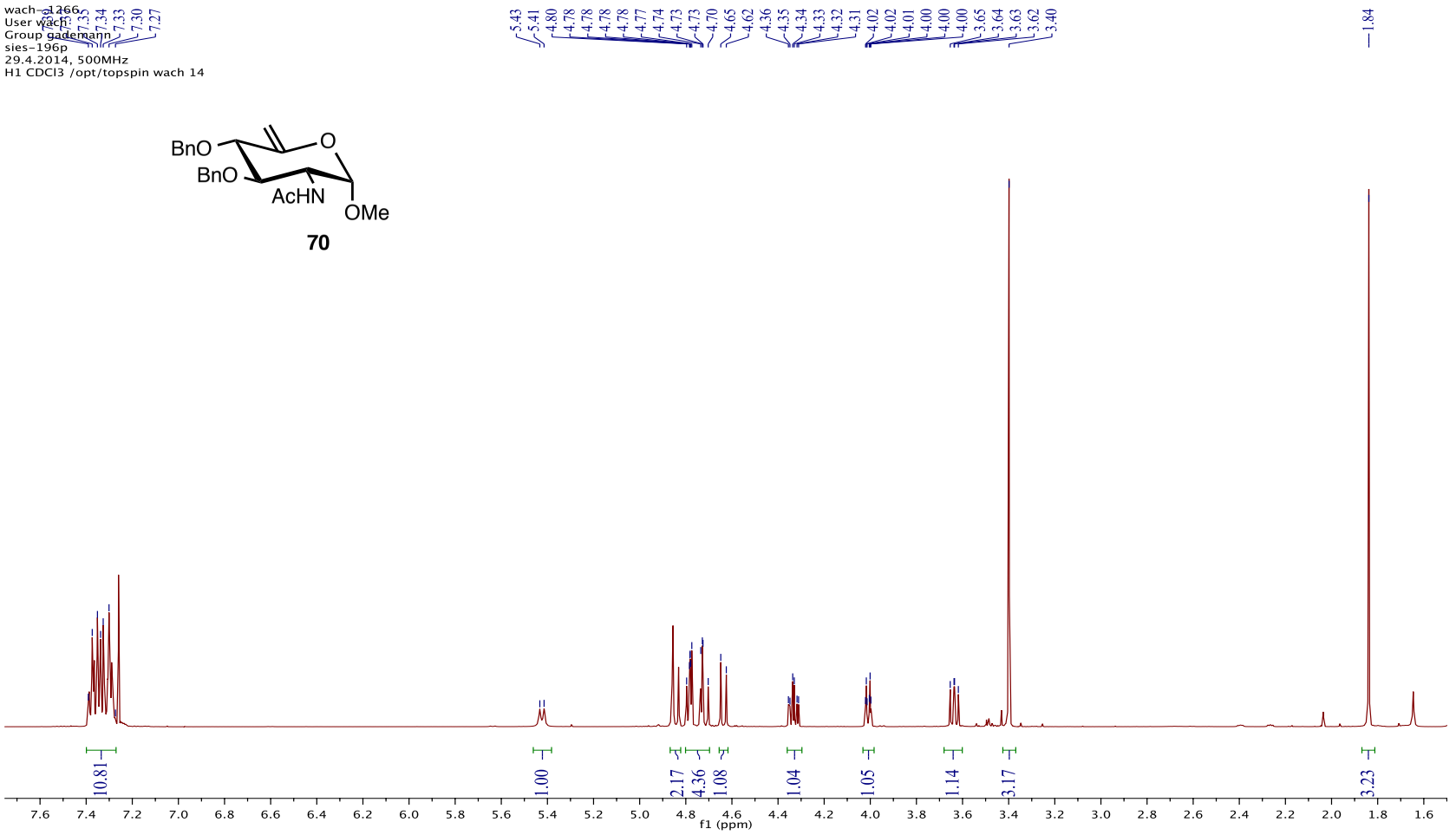
wach-1266
User wach
Group gademann
sies-196p
29.4.2014, 500MHz
H1 CDCl3 /opt/topspin wach 14
BnO
BnO
AcHN
O
OMe
70
f1 (ppm)

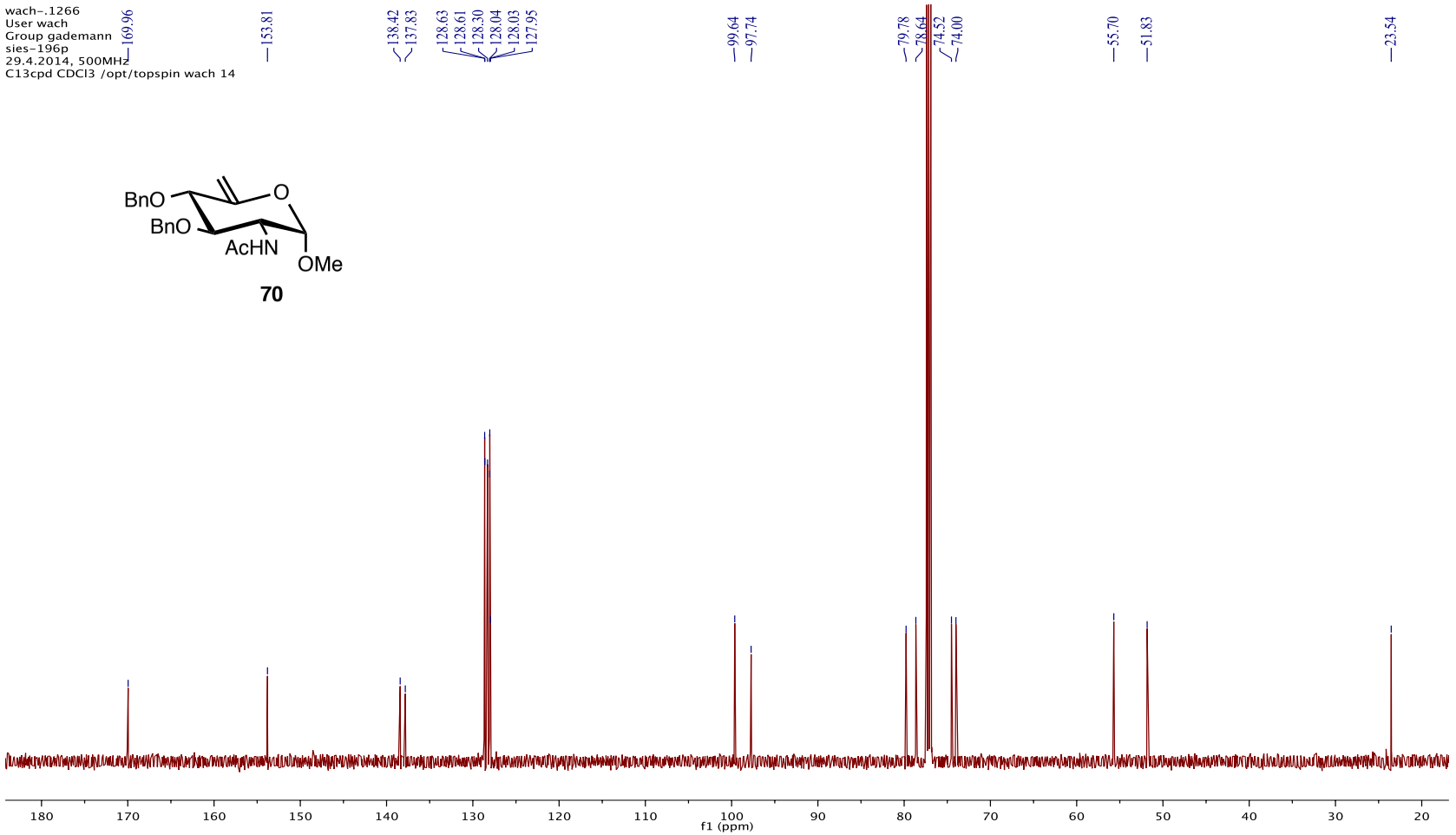
wach-.1266
User wach
Group gademann
sies-196p
29.4.2014, 500MHz
C13cpd CDCl3 /opt/topspin wach 14
169.96
153.81
138.42
137.83
128.63
128.61
128.30
128.04
128.03
127.95
99.64
97.74
79.78
78.64
74.52
74.00
55.70
51.83
23.54
BnO
BnO
AcHN
O
OMe
70
180
170
160
150
140
130
120
110
100
90
80
70
60
50
40
30
20
f1 (ppm)

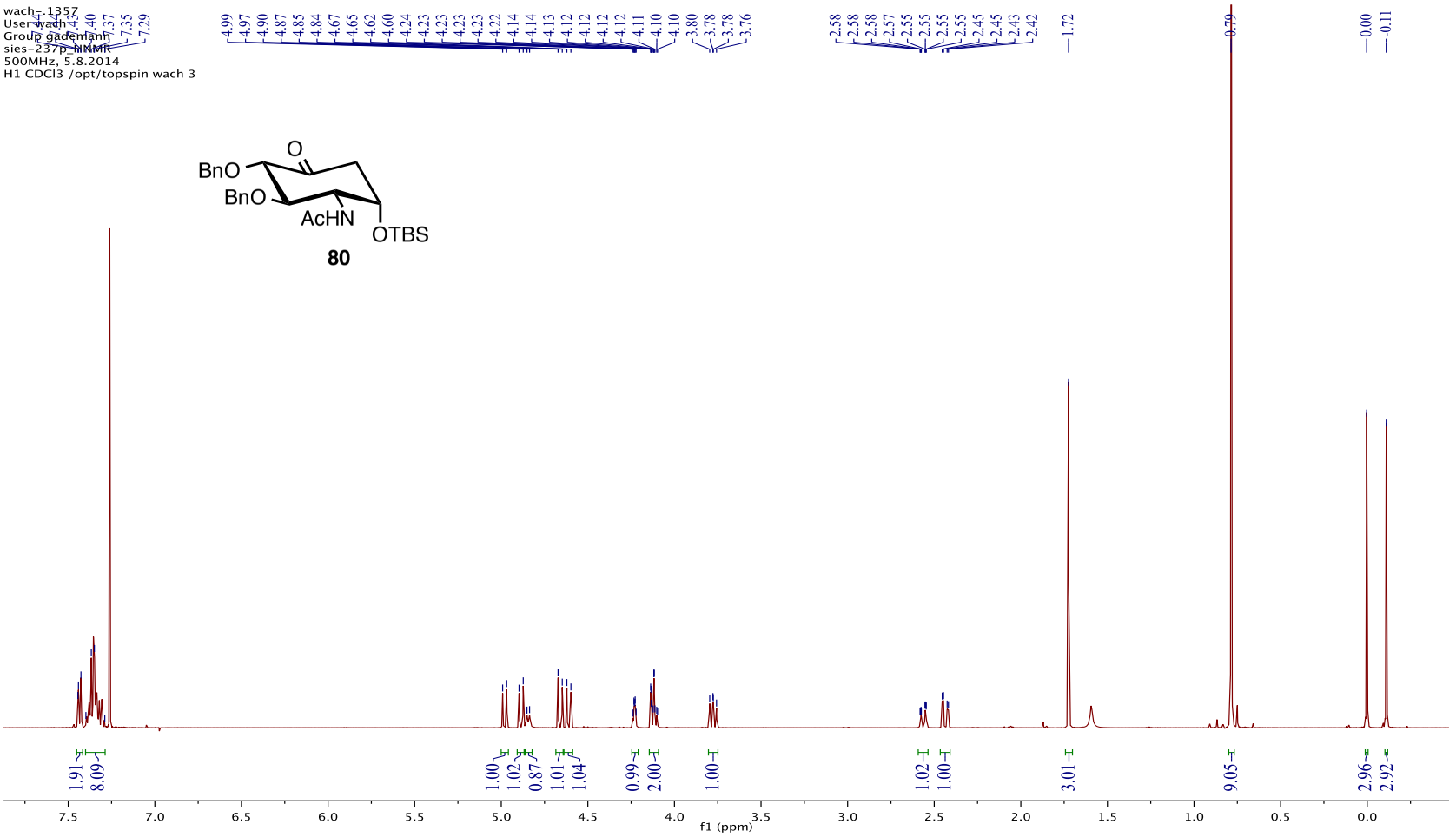
wach_1357
User wach
Group ademann
sies-237p_HNMR
500MHz, 5.8.2014
H1 CDCl3 /opt/topspin wach 3
BnO
BnO
AcHN
OTBS
O
80
f1 (ppm)

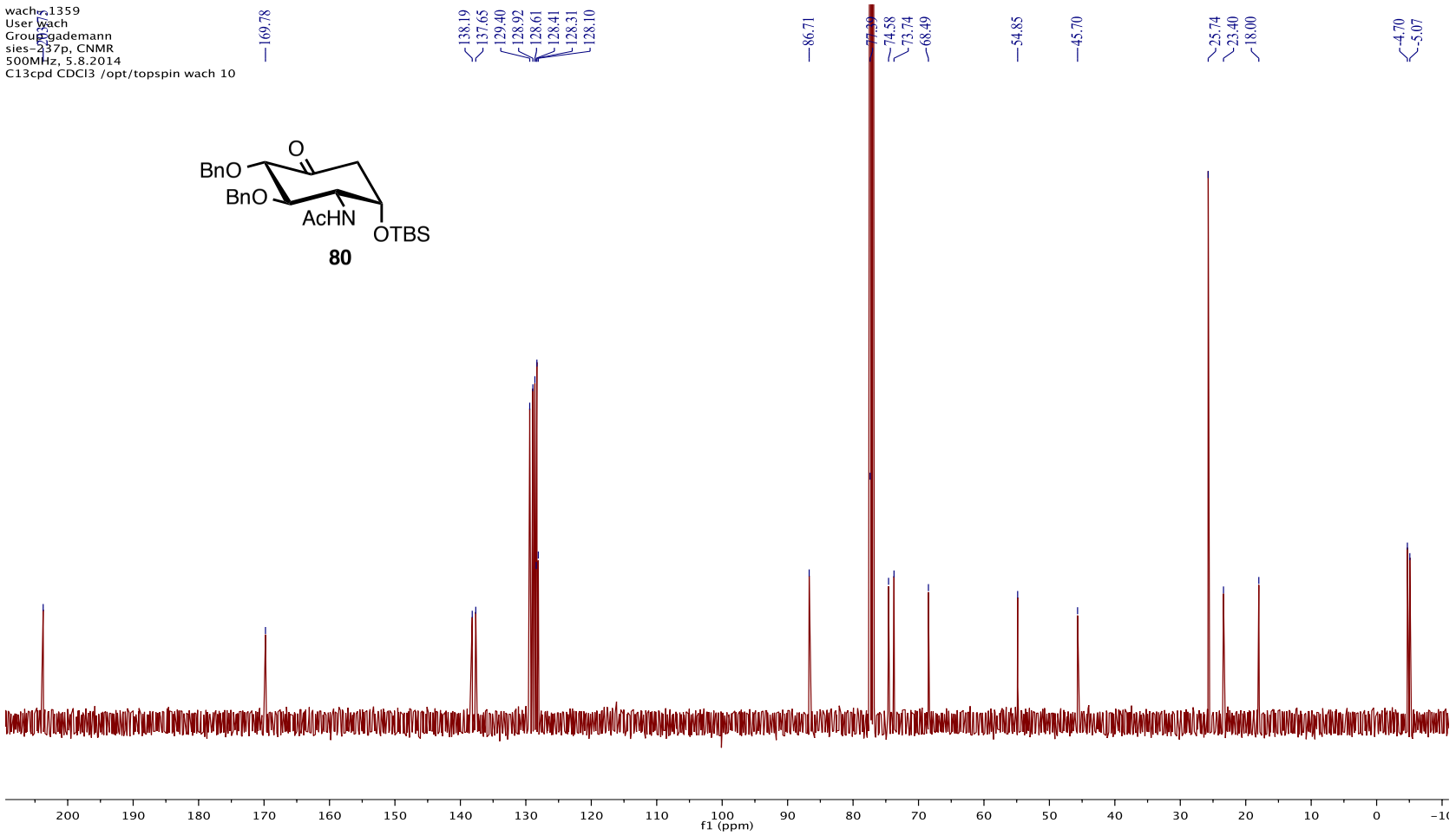
wach-1359
User wach
Group gademann
sies-237p, CNMR
500MHz, 5.8.2014
C13cpd CDCl3 /opt/topspin wach 10
169.78
138.19
137.65
129.40
128.92
128.61
128.41
128.31
128.10
86.71
77.39
74.58
73.74
68.49
54.85
45.70
25.74
23.40
18.00
-4.70
-5.07
O
BnO
BnO
AcHN
OTBS
80
f1 (ppm)

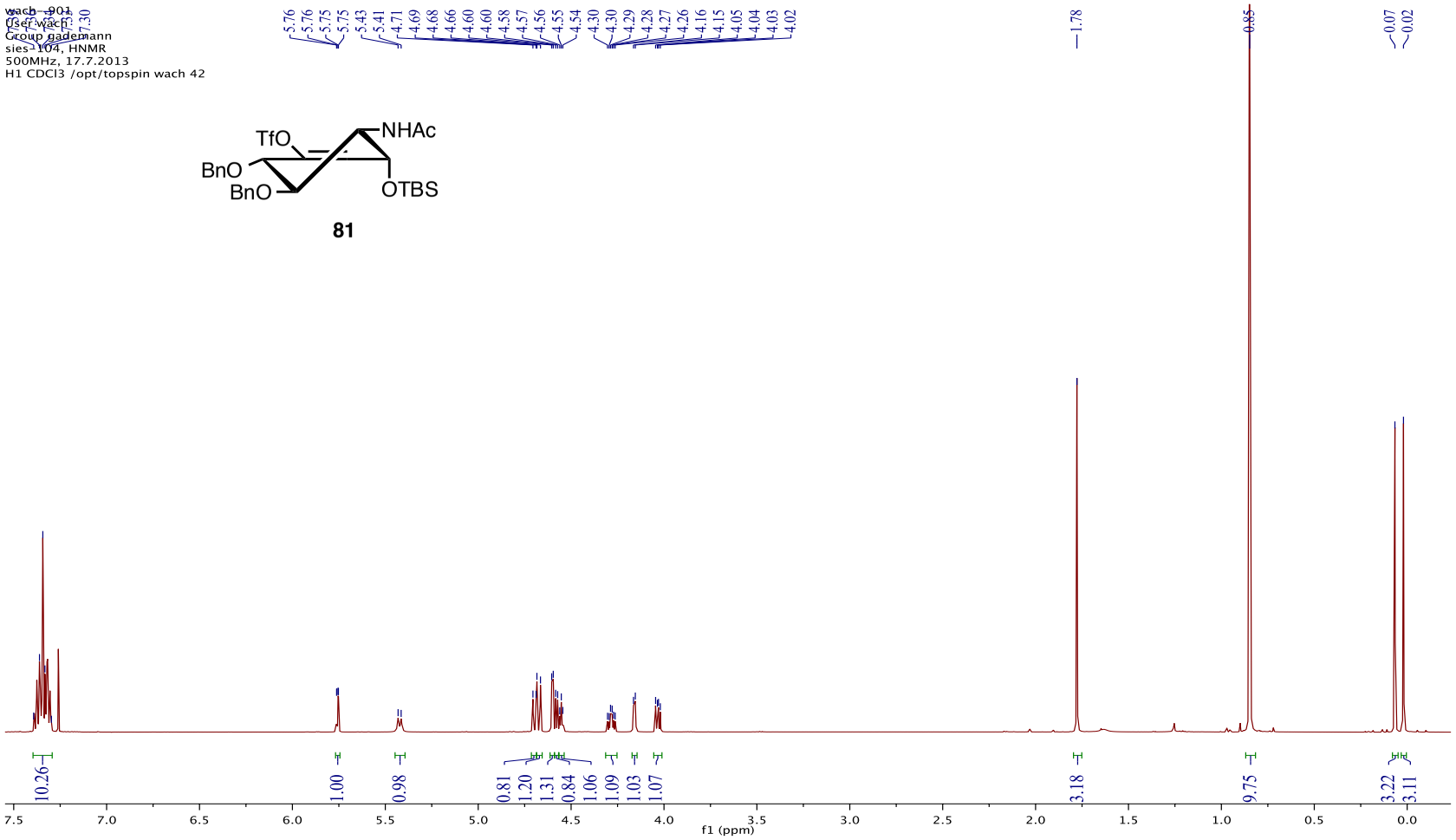
wach_901
C:\Users\wach\...
Group gademann
sies-104, HNMR
500MHz, 17.7.2013
H1 CDCl3 /opt/topspin wach 42
TfO
NHAc
BnO
BnO
OTBS
81
f1 (ppm)

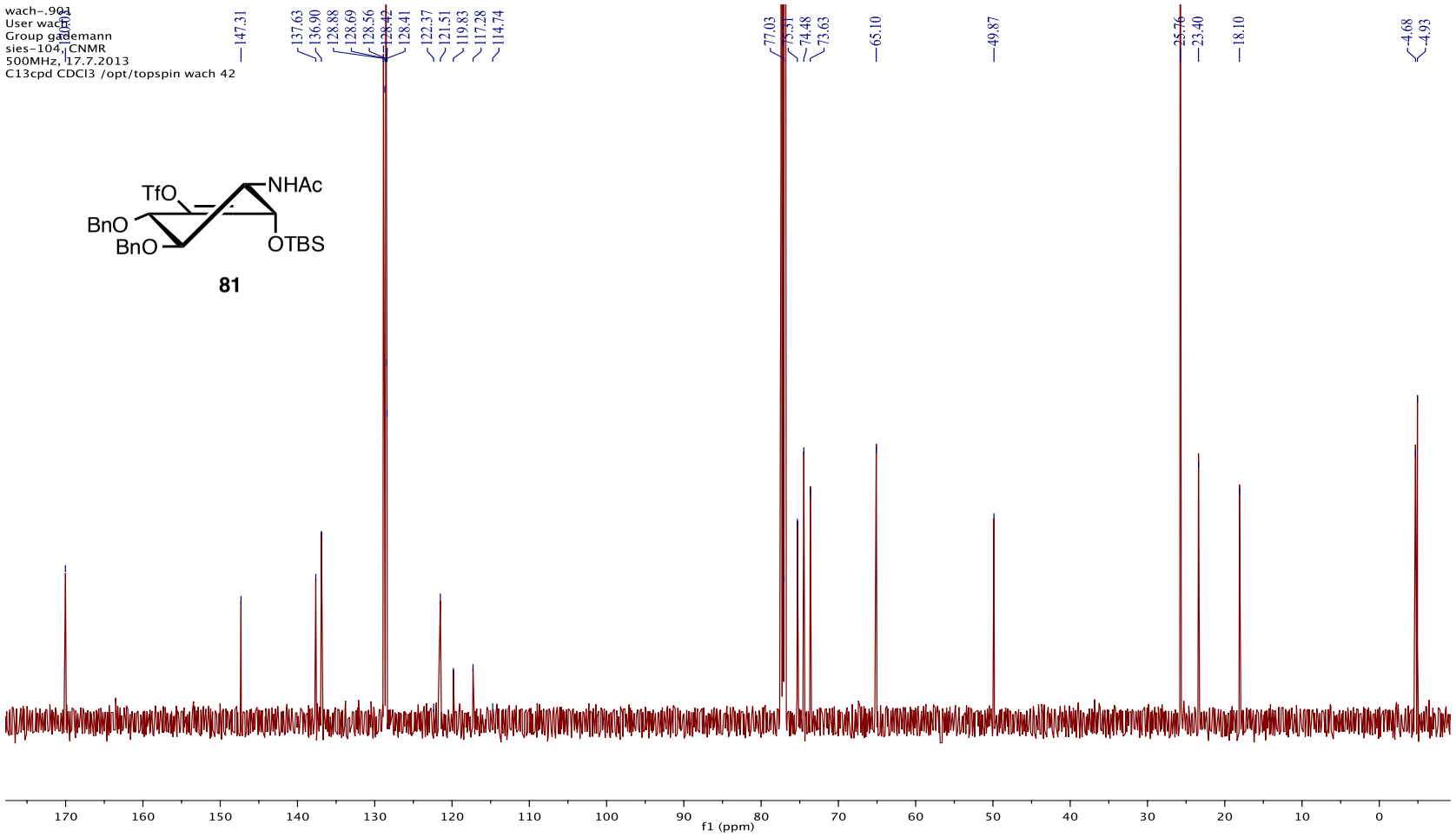
wach-.901
User wach
Group gademann
sies-104, CNMR
500MHz, 17.7.2013
C13cpd CDCl3 /opt/topspin wach 42
147.31
137.63
136.90
128.88
128.69
128.56
128.42
128.41
122.37
121.51
119.83
117.28
114.74
77.03
75.31
74.48
73.63
65.10
49.87
25.76
23.40
18.10
-4.68
-4.93
TfO
NHAc
BnO
BnO
OTBS
81
f1 (ppm)

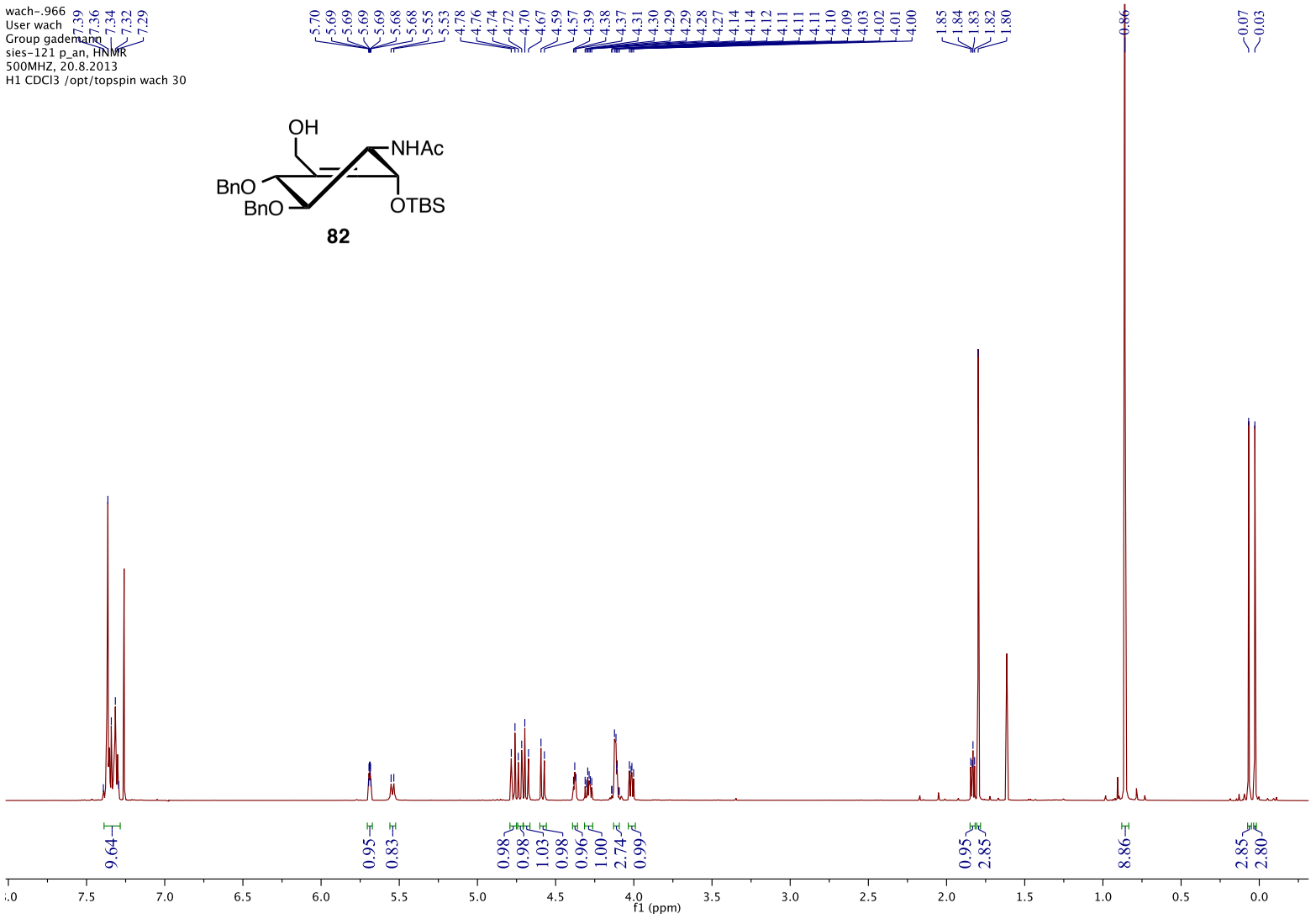
wach-.966
User wach
Group gademann
sies-121 p_an, HNMR
500MHZ, 20.8.2013
H1 CDCl3 /opt/topspin wach 30
OH
NHAc
BnO
BnO
OTBS
82
f1 (ppm)

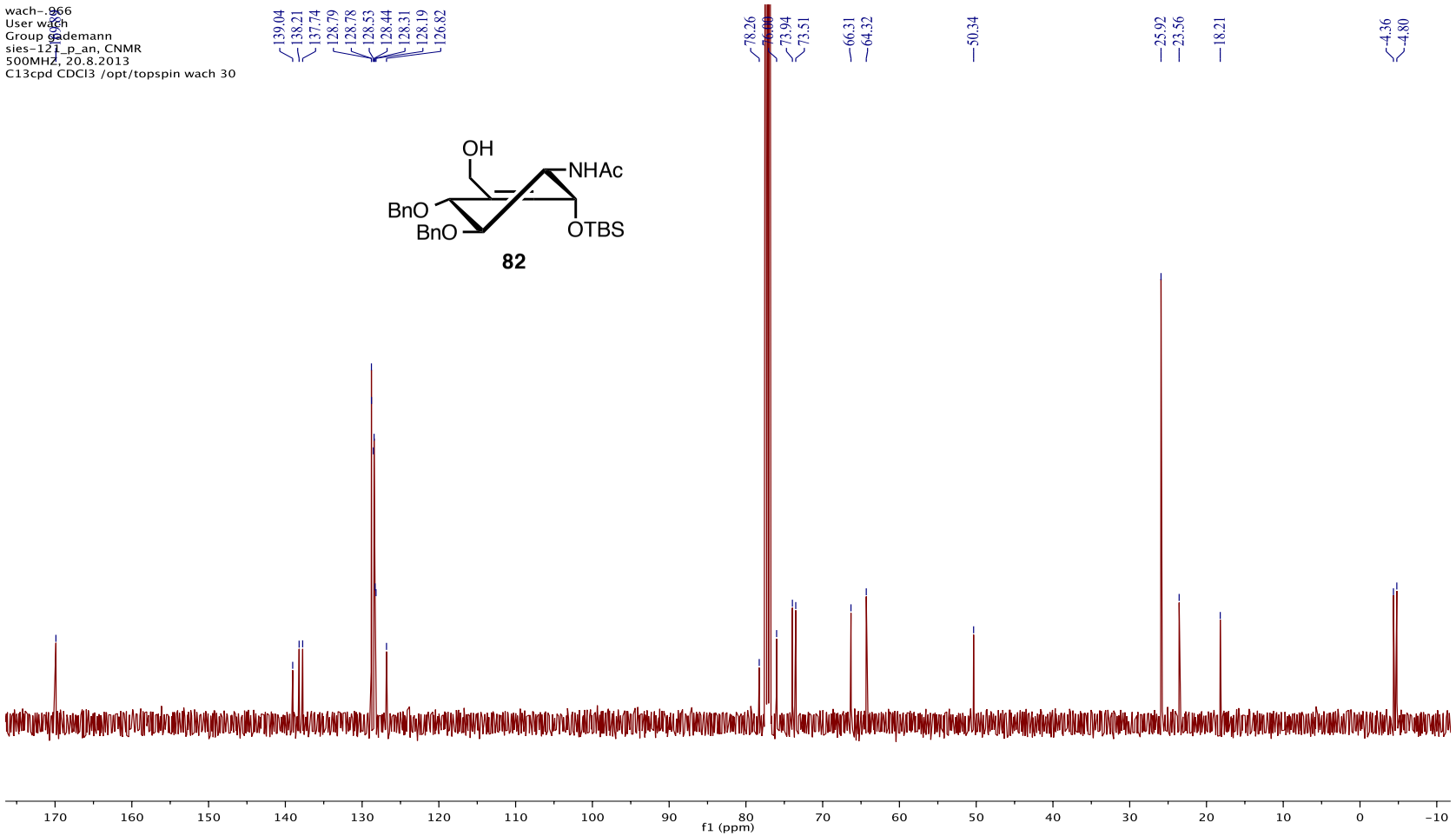
wach-.966
User wach
Group gademann
sies-127_p_an, CNMR
500MHz, 20.8.2013
C13cpd CDCl3 /opt/topspin wach 30
139.04
138.21
137.74
128.79
128.78
128.53
128.44
128.31
128.19
126.82
78.26
76.80
73.94
73.51
66.31
64.32
50.34
25.92
23.56
18.21
-4.36
-4.80
OH
NHAc
BnO
BnO
OTBS
82
f1 (ppm)

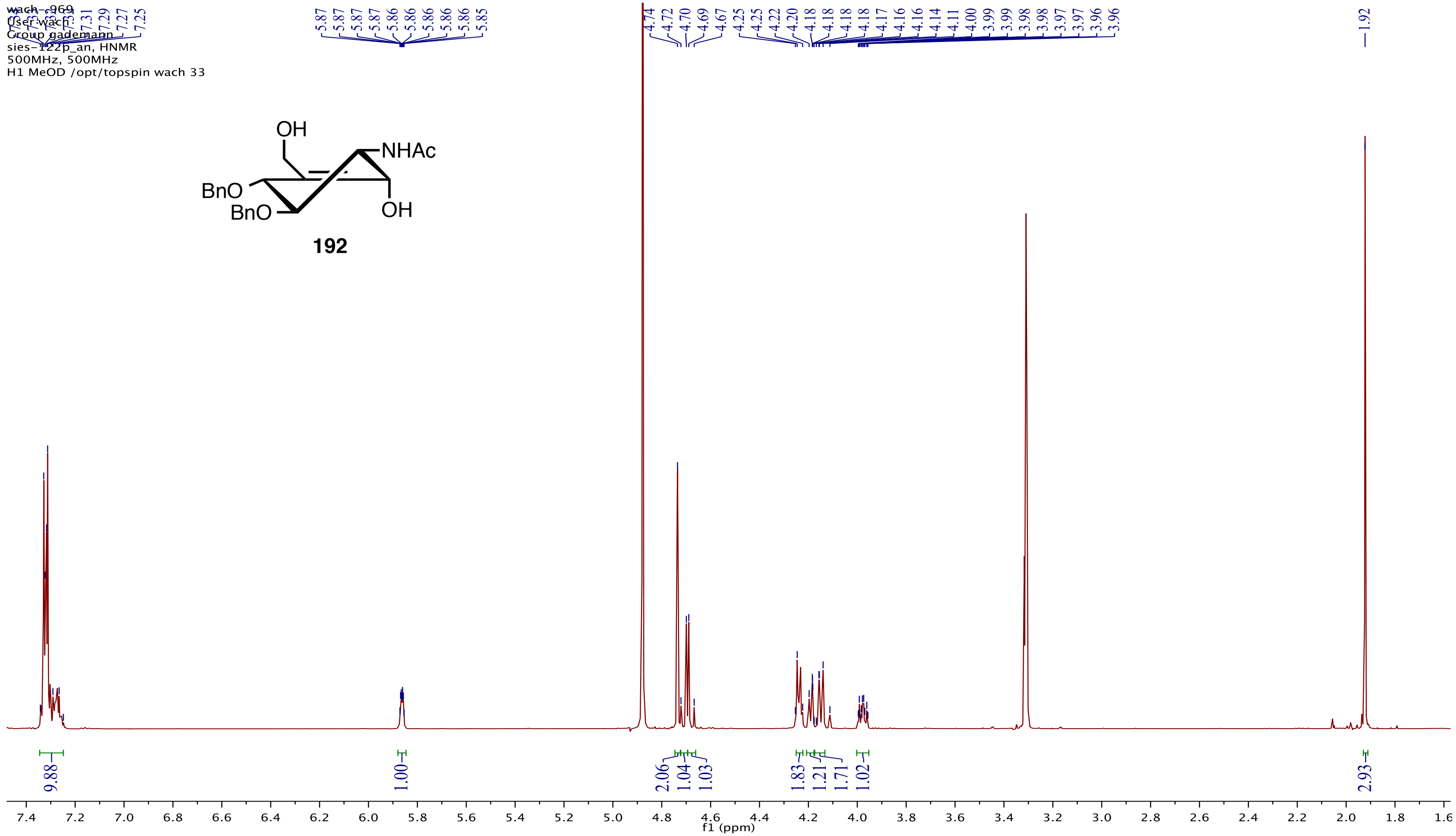
wach-969
User wach
Group gademann
sies-122p_an, HNMR
500MHz, 500MHz
H1 MeOD /opt/topspin wach 33
7.31
7.29
7.27
7.25
5.87
5.87
5.87
5.87
5.86
5.86
5.86
5.86
5.86
5.85
4.74
4.72
4.70
4.69
4.67
4.25
4.25
4.22
4.20
4.18
4.18
4.18
4.18
4.17
4.16
4.16
4.14
4.11
4.00
3.99
3.99
3.98
3.98
3.97
3.97
3.96
3.96
1.92
OH
NHAc
BnO
BnO
OH
192
9.88
1.00
2.06
1.04
1.03
1.83
1.21
1.71
1.02
2.93
7.4
7.2
7.0
6.8
6.6
6.4
6.2
6.0
5.8
5.6
5.4
5.2
5.0
4.8
4.6
4.4
4.2
4.0
3.8
3.6
3.4
3.2
3.0
2.8
2.6
2.4
2.2
2.0
1.8
1.6
f1 (ppm)

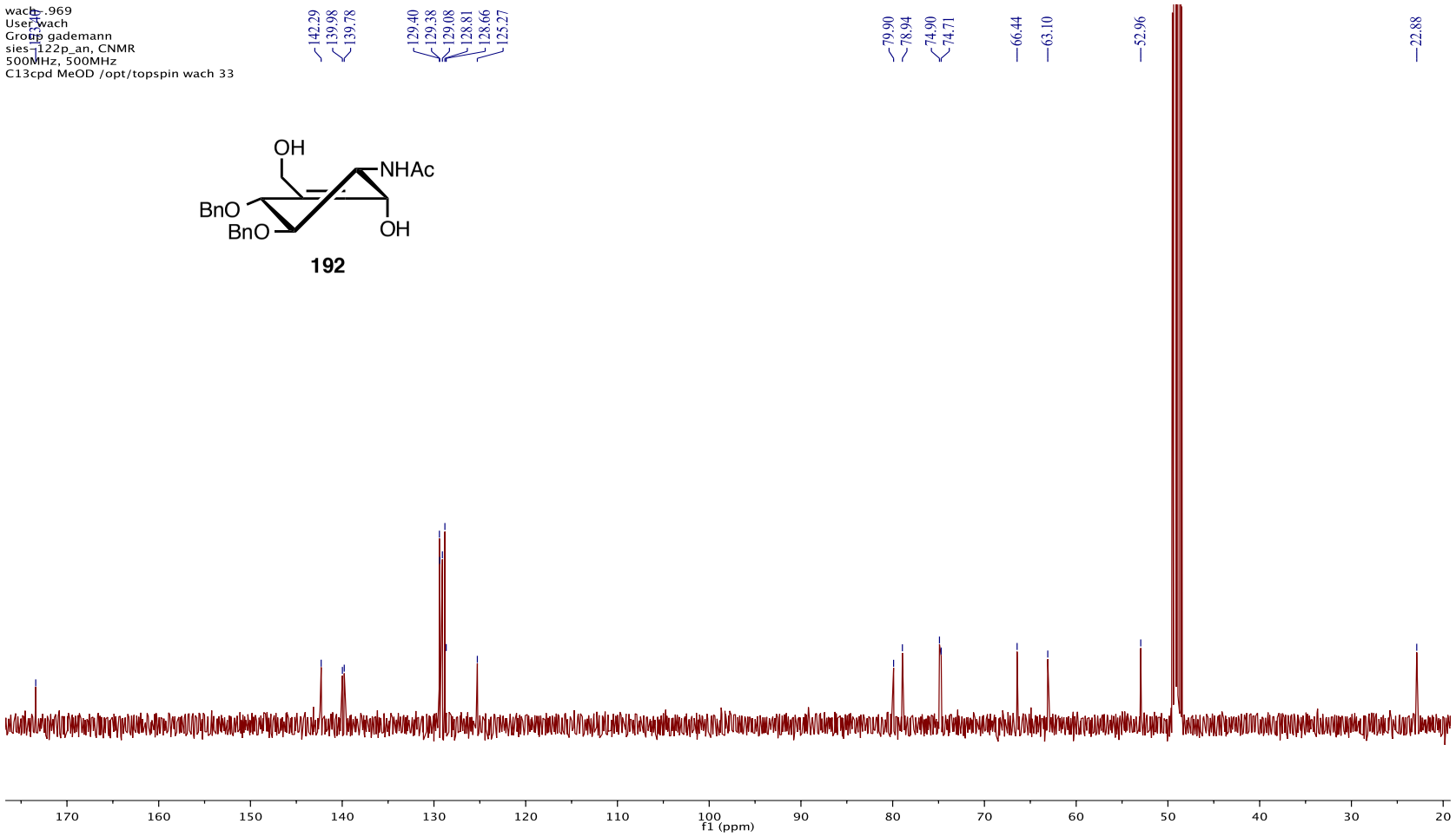
wach_.969
User wach
Group gademann
sies-122p_an, CNMR
500MHz, 500MHz
C13cpd MeOD /opt/topspin wach 33
142.29
139.98
139.78
129.40
129.38
129.08
128.81
128.66
125.27
79.90
78.94
74.90
74.71
66.44
63.10
52.96
22.88
OH
NHAc
BnO
BnO
OH
192
170
160
150
140
130
120
110
100
90
80
70
60
50
40
30
20
f1 (ppm)

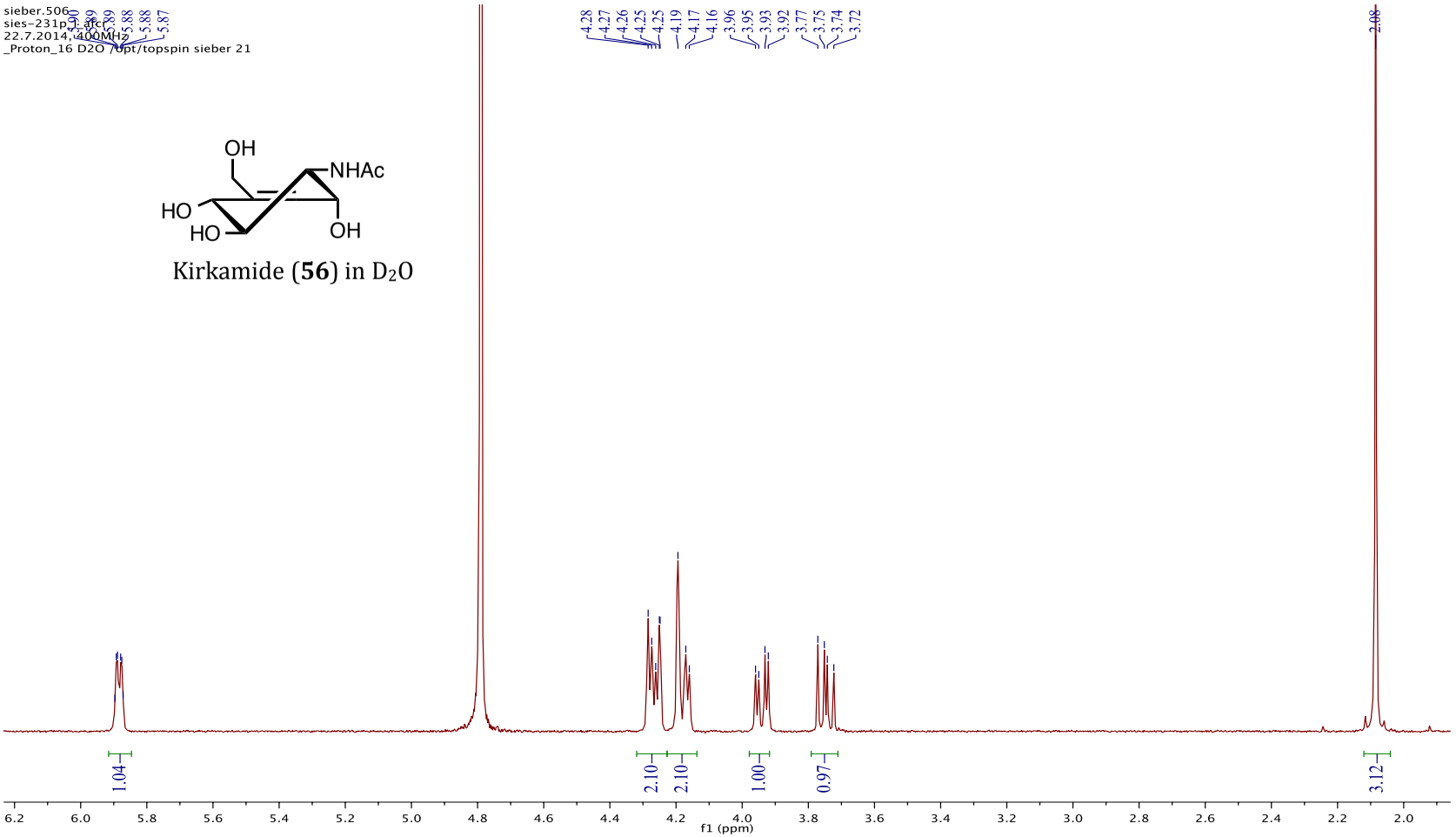
sieber.506
sies-231p01-1.afc
22.7.2014, 400MHz
_Proton_16 D2O /opt/topspin sieber 21
OH
NHAc
HO
HO
OH
Kirkamide (56) in D2O
1.04
2.10
2.10
1.00
0.97
3.12
f1 (ppm)

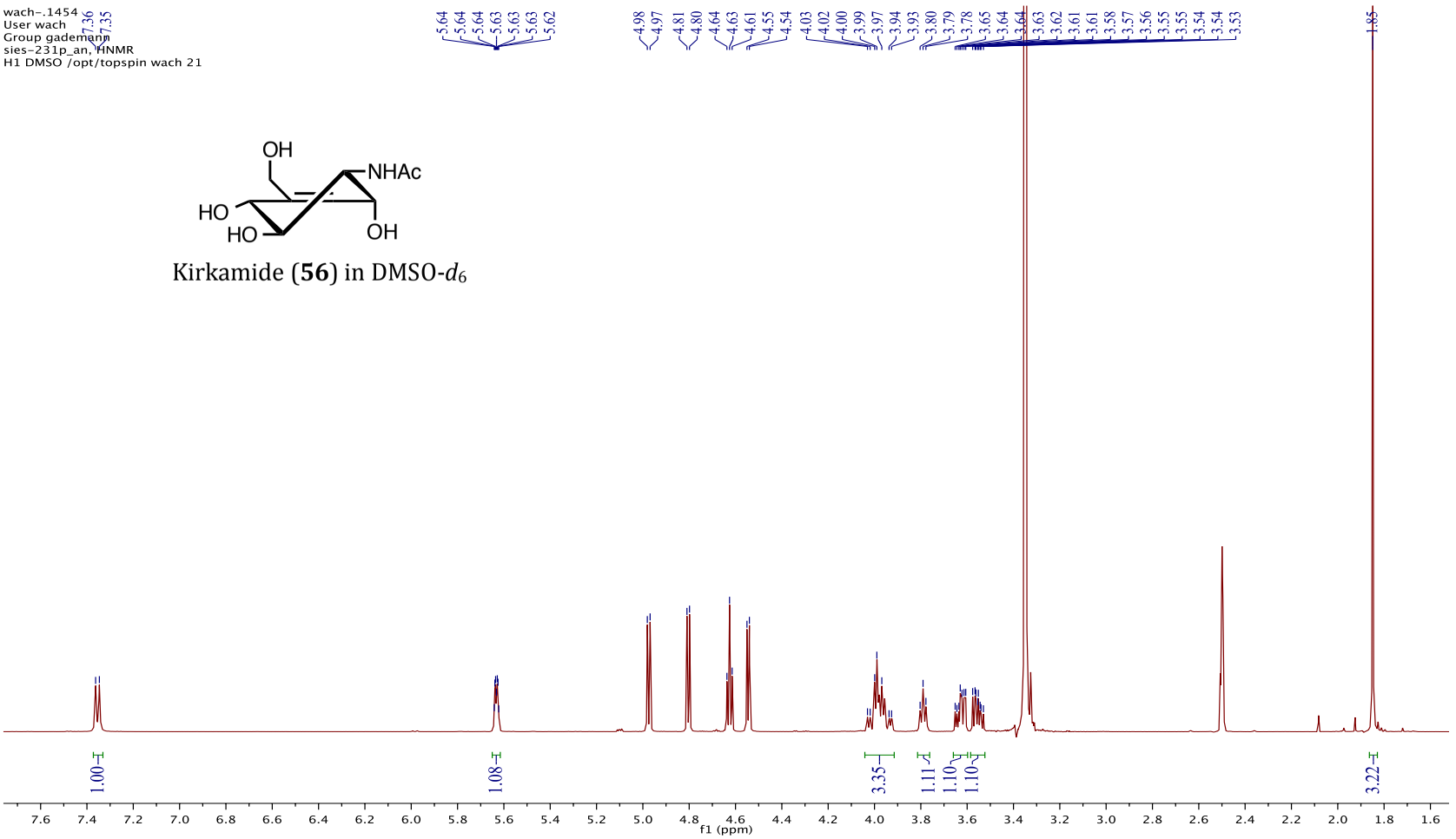

Kirkamide (**56**) in DMSO-d_6

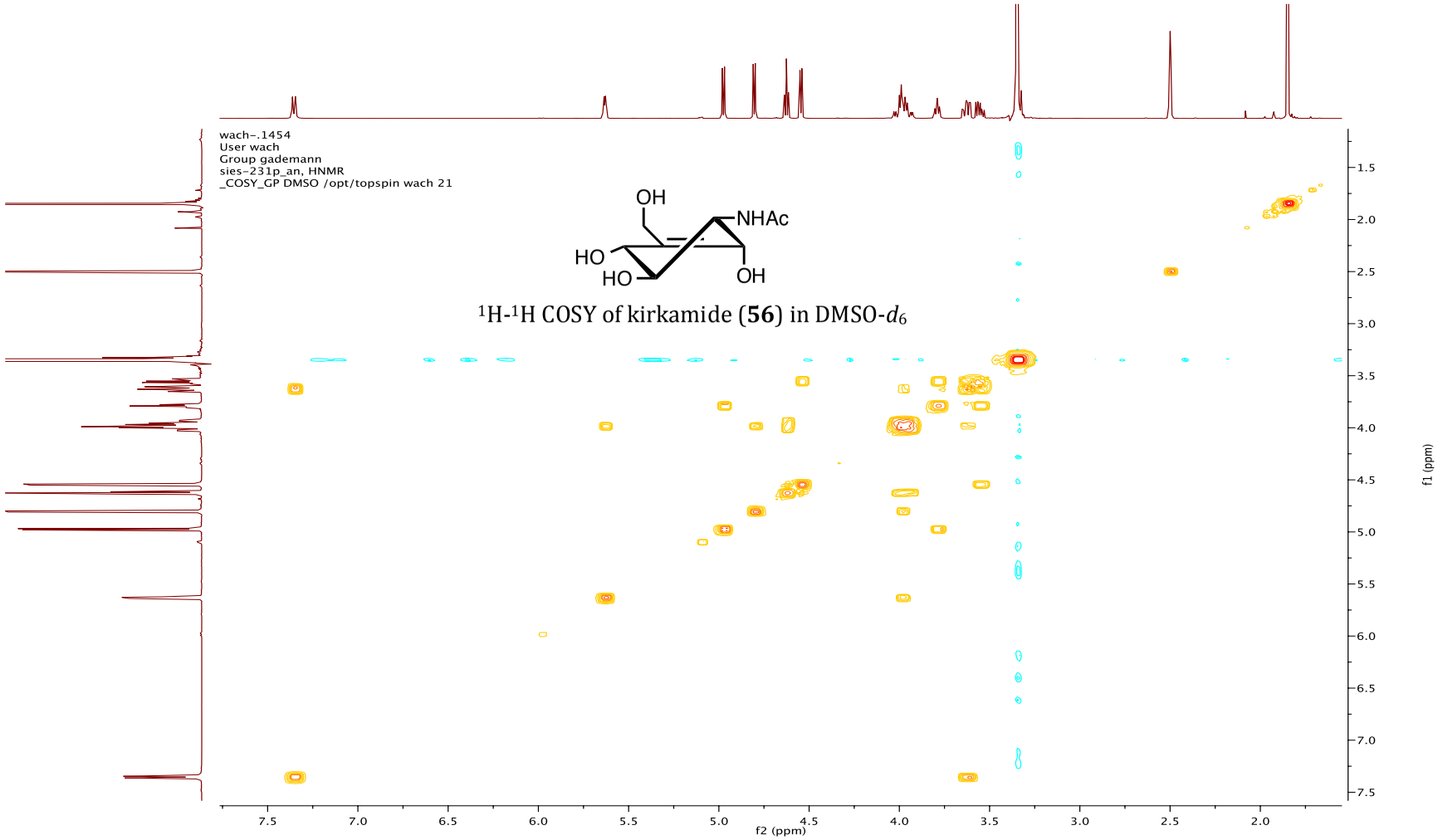

^{1}H-^{1}H COSY of kirkamide (**56**) in DMSO-d_6

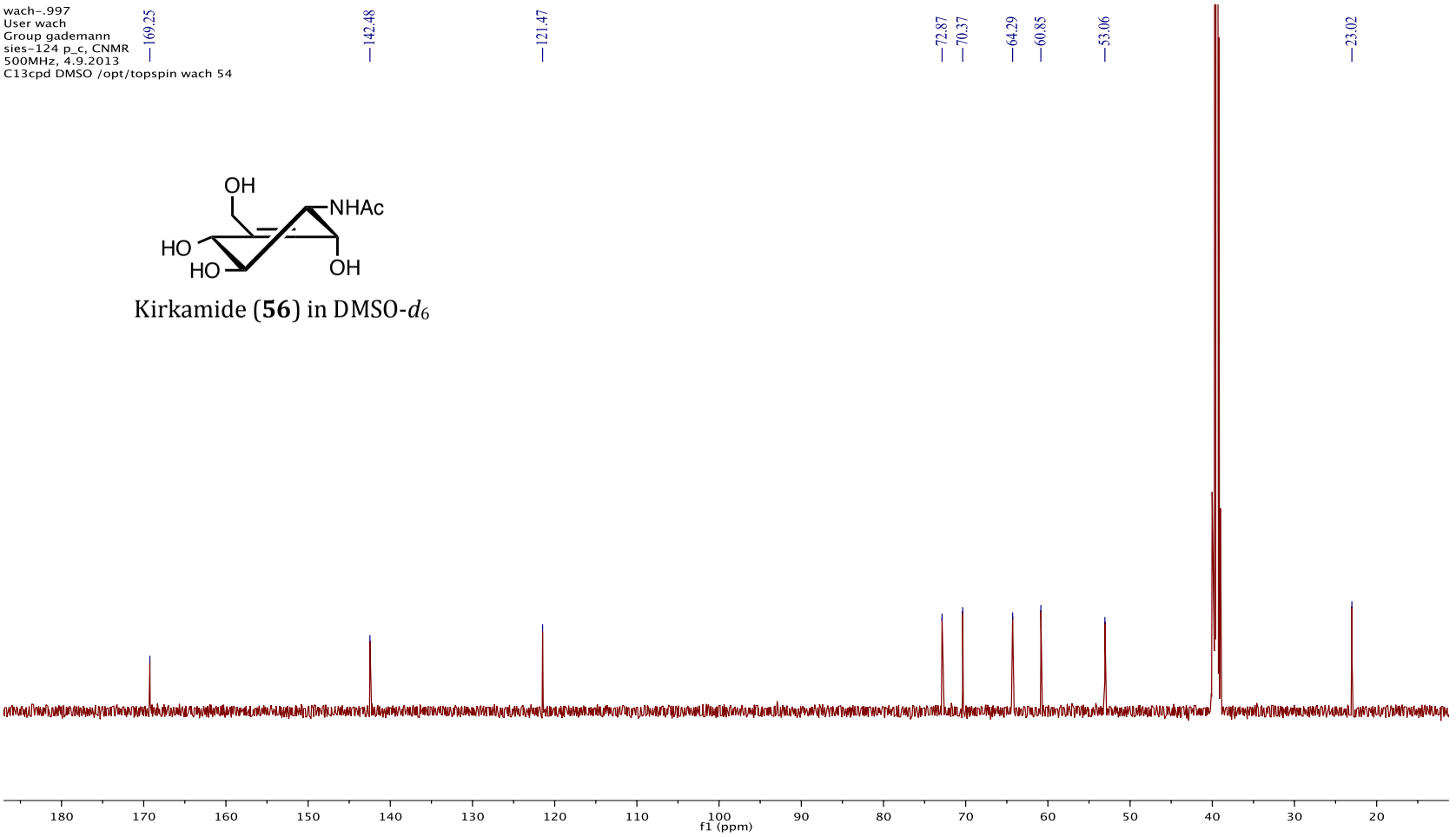

Kirkamide (**56**) in DMSO-d_6

NMR Spectra of Streptol Glucoside

^{1}H NMR spectrum of streptol glucoside (**57**) in DMSO-d_6 (600 MHz).

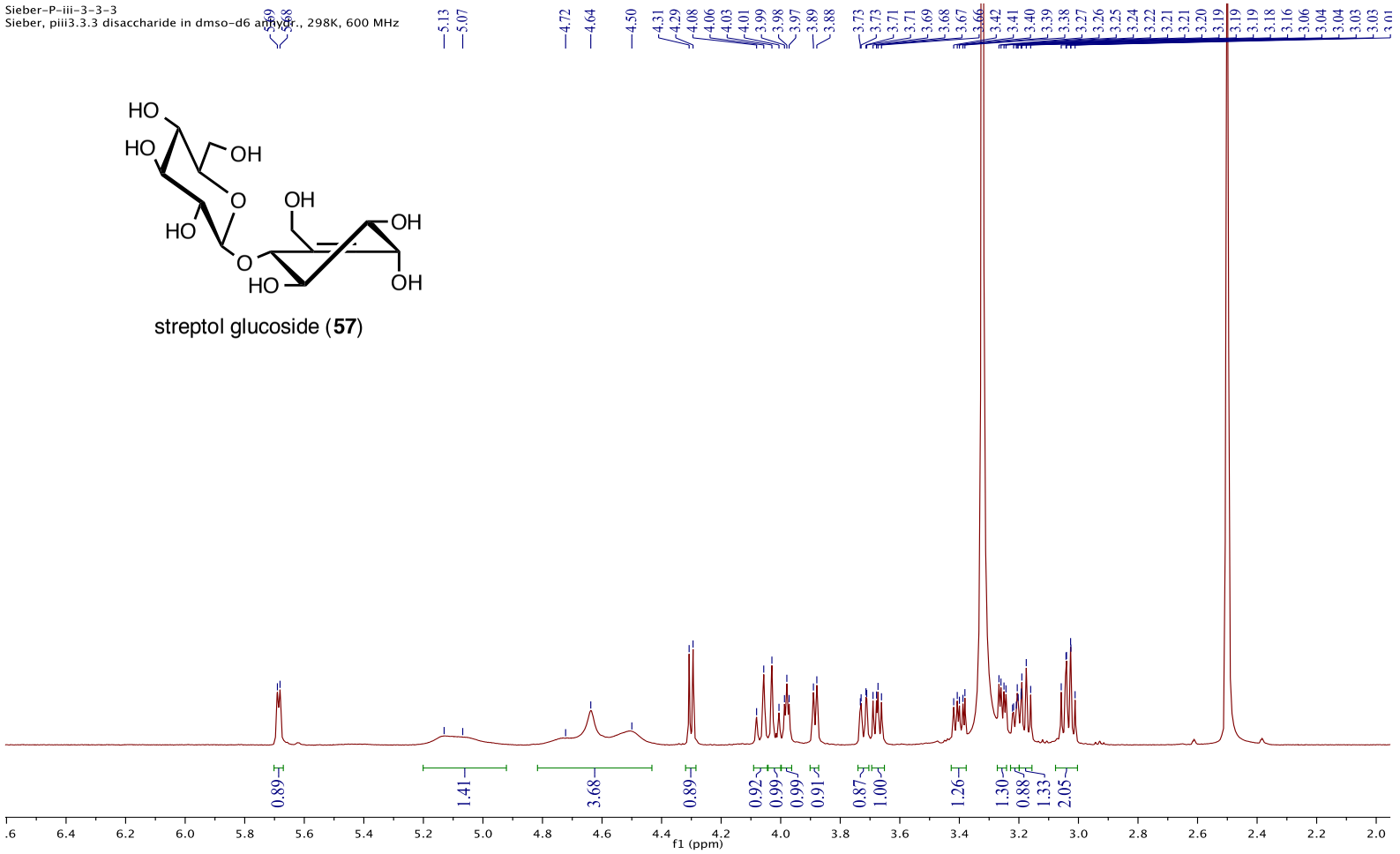

^{1}H-^{1}H COSY NMR spectrum of streptol glucoside (**57**) in DMSO-d_6 (600 MHz).

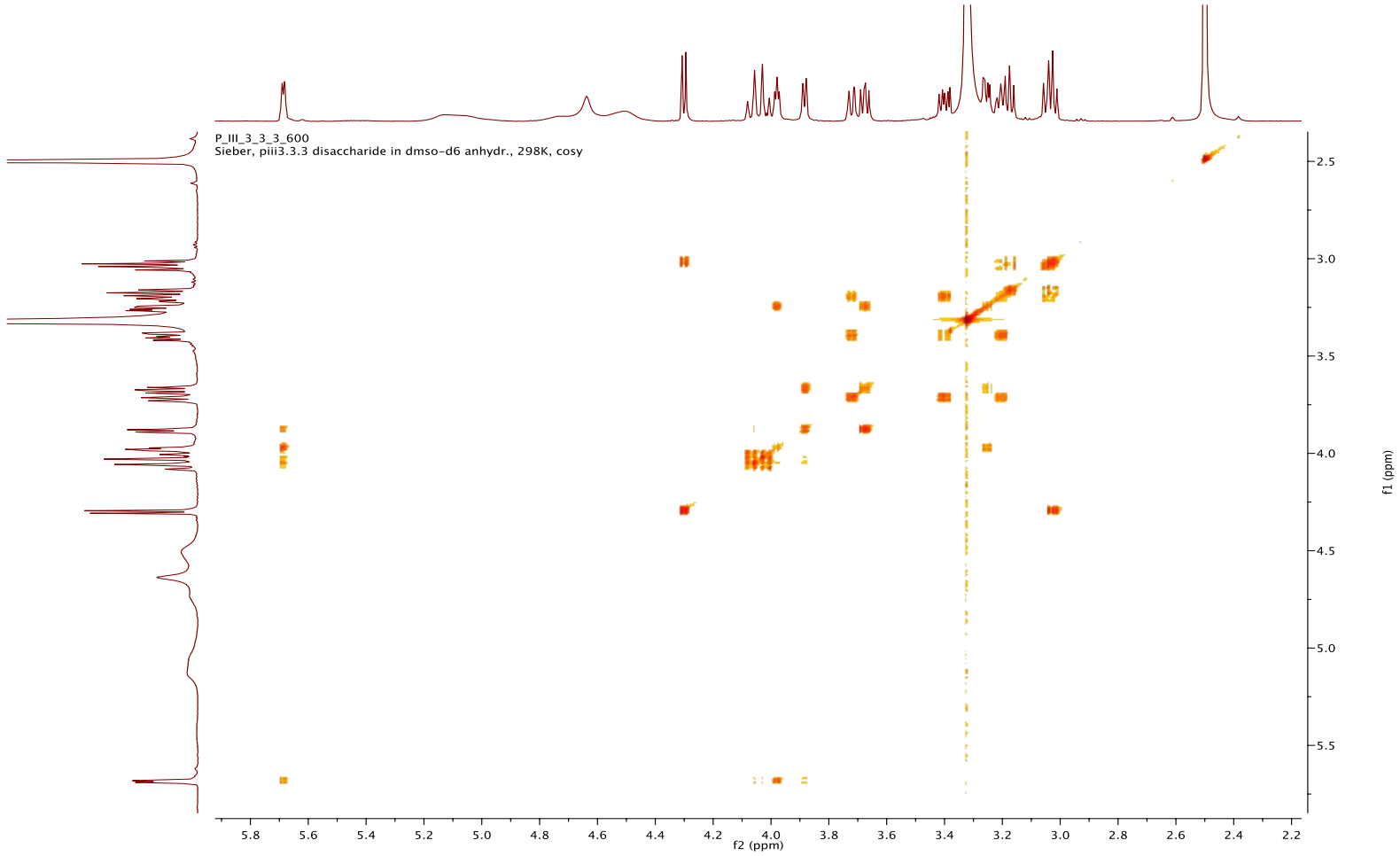

^{1}H-^{13}C HMQC NMR spectrum of streptol glucoside (**57**) in DMSO-d_6 (600 MHz).

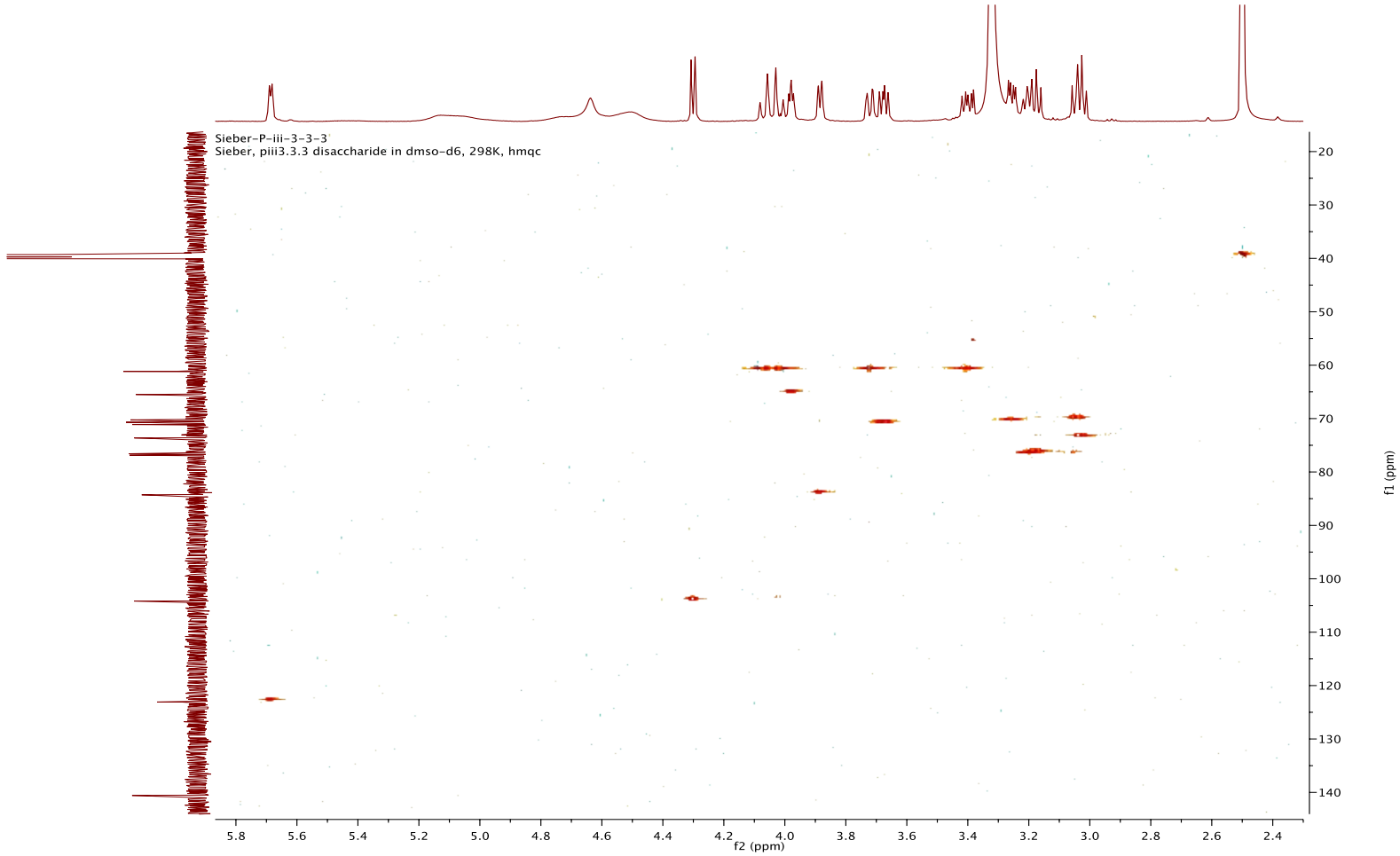

^{1}H-^{13}C HMBC NMR spectrum of streptol glucoside (**57**) in DMSO-d_6 (600 MHz).

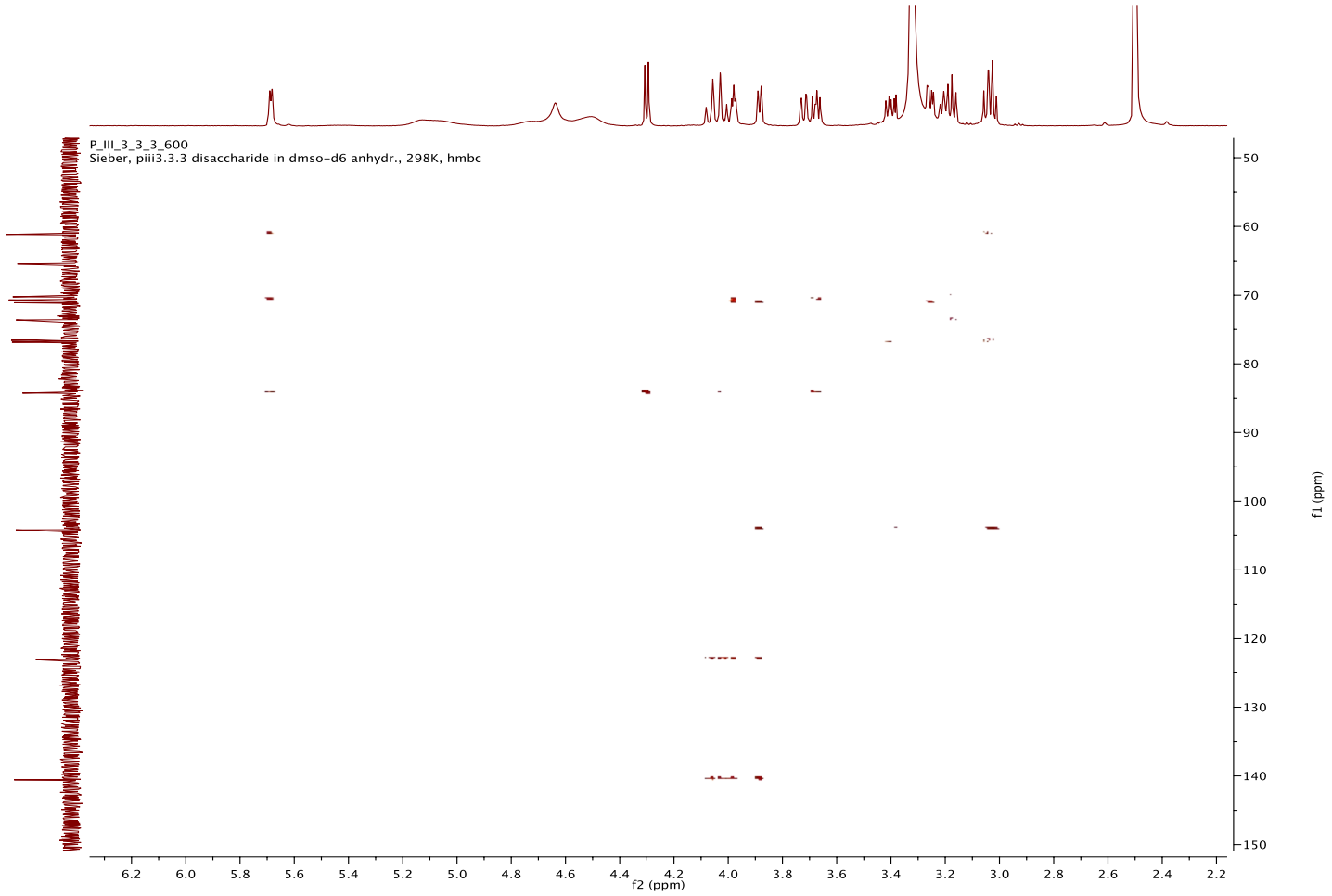

^{13}C NMR Spectrum of streptol glucoside (**57**) in DMSO-d_6 (600 MHz).

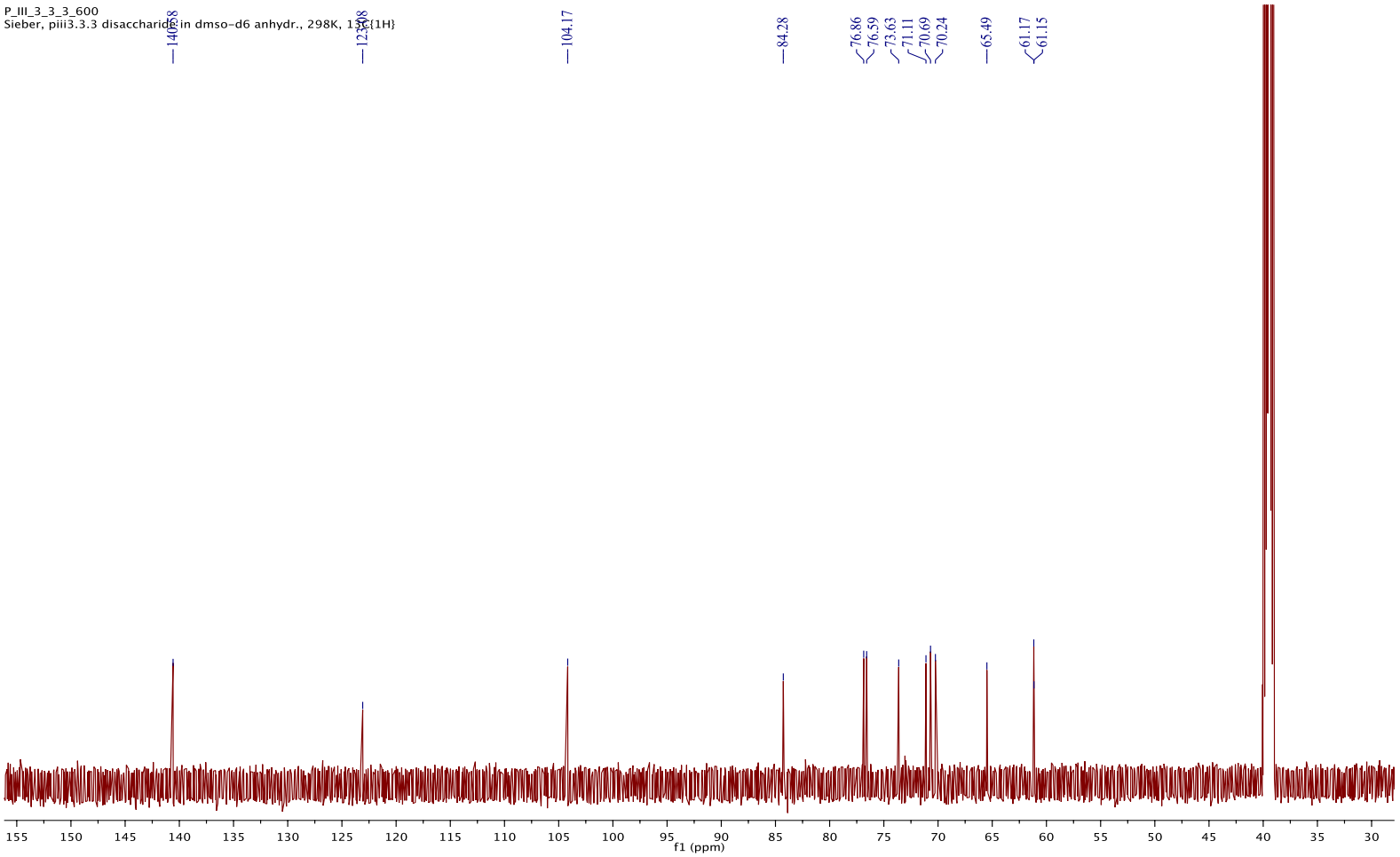

^{1}H NMR Spectrum of streptol glucoside (**57**) in D_2O (500 MHz).

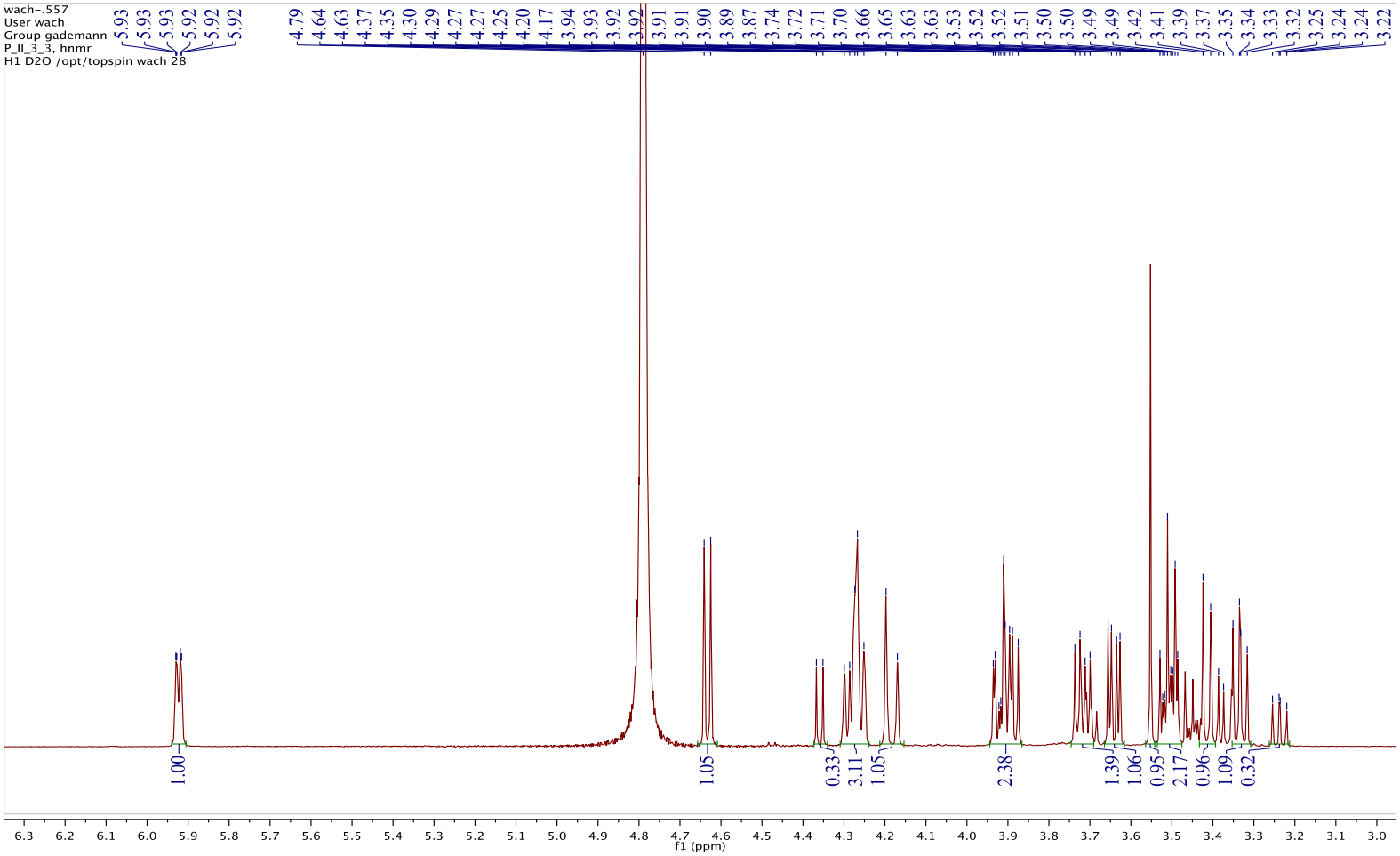

GC-MS Chromatograms for the Detection of Kirkamide

GC spectrum of kirkamide (**56**) after MSTFA derivatization and MS spectrum of the peak a 27.73 min.

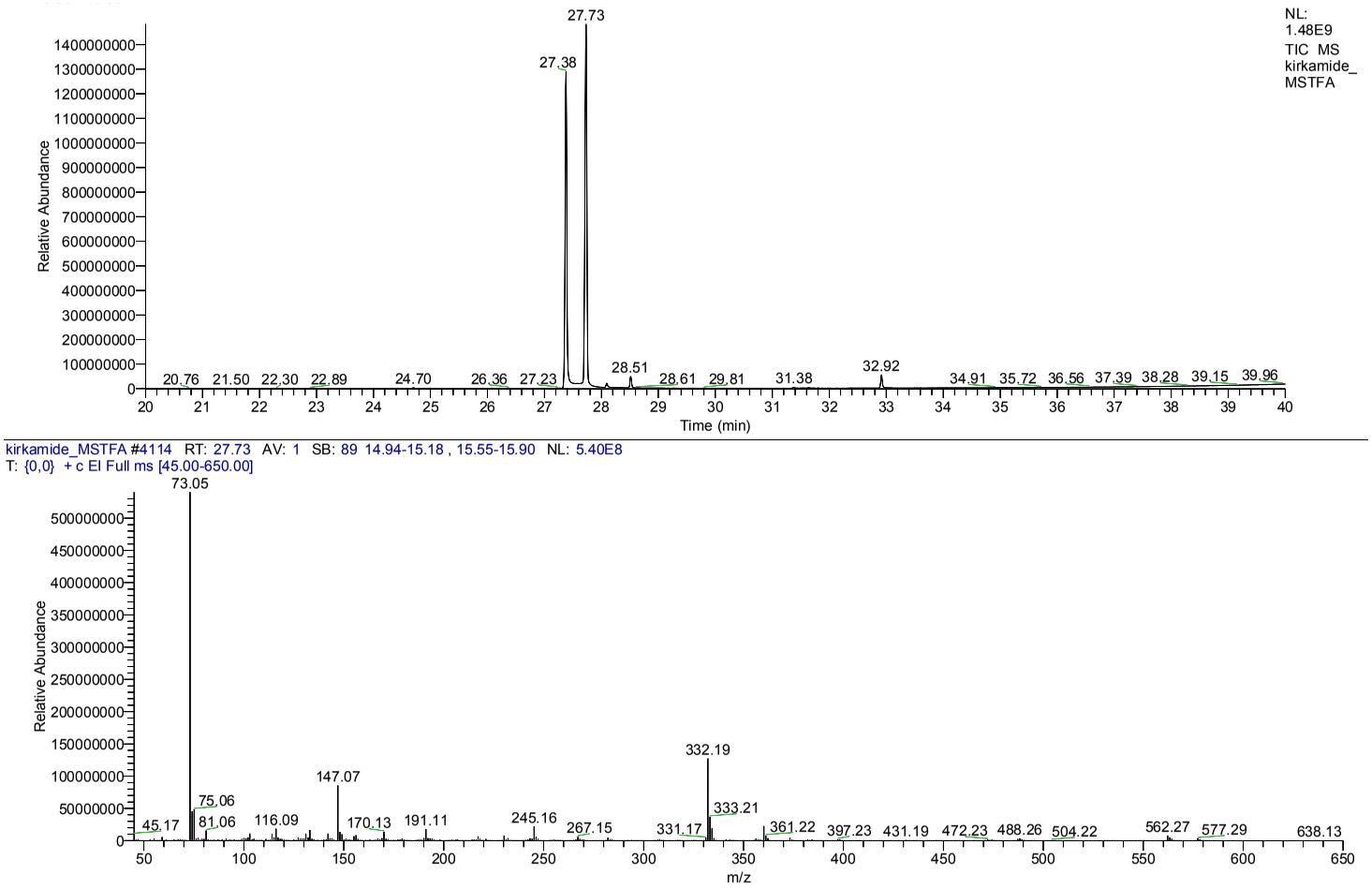

GC spectrum of kirkamide (**56**) after MSTFA derivatization and MS spectrum from 400 to 600 *m/z* of the peak a 27.73 min.

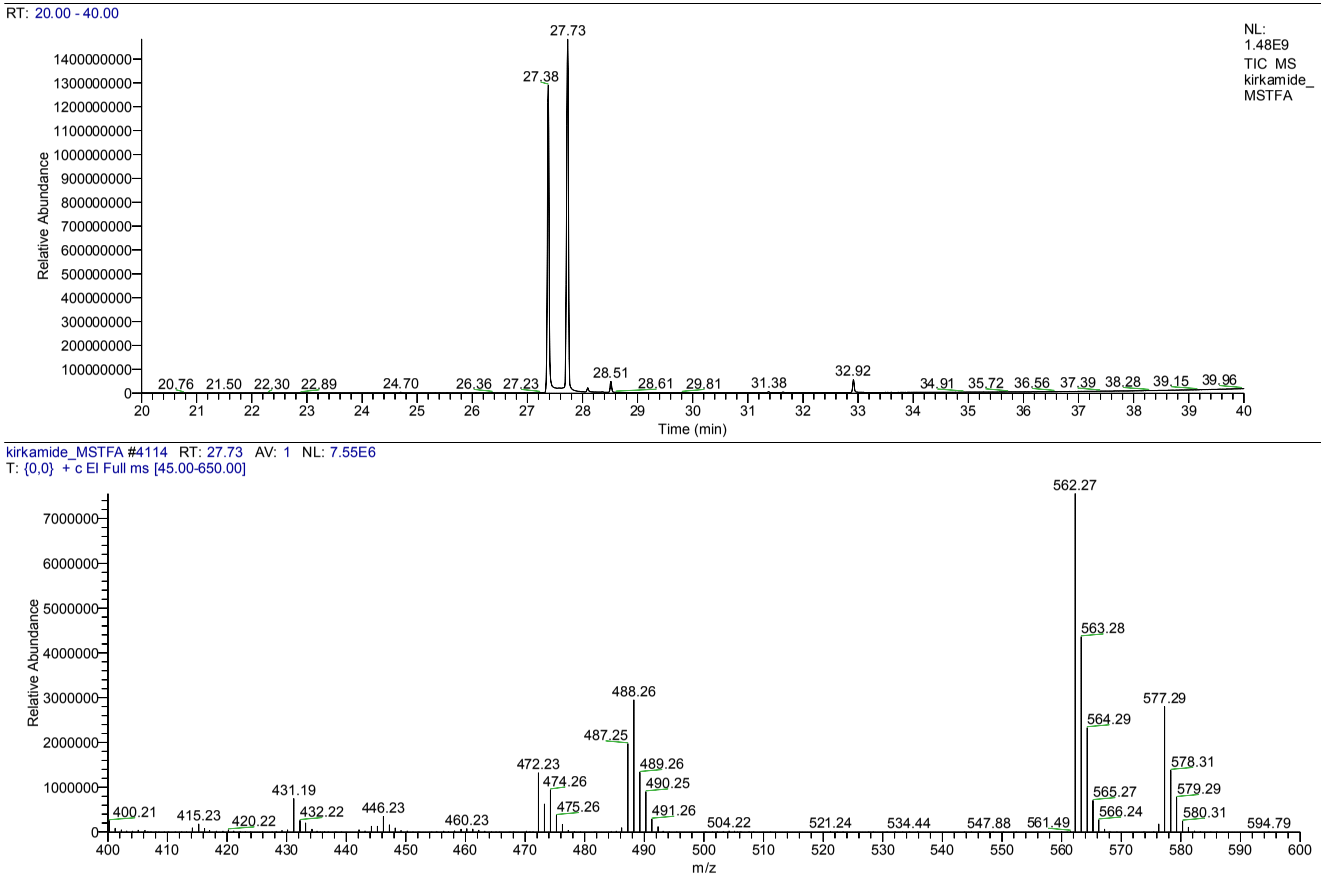

GC spectrum of kirkamide (**56**) after MSTFA derivatization and MS spectrum of the peak a 27.38 min.

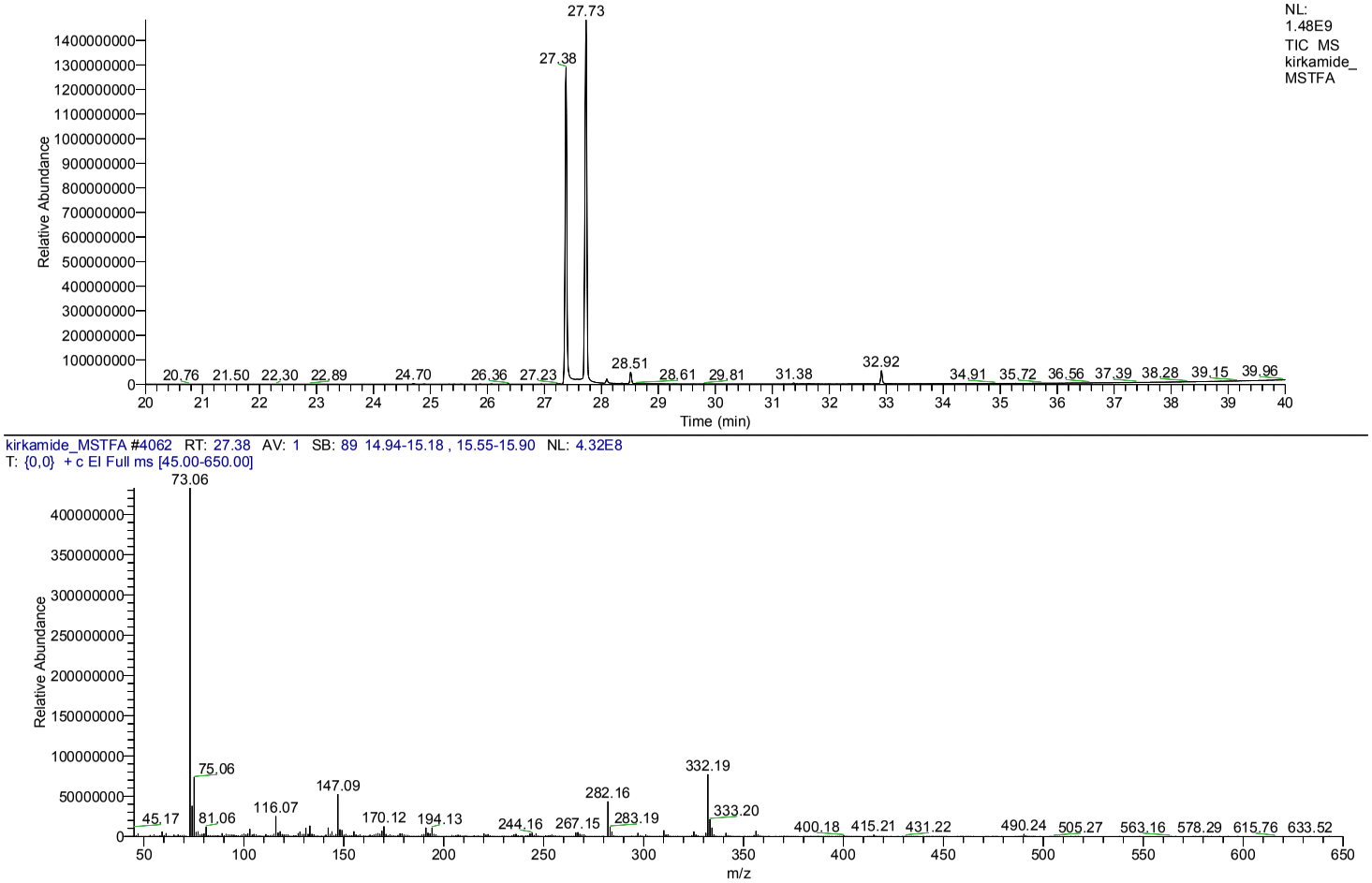

GC spectrum of kirkamide (**56**) after MSTFA derivatization and MS spectrum from 400 to 600 *m/z* of the peak a 27.38 min.

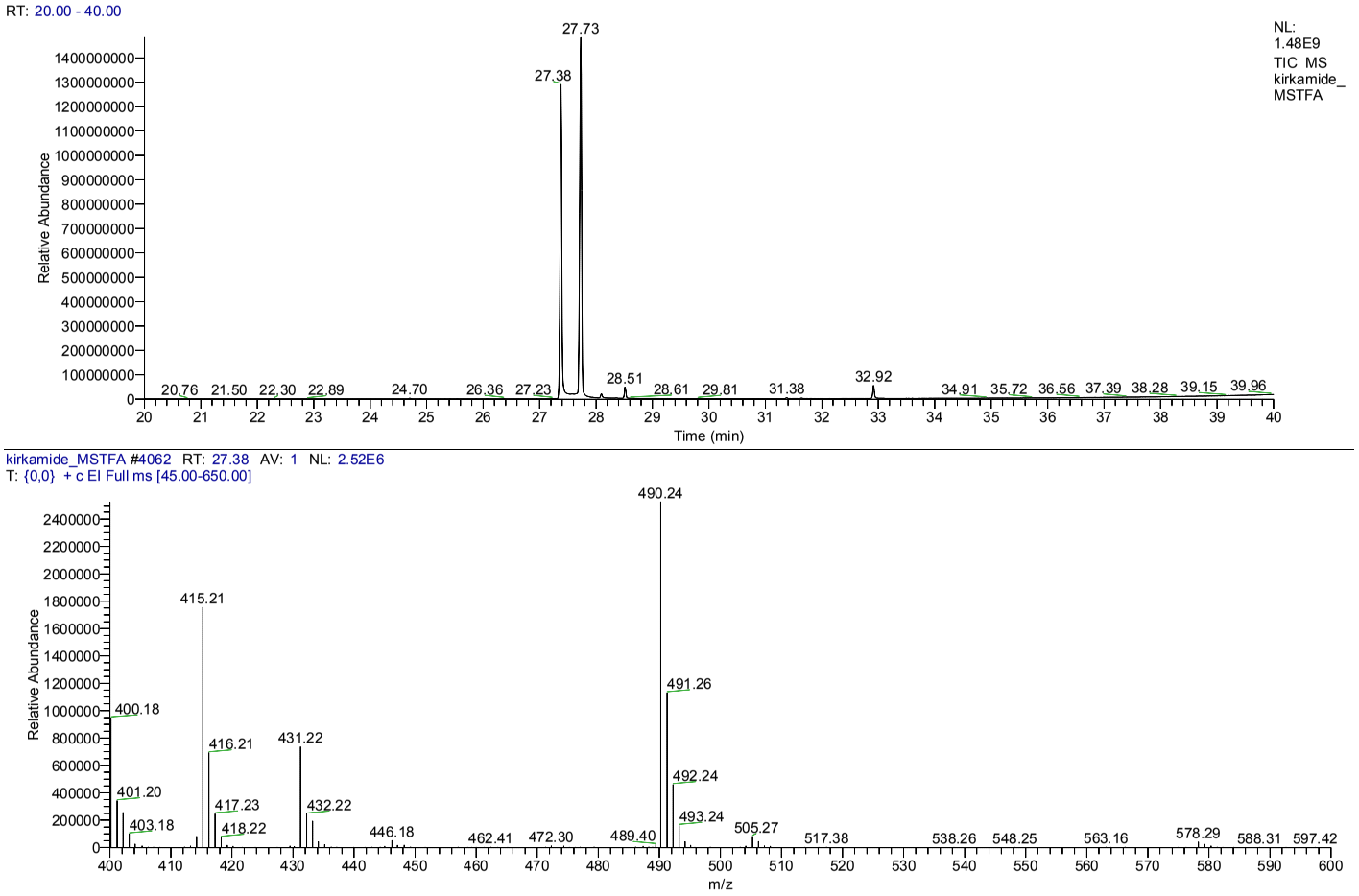

GC spectrum of *Psychotria humilis* leaves extract after MSTFA derivatization and MS spectrum from 400 to 600 *m/z* of the peak a 27.29 min.

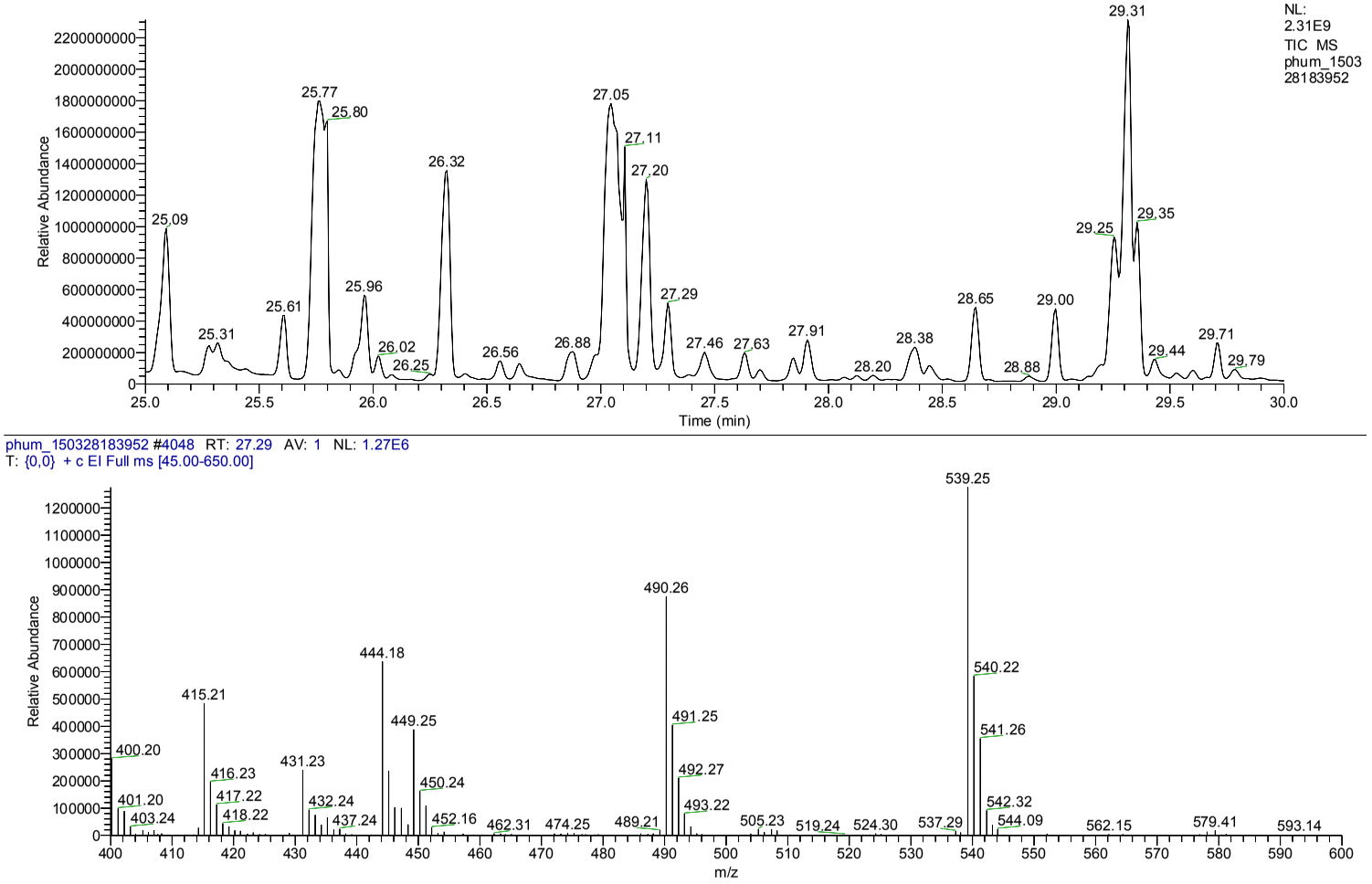

GC spectrum of *Psychotria humilis* leaves extract after MSTFA derivatization and MS spectrum from 400 to 600 *m/z* of the peak a 27.63 min.

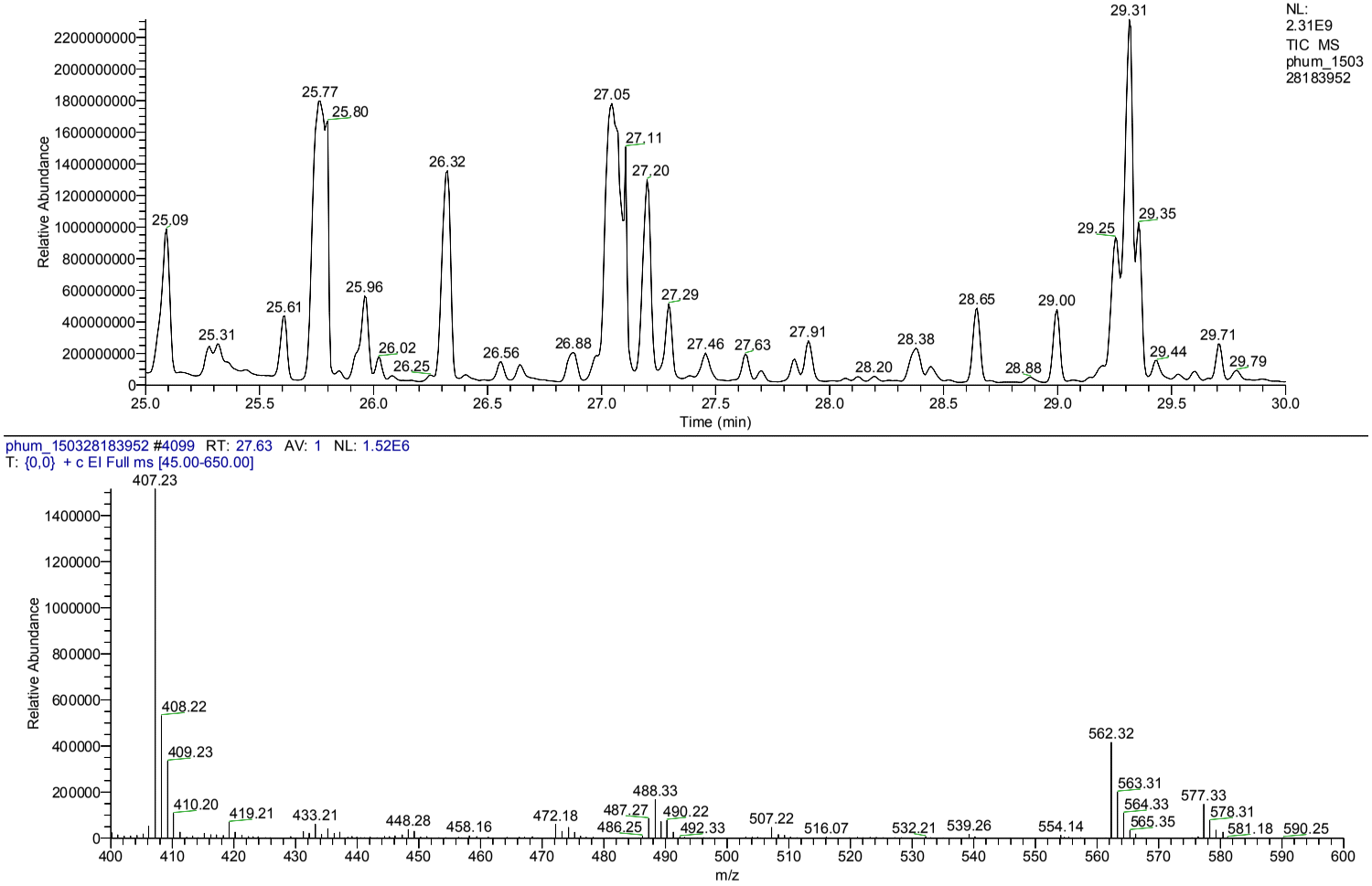

GC spectrum of *Psychotria verschuerenii* leaves extract after MSTFA derivatization and MS spectrum from 400 to 600 *m/z* of the peak a 27.28 min.

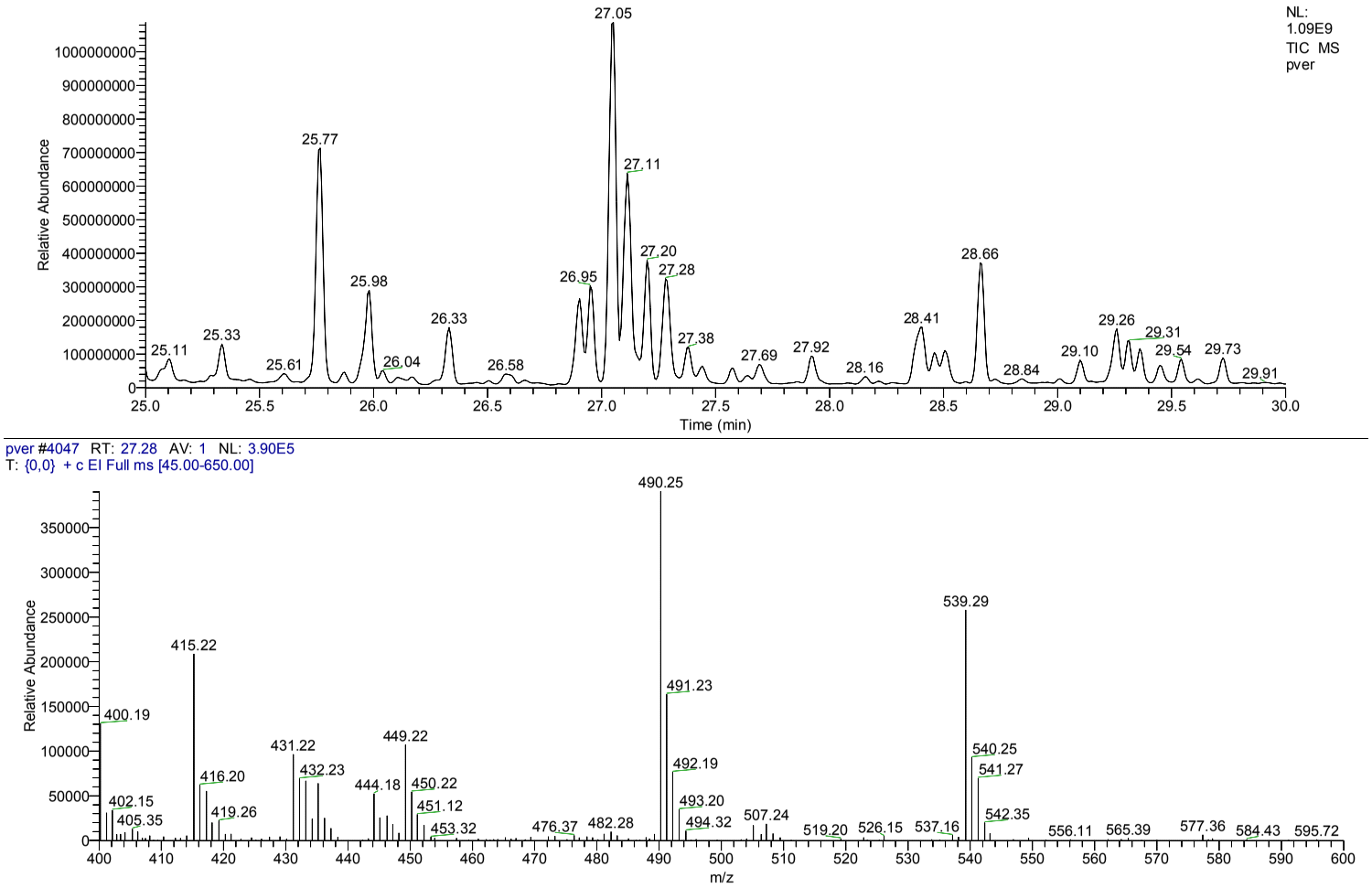

GC spectrum of *Psychotria verschuerenii* leaves extract after MSTFA derivatization and MS spectrum from 400 to 600 *m/z* of the peak a 27.64 min.

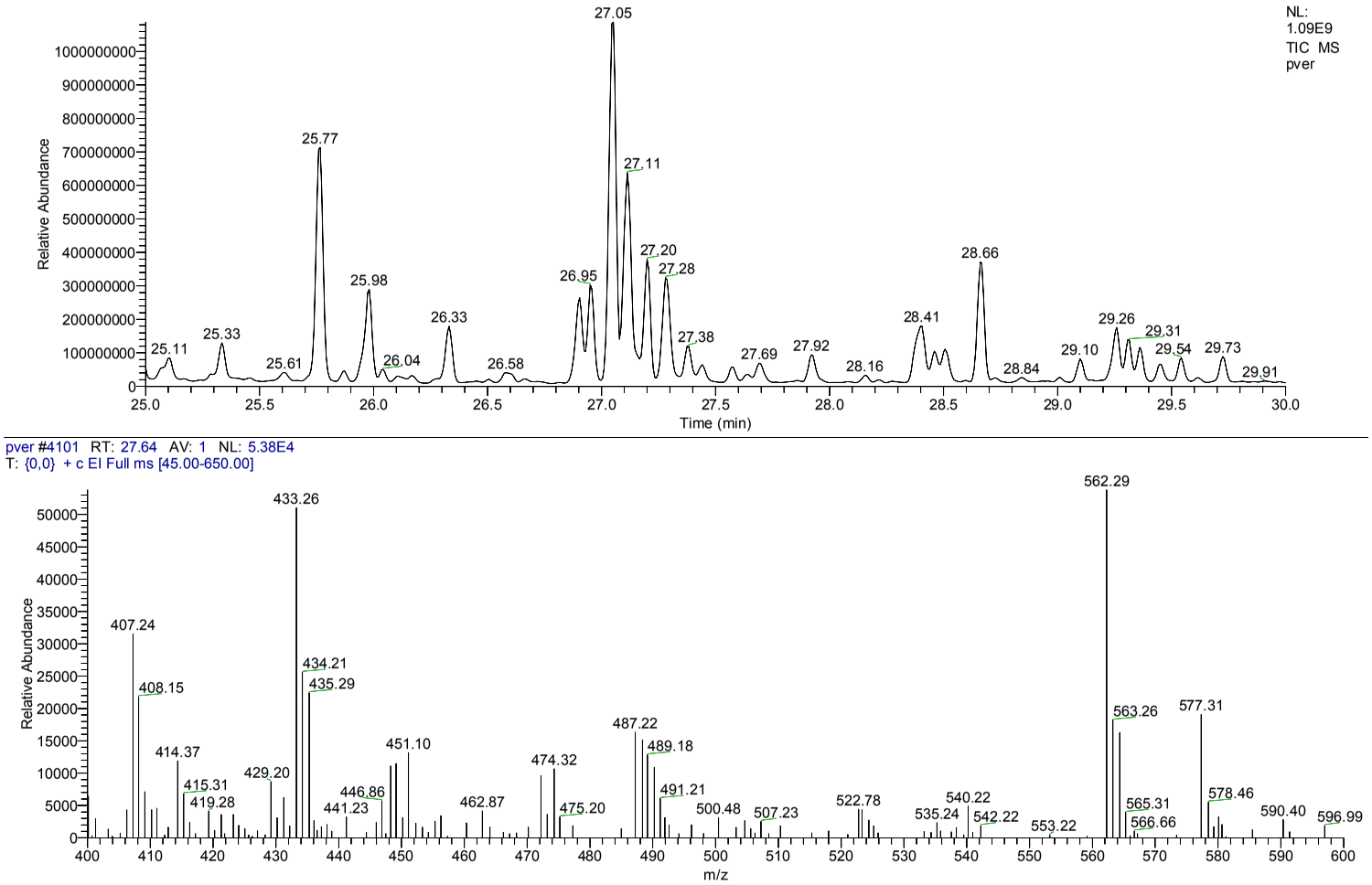

GC spectrum of *Psychotria kirkii* leaves extract after MSTFA derivatization and MS spectrum from 400 to 600 *m/z* of the peak a 27.25 min.

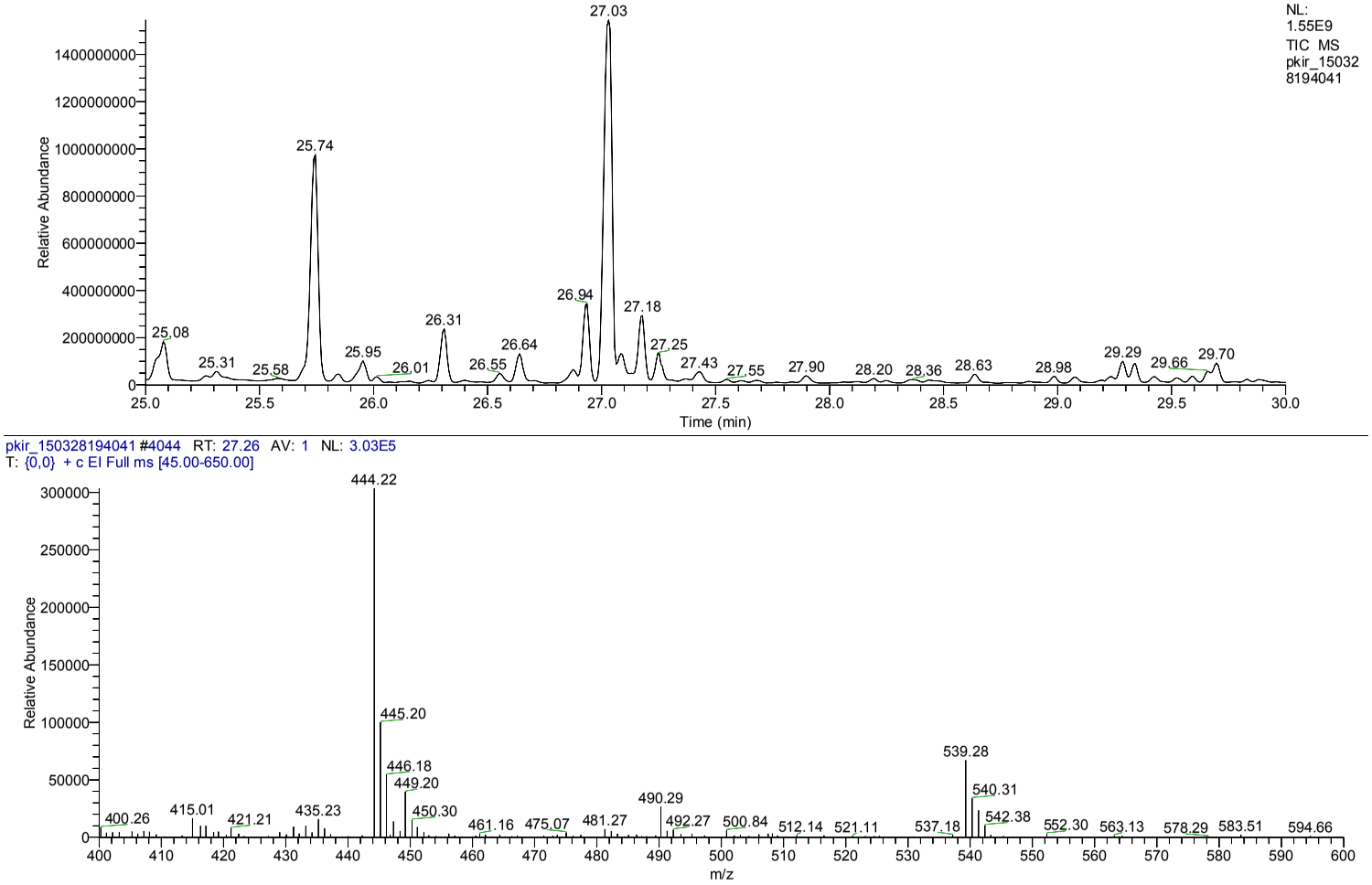

GC spectrum of *Psychotria kirkii* leaves extract after MSTFA derivatization and MS spectrum from 400 to 600 m/z of the peak a 27.62 min.

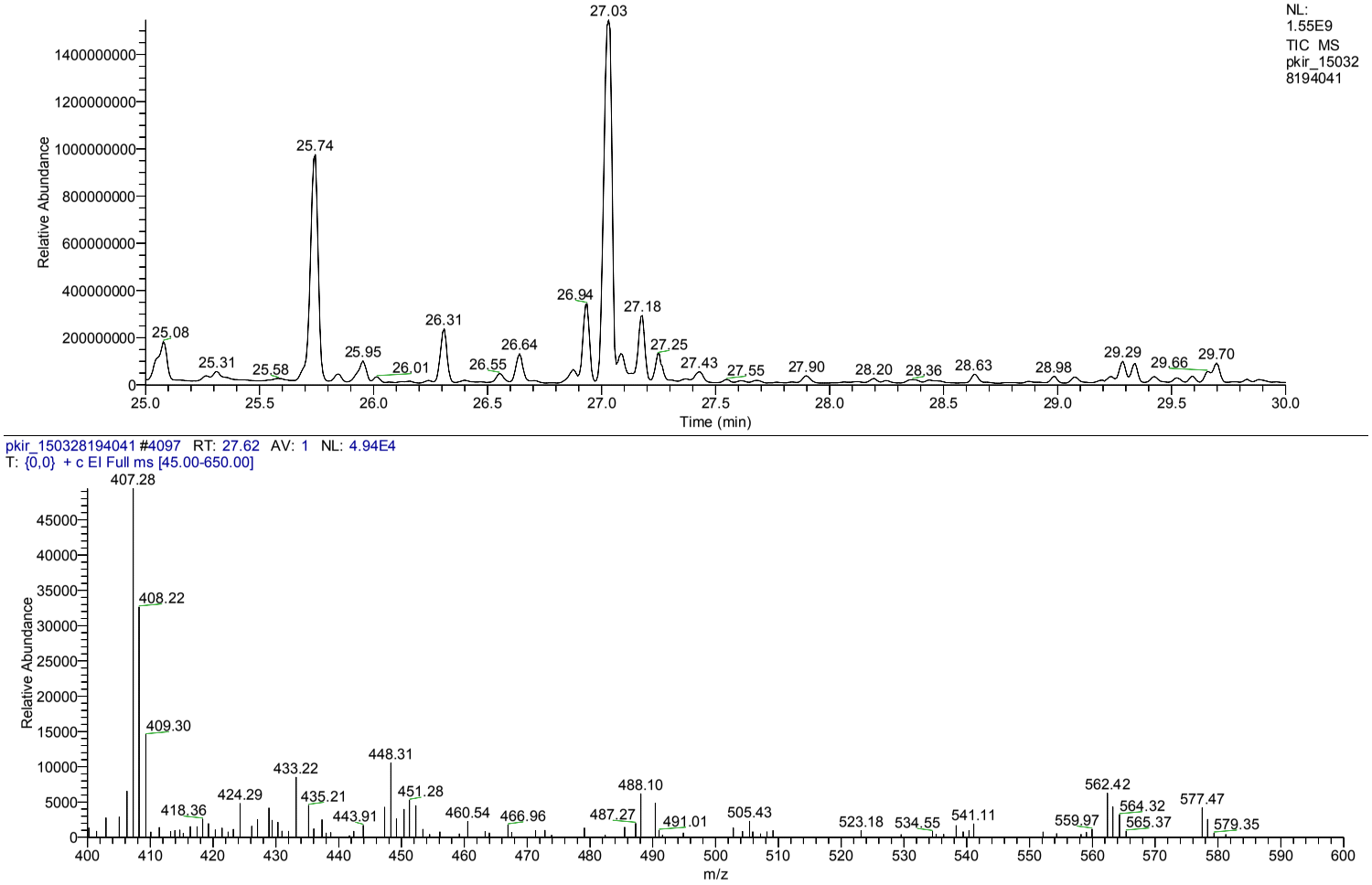

GC spectrum of *Psychotria pumila* leaves extract after MSTFA derivatization and MS spectrum from 400 to 600 *m/z* of the peak a 27.27 min.

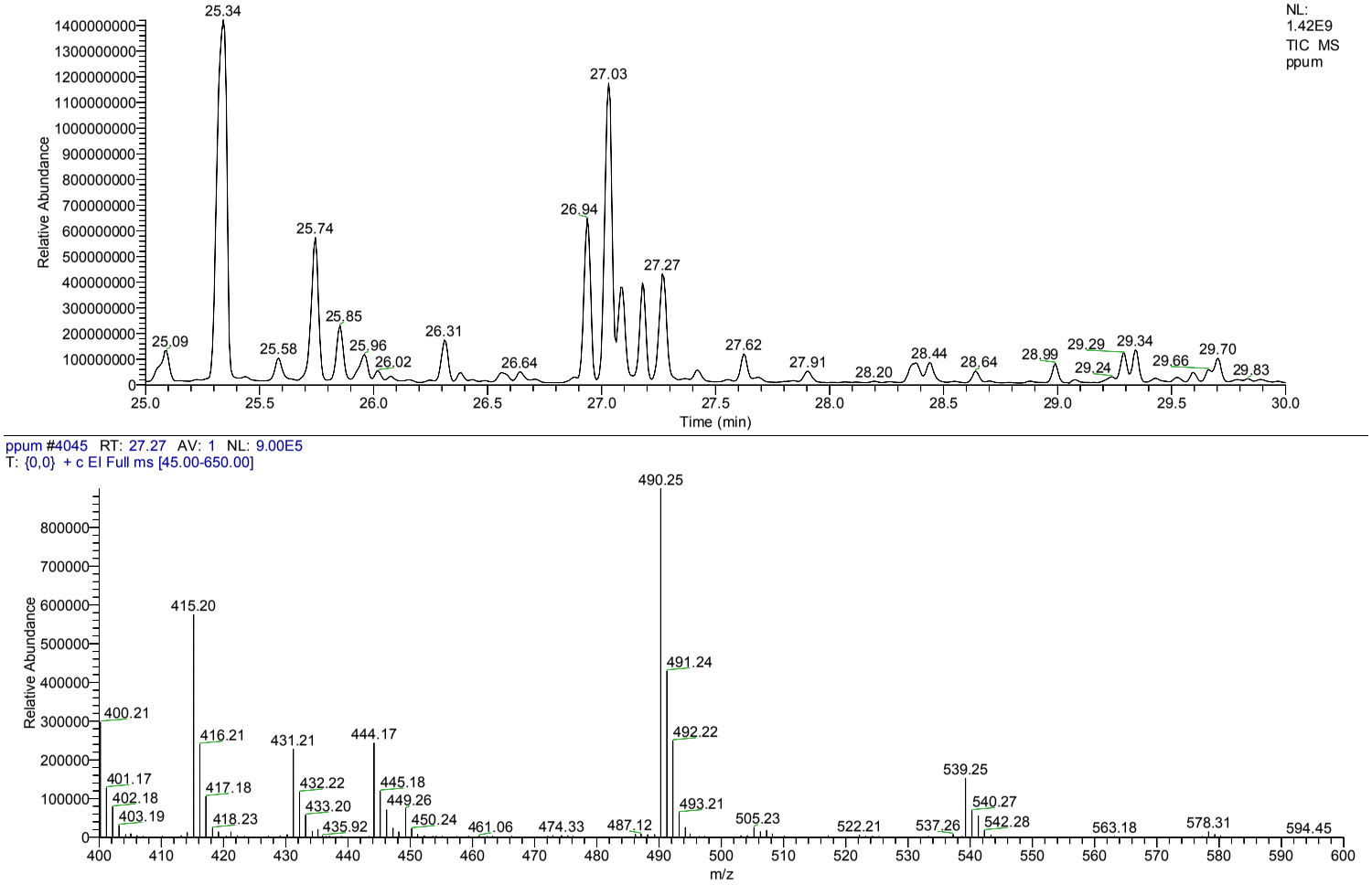

GC spectrum of *Psychotria pumila* leaves extract after MSTFA derivatization and MS spectrum from 400 to 600 *m/z* of the peak a 27.62 min.

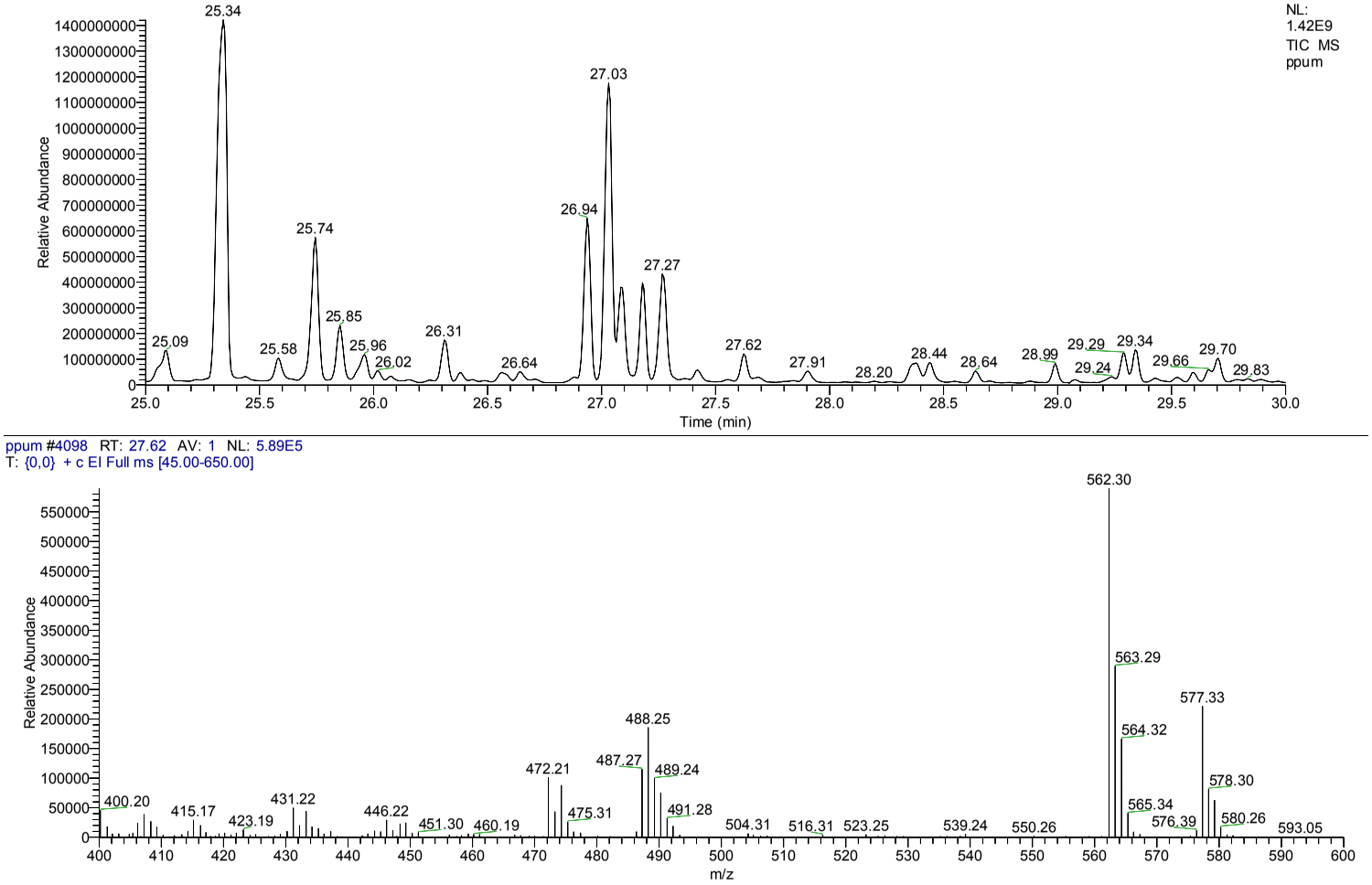

GC spectrum of *Psychotria punctata* leaves extract after MSTFA derivatization and MS spectrum from 400 to 600 *m/z* of the peak a 27.30 min.

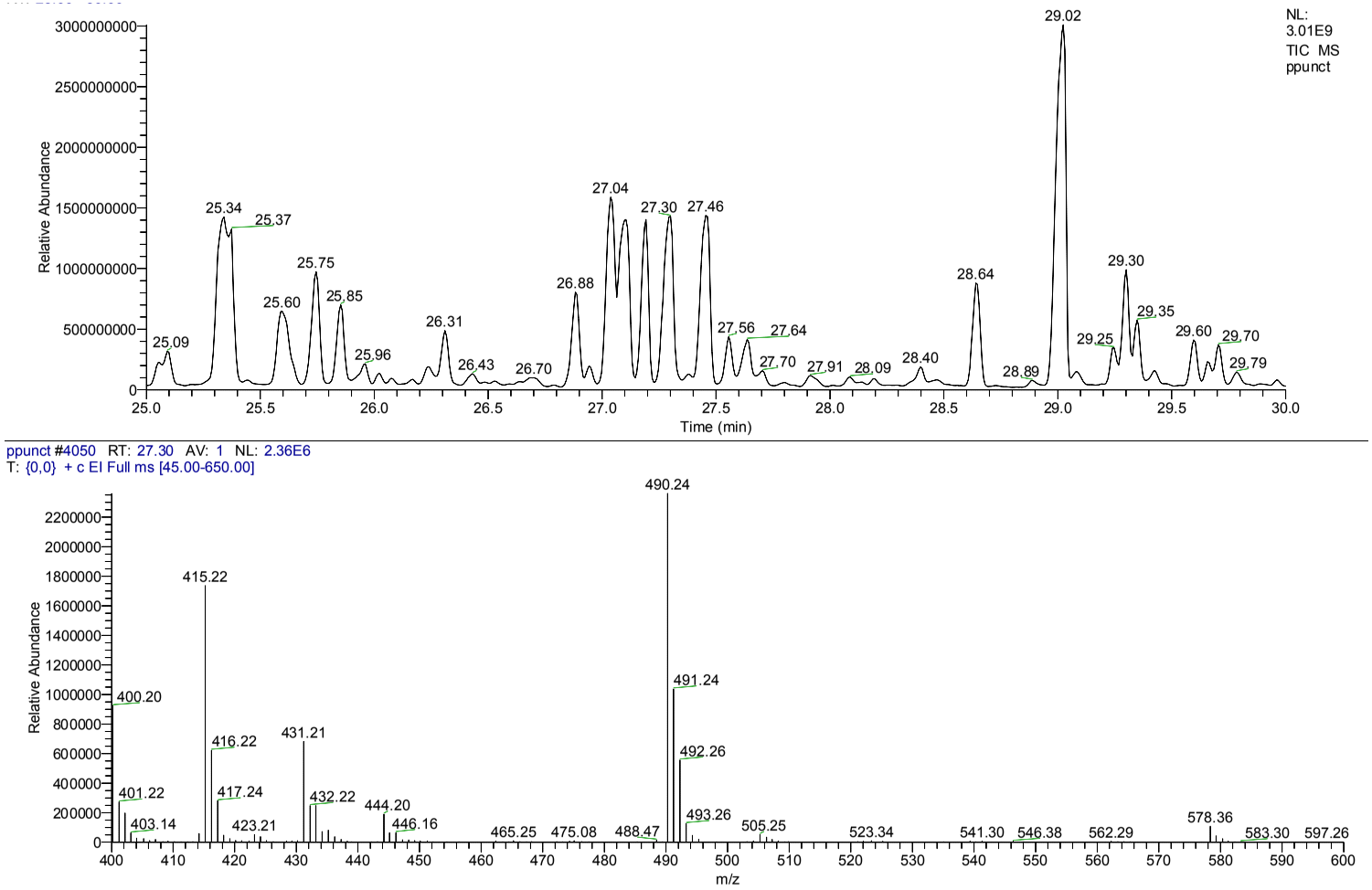

NMR Spectra for the Quantification of Kirkamide, Streptol glucoside and Asperuloside

^{1}H NMR Spectrum of leaves extract from *Psychotria kirkii* in D_2O (500 MHz).

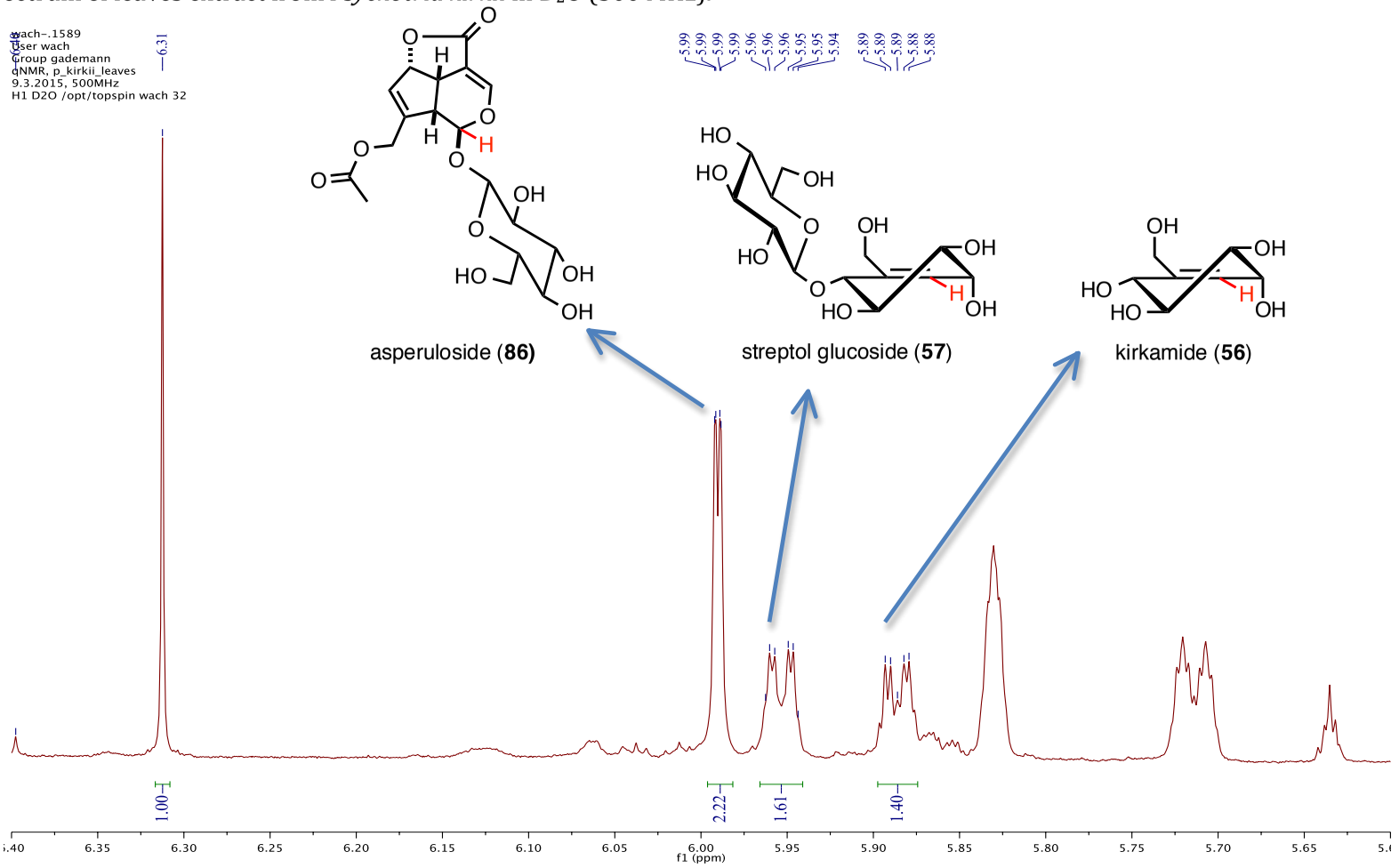

^{1}H NMR Spectrum of shoot extract from *Psychotria kirkii* in D_2O (500 MHz).

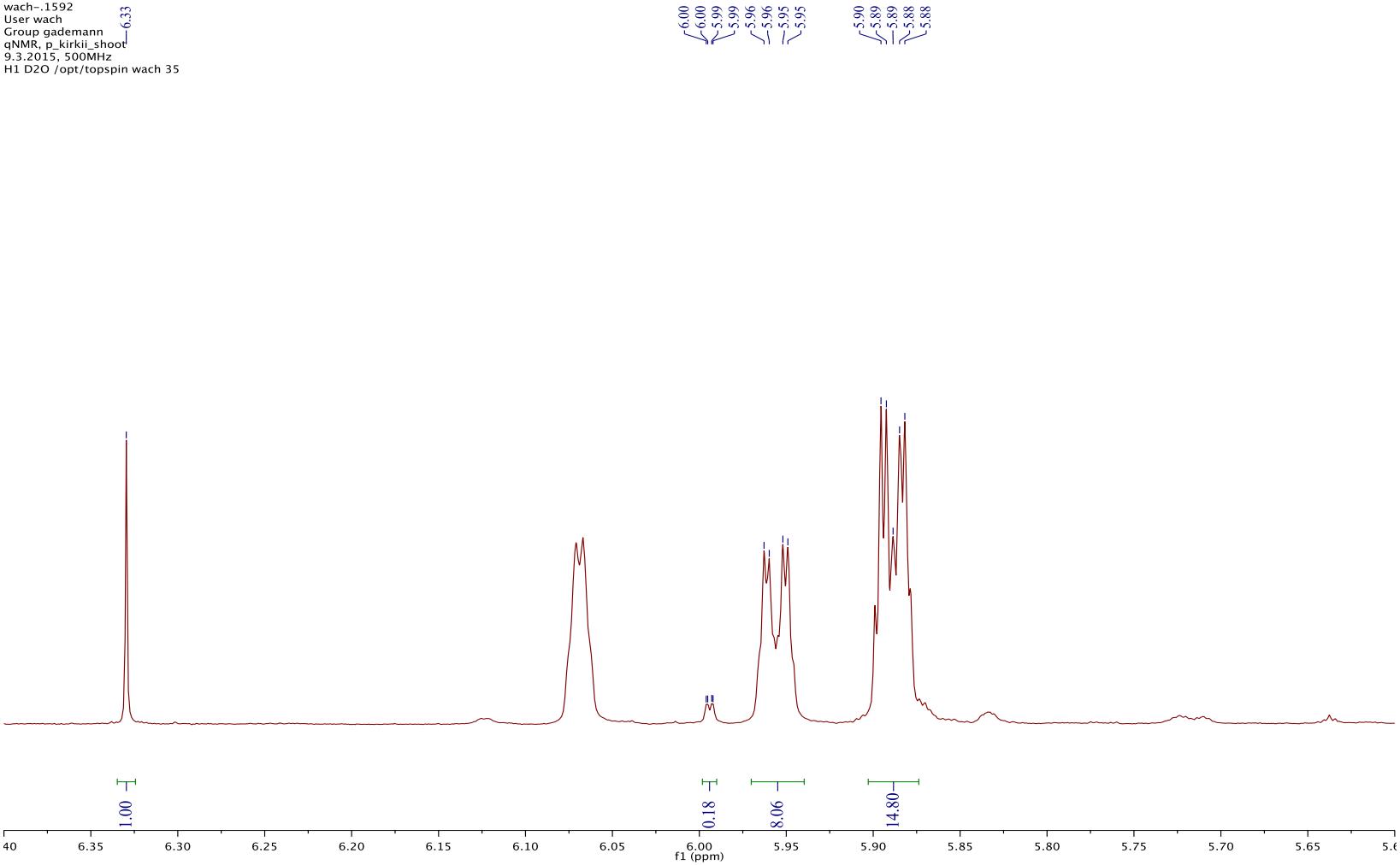

^{1}H NMR Spectrum of root extract from *Psychotria kirkii* in D_2O (500 MHz).

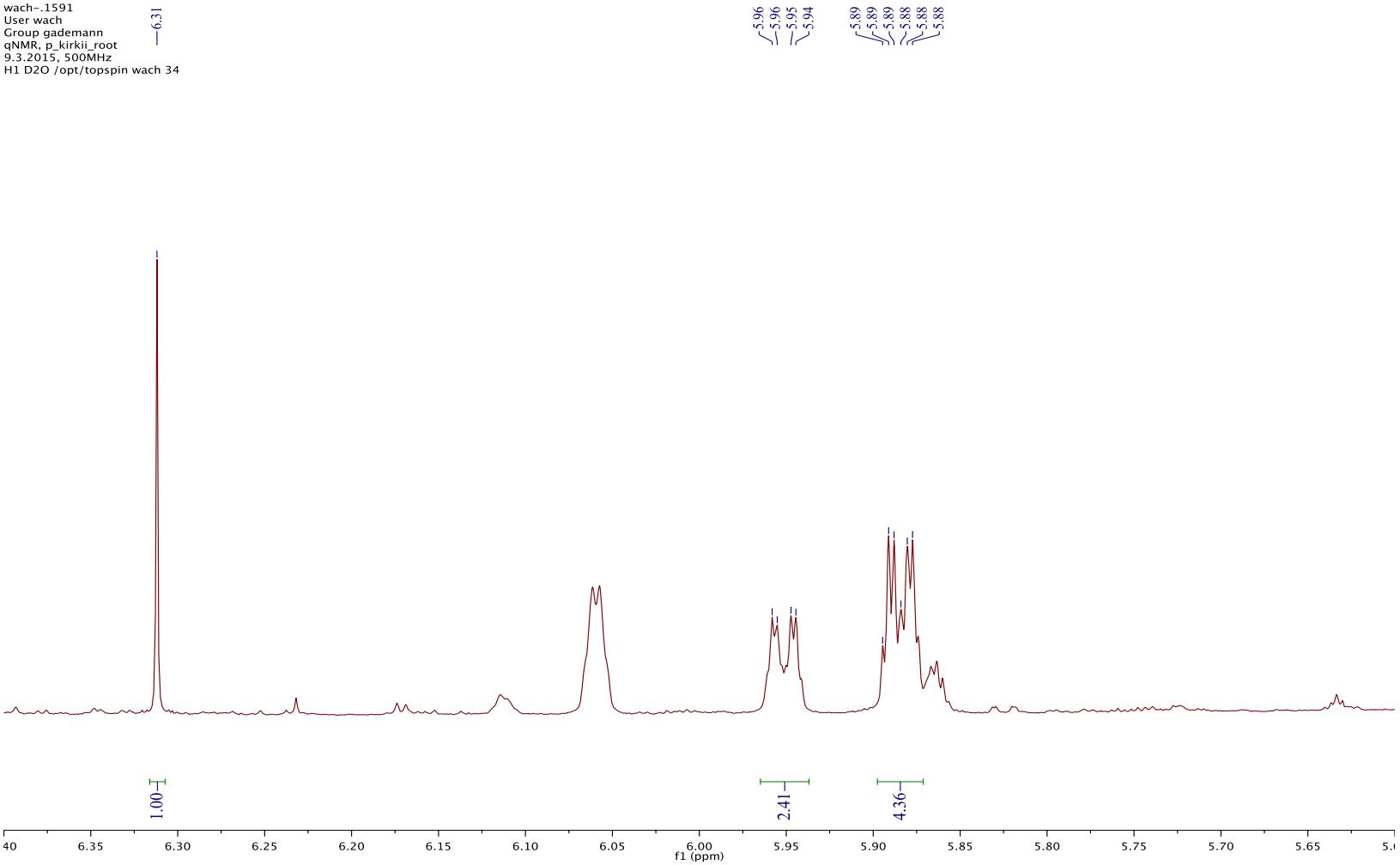

^{1}H NMR Spectrum of soil extract from *Psychotria kirkii* in D_2O (500 MHz).

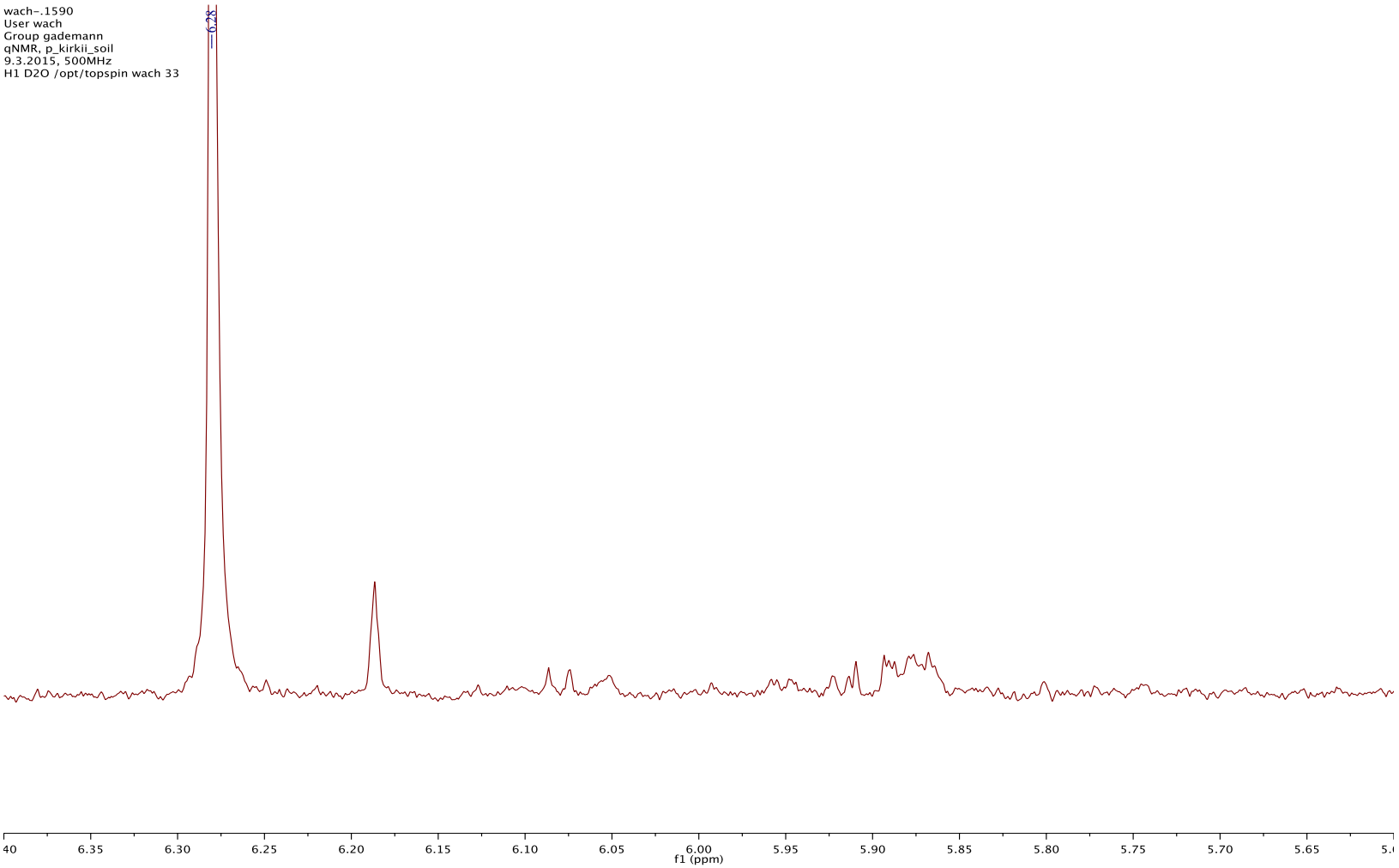

^{1}H NMR Spectrum of *Psychotria kirkii* leaves in D_2O (500 MHz).

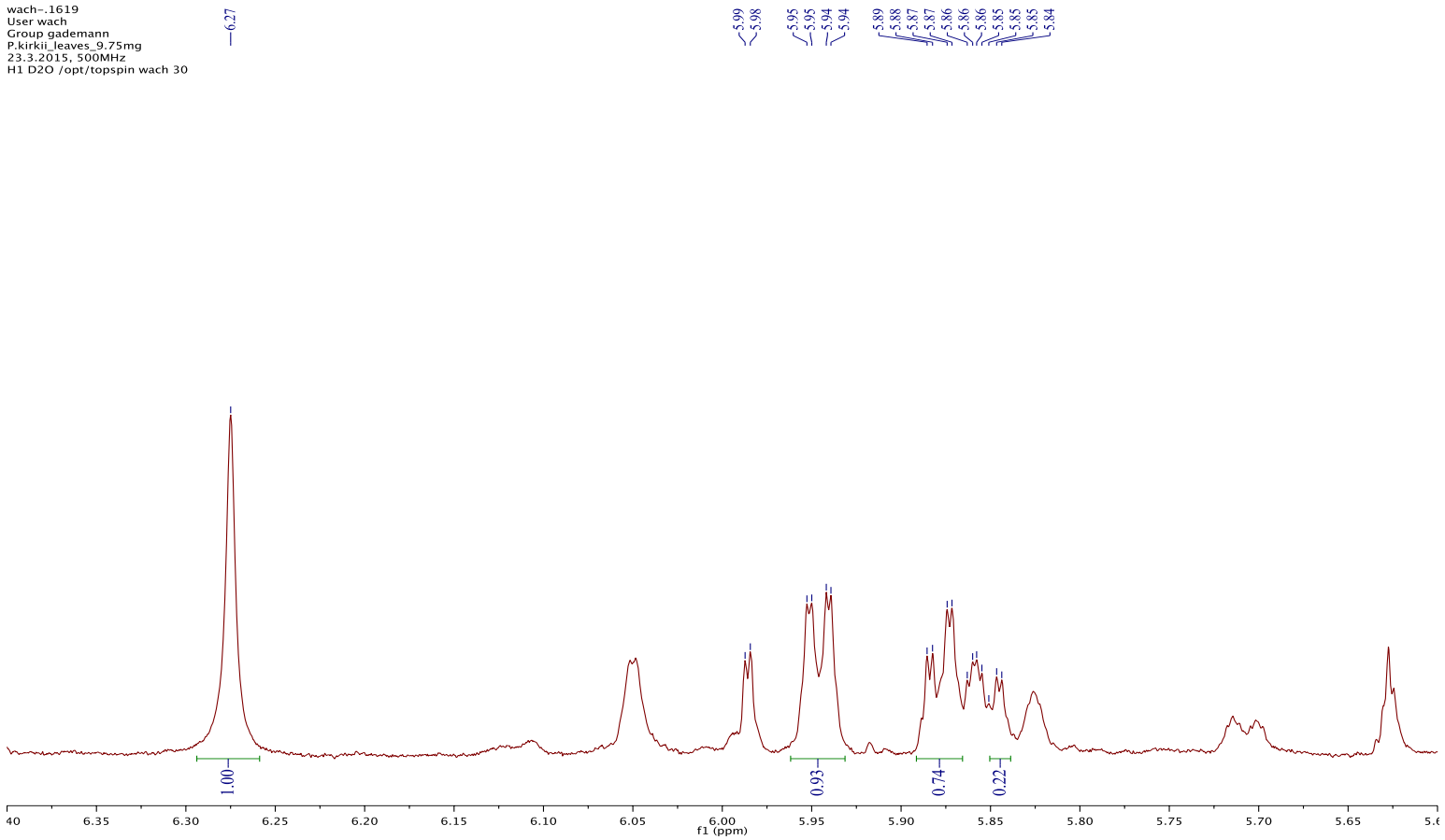

^{1}H NMR Spectrum of *Psychotria kirkii* leaves mixed with kirkamide (40 µg) in D_2O (500 MHz).

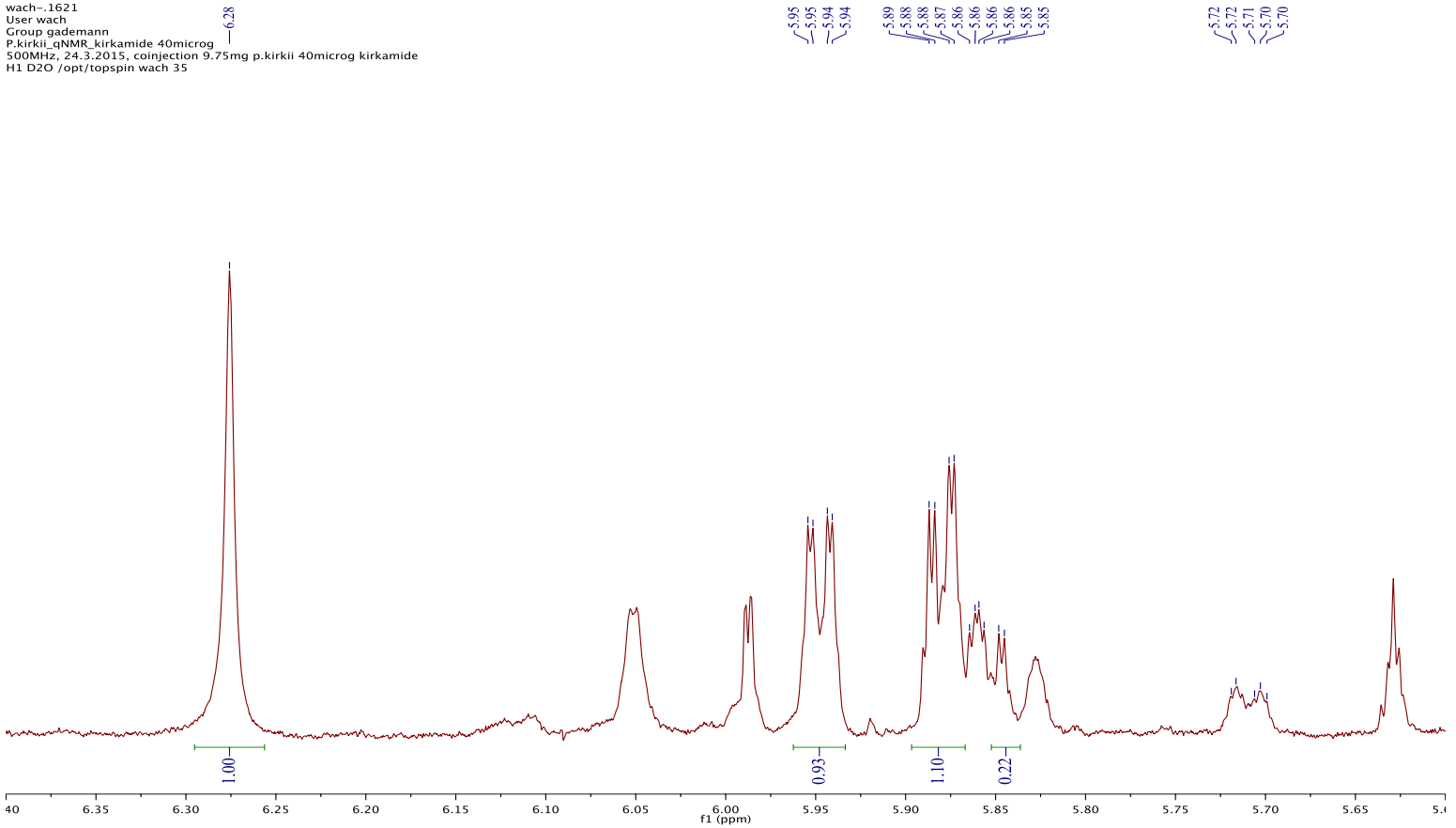

^{1}H NMR Spectrum of *Psychotria punctata* leaves in D_2O (500 MHz).

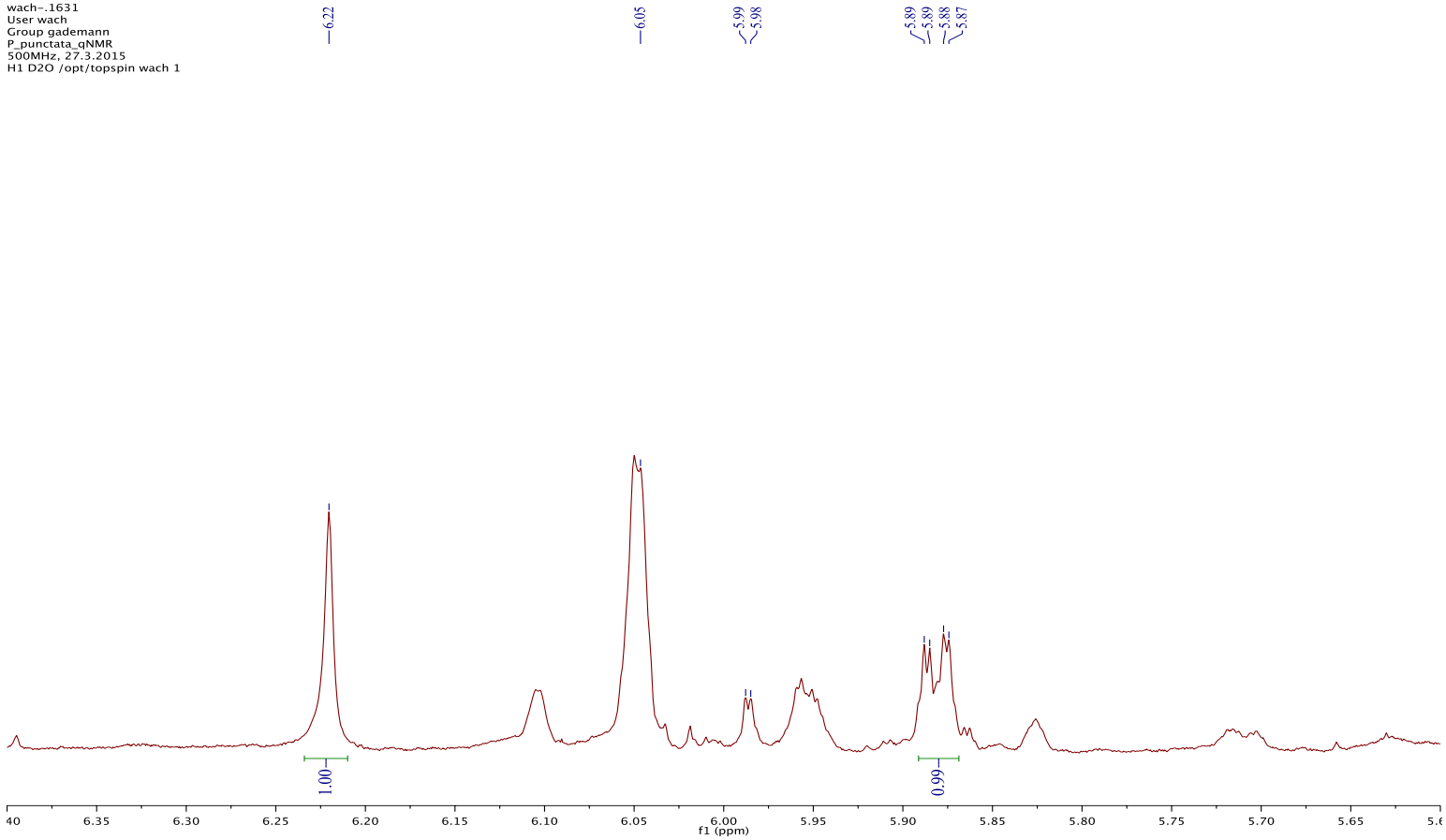

NMR Spectra of Fragin

^{1}H NMR Spectrum of fragin (**133**) in $CDCl_3$ (500 MHz).

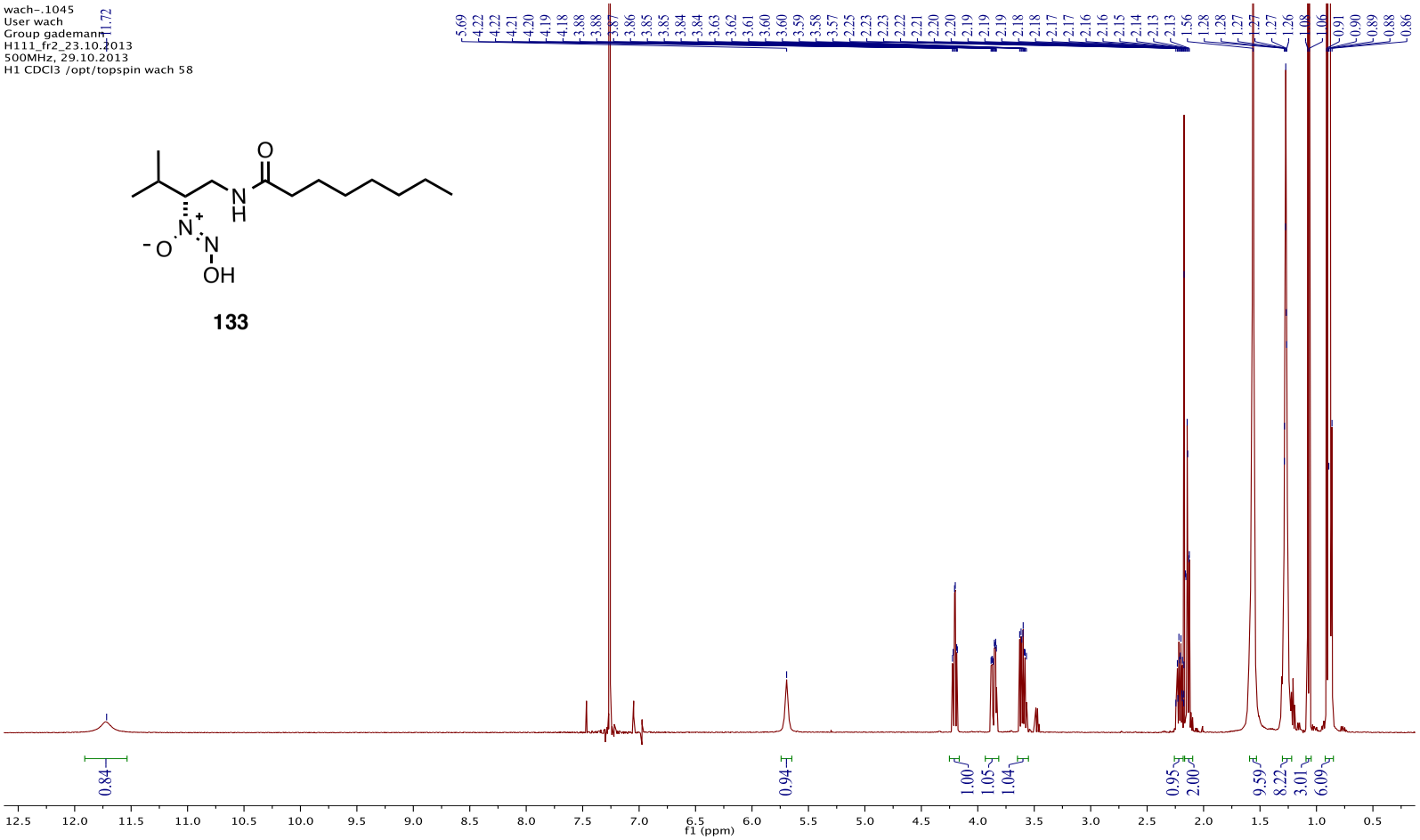

^{1}H-^{1}H COSY NMR Spectrum of fragin (**133**) in $CDCl_3$ (500 MHz).

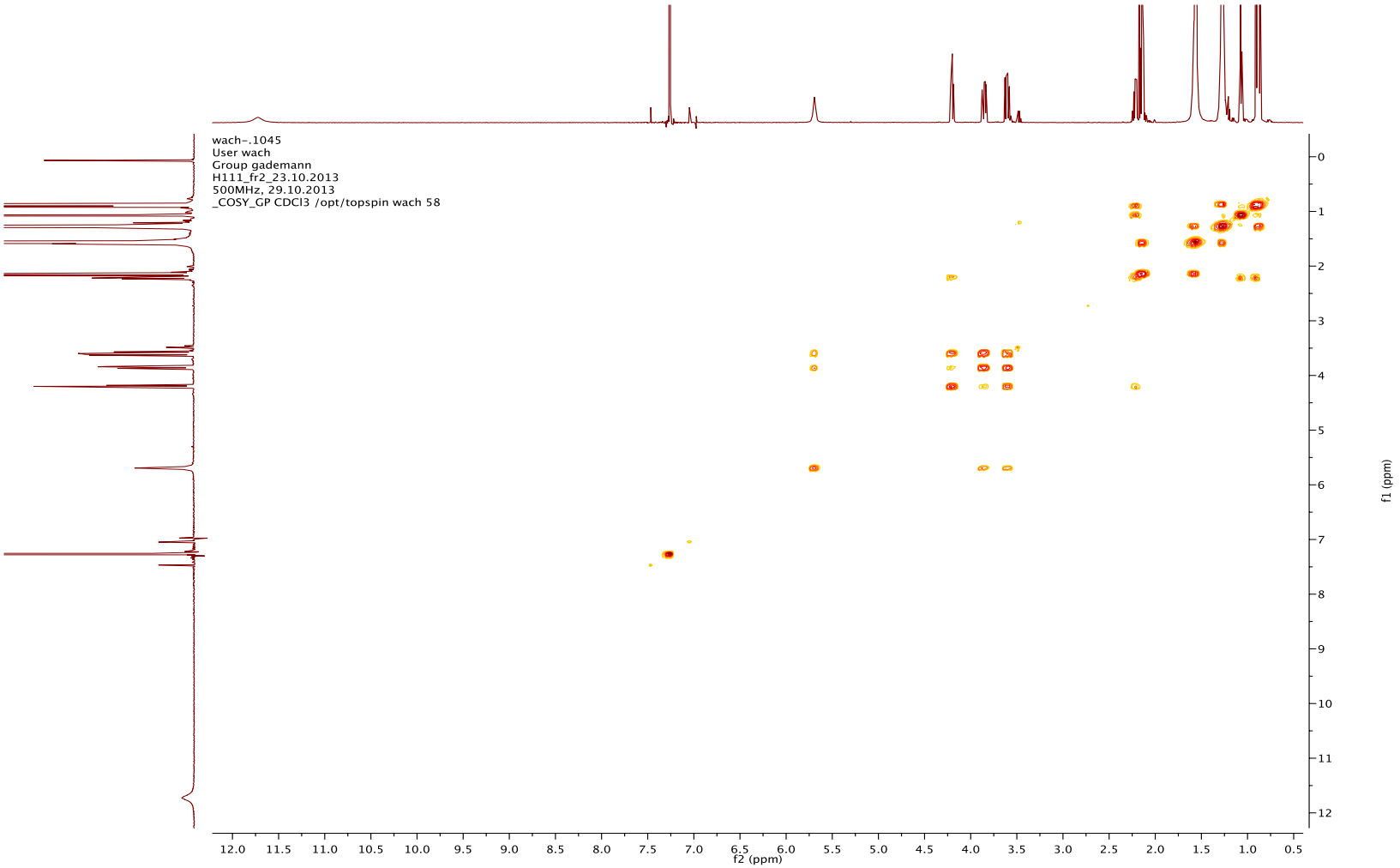

^{1}H-^{13}C HMQC NMR Spectrum of fragin (**133**) in $CDCl_3$ (500 MHz).

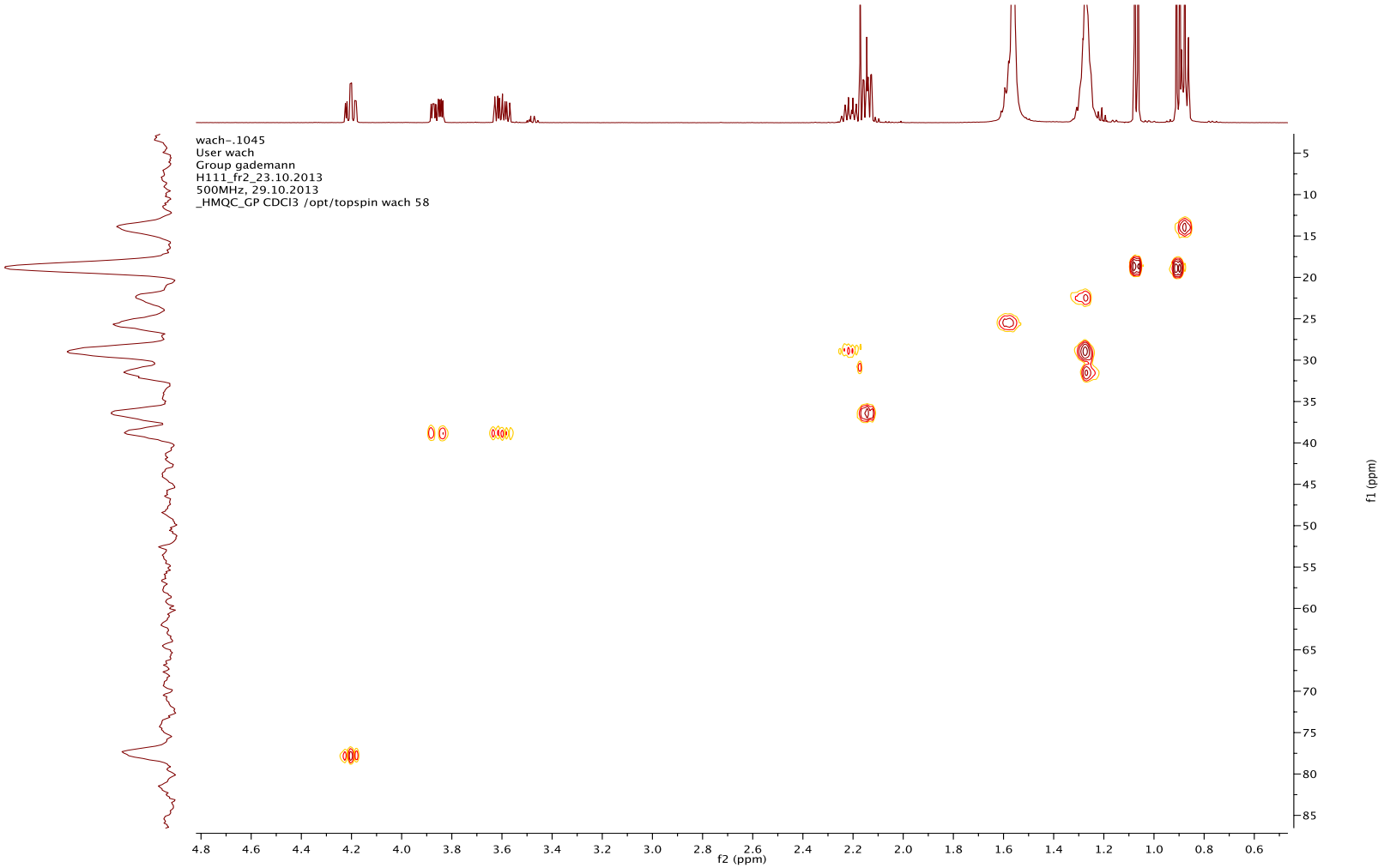

^{1}H NMR Spectra comparison between synthetic and isolated fragin (**133**) in $CDCl_3$ (500 MHz).

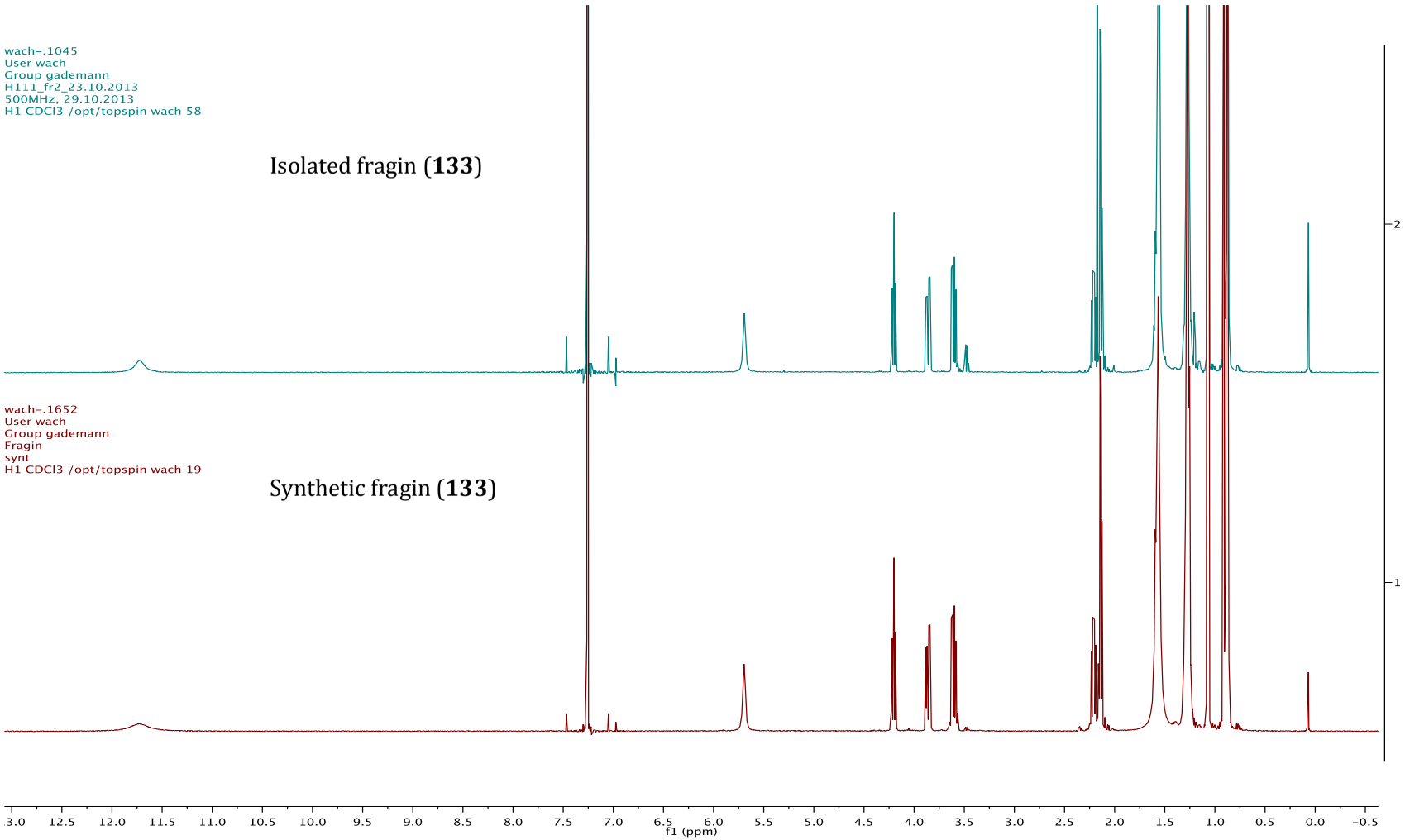

^{13}C NMR Spectrum of synthetic fragin (**133**) in $CDCl_3$ (500 MHz).

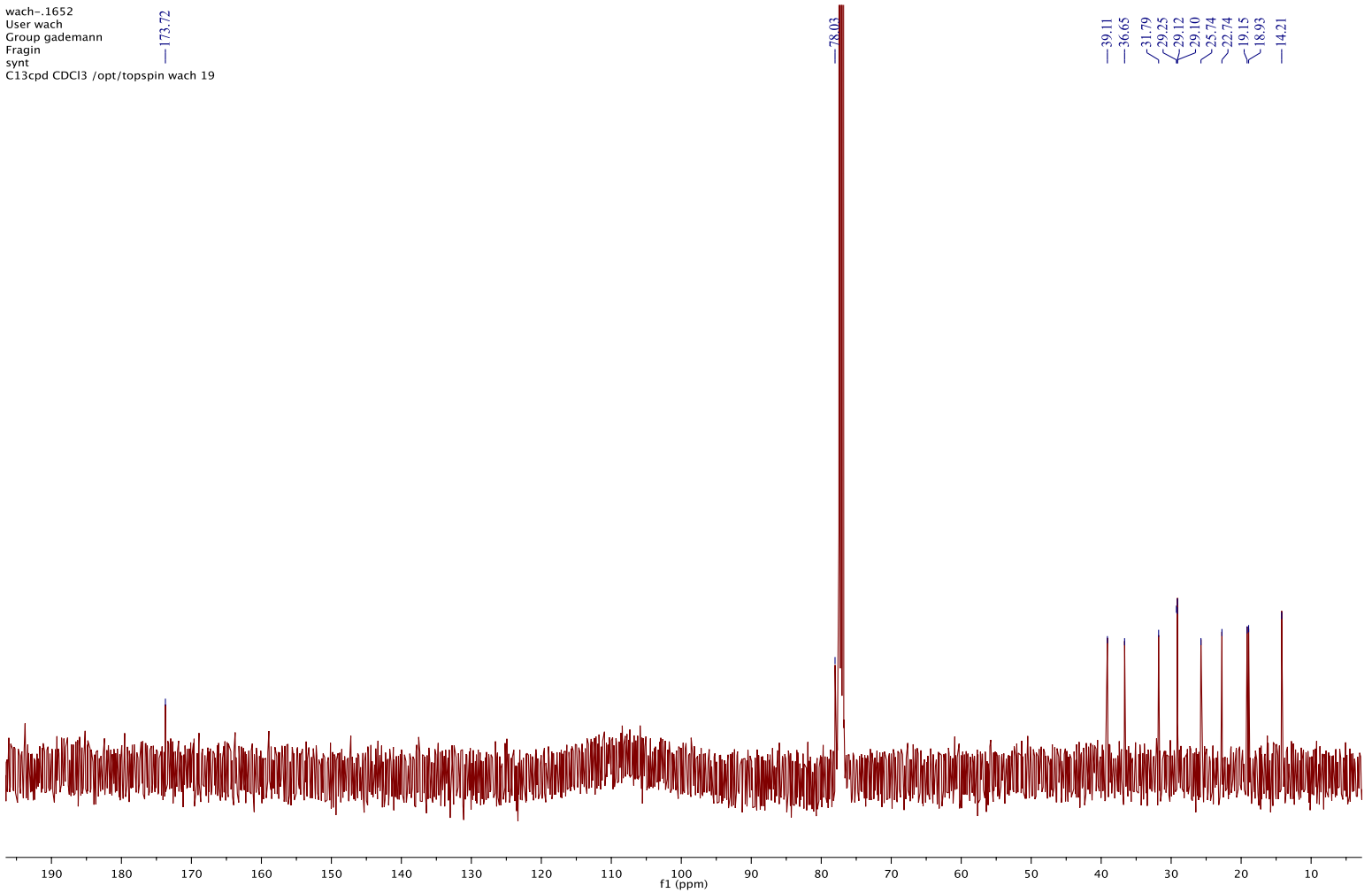

Chromatograms of the Proposed Intermediates Involved in the Biosynthetis of Fragin

Mass chromatograms of *B. cenocepacia H111* crude extract and amine **143** extract at 229 Da.

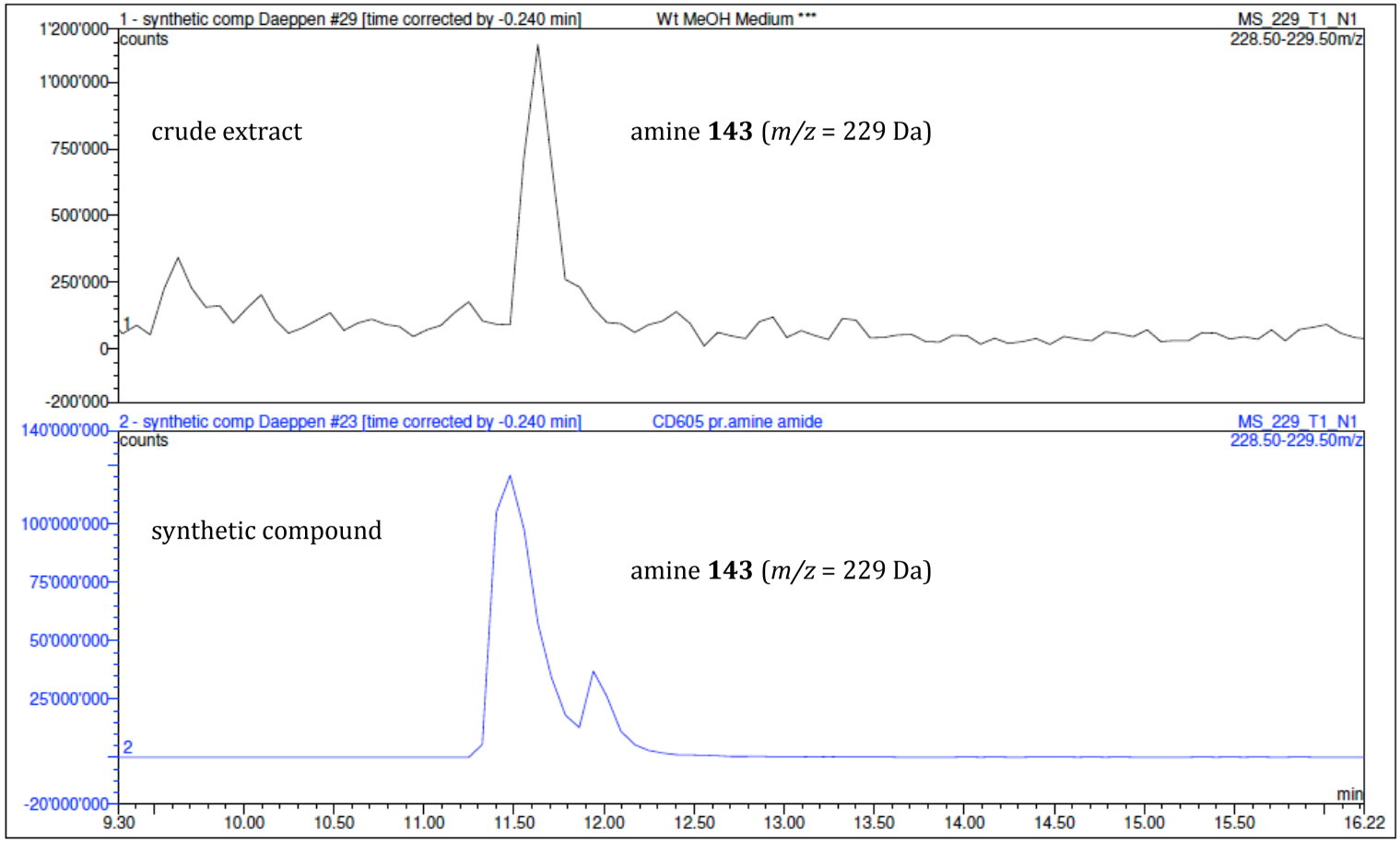

Mass chromatograms of *B. cenocepacia H111* crude extract and hydroxylamine **144** extract at 245 Da.

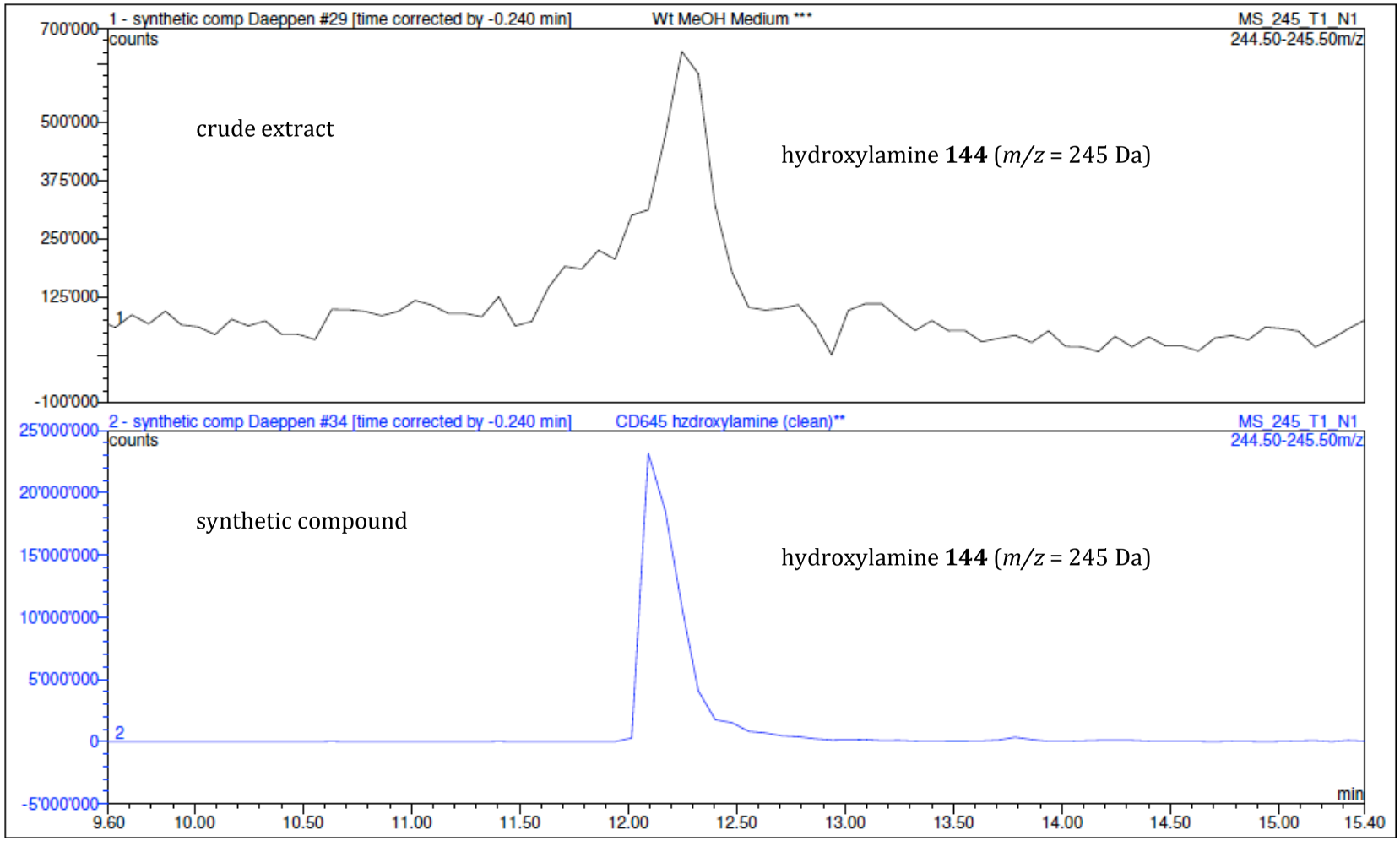

Mass chromatograms of *B. cenocepacia H111* crude extract, oxime **145** and nitroso **146** extract at 243 Da.

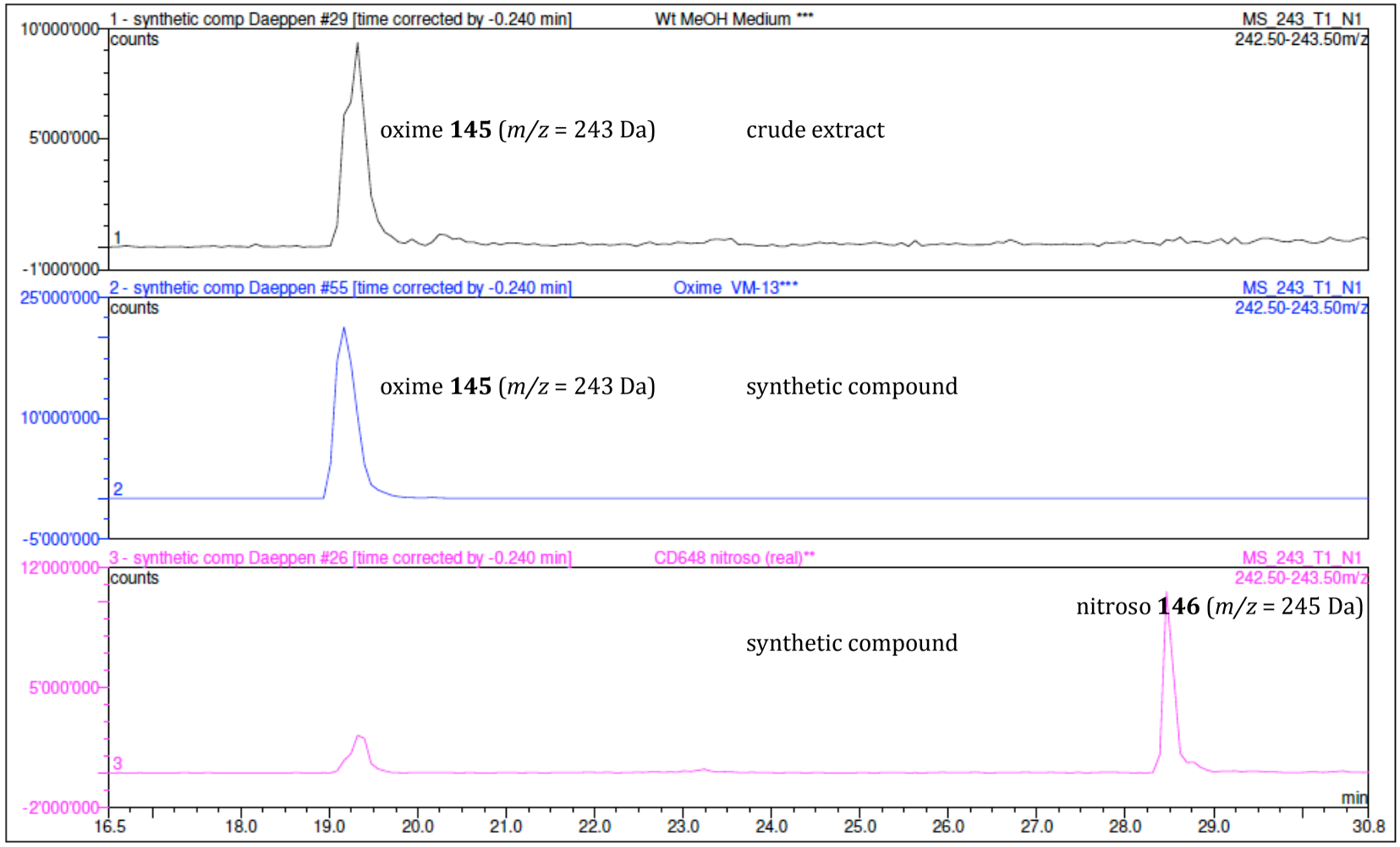

HPLC and Mass Chromatograms of the Hydroxylamine 144 in Various Conditions

Mass chromatograms of the reaction between **144** and various salts (from top to bottom: NH_4CO_2H, NH_4OAc, $NaNO_3$, $NaNO_2$, NH_4NO_3 and without).

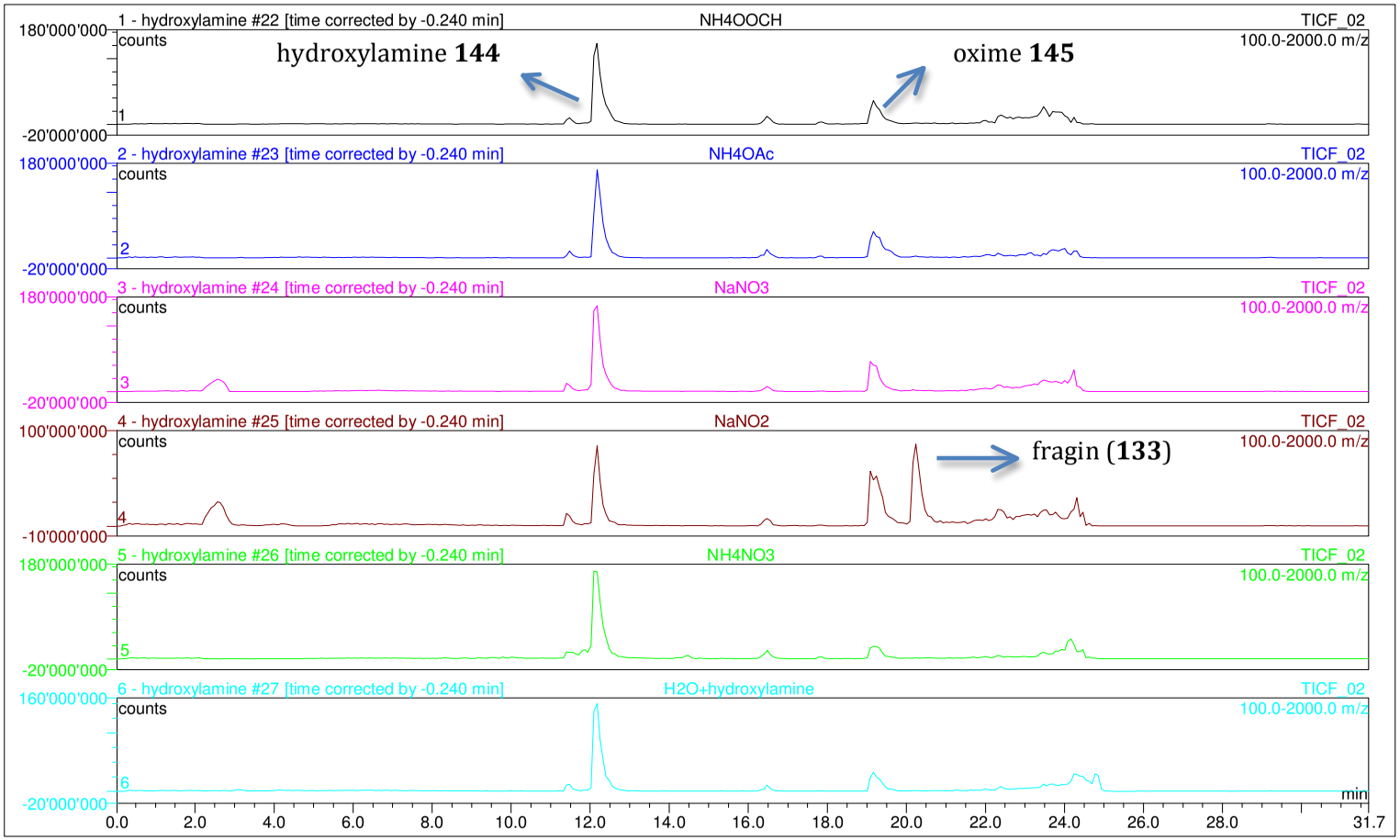

HPLC and mass chromatograms extracted at 229, 243, 245 and 300 Da of reaction between the hydroxylamine **144** and $NaNO_2$.

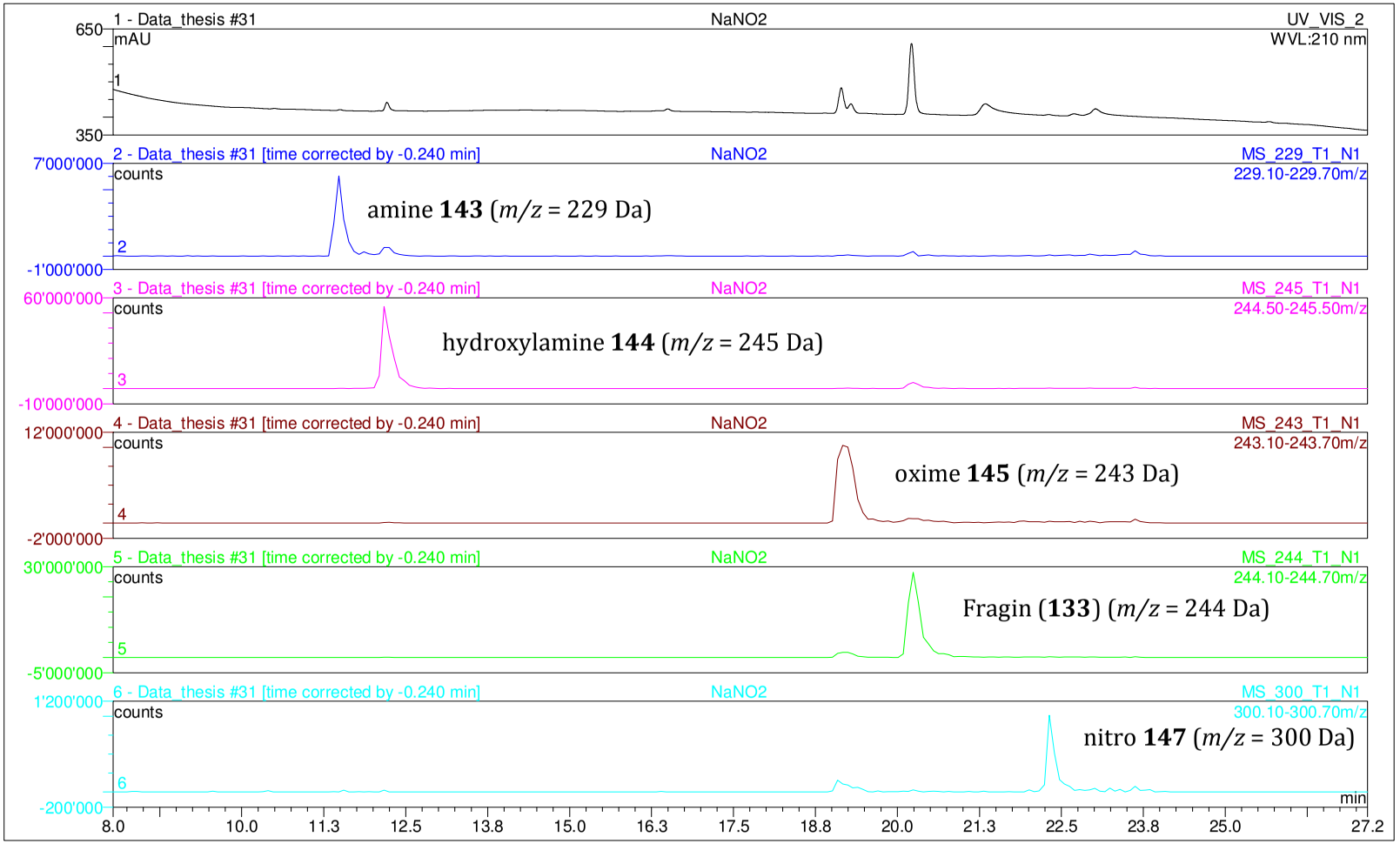

Comparison of HPLC chromatograms of the hydroxylamine **144** with $NaNO_2$ without buffer and with buffer at pH = 6.5 and 7.85.

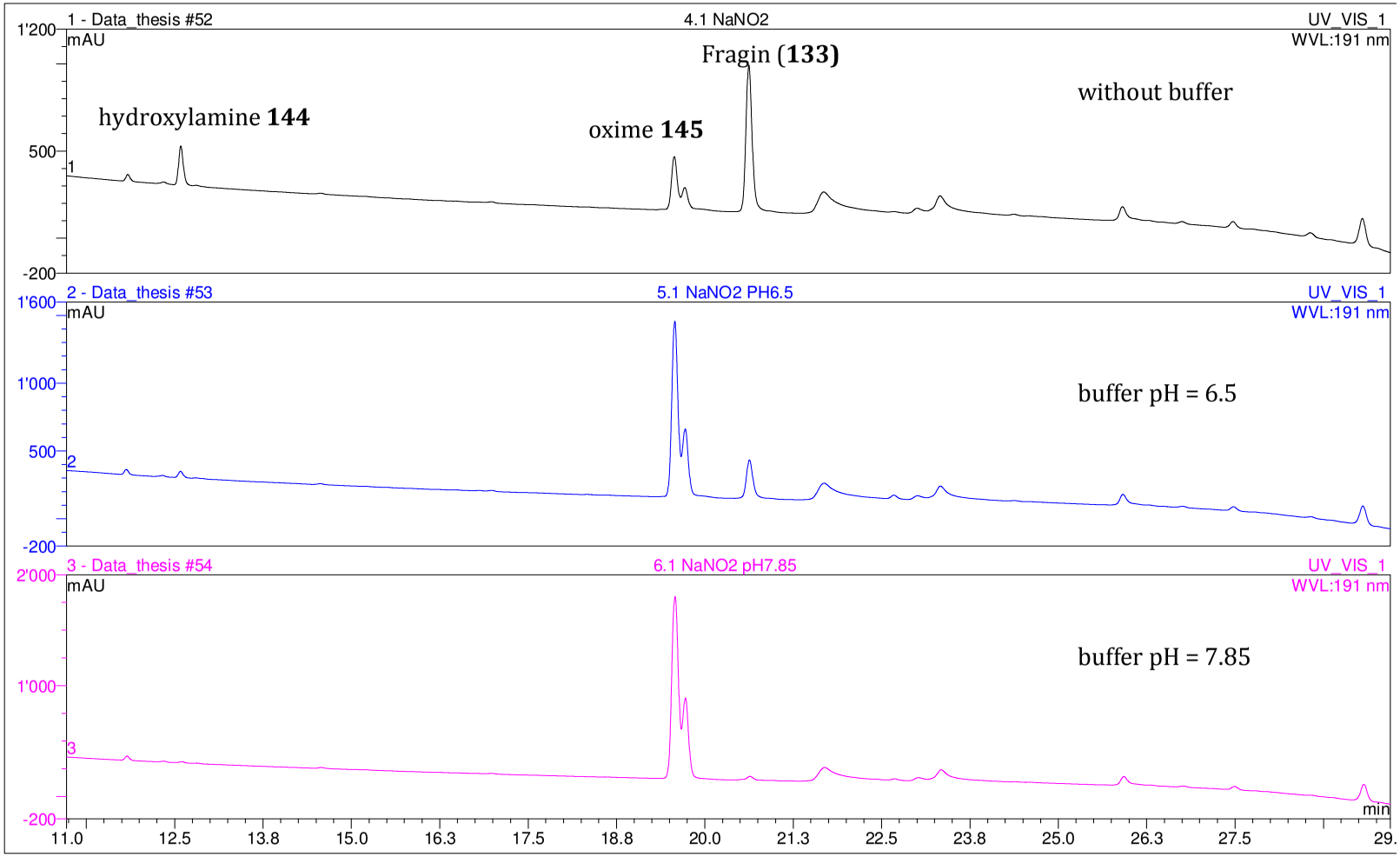

HPLC and mass chromatograms extracted at 229, 243, 245 and 300 Da of the reaction between hydroxylamine **144** and $NaNO_2$ with Buffer at pH = 6.5.

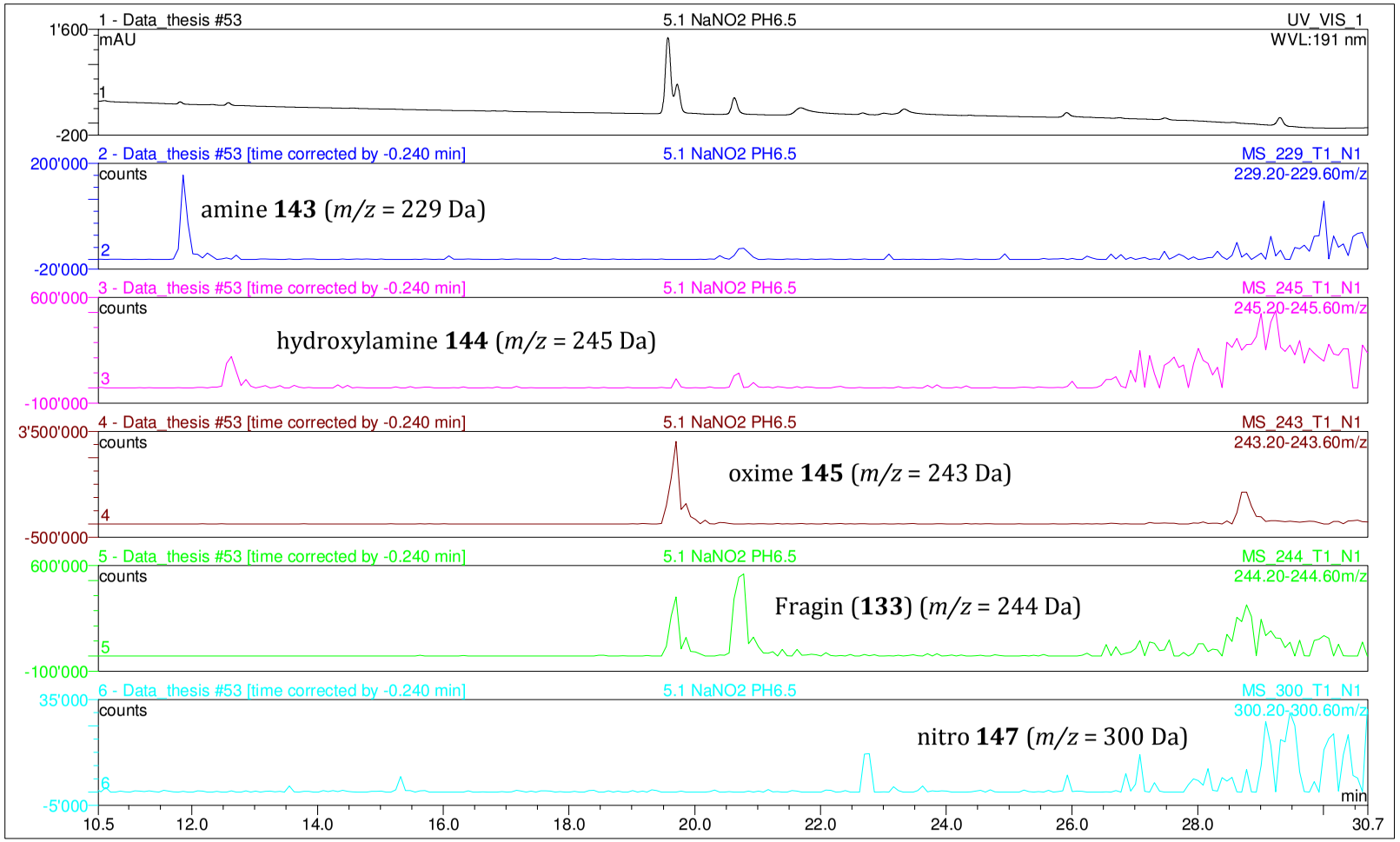

HPLC and mass chromatograms extracted at 229, 243, 245 and 300 Da of the reaction between hydroxylamine **144** and $NaNO_2$ with Buffer at pH = 7.85.

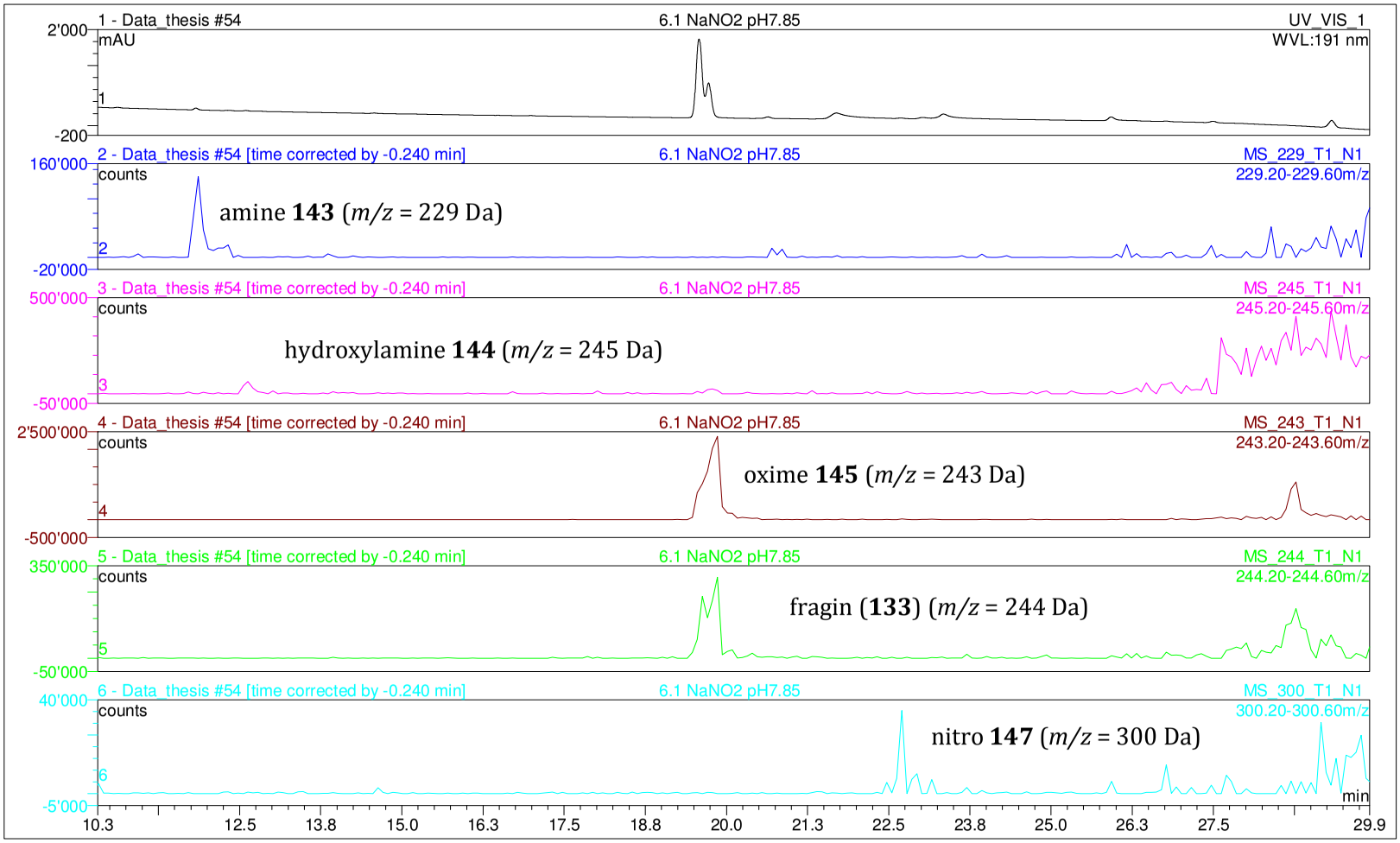

Comparison of HPLC chromatograms of hydroxylamine **144** with $NaN^{15}O_2$ at three different reaction times.

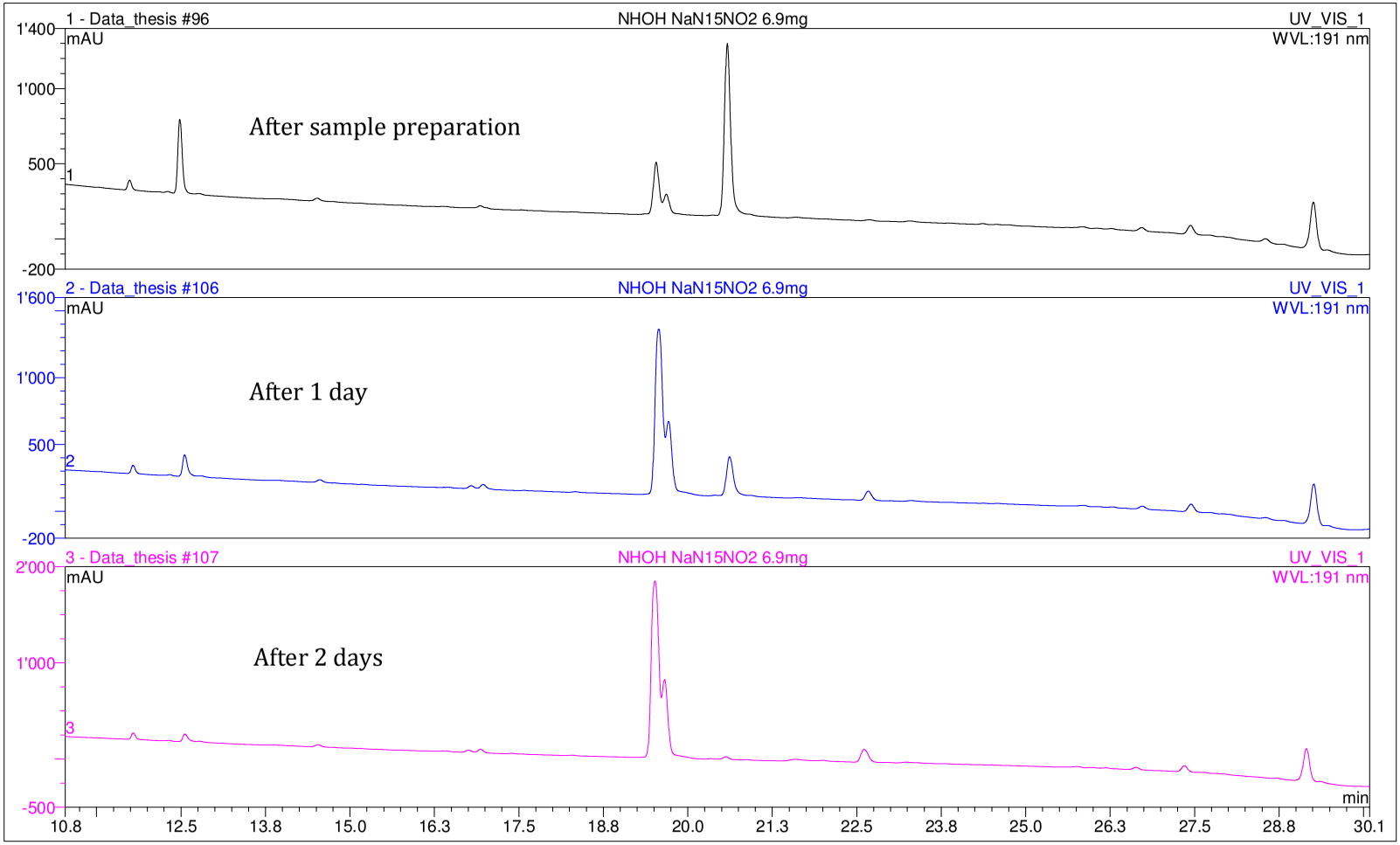

Mass chromatograms extracted at 229 Da of the reaction between the hydroxylamine **144** and $NaN^{15}O_2$ at three different reaction times.

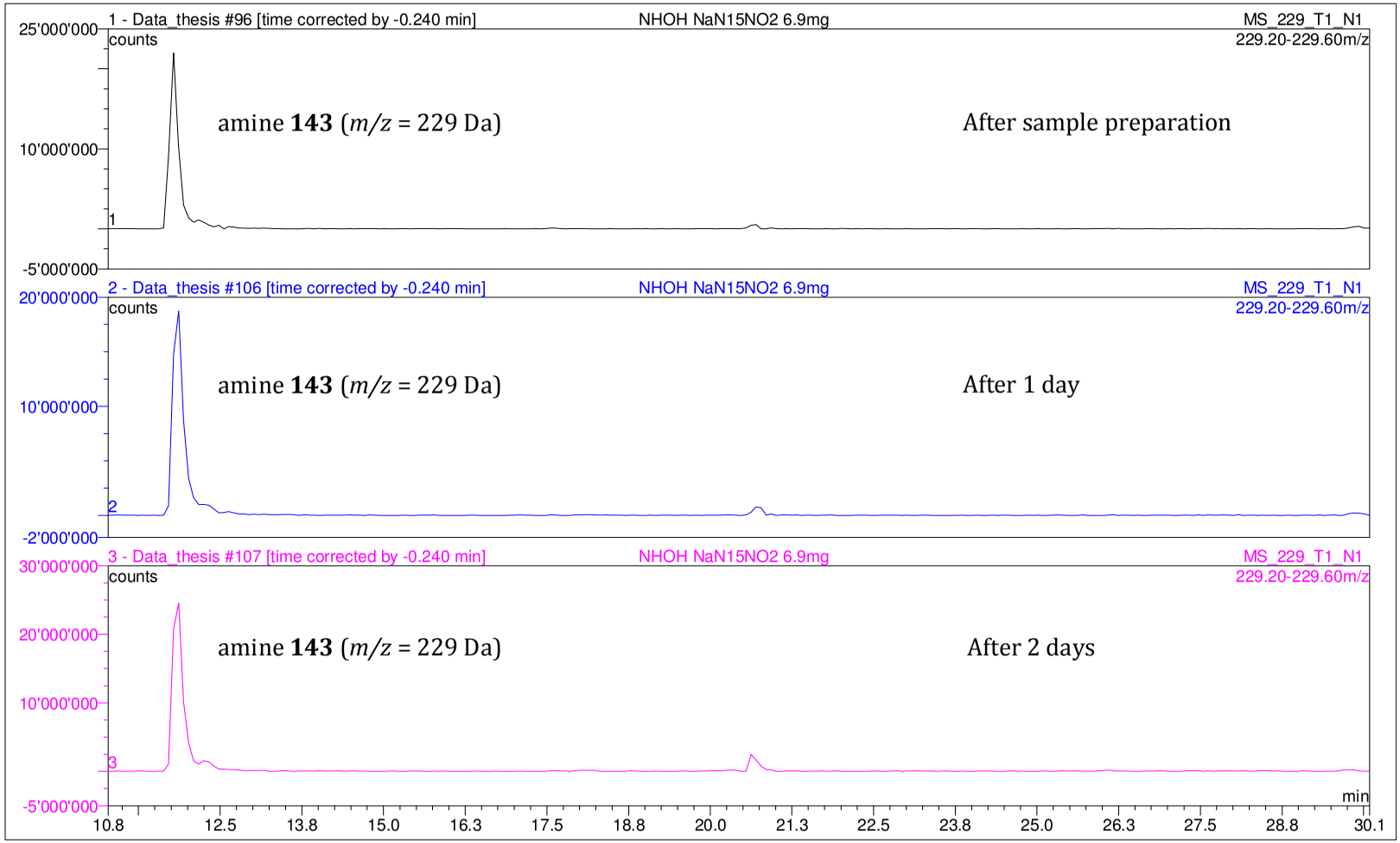

Mass chromatograms extracted at 245 Da of the reaction between the hydroxylamine **144** and $NaN^{15}O_2$ at three different reaction times.

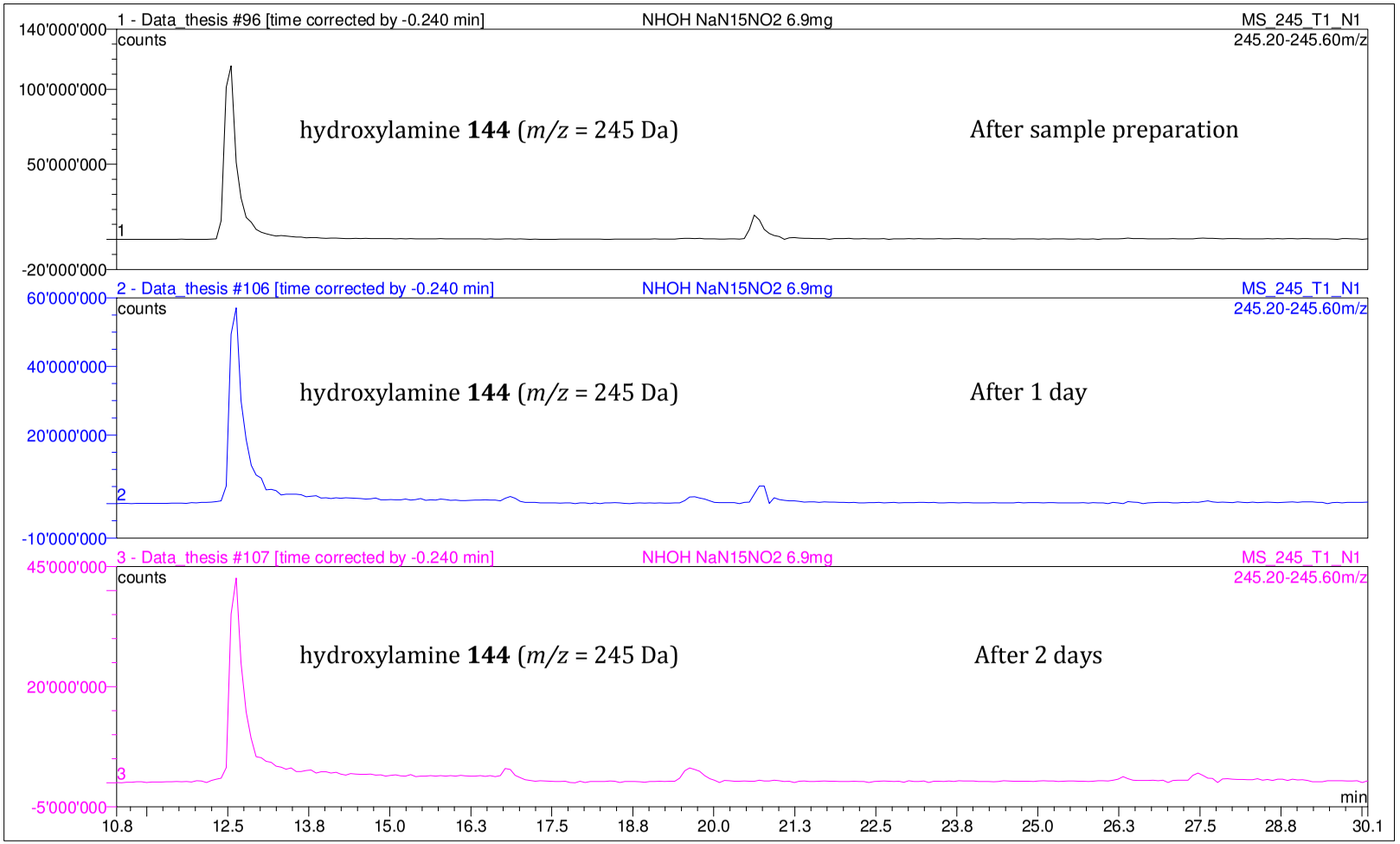

Mass chromatograms extracted at 243 Da of the reaction between the hydroxylamine **144** and $NaN^{15}O_2$ at three different reaction times.

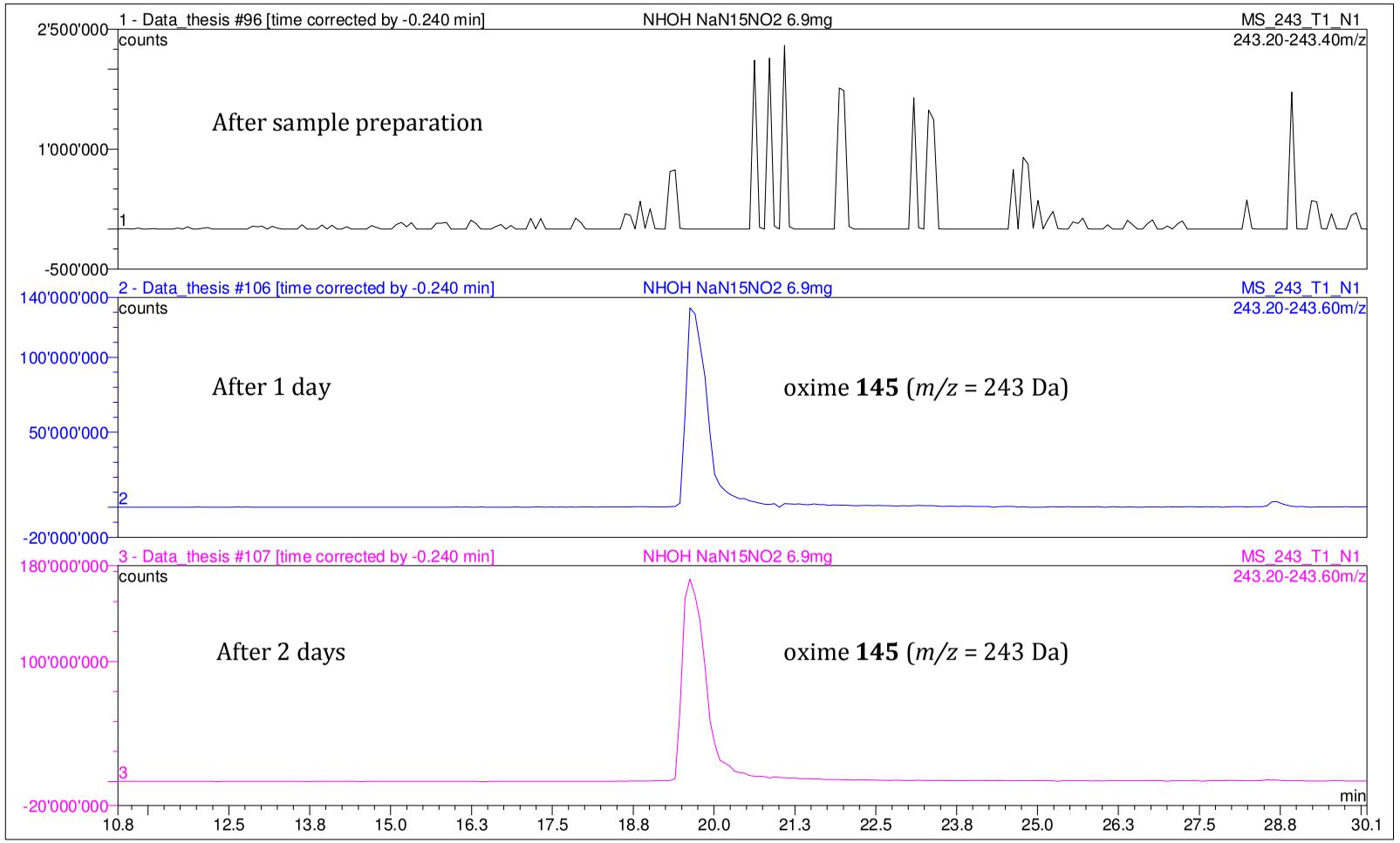

Mass chromatograms extracted at 275 Da of the reaction between the hydroxylamine **144** and $NaN^{15}O_2$ at three different reaction times.

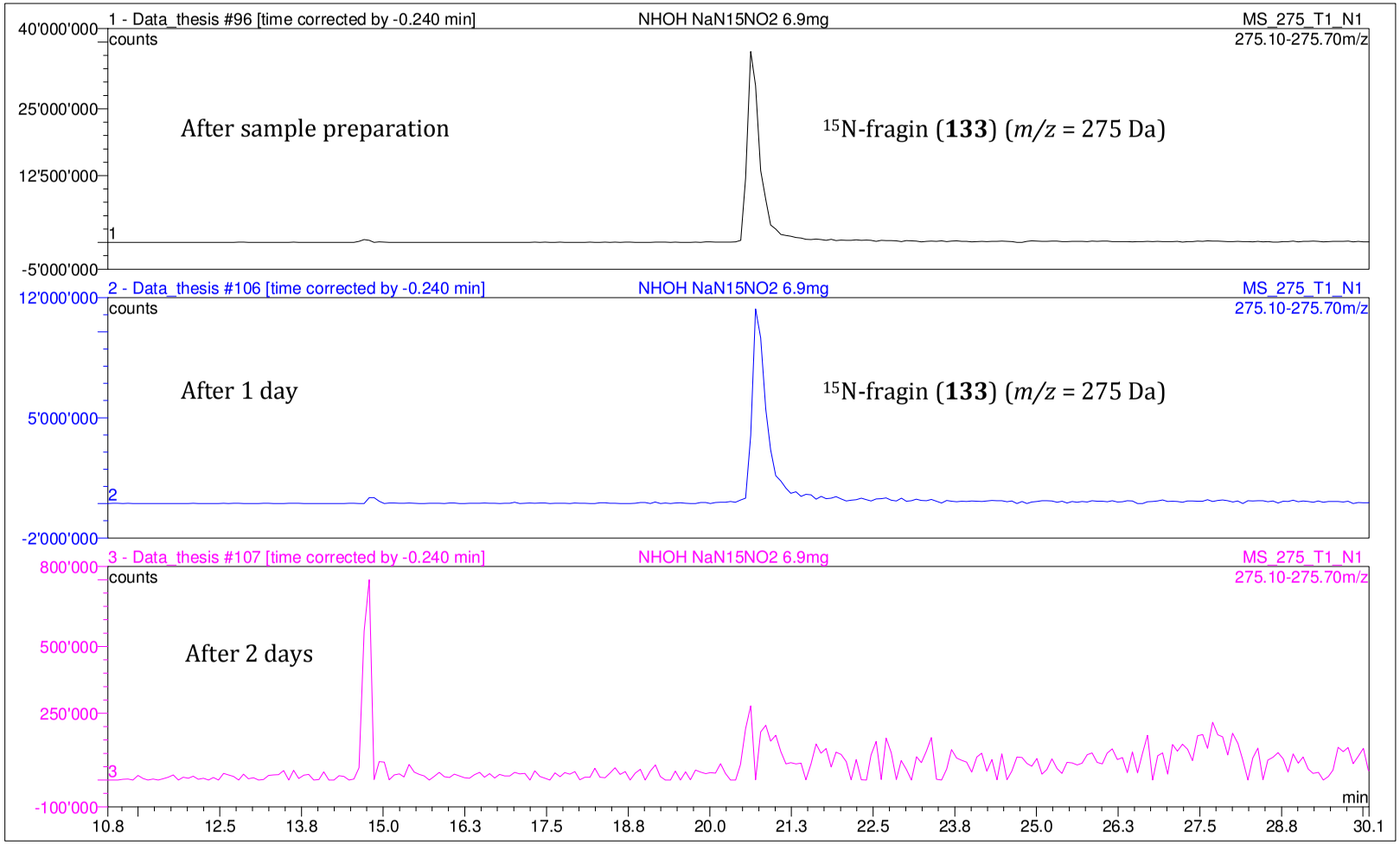

Mass chromatograms extracted at 228 Da of the reaction between the hydroxylamine **144** and $NaN^{15}O_2$ at three different reaction times.

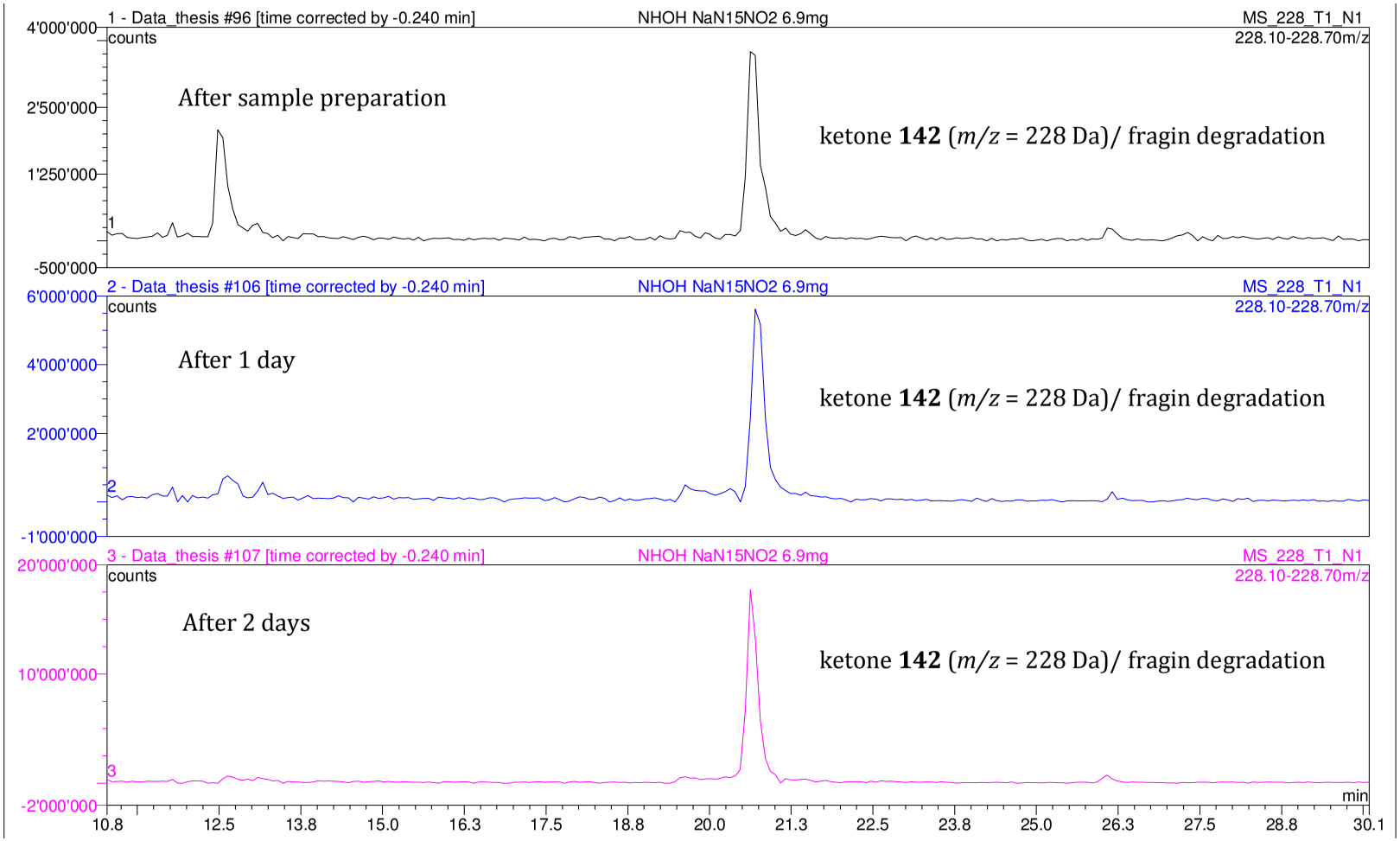

Mass chromatograms extracted at 300 Da of the reaction between the hydroxylamine **144** and $NaN^{15}O_2$ at three different reaction times.

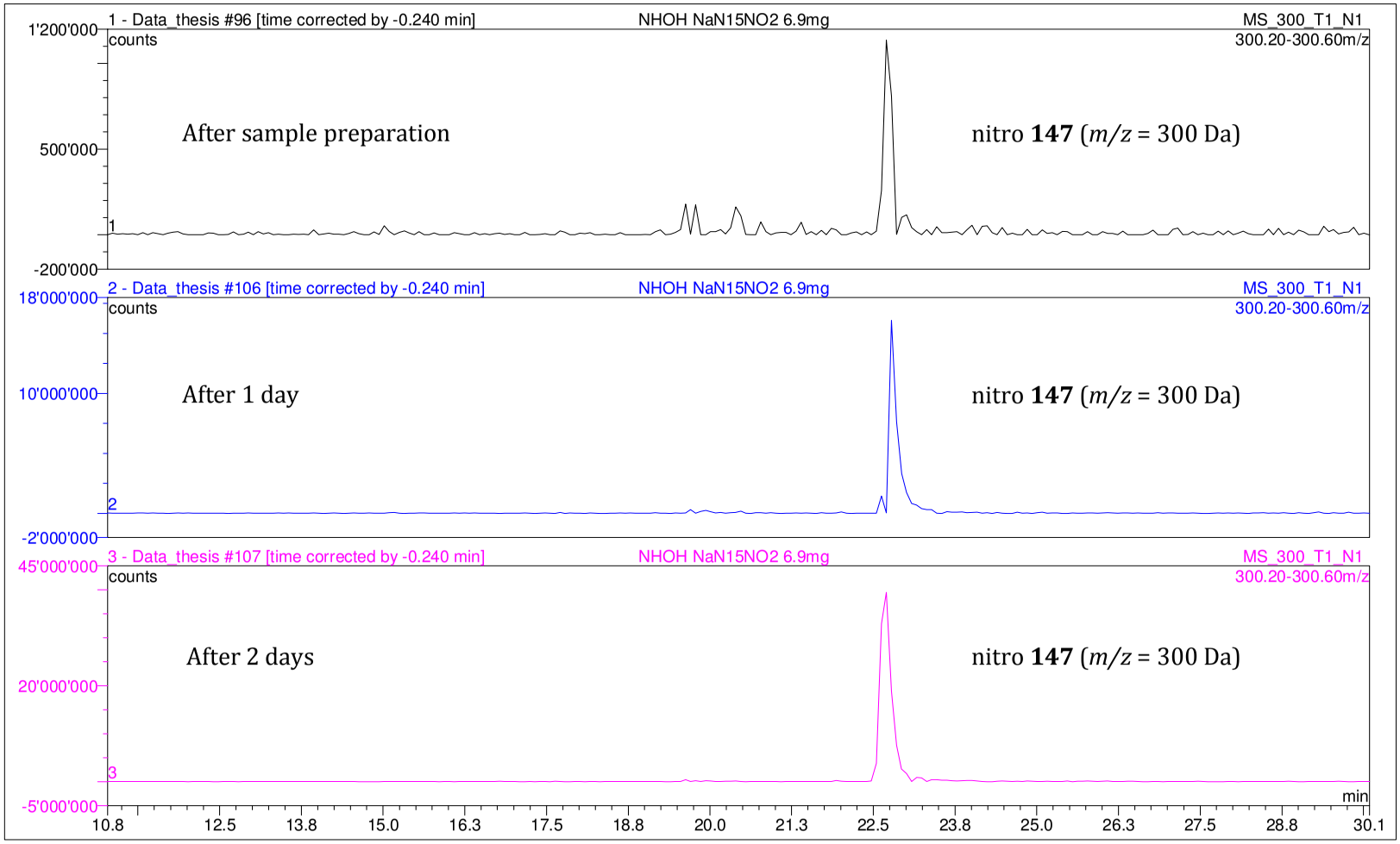

Mass chromatograms and NMR Spectra of the Project on Glycolipopetides

HRMS^2 spectrum of the pseudomolecular ion $[M+2H]^{2+}$ with a *m/z* of 817.90078 Da corresponding to GPLC-1 (**182**).

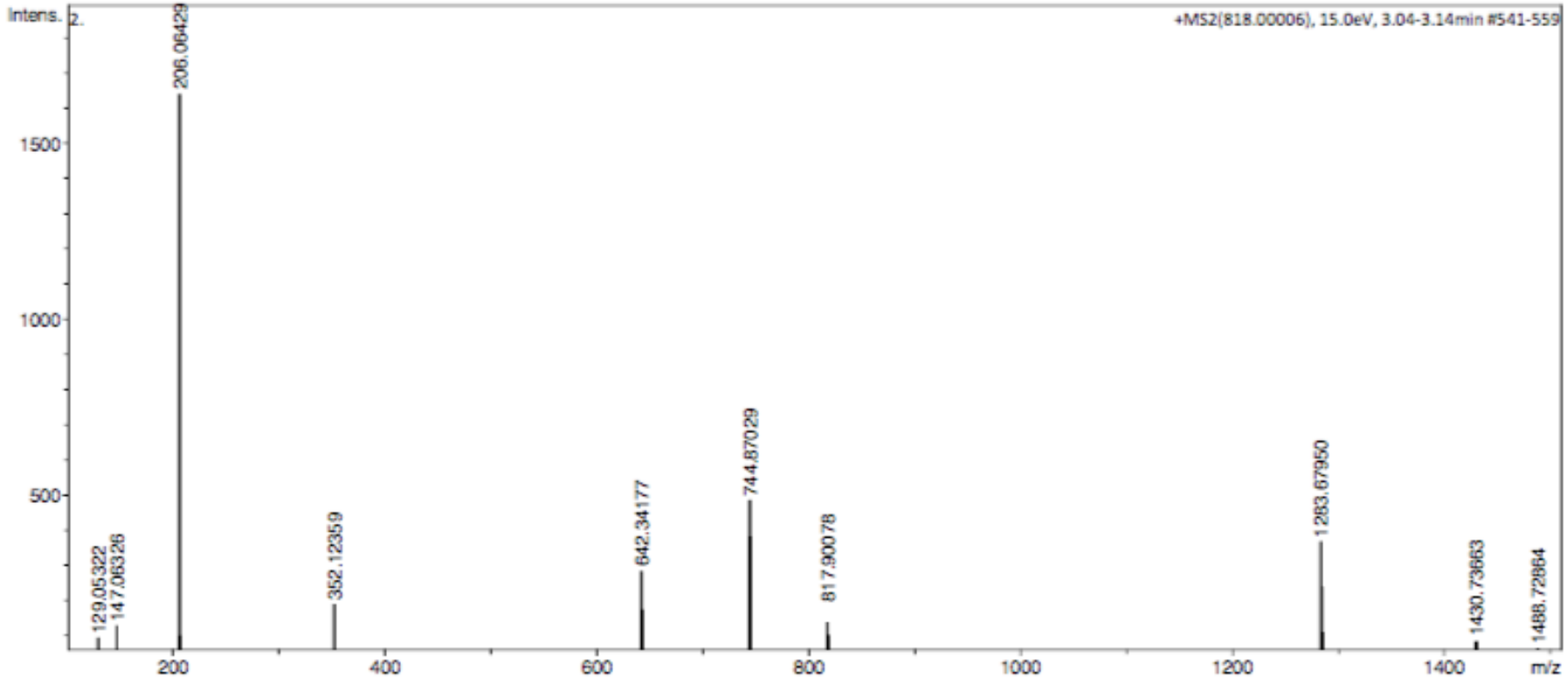

HRMS^2 spectrum of the pseudomolecular ion $[M+2H]^{2+}$ with a *m/z* of 839.40274 Da corresponding to GPLC-2 (**183**).

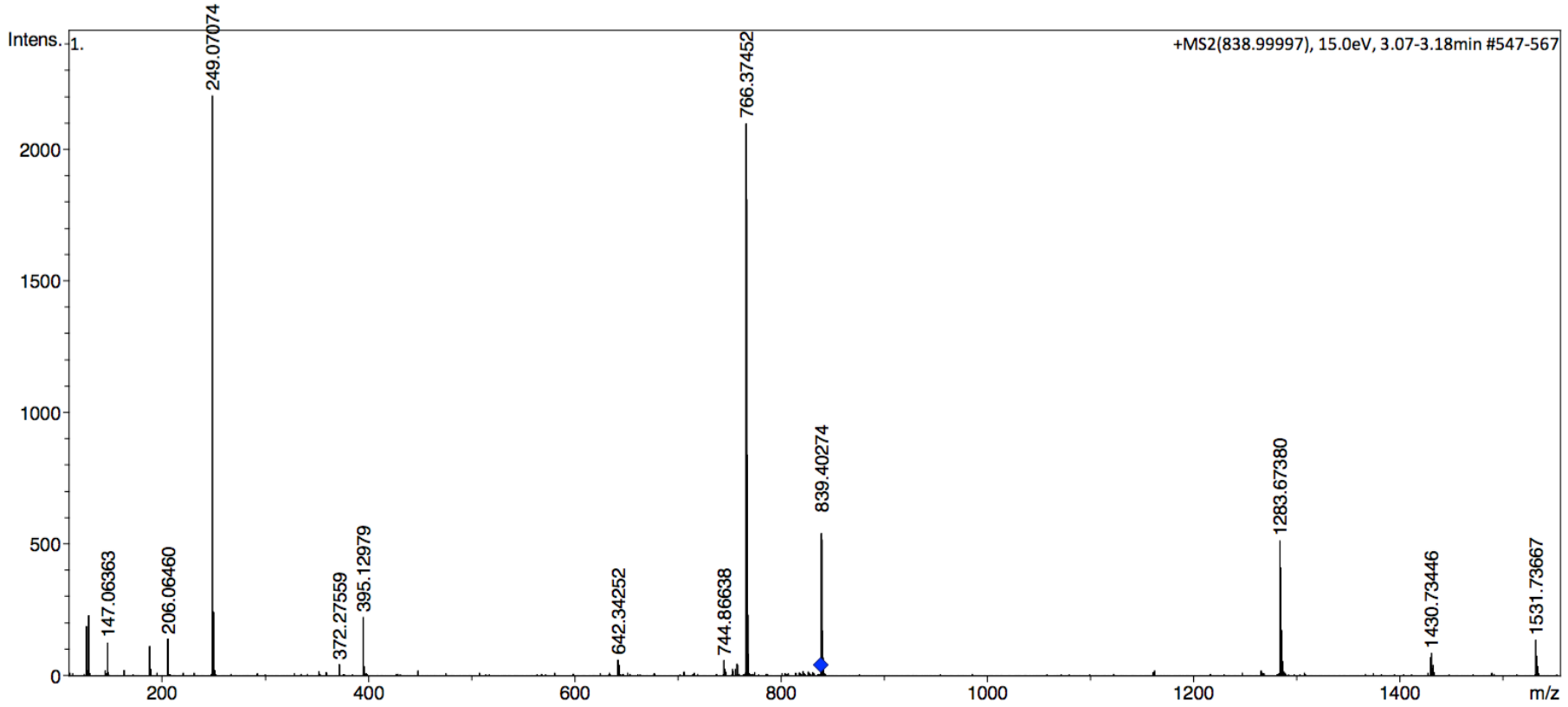

^{1}H-NMR Spectrum of GPLC-2 (**183**) with the lactone opened.

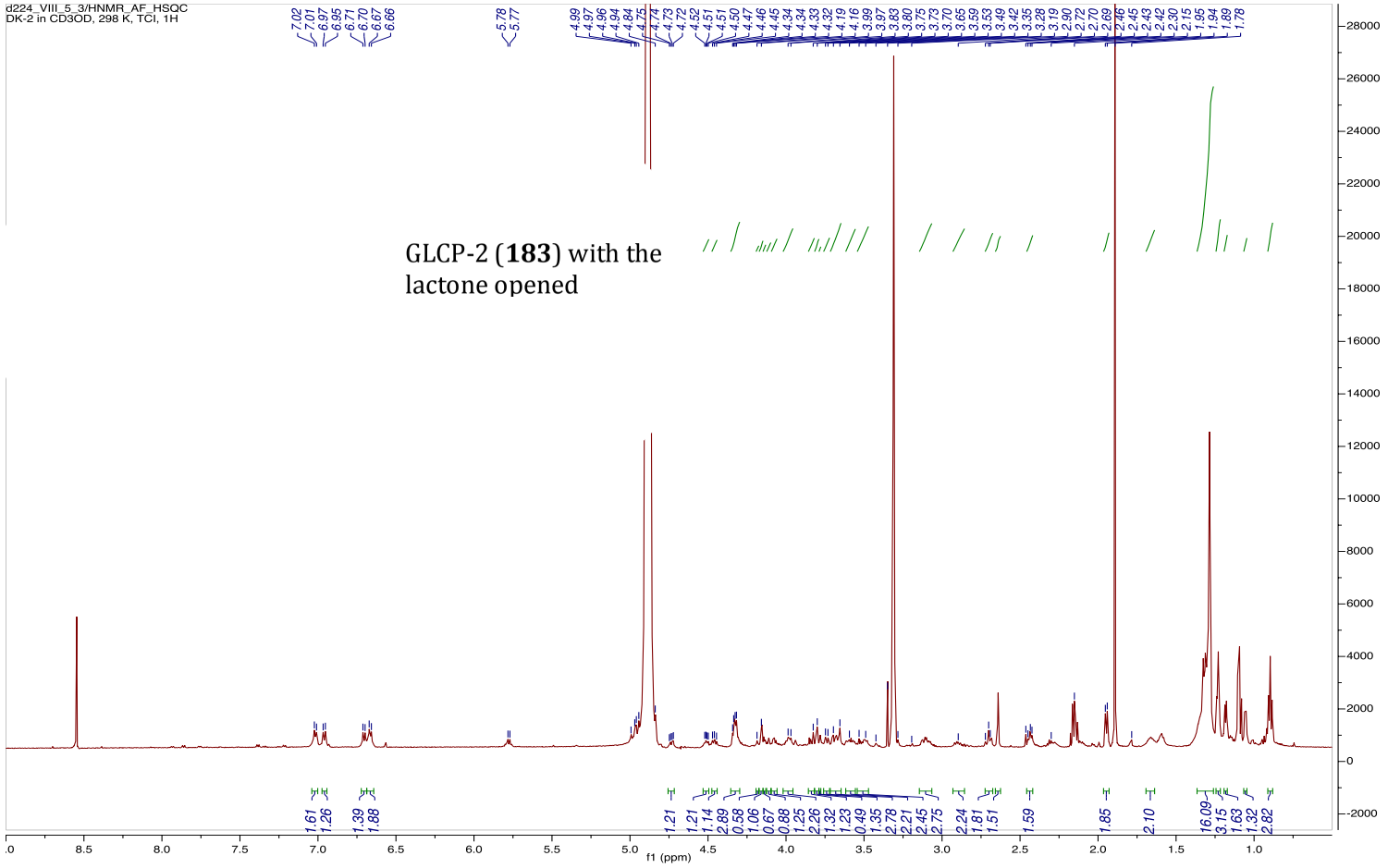

HSQC Spectrum of GPLC-2 (**183**) with the lactone opened.

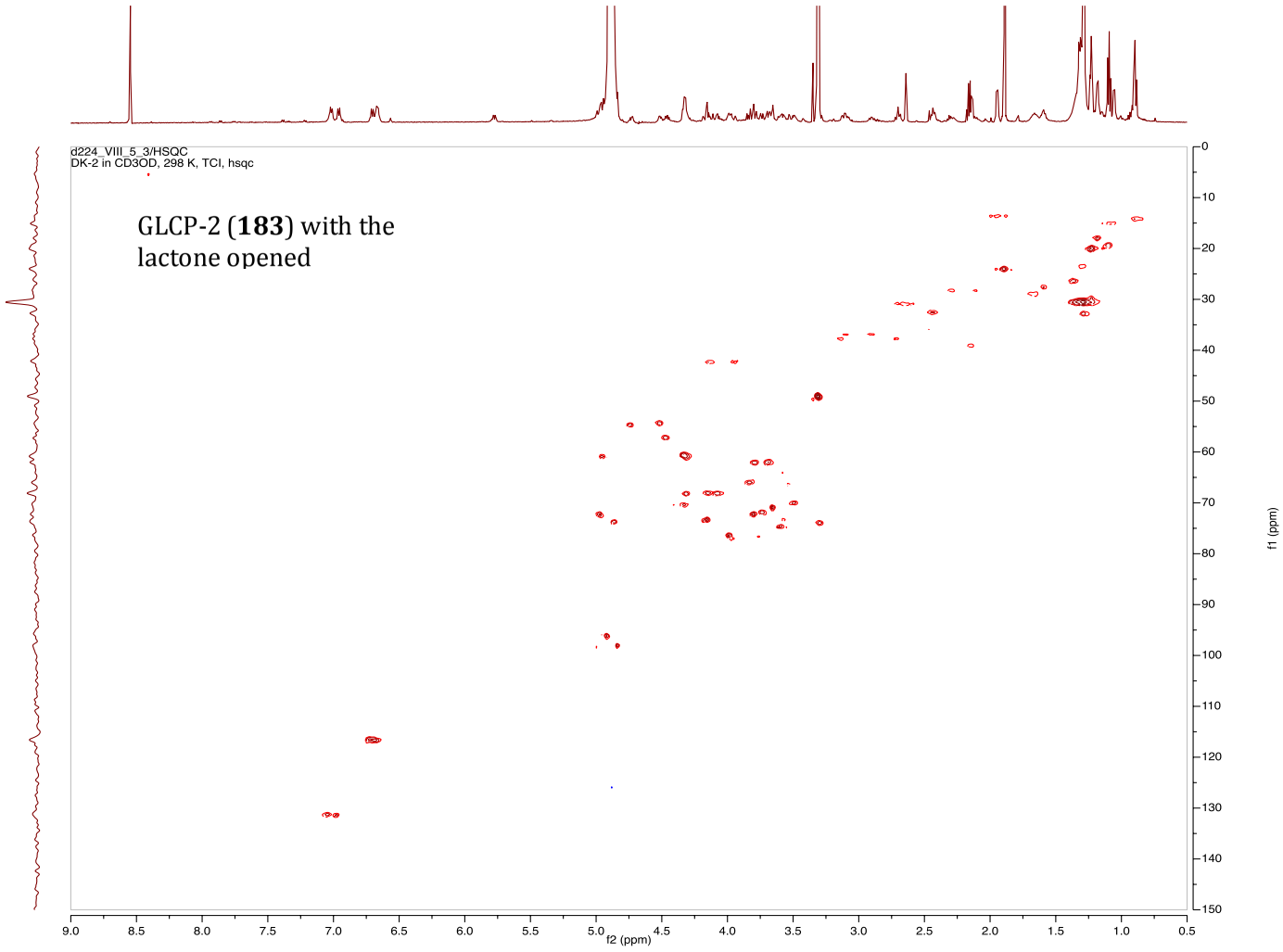

GLCP-2 (**183**), mass chromatograms monitored at *m/z* 686 for the protonated tyrosine Marfey's derivatives. **183** was hydrolyzed prior to derivatization.

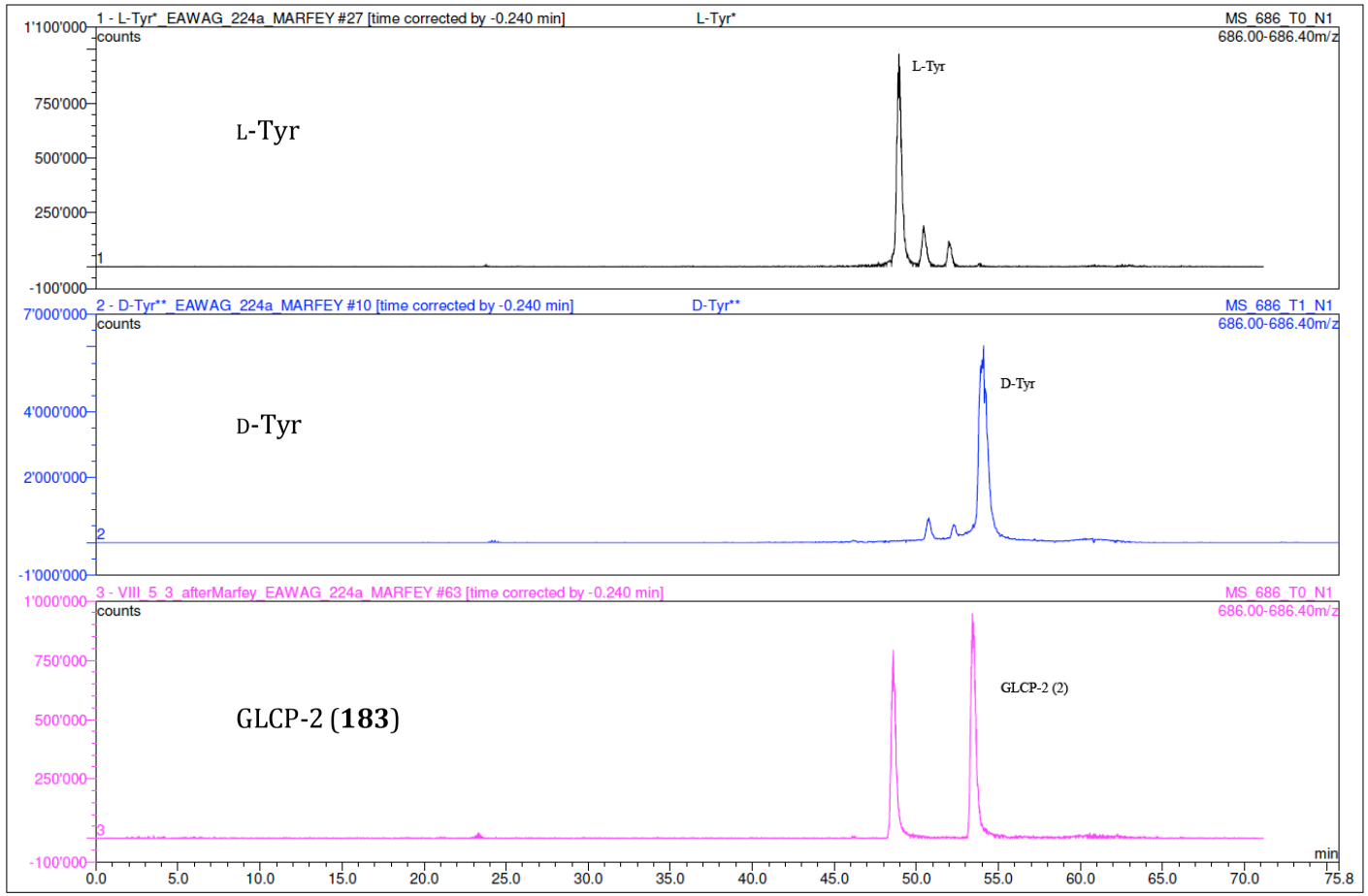

GLCP-2 (**183**), mass chromatograms monitored at *m/z* 400 for the protonated glutamine Marfey's derivatives. **183** was hydrolyzed prior to derivatization.

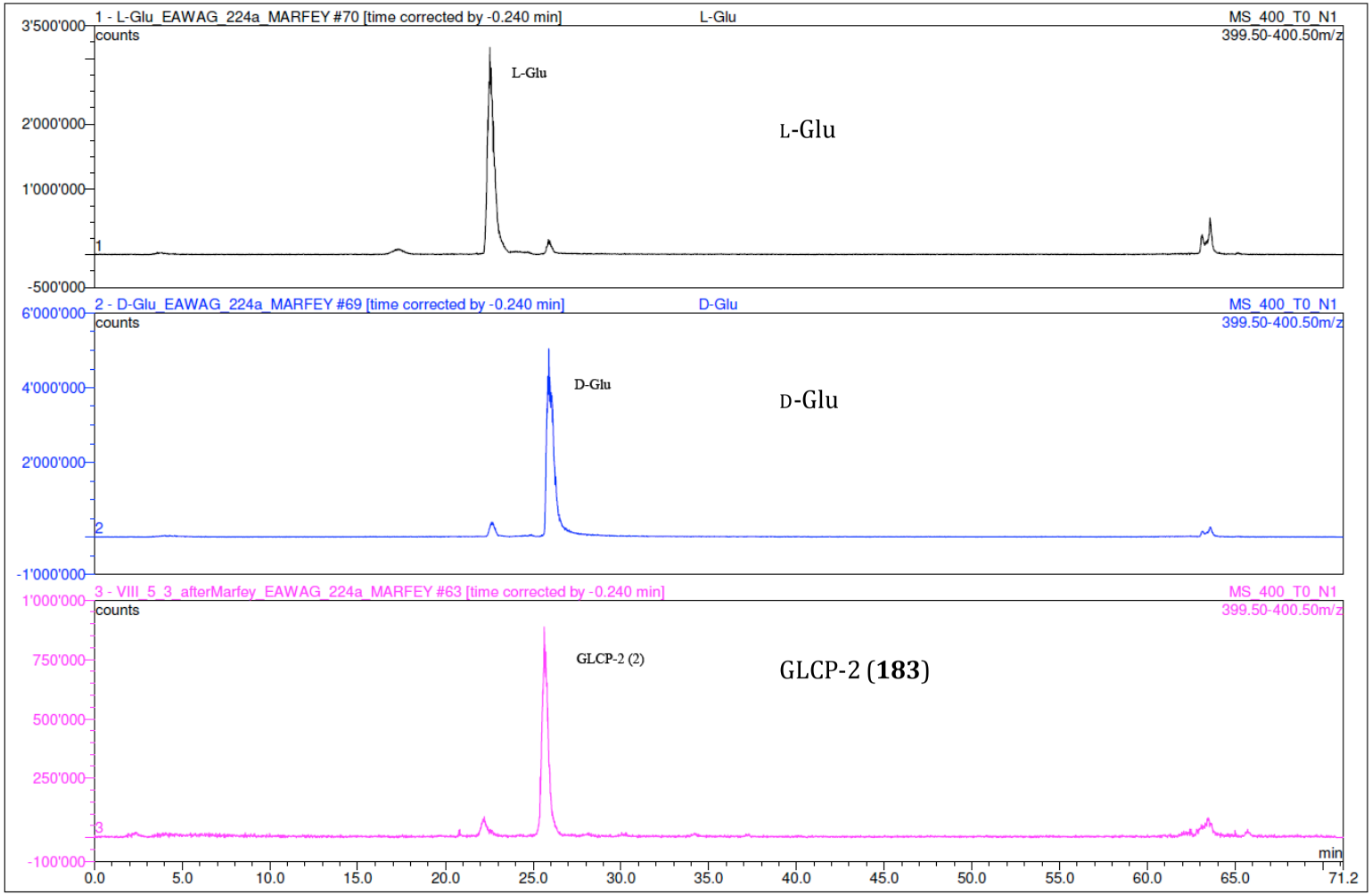

GLCP-2 (**183**), mass chromatograms monitored at *m/z* 372 for the protonated threonine Marfey's derivatives. **183** was hydrolyzed prior to derivatization.

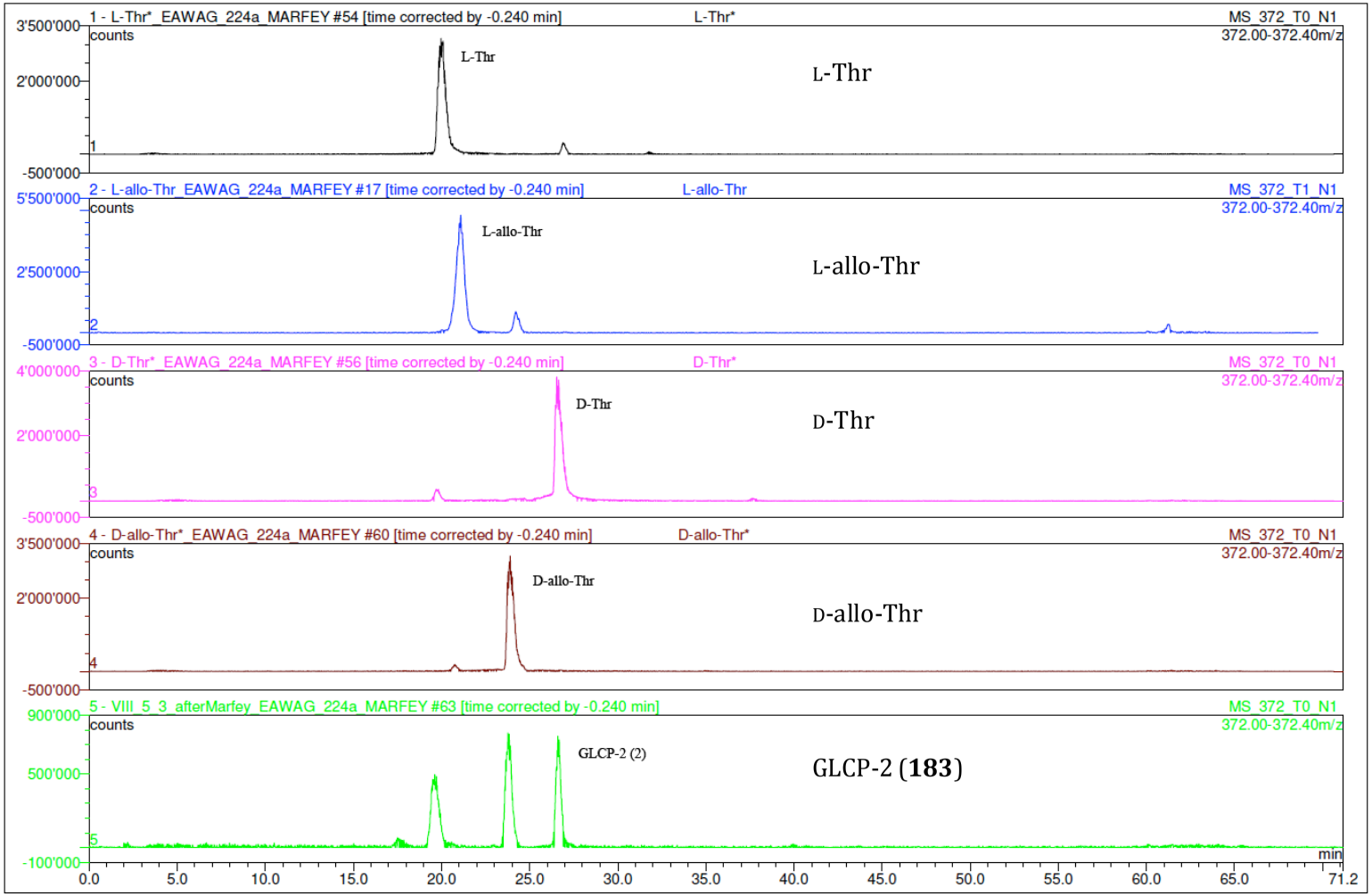

GLCP-2 (**183**), mass chromatograms monitored at *m/z* 372 for the protonated threonine Marfey's derivatives. **183** was hydrolyzed prior to derivatization.

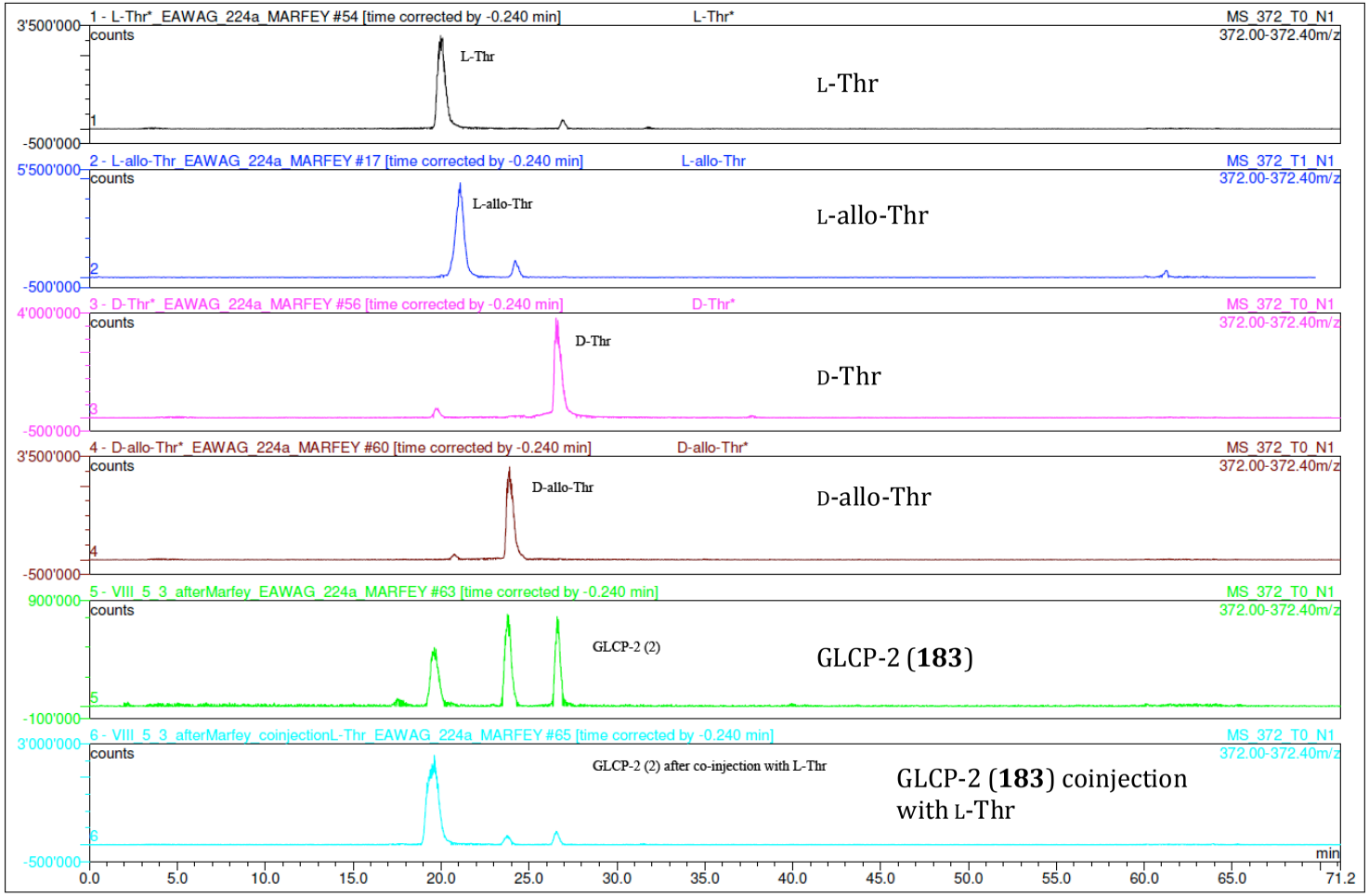

GLCP-2 (**183**), mass chromatograms monitored at *m/z* 328 for the protonated glutamine Marfey's derivatives. **183** was hydrolyzed prior to derivatization.

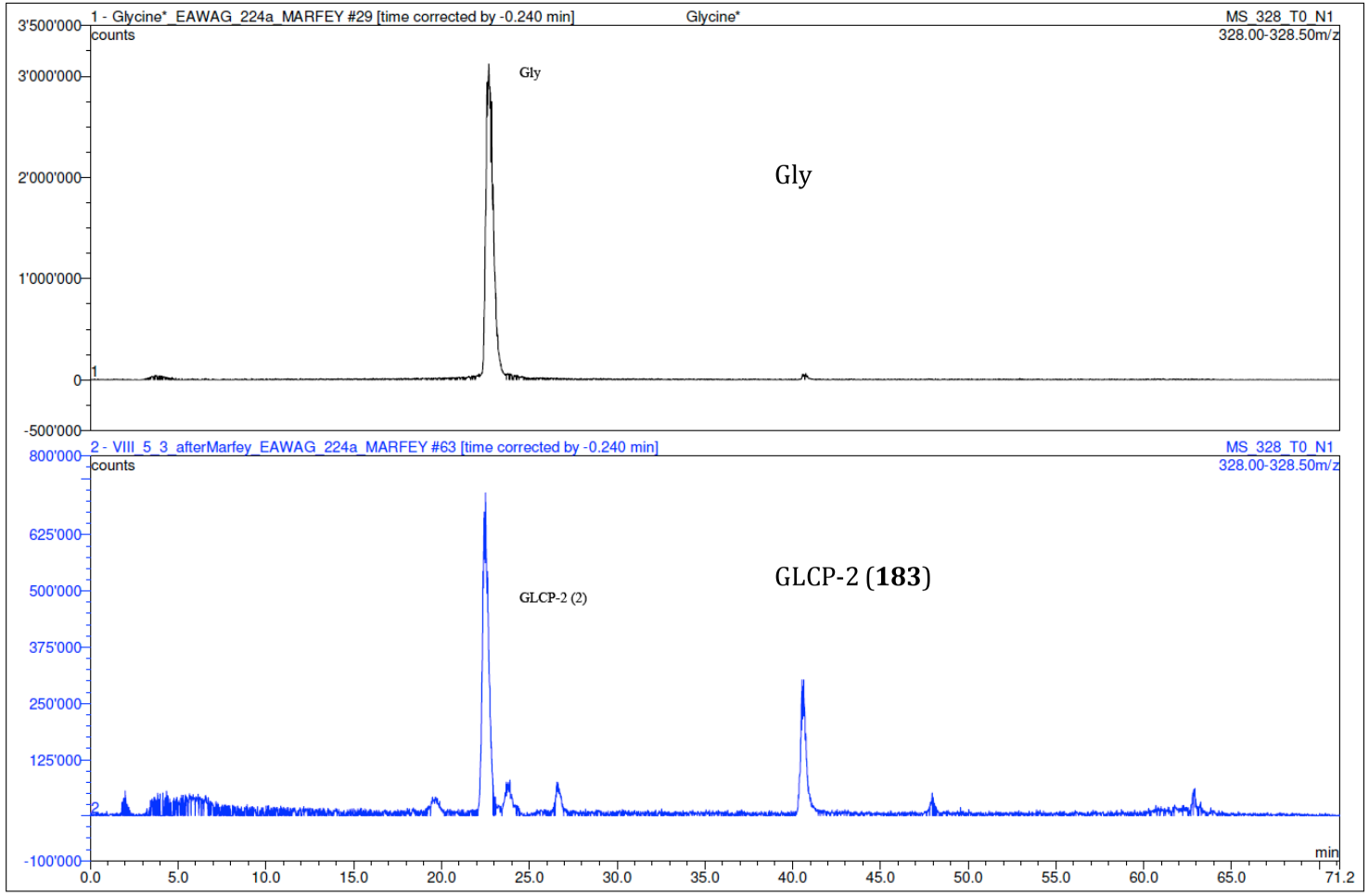

GLCP-2 (**183**), mass chromatograms monitored at *m/z* 386 for the protonated *N*-methylate threonine Marfey's derivatives. **183** was hydrolyzed prior to derivatization.

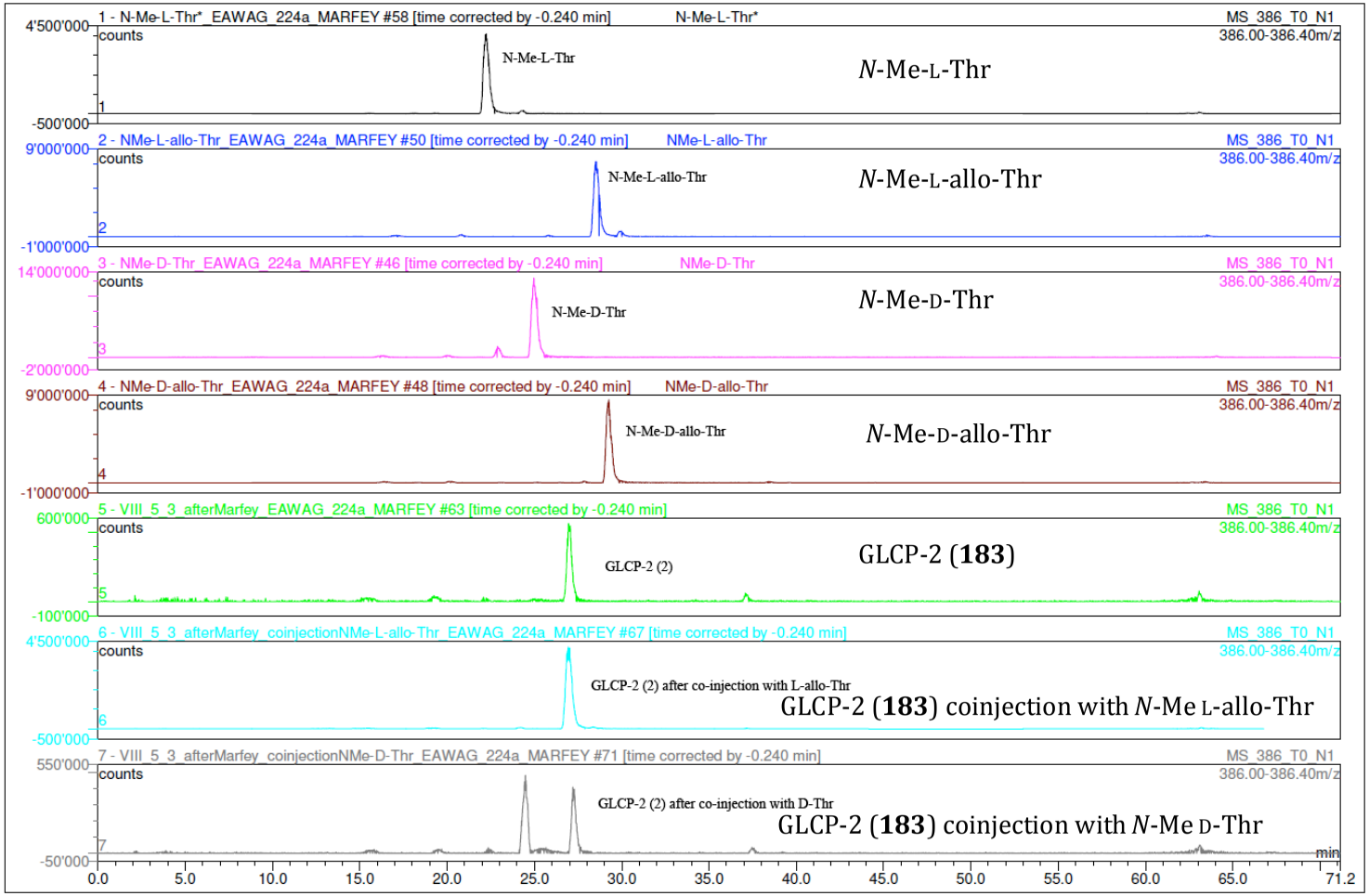

Amino Acid Analysis of Balgacyclamides

Balgacyclamide A (**177**), mass chromatograms monitored at *m/z* 368 with negative APCI mode for the deprotonated valine Marfey's derivatives. **177** was ozonolyzed and hydrolyzed prior to the derivatization.

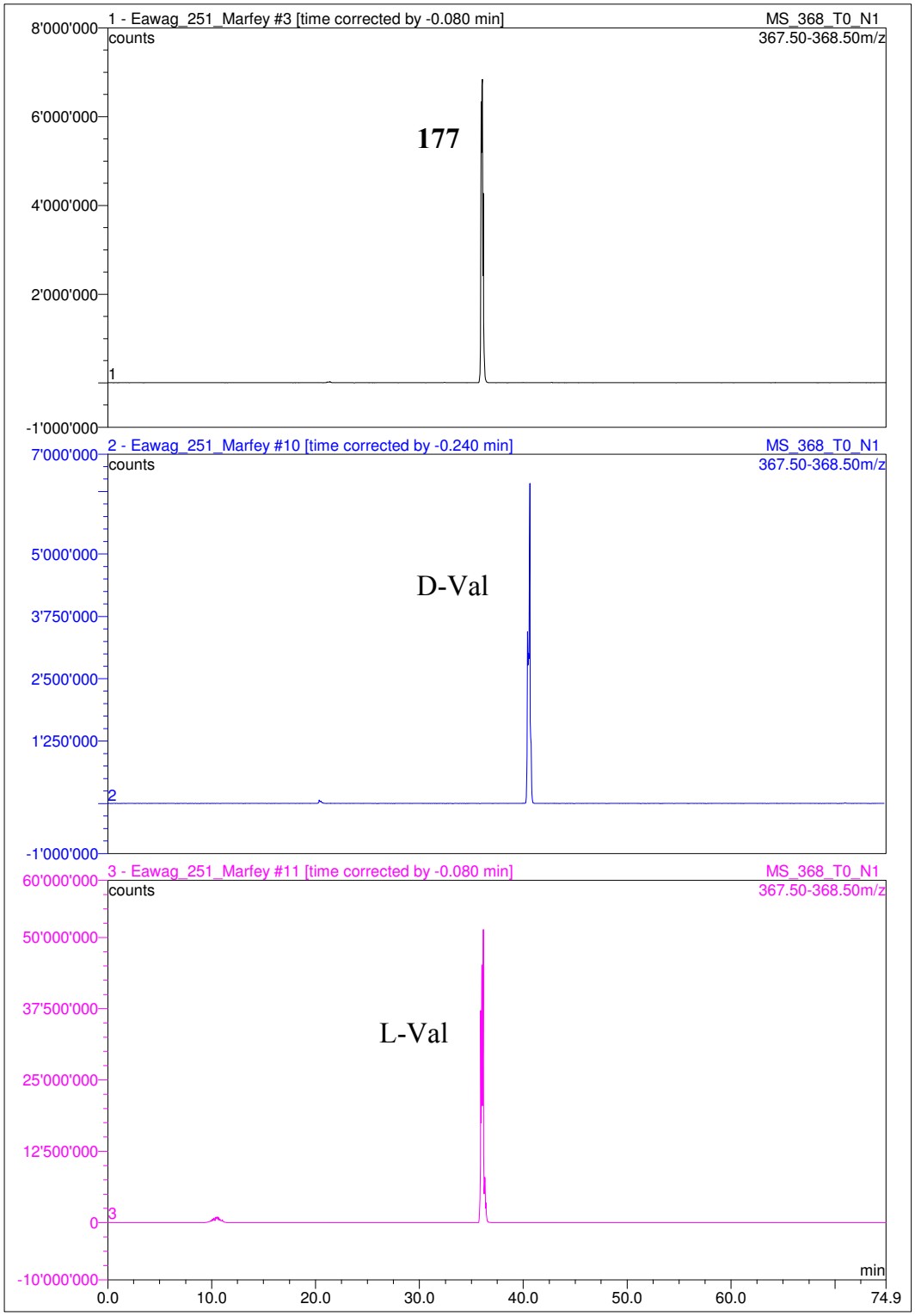

Balgacyclamide A (**177**), mass chromatograms monitored at *m/z* 340 with negative APCI mode for the deprotonated alanine Marfey's derivatives. **177** was ozonolyzed and hydrolyzed prior to the derivatization.

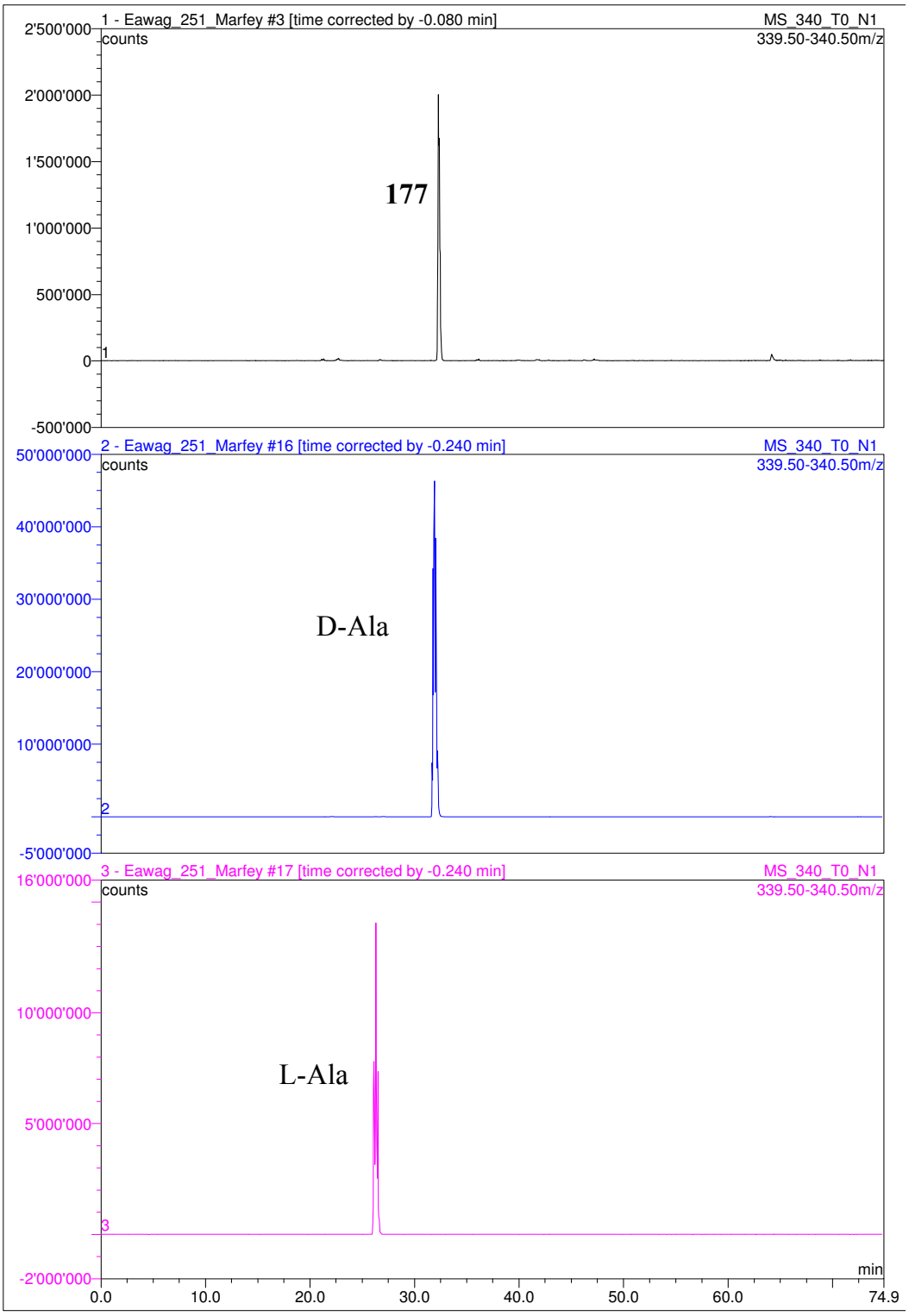

Balgacyclamide A (**177**), mass chromatograms monitored at *m/z* 382 with negative APCI mode for the deprotonated isoleucine Marfey's derivatives. **177** was ozonolyzed and hydrolyzed prior to the derivatization.

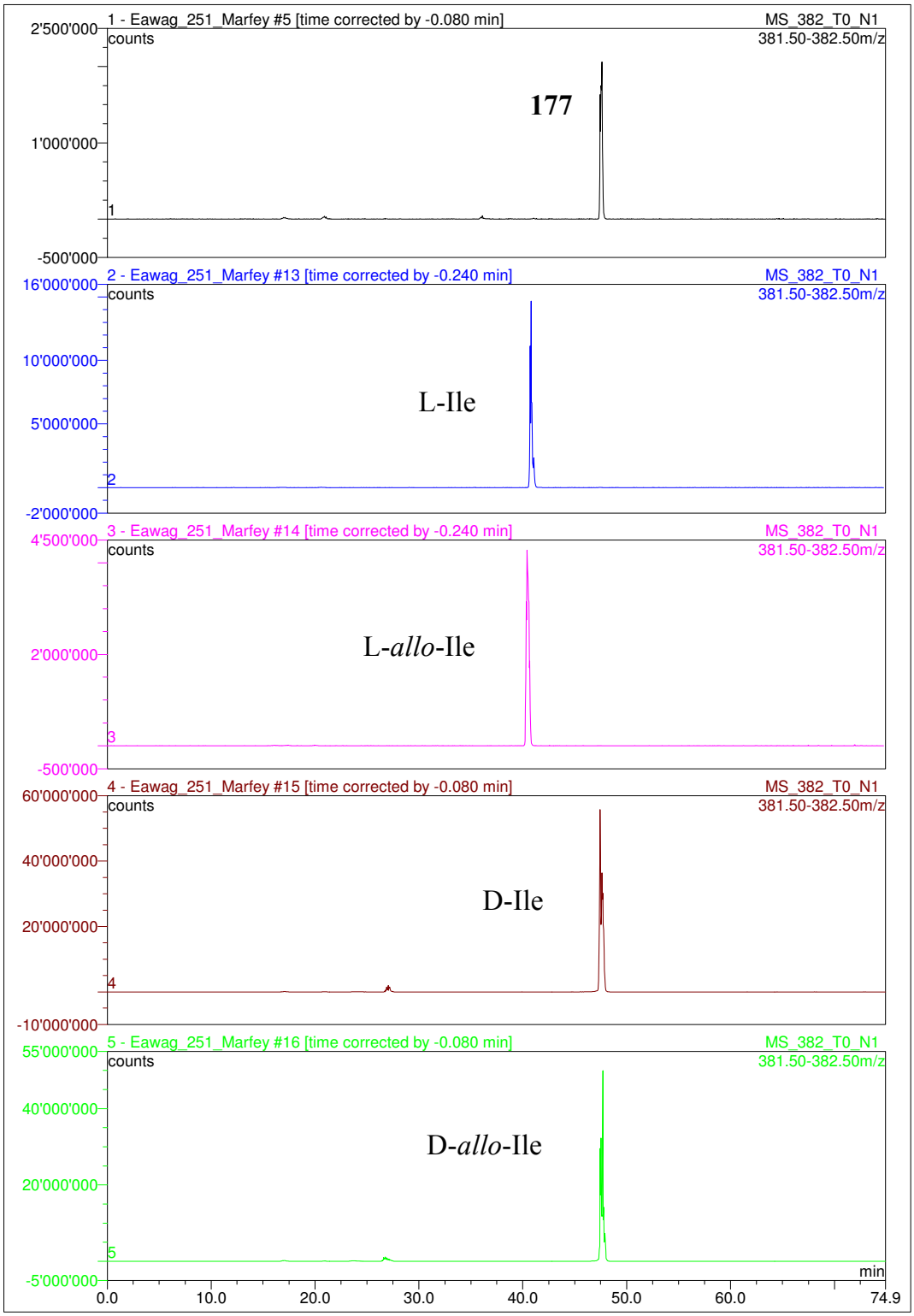

Balgacyclamide A (**177**), mass chromatograms monitored at *m/z* 370 with negative APCI mode for the deprotonated threonine Marfey's derivatives. **177** was ozonolyzed and hydrolyzed prior to the derivatization.

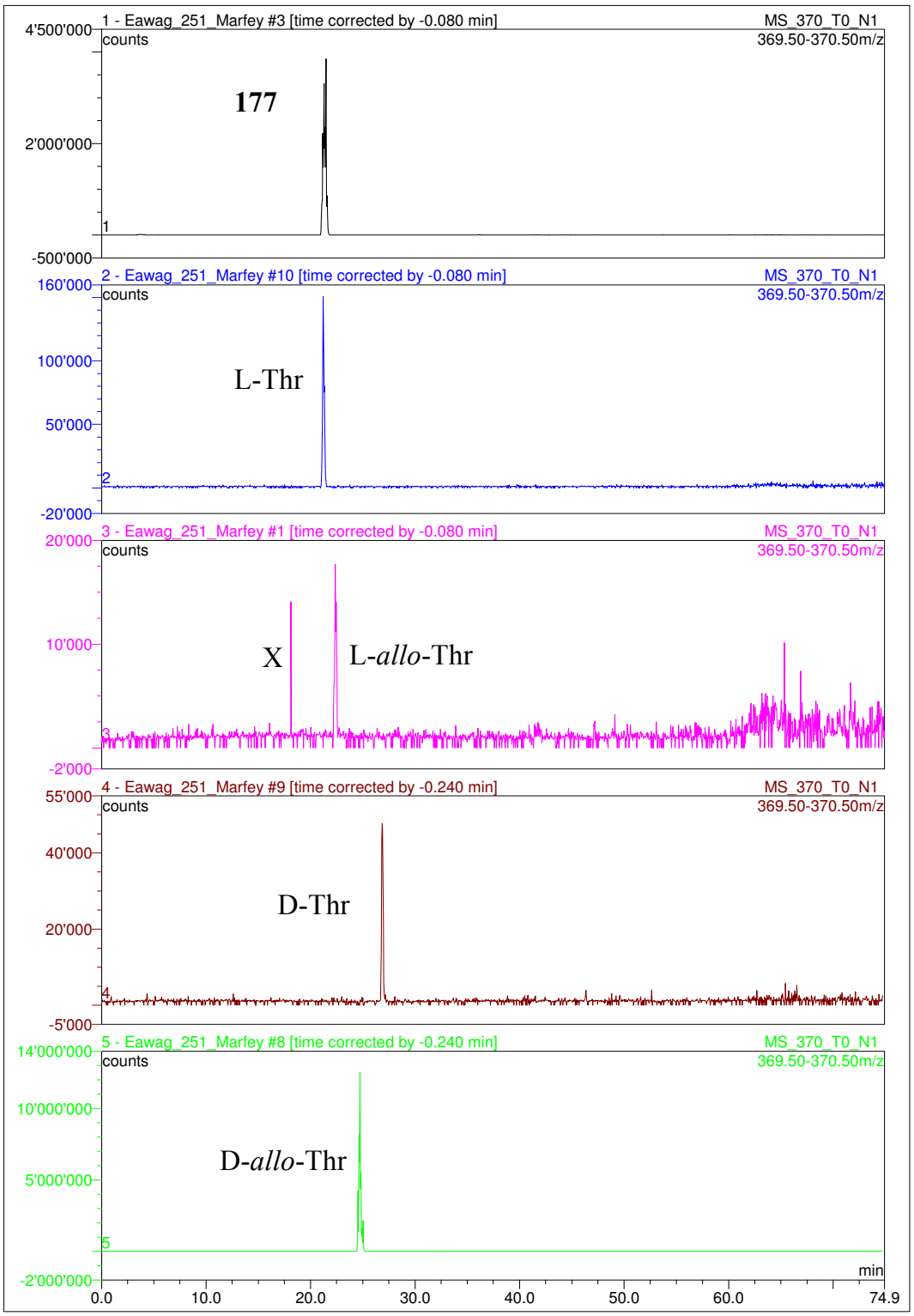

Balgacyclamide A (**177**), mass chromatograms monitored at *m/z* 370 with negative APCI mode for the deprotonated threonine Marfey's derivatives, L-Thr and L-*allo*-Thr, and coinjection of **177** with L-*allo*-Thr. **177** was ozonolyzed and hydrolyzed prior to the derivatization.

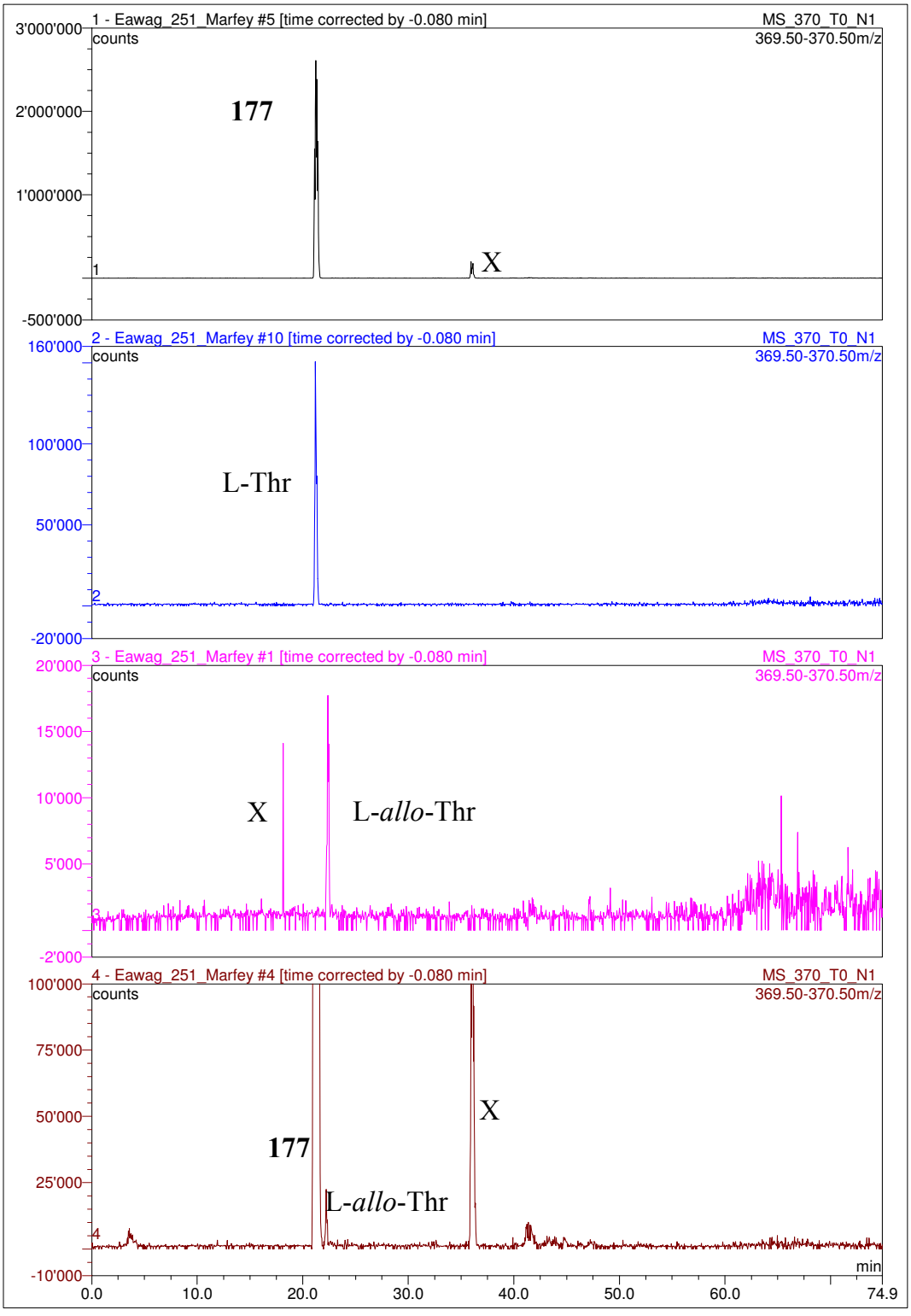

Balgacyclamide A (**177**), GC chromatograms of the derivatized D-*allo*-Ile, D-Ile and coinjection of derivatized **177** with D-Ile. **177** was hydrolyzed prior to derivatization with trifluoroacetic acid.

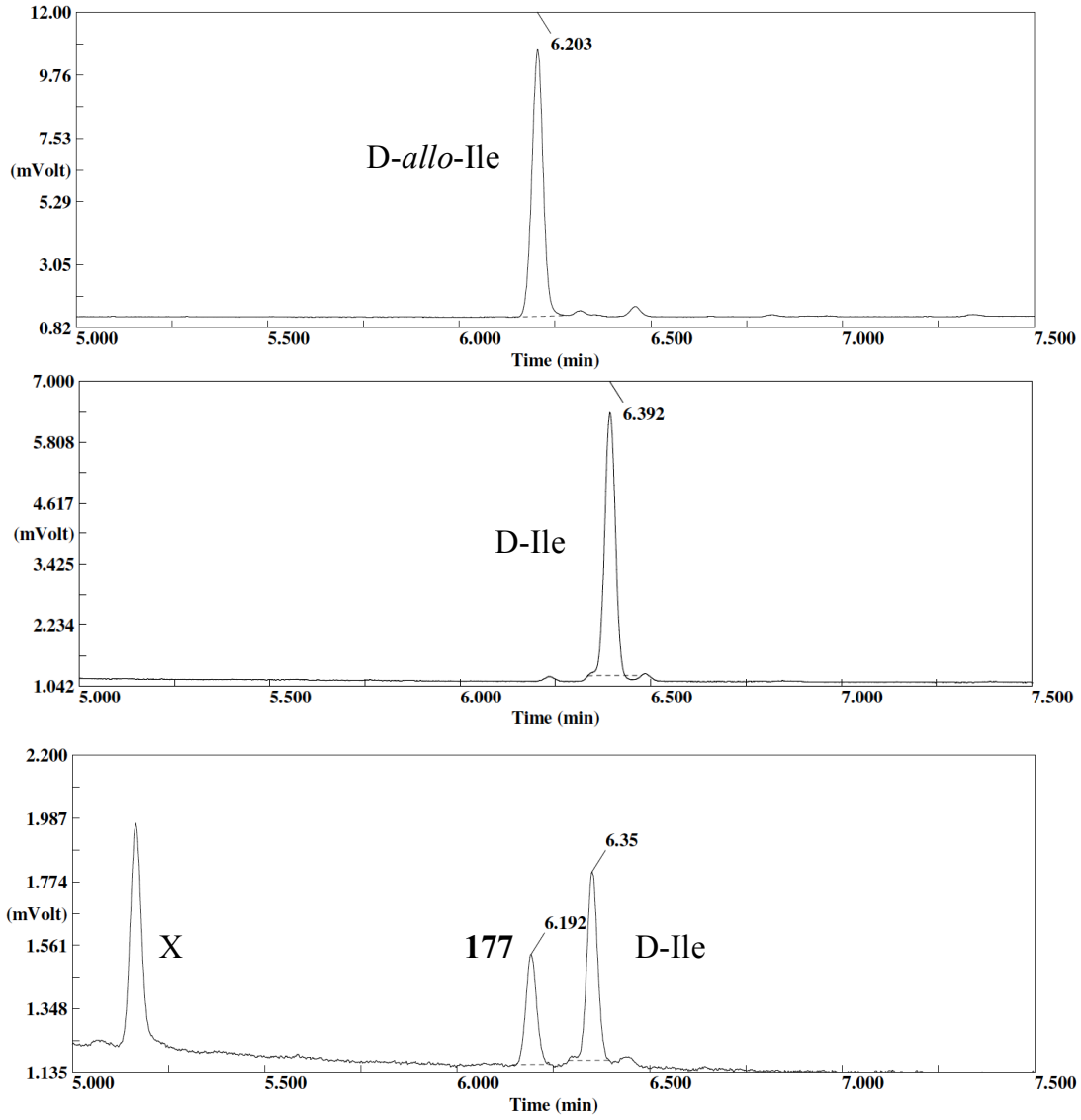

Balgacyclamide B (**178**), mass chromatograms monitored at *m/z* 368 with negative APCI mode for the deprotonated valine Marfey's derivatives. **178** was ozonolyzed and hydrolyzed prior to the derivatization.

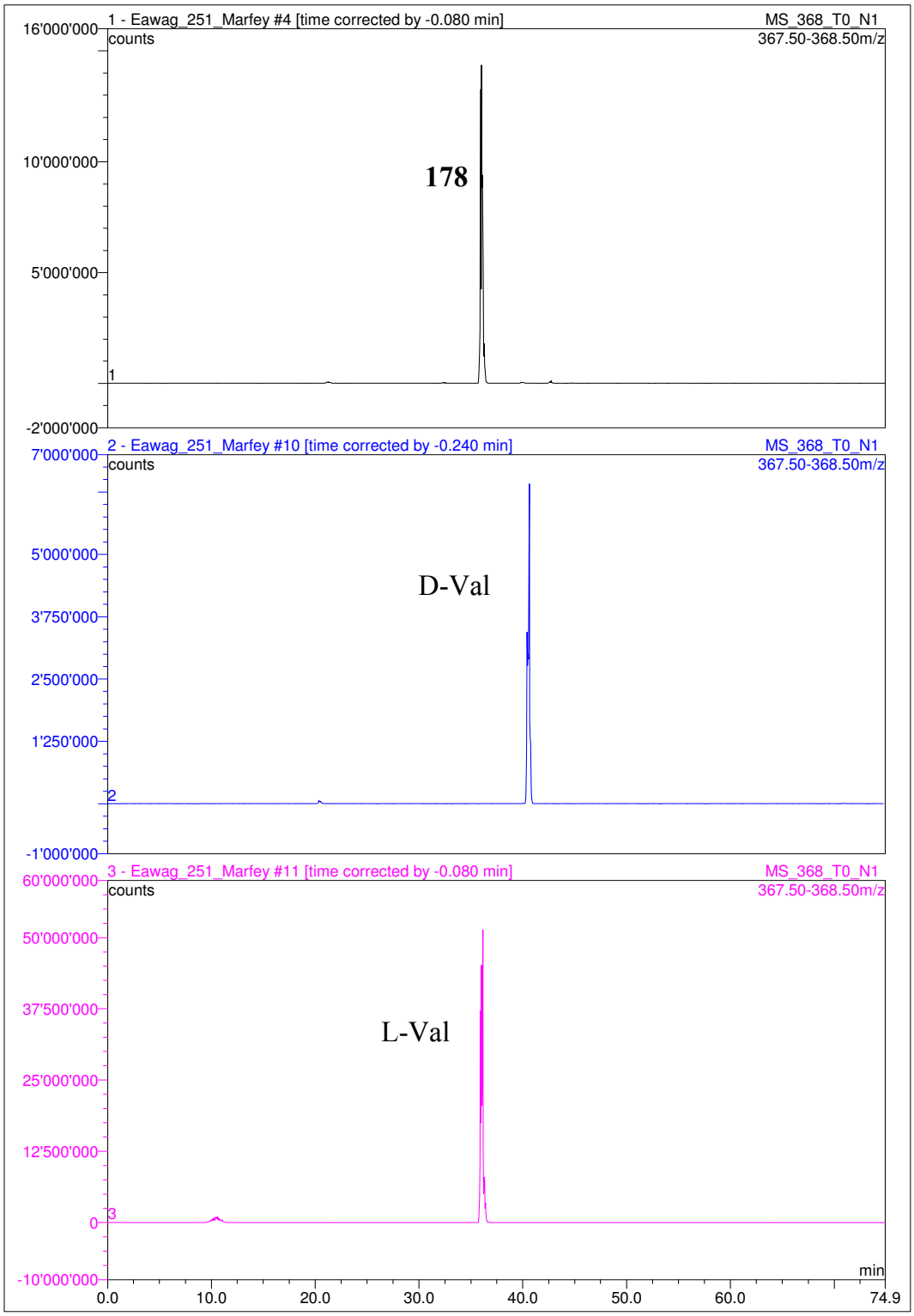

Balgacyclamide B (**178**), mass chromatograms monitored at *m/z* 340 with negative APCI mode for the deprotonated alanine Marfey's derivatives. **178** was ozonolyzed and hydrolyzed prior to the derivatization.

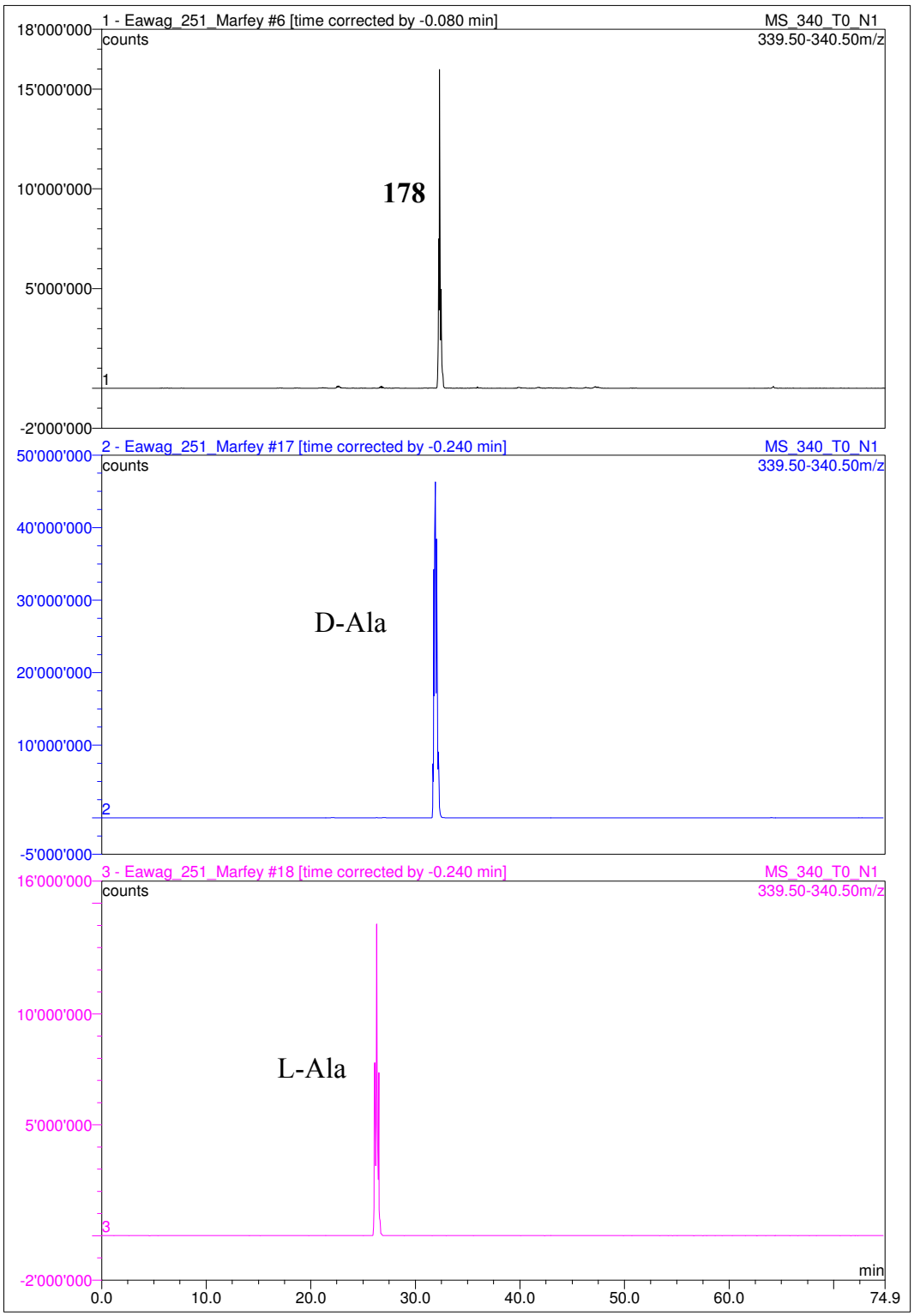

Balgacyclamide B (**178**), mass chromatograms monitored at *m/z* 382 with negative APCI mode for the deprotonated isoleucine Marfey's derivatives. **178** was ozonolyzed and hydrolyzed prior to the derivatization.

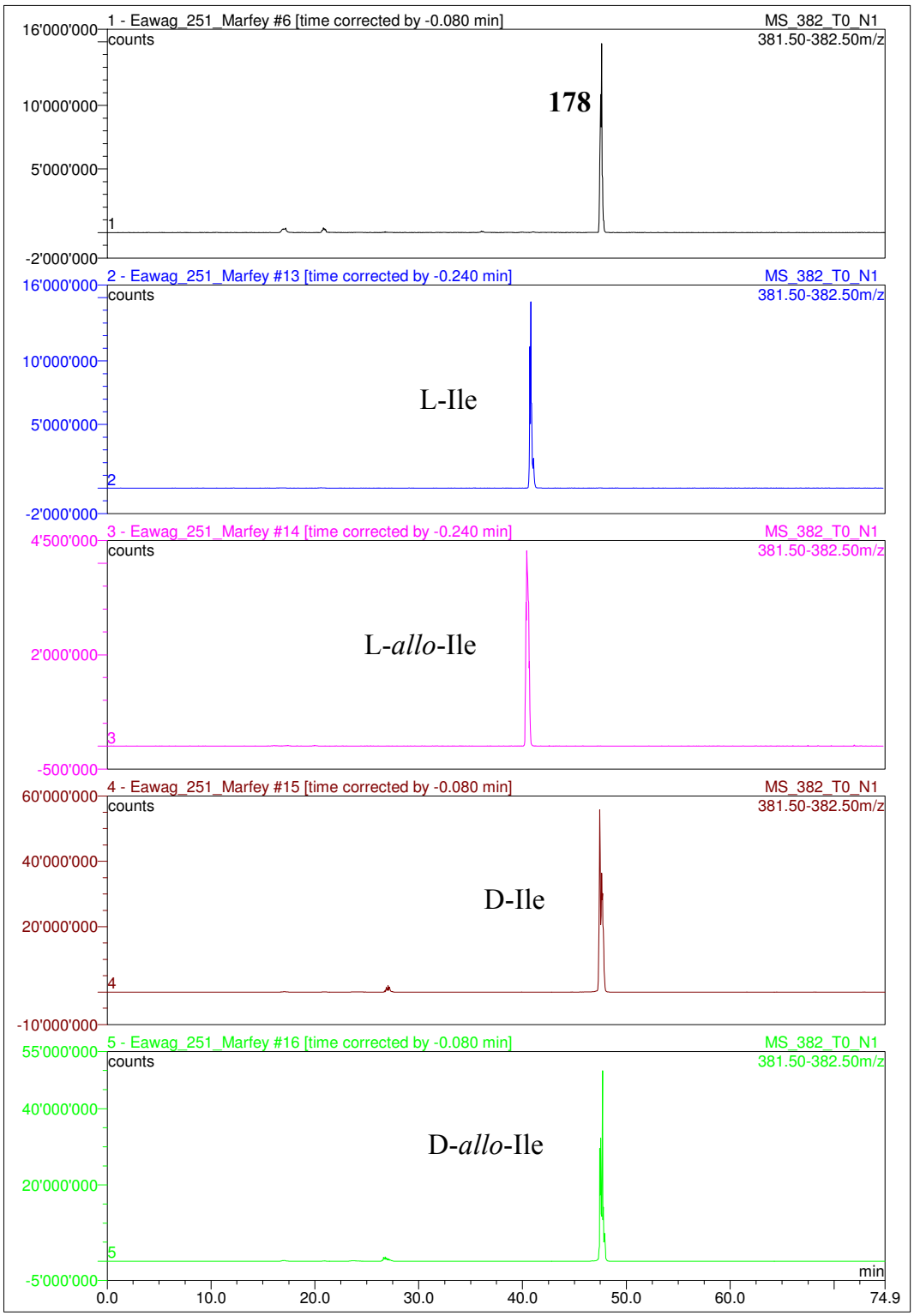

Balgacyclamide B (**178**), mass chromatograms monitored at *m/z* 370 with negative APCI mode for the deprotonated threonine Marfey's derivatives. **178** was ozonolyzed and hydrolyzed prior to the derivatization.

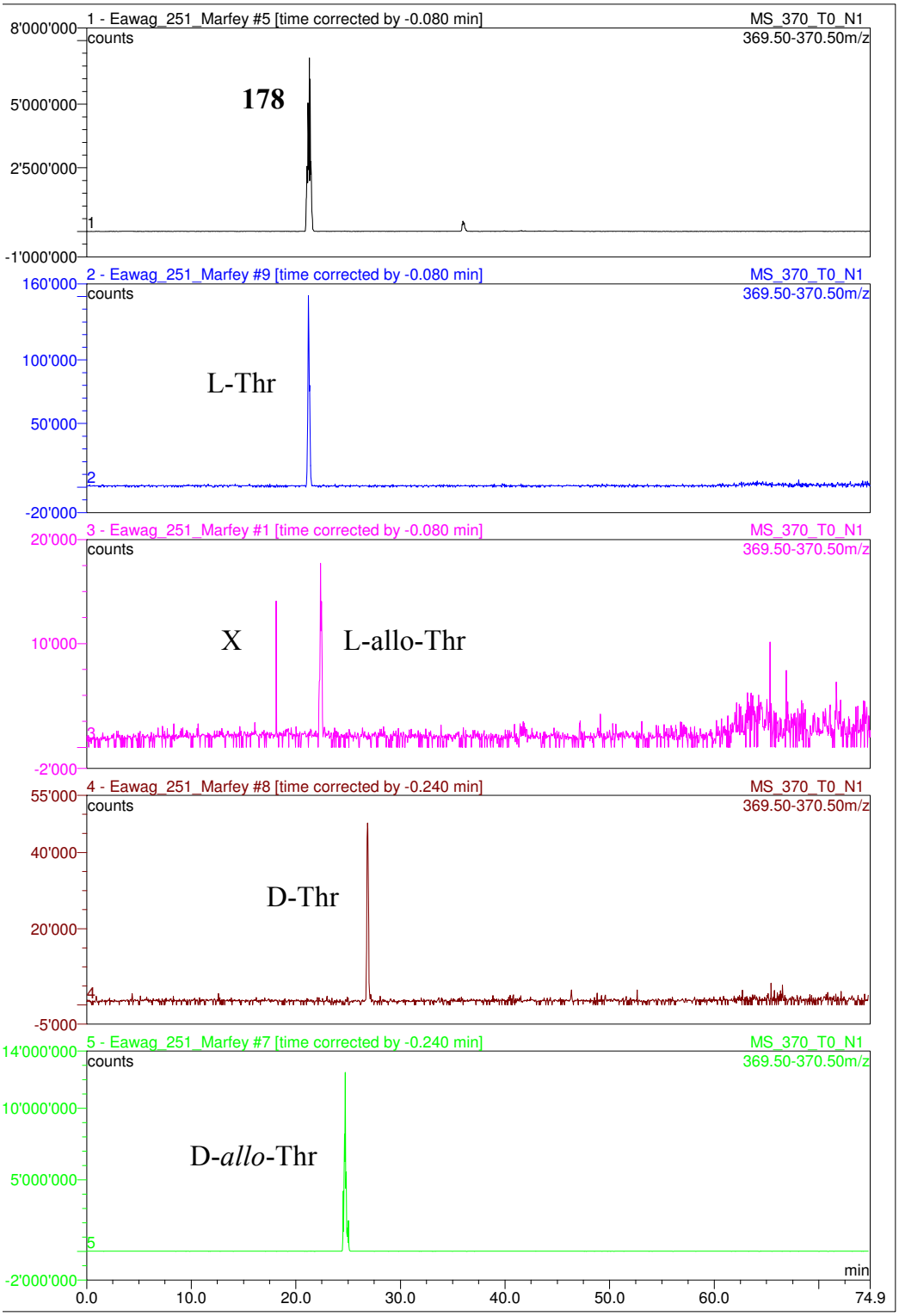

Balgacyclamide B (**178**), GC chromatograms of the derivatized D-*allo*-Ile, D-Ile and coinjection of derivatized **178** with D-Ile. **178** was hydrolyzed prior to derivatization with trifluoroacetic acid.

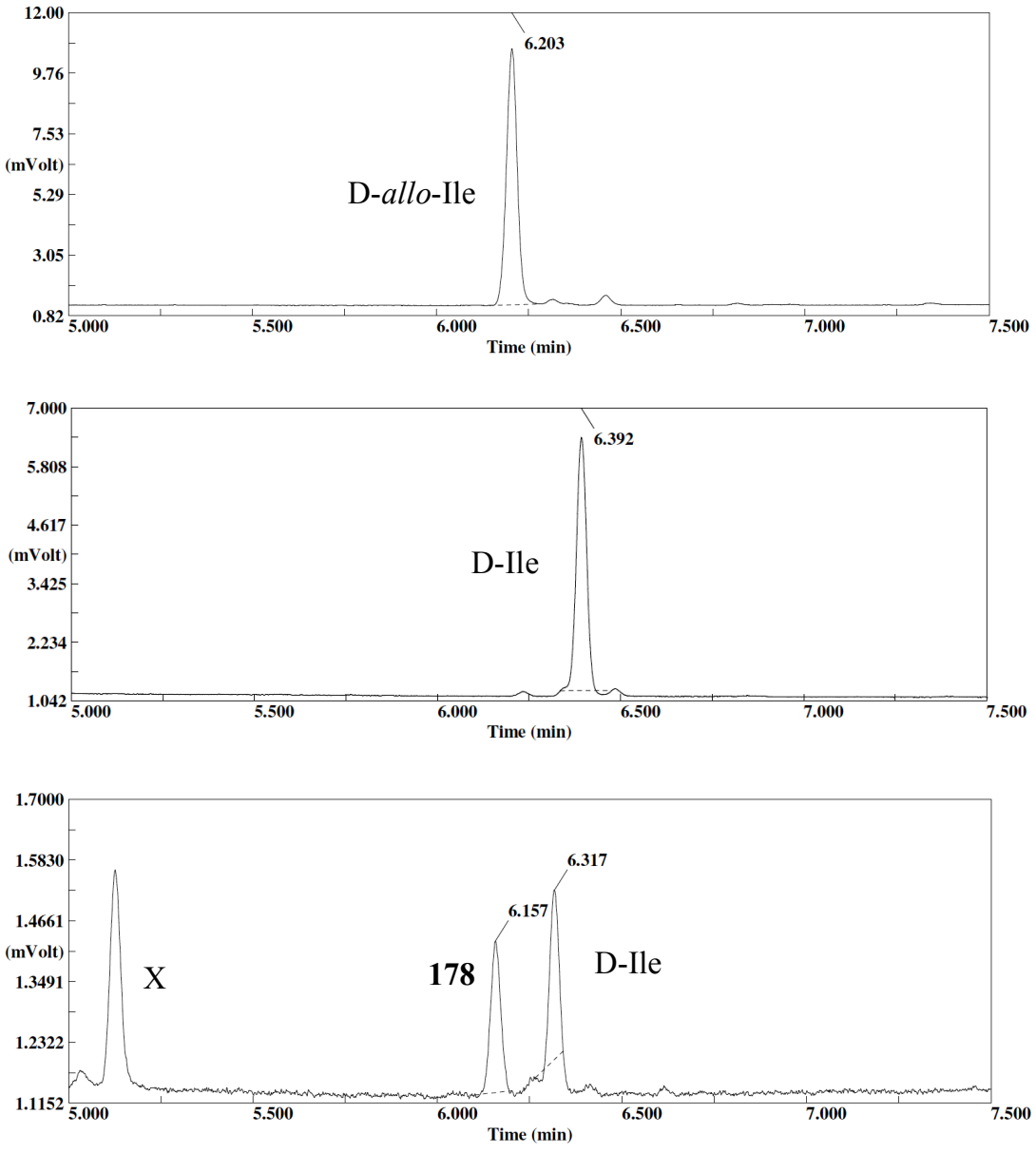

Balgacyclamide C (**179**), mass chromatograms monitored at *m/z* 416 with negative APCI mode for the deprotonated phenylalanine Marfey's derivatives. **179** was ozonolyzed and hydrolyzed prior to the derivatization.

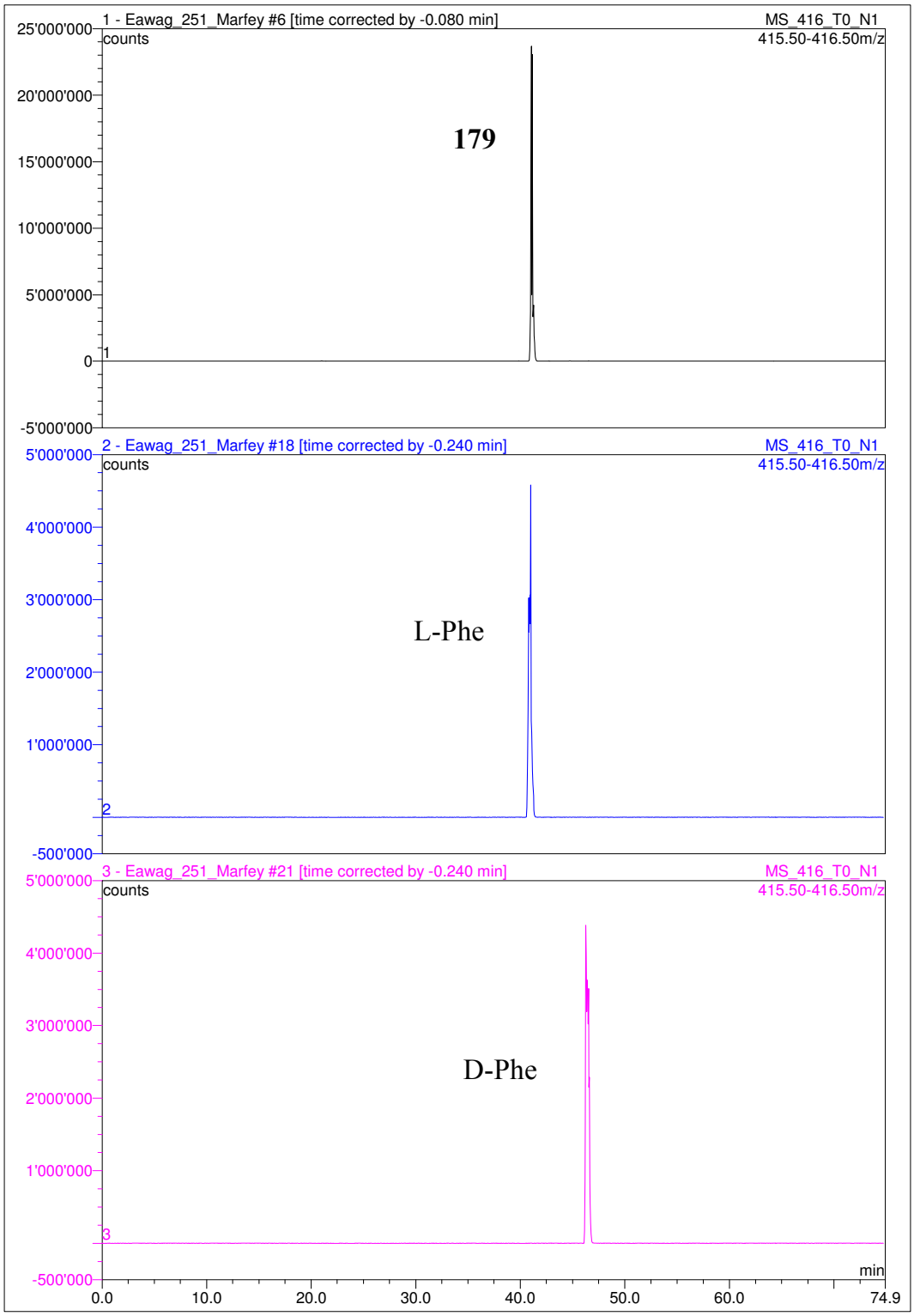

Balgacyclamide C (**179**), mass chromatograms monitored at *m/z* 382 with negative APCI mode for the deprotonated isoleucine Marfey's derivatives. **179** was ozonolyzed and hydrolyzed prior to the derivatization.

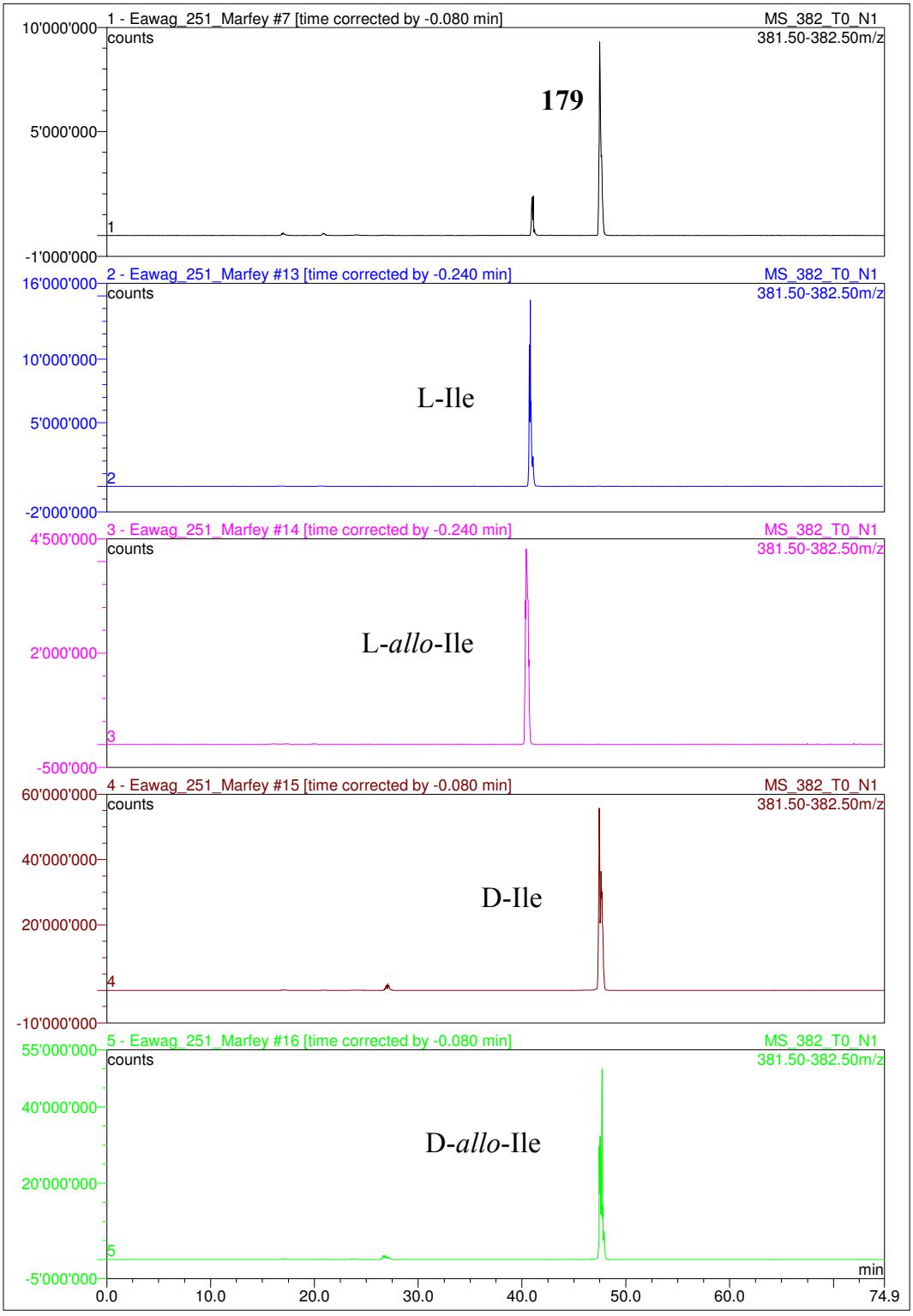

Balgacyclamide C (**179**), mass chromatograms monitored at *m/z* 370 with negative APCI mode for the deprotonated threonine Marfey's derivatives. **179** was ozonolyzed and hydrolyzed prior to the derivatization.

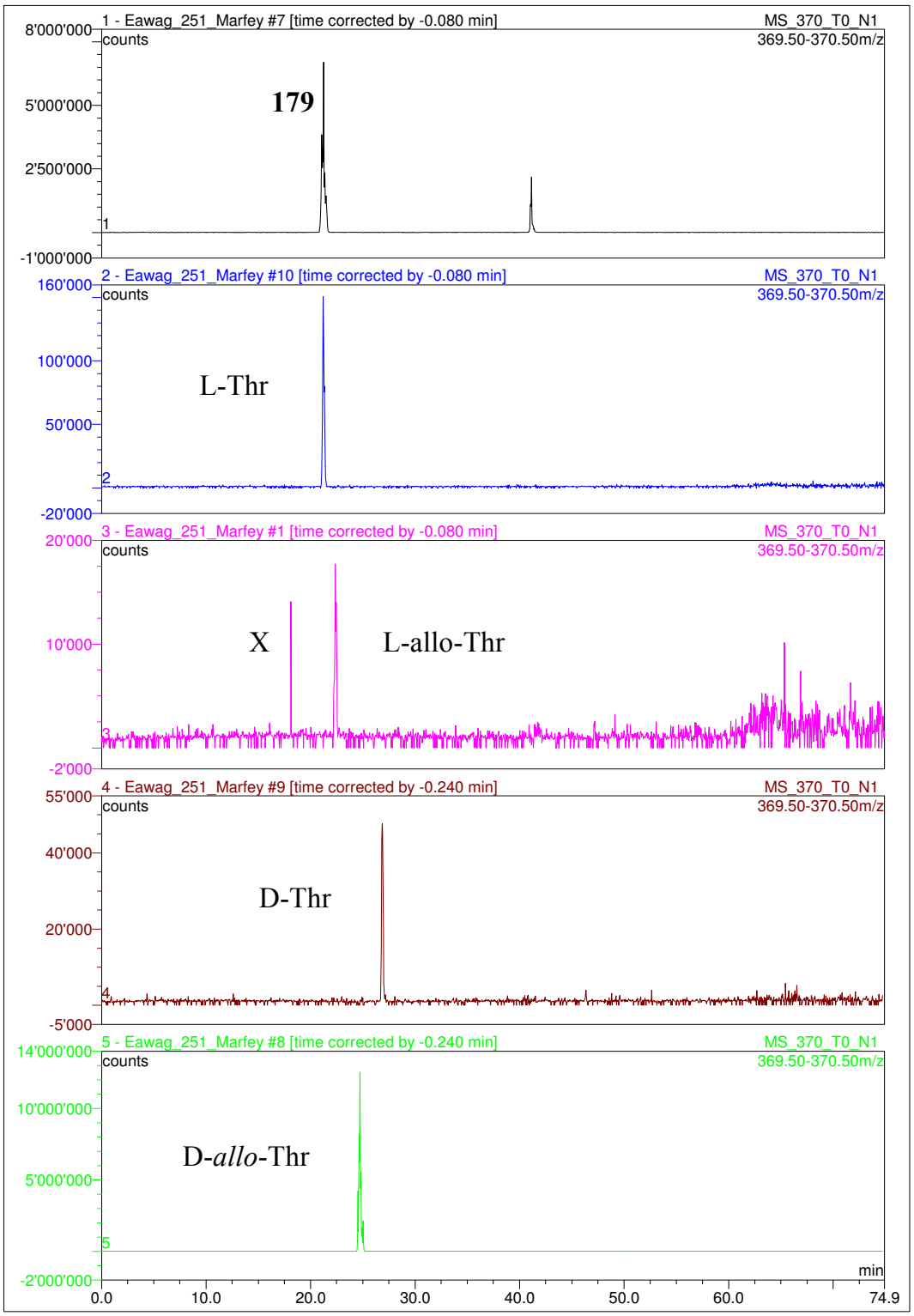

Balgacyclamide C (**179**), GC chromatograms of the derivatized D-*allo*-Ile, D-Ile and coinjection of **179** with D-Ile. **179** was hydrolyzed prior to derivatization with trifluoroacetic acid.